

The 19th International Symposium on Polar Sciences

Toward Better Understanding of Climate Change in the Arctic



October 16–18, 2013
Korea Polar Research Institute
Incheon, Republic of Korea

<http://symposium.kopri.re.kr>



26, Songdomirae-ro, Yeonsu-gu, Incheon 406-840, Korea

The 19th International Symposium on Polar Sciences

- Toward Better Understanding of Climate Change in the Arctic -

**Oct 16 - 18, 2013
Korea Polar Research Institute
Incheon, Republic of Korea**

**Organized by
Korea Polar Research Institute**



Schedule

	Oct. 15	Oct. 16	Oct. 17	Oct. 18			
0900	<p>KOPRI-OUJ Joint Workshop</p> <p>International Meeting Room (3F)</p>	Registration	Registration	<p>Pacific Arctic Group (PAG) Meeting</p> <p>International Meeting Room (3F)</p>	<p>Permafrost Group Meeting</p> <p>Seminar Room (3F)</p>		
		Opening Ceremony & Group Photo	Plenary Speech				
1000		Plenary Speech	Coffee Break				
1100			Session 3: Permafrost				
1200		Lunch	Lunch				
1300		<p>Planning Meeting for Collaborative Observational Study in the Seasonal Ice Zone near Svalbard</p> <p>Seminar Room (3F)</p>	Session 1: Atmosphere			Session 4: Arctic Terrestrial Ecosystems	
1400						Coffee Break & Poster Session	
1500			Session 2: Ice and Ocean			Session 5: Arctic Paleocyanography	<p>Arctic Terrestrial Ecosystem Group Meeting</p> <p>International Meeting Room (3F)</p>
1600						Session 6: Northern Route	
1700							
1800							
1900			Banquet				
2000		Icebreaker					

SYMPOSIUM PROGRAM

OCT 16 (WEDNESDAY)

TIME	SCHEDULE
09:00-09:30	Registration <i>Information desk, Auditorium Hall</i>
09:30-09:50	Opening Ceremony <i>Auditorium</i>
09:50-10:00	Group Photo <i>Auditorium</i>
10:00-10:10	Coffee Break <i>Auditorium Hall</i>
10:10-10:55	Plenary Speech 1: Toward Better Understanding of Climate Changes in the Arctic <i>Mojib Latif</i> <i>GEOMAR, Germany</i>
10:55-11:40	Plenary Speech 2: Biological Hotspots in The Pacific Arctic: Physical Drivers, Ecosystem Productivity and Sensitivity to Climate Change <i>Jackie Grebmeier</i> <i>University of Maryland Center for Environmental Science, USA</i>
11:40-13:00	Lunch
13:00-15:00	ATMOSPHERE <i>Session Chair: Seong-Joong Kim</i>
13:00-13:15	Recent Arctic Climate Change and Its Impact on Mid-latitudes <i>Seong-Joong Kim</i> <i>Korea Polar Research Institute</i>
13:15-13:30	Association of Indian Ocean ITCZ Variations with the Arctic Oscillation during Boreal Winter <i>Dao-Yi Gong</i> <i>Beijing Normal University, China</i>
13:30-13:45	Study on the Influence of Arctic Sea-Ice Loss on the Tropical Pacific SST Variability <i>Sang-Wook Yeh</i> <i>Hanyang University, Korea</i>
13:45-14:00	Relationship Between the Arctic Oscillation and Arctic Amplification <i>Hiroshi Tanaka</i> <i>University of Tsukuba, Japan</i>
14:00-14:15	Role of Biological Feedback in Arctic Amplification <i>Jong-Seong Kug</i> <i>Korea Institute of Ocean Science and Technology, Korea</i>
14:15-14:30	Interannual Variability and Long-Term Changes of Atmospheric Circulation over the Chukchi and Beaufort Seas <i>Qigang Wu</i> <i>Nanjing University, China</i>
14:30-14:45	Arctic Cloud Microphysical Characteristics from Space-Based Lidar Caliop <i>Sang-Woo Kim</i> <i>Seoul National University, Korea</i>

14:45- 15:00	Changing Relation Between Arctic Sea Ice and Asian Dust Associated with Global Warming <i>Jeong-Hyun Park</i> <i>Seoul National University, Korea</i>
15:00- 16:00	Poster Session <i>Auditorium Hall</i>
16:00- 18:15	ICE AND OCEAN <i>Session Chair: Ho Kyung Ha</i>
16:00- 16:15	Carbon Contribution of Sea Ice floes in the Arctic Ocean <i>Sang H Lee</i> <i>Pusan National University, Korea</i>
16:15- 16:30	Using Pelagic Ciliated Microzooplankton Communities as an Indicator for Monitoring Environmental Condition under Impact of Summer Sea-Ice Reduction in Western Arctic Ocean <i>Yong Jiang</i> <i>Korea Polar Research Institute</i>
16:30- 16:45	Projection of Ship-accessible Days in the Arctic Sea based on IPCC Climate Change Scenarios <i>Jai-Ho Oh</i> <i>Pukyong National University, Korea</i>
16:45- 17:00	No-Rebound Reduction of Sea Ice in the Arctic Ocean: Role of "Inertia" Effect of the Ocean <i>Koji Shimada</i> <i>Tokyo University, Japan</i>
17:00- 17:15	Optical Properties around Mendeleev Ridge Related to the Physical Features of Water Masses <i>Jinping Zhao</i> <i>Ocean University of China, China</i>
17:15- 17:30	Subseasonal to seasonal prediction of Arctic sea-ice concentration by seasonal Empirical Orthogonal Function (EOF) method <i>Baek-Min Kim</i> <i>Korea Polar Research Institute</i>
17:30- 17:45	The Effect of Poleward Moisture Flux on Arctic Winter Sea-Ice Melting <i>Hyo-Seok Park</i> <i>Seoul National University, Korea</i>
17:45- 18:00	Energy Budget of First-Year Arctic Sea Ice in Advanced Stages of Melt <i>Stephan Hudson</i> <i>Norwegian Polar Institute, Norway</i>
18:00- 18:15	Solar Energy Budget of First-Year Sea Ice in the Central Arctic - Autonomous Observations from Two Summer Melt Seasons <i>M. A. Granskog</i> <i>Norwegian Polar Institute, Norway</i>
19:00- 21:00	Icebreaker

October 17 (THURSDAY)

TIME	SCHEDULE
09:00-09:30	Registration <i>Information desk, Auditorium Hall</i>
09:30-10:00	Plenary Speech 1: The Interaction of Atmospheric, Hydrologic, Geomorphic and Ecosystem Processes on the Arctic Coastal Plain <i>Larry Hinzman</i> <i>International Arctic Research Center, University of Alaska Fairbanks, USA</i>
10:00-10:30	Plenary Speech 2: Projections and Implications of 21st Century Permafrost Thaw <i>David Lawrence</i> <i>National Center for Atmospheric Research, USA</i>
10:30-10:45	Coffee Break <i>Auditorium Hall</i>
10:45-12:00	<p style="text-align: center;">PERMAFROST – ATMOSPHERE INTERACTIONS</p> <p style="text-align: center;"><i>Session Chair: Taejin Choi</i></p>
10:45-11:00	Climate and Permafrost Change in Western Alaska: 115 Years of Measurements on the Seward Peninsula <i>Jessica Cherry</i> <i>University of Alaska Fairbanks, USA</i>
11:00-11:15	Greenhouse Gas Exchange at an Alaska Permafrost Region <i>Sang-Jong PARK</i> <i>Korea Polar Research Institute</i>
11:15-11:30	The Permafrost-Dominated Ecosystems in a Changing Climate <i>Trofim Maximov</i> <i>Institute for Biological Problems of Cryolithozone of SB RAS, Russia</i>
11:30-11:45	Structure of the Atmospheric Boundary Layer at Ny-Alesund: Statistics and Case Studies <i>Angelo P. Viola</i> <i>CNR Institute of Atmospheric Sciences and Climate, Italy</i>
11:45-12:00	Simultaneous Measurements of Carbon Exchange over Three Permafrost Sites at the Arctic <i>Taejin Choi</i> <i>Korea Polar Research Institute</i>
12:00-13:00	Lunch
13:00-14:30	<p style="text-align: center;">ARCTIC TERRESTRIAL ECOSYSTEMS</p> <p style="text-align: center;"><i>Session Chair: Yoo Kyung Lee</i></p>
13:00-13:15	The Future Terrestrial Arctic: Projections for Permafrost and Snow <i>Andrew Slater</i> <i>National Snow and Ice Data Center, University of Colorado, USA</i>
13:15-13:30	Methane Dynamics under Melting Excess Ice And Permafrost Thaw in the Community Land Model 4.5 <i>Hanna Lee</i> <i>National Center for Atmospheric Research, Boulder, Colorado, USA</i>
13:30-13:45	'Dynamic Disequilibria' in the Arctic Terrestrial Realm: Landscapes and Ecosystems in Transition <i>Philip A. Wookey</i> <i>Heriot Watt University, UK</i>

13:45- 14:00	Circum-Polar Vegetation and Environmental Conditions <i>Eun Ju Lee</i> <i>Seoul National University, Korea</i>
14:00- 14:15	Soil Microbial Communities in Arctic and Other Cold Ecosystems <i>Haiyan Chu</i> <i>Institute of Soil Science, Chinese Academy of Sciences, China</i>
14:15- 14:30	Climate Change and Soil Ecosystem <i>Yoo Kyung Lee</i> <i>Korea Polar Research Institute</i>
14:30- 15:30	Coffee Break & Poster Session <i>Auditorium Hall</i>
15:30- 16:45	ARCTIC PALEOCEANOGRAPHY: LESSON FROM THE PAST <i>Session Chair: Seung-II Nam</i>
15:30- 16:00	Plenary Speech 3: Repeated Pleistocene glaciation of the East Siberian continental margin <i>Frank Niessen</i> <i>Alfred Wegener Institute, Germany</i>
16:00- 16:15	Interpretation of Lipids Biomarkers in the Sediment of Western Arctic Ocean: Last 100 Years Records of Organic Sources, Storage and Surface Seawater Temperature <i>Adegoke.O Badejo</i> <i>Hanyang University, Korea</i>
16:15- 16:30	Stable Isotope Compositions of Authigenic Carbonates in Pelagic Sediments of the Mendeleev Ridge (Arctic Ocean): Their Implications for Paleooceanography <i>Kyung Sik Woo</i> <i>Kangwon National University, Korea</i>
16:30- 16:45	Preliminary Results of 3rd/4th RV ARAON Expeditions (ARA04B/4C, 2013) into the Western Arctic Ocean <i>Seung Il Nam</i> <i>Korea Polar Research Institute</i>
16:45- 17:30	NORTHERN ROUTE <i>Session Chair: Baek-Min Kim</i>
16:45- 17:00	Summer CDOM Optical Properties in the Western Arctic under Low Sea Ice Conditions <i>Eurico D'Sa</i> <i>Department of Oceanography and Coastal Sciences, Louisiana State University, USA</i>
17:00- 17:15	Conceptual Design of A Satellite-Based Ice Navigation Supporting System for the Northern Sea Route <i>Sun-Hwa Kim</i> <i>Korea Institute of Ocean Science and Technology</i>
17:15- 17:30	Preconditioning effect of absorbed shortwave radiation on Arctic sea-ice variation in summer <i>Baek-Min Kim</i> <i>Korea Polar Research Institute</i>
18:30- 20:30	Banquet

POSTER SESSION

ATMOSPHERE (PS-AXX)	
PS-A01	Impact of Arctic Sea-Ice on the 2009/2010 Eurasian Cold Winter <i>Taehyoun Shim</i> <i>Korea Polar Research Institute</i>
PS-A02	Arctic Greening can Cause Earlier Seasonality of Polar Amplification <i>Yoo-jeong Chae</i> <i>Ulsan National Institute of Science and Technology, Korea</i>
PS-A03	The Atmospheric Mode Related to Climate Change in Arctic Region <i>Euihyun Jung</i> <i>Seoul National University, Korea</i>
PS-A04	Asymmetric Change of Global Rainy Season Pattern on Global Warming Scenarios <i>Yechul Shin</i> <i>Ulsan National Institute of Science and Technology, Korea</i>
PS-A05	The Response of the ITCZ to Thermal Forcing with the Change of Perturbed Latitude <i>Jeongbin. Seo</i> <i>Ulsan National Institute of Science and Technology, Korea</i>
PS-A06	The High Heat Flux Event in the Barents/Kara Seas in the Winter of 2011/12 <i>Joo-Hong Kim</i> <i>Korea Polar Research Institute</i>
PS-A07	Climate Impact of Changes in Eurasian Arctic Vegetation on the East Asian Summer Monsoon <i>Ah-Ryeon Yang</i> <i>Korea Polar Research Institute</i>
PS-A08	How Much Winter Stratospheric Polar-Cap Warming Is Explained by Upward-Propagating Planetary Waves in CMIP5 Models?: Part 1. An Indirect Approach Using a Wave Interference Index <i>Ji-Won Kim</i> <i>Korea Polar Research Institute</i>
PS-A09	Change in Winter SST over the North Pacific Induced by Sea Ice Loss in Barents - Kara Sea <i>Hyerim Kim</i> <i>Korea Polar Research Institute</i>
PS-A10	AGCM Simulations of Atmospheric Responses to Arctic Sea Ice and SST Anomaly During Boreal Winter: Impacts of Cloud <i>Jung Ok</i> <i>Korea Polar Research Institute</i>
PS-A11	Prediction of The Arctic Oscillation in Boreal Winter by Seasonal Forecasting Systems: Stratospheric Connection <i>Daehyun Kang</i> <i>Ulsan National Institute of Science and Technology, Korea</i>
PS-A12	Ship-Borne Lidar Measurements of Aerosol Vertical Distribution and Optical Properties in Arctic and Antarctic Region <i>Youngmin Noh</i> <i>Gwangju Institute of Science and Technology, Korea</i>
PS-A13	Impact of Sea Ice on Arctic Warming on CMIP5 <i>Bo Young Yim</i> <i>Korea Institute of Ocean Science & Technology, Korea</i>

PS-A14	Temperature Variation over East Asia in Association with Stratospheric Polar Vortex During the Boreal Winter Season <i>Sung-Ho Woo</i> <i>Korea Institute of Ocean Science and Technology, Korea</i>
PS-A15	Influences of Arctic Sea Ice Variability on the Summer North Atlantic Oscillation (SNAO) <i>Hans W Linderholm</i> <i>University of Gothenburg, Sweden</i>
PS-A16	Recent Changes in Winter Arctic Cloud and Its Relation to Atmospheric States over the Surrounding Region <i>Sang-Yoon Jun</i> <i>Korea Institute of Atmospheric Prediction Systems, Korea</i>
PS-A17	Understanding of Circulation Characteristics in Different Types of Sudden Stratospheric Warming Using WACCM <i>Hyesun Choi</i> <i>Korea Polar Research Institute</i>
PS-A18	Interannual Variation of Arctic Sea Ice Concentration in Summer in Response to Precursory Absorbed Shortwave Radiation <i>Yong-Sang Choi</i> <i>Ewha Womans University, Korea</i>
PS-A19	Detecting Human Influence on Arctic Sea-Ice <i>Seung-Ki Min</i> <i>Pohang University of Science and Technology, Korea</i>
PS-A20	Variation of Atmospheric Carbon Monoxide over the Arctic Ocean and the Northwestern Pacific During Summer 2012 <i>Keyhong Park</i> <i>Korea Polar Research Institute</i>
PS-A21	Spatial Distribution of Trace Gases in the East Sea, North Pacific, and Bering Sea along R/V ARAON's cruise track in 2012 <i>Tae Siek Rhee</i> <i>Korea Polar Research Institute</i>
PS-A22	Maritime Boundary Layer Research at Polar Oceans Based on ARAON <i>Sang Jong Park</i> <i>Korea Polar Research Institute</i>

ICE AND OCEAN (PS-IXX)

PS-I01	Distribution of Microbial Populations and Their Relationships with Environmental Factors in the Prydz Bay and Its Adjacent Southern Ocean, Antarctic <i>Min Wang</i> <i>Ocean University of China, China</i>
PS-I02	Asymmetry Variability Between the Arctic and Antarctic Sea Ice <i>Fei Huang</i> <i>Ocean University of China, China</i>
PS-I03	Pyrosequencing Assessment of Prokaryotic Community in the Chukchi Sea During Summer 2012 <i>Chung Y. Hwang</i> <i>Korea Polar Research Institute</i>
PS-I04	Rapid Robotic Bioassessment Method for Herbicides Using Male Gametophyte of Polar Brown Algae <i>Saccharina Latissima</i> <i>Hoon Choi</i> <i>Incheon National University, Korea</i>

PS-I05	Phytoplankton Communities in the Western Arctic Ocean During Late Summer <i>Hyoung Min Joo</i> <i>Korea Polar Research Institute</i>
PS-I06	Under-Ice Measurement of Suspended Particulate Matter, Chukchi Sea <i>Hyun Jung Lee</i> <i>Korea Polar Research Institute</i>
PS-I07	Sinking Particle Flux and Radiocarbon Values of Particulate Organic Carbon in the Deep Canada Basin <i>Minkyoung Kim</i> <i>Pohang University of Science and Technology, Korea</i>
PS-I08	Population Dynamics of Bacterial Assemblages in the Arctic Seafloor <i>Dukki Han</i> <i>Gwangju Institute of Science and Technology, Korea</i>
PS-I09	Study on the Distribution of Dissolved Organic Carbon (DOC) in the Western Arctic <i>Jun-Oh Min</i> <i>Korea Polar Research Institute</i>
PS-I10	Determination of the Production Rate of Mycosporine-Like Amino Acids Through Carbon Stable Isotope Analysis in Arctic Melt Ponds <i>Sun-Yong Ha</i> <i>Korea Polar Research Institute</i>
PS-I11	Numerical Study On The Arctic Sea Ice Variation Using An Ice-Ocean Coupled Model <i>Mi Ok Kwon</i> <i>Korea Maritime and Ocean University, Korea</i>
PS-I12	Temporal and Spatial Variation of Pacific-Origin Summer Water in the Chukchi Borderland, Arctic Ocean <i>T.W. Kim</i> <i>Korea Polar Research Institute</i>
PS-I13	Regional Productivity of Phytoplankton in the Northeast Chukchi Sea and Western Canada Basin During Early Summer in 2010 <i>Mi Sun Yun</i> <i>Pusan National University, Korea</i>
PS-I14	Macromolecular Productivity of Phytoplankton in the Amundsen Sea <i>HuiTae Joo</i> <i>Pusan National University, Korea</i>
PS-I15	Macromolecular Compositions of Phytoplankton in the Arctic Ocean in 2012 <i>Jae Joong Kang</i> <i>Pusan National University, Korea</i>
PS-I16	Lipid Concentration of Phytoplankton in the Northern Chukchi Sea, Arctic <i>Su Min Kim</i> <i>Pusan National University, Korea</i>
PS-I17	Study on Recent International Trend in Bipolar Oceans and Korea's Future Policy <i>Su jin Park</i> <i>Korea Maritime Institute, Korea</i>
PS-I18	Comparative Response of Arctic and Temperate Microalgae to Temperature Elevation <i>Sreejith Kottuparambil</i> <i>Incheon National University, Korea</i>
PS-I19	Biochemical Compositons of Particulate Organic Matter in the Northern Chukchi Sea, 2011 <i>Bo Kyung Kim</i> <i>Pusan National University, Korea</i>

PERMAFROST – ATMOSPHERE INTERACTIONS (PS-PXX)

PS-P01	Greenhouse Gas Flux Measurement Network of KOPRI at Circum-Polar Permafrost Sites <i>Jaeill Yoo</i> <i>Korea Polar Research Institute</i>
PS-P02	Measurements of Environmental Factors in Polar Regions Based on a Ubiquitous Sensor Network <i>Namyi Chae</i> <i>Yonsei University, Korea</i>
PS-P03	Carbon Dioxide Exchange over the Arctic Tundra in Council, Alaska: Controlling Factors and Contribution of Vegetation to Carbon Cycle <i>Namyi Chae</i> <i>Yonsei University, Korea</i>
PS-P04	Geochemical Analysis of Alaskan Permafrost Soil: Defining Gas Permeable Layer and Quantifying Gas Transport <i>Eunji Byun</i> <i>Seoul National University, Korea</i>

ARCTIC TERRESTRIAL ECOSYSTEMS (PS-TXX)

PS-T01	Temperature and Precipitation Manipulation Experiment in Cambridge Bay, Canadian High Arctic <i>Hyeyoung Kwon</i> <i>Korea Polar Research Institute</i>
PS-T02	Geographical Analysis of Microbial Activity in Arctic Soils <i>Inyoung Jang</i> <i>Yonsei University, Korea</i>
PS-T03	Comparisons of Metabolic Profiles of <i>Dryas Integrifolia</i> in Relation with Soil Microbial Community Changes from an Open Top Chamber Experiment in Cambridge Bay, Canada <i>Dongwoo Yang</i> <i>Ajou University, Korea</i>
PS-T04	Spatial Distribution of Bacterial Community Structure in Tundra Soil, Alaska <i>Hye Min Kim</i> <i>Korea Polar Research Institute</i>
PS-T05	Changes in Community Structure and Degradative Capacity of Soil Humic Substances-Degrading Bacteria from Cold Environments <i>Ha Ju Park</i> <i>Korea Polar Research Institute</i>
PS-T06	Effects of Svalbard Reindeer (<i>Rangifer Tarandus Platyrhynchus</i>) Grazing on GC-MS Metabolic Profiles of Dwarf Willow (<i>Salix Polaris</i>) Leaves in an Arctic Region <i>Donguk Han</i> <i>Seoul National University, Korea</i>
PS-T07	Turnover Time of Soil Organic Carbon in Permafrost Using Radiocarbon and Their Application for Determining Long and Short Terms Carbon Balances: Case Study in Alaskan Tundra and Boreal Forest <i>Miyuki Kondo</i> <i>National Institute for Environmental Studies, Japan</i>
PS-T08	Effects of Climate Manipulations on Soil Organic Matter under <i>Cassiope Tetragona</i> in Zackenberg, Greenland <i>Ji Young Jung</i> <i>Korea Polar Research Institute</i>

ARCTIC PALEOCEANOGRAPHY: LESSON FROM THE PAST (PS-LXX)

PS-L01	Sedimentary Facies Analysis of Late Pleistocene Core Sediments Recovered from the Chukchi Sea, the Western Arctic Ocean <i>Young-Jin Joe</i> <i>Jeju National University, Korea</i>
PS-L02	Paleoceanographic Records in the Chukchi Plateau, Western Arctic Ocean <i>Boo-Keun Khim</i> <i>Pusan National University, Korea</i>
PS-L03	A High Precision Gas Extraction System for Measurement of Atmospheric Methane and Total Air Content in Polar Ice Core <i>Jiwoong Yang</i> <i>Seoul National University, Korea</i>
PS-L04	Vegetation Changes in the Western Arctic During the Holocene: Preliminary Results from Pollen and Spore Records from the Shelf Sediments in the Chukchi Sea <i>So-Young Kim</i> <i>Korea Polar Research Institute</i>
PS-L05	Sedimentary Organic Matter Variations in the Chukchi Borderland over the Last 155 Kyr <i>Masao Uchida</i> <i>National Institute for Environmental Studies, Japan</i>
PS-L06	Multibeam Bathymetric and Sediment Profiler Evidences for Pockmarks and Ice Grounding Scours on the Chukchi <i>Masao Uchida</i> <i>National Institute for Environmental Studies, Japan</i>
PS-L07	Terrestrial N-Alkanes Signatures in Sediment of the North Atlantic ODP Site 980: Paleoclimatological Implications <i>Sangmin Hyun</i> <i>Korea Institute of Ocean Science and Technology</i>
PS-L08	Neogene Biostratigraphy and Paleoenvironment across the Fram Strait Gateway - Reappraisal for the application of dinocysts in Arctic deep time reconstruction - <i>Michael Shreck</i> <i>Korea Polar Research Institute</i>

SIDE MEETINGS

KOPRI – OUC JOINT WORKSHOP

- Date & Time: 10:00-16:00, 15 October, 2013
- Meeting place: International Meeting Room
- Contact: Dr. Hyoung Chul Shin (hcshin@kopri.re.kr)

PLANNING MEETING FOR COLLABORATIVE OBSERVATIONAL STUDY IN THE SEASONAL ICE ZONE NEAR SVALBARD

- Date & Time: 14:00-18:30, 15 October, 2013
- Meeting place: Seminar Room
- Contact: Dr. Baek-Min Kim (bmkim@kopri.e.kr)

ARCTIC TERRESTRIAL ECOSYSTEM GROUP MEETING

- Date & Time: 15:30-18:00, 17 October, 2013
- Meeting place: International Meeting Room
- Contact: Dr. Yoo Kyung Lee (yklee@kopri.re.kr)

PERMAFROST GROUP MEETING

- Date & Time: 09:00-18:30, 18 October, 2013
- Meeting place: Seminar Room
- Contact: Dr. Baek-Min Kim (bmkim@kopri.e.kr)

PACIFIC ARCTIC GROUP (PAG) MEETING

- Date & Time: 09:00-18:30, 18 October, 2013
- Meeting place: International Meeting Room
- Contact: Sung-Ho Kang (shkang@kopri.re.kr)

TRANSPORT INFORMATION

BETWEEN INCHEON INT'L AIRPORT AND SONGDO PARK HOTEL

If you will stay at Songdo Park Hotel, you can reach the hotel by KAL Limousine Bus.

Further information is available at following website:

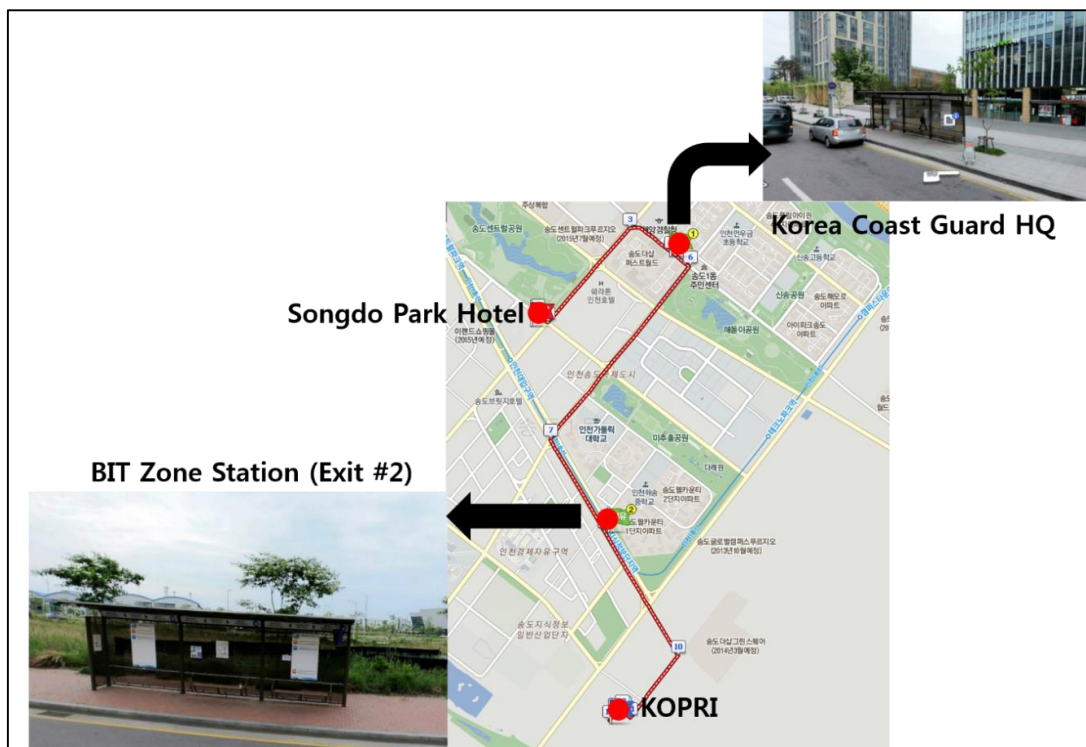
http://symposium.kopri.re.kr/docs/Trans_info_Airport-SongParkHotel.pdf

BETWEEN KOPRI AND SONGDO PARK HOTEL

Shuttle Bus between KOPRI and Songdo Park Hotel will be provided on 16-17 October. Bus will stop at the middle in BIT Zone Station (Incheon Subway). You can find shuttle time table below;

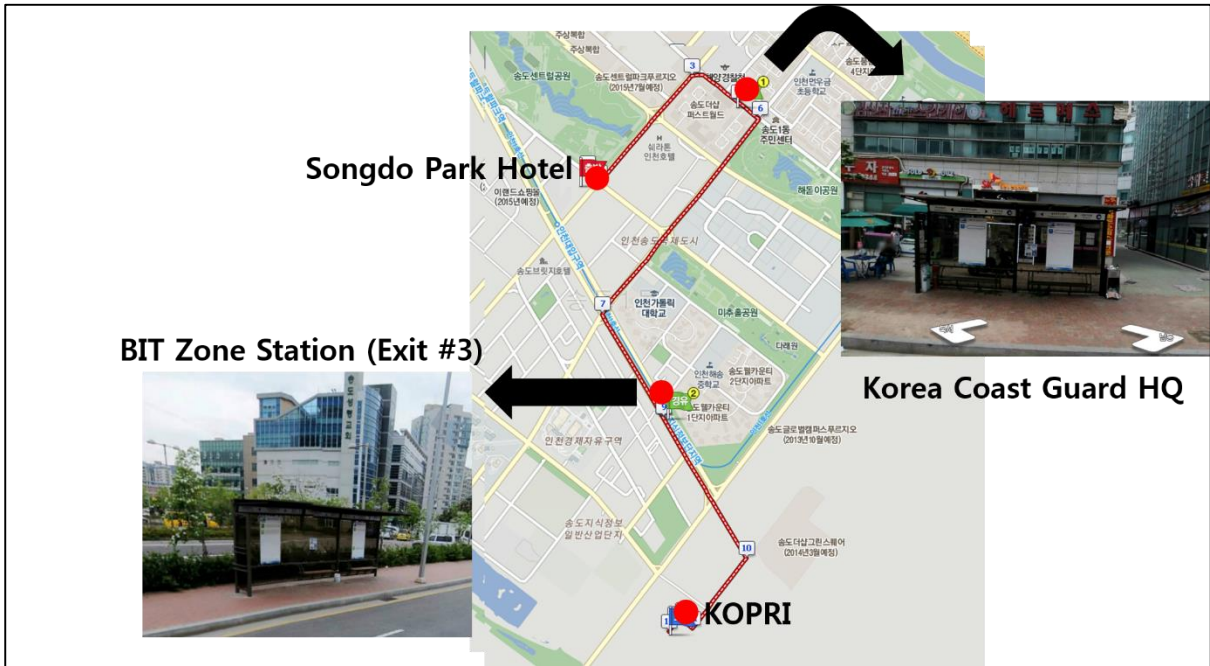
From Songdo Park Hotel to KOPRI

	Songdo Park Hotel	Korea Coast Guard HQ	BIT Zone Station (Exit #2)	KOPRI
1	08:30	-	08:40	08:50
2	09:10	-	09:20	09:30
3	12:40	12:45	12:50	12:55
4	13:15	13:20	13:25	13:30
5	15:30	-	15:40	15:45
6	18:00	-	18:10	18:20
7	18:45	-	18:55	19:00



From KOPRI to Songdo Park Hotel

	KOPRI	BIT Zone Station (Exit #3)	Korea Coast Guard HQ	Songdo Park Hotel
1	11:45	11:50	11:55	12:00
2	12:20	12:25	12:30	12:35
3	15:10	15:15	-	15:25
4	17:40	17:45	-	17:55
5	18:25	18:30	-	18:40



PARTICIPANT LIST

No	First Name	Last Name	Country	Affiliation
1	Sangkyu	Park	Korea	Ajou University
2	Dongwoo	Yang	Korea	Ajou University
3	Aleksey	Ostrovskiy	Russia	Alliance Group LLC
4	Frank	Niessene	Germany	AWI
5	Daoyi	Gong	China	Beijing Normal University
6	YangSoo	Cho	Korea	Beta Analytic Inc.
7	Kyungmin	Kim	Korea	Chonnam university
8	Mauro	Mazzola	Italy	CNR- ISAC
9	angelo pietro	Viola	italy	CNR- ISAC
10	Francesco	Canganella	italy	Embassy of Italy
11	Alexander	Bantov	Russia	Embassy of the Russian Federation
12	Yong-Sang	Choi	Korea	Ewha Womans University
13	Ha-Rim	Kim	Korea	Ewha Womans University
14	Youngsim	Hwang	Korea	GeoBook
15	Mojib	Latif	Germany	GEOMAR
16	Wonsun	Park	Germany	GEOMAR
17	Dukki	Han	Korea	Gwangju Institue of Sci. and Tech.
18	KyoungHoon	Shin	Korea	Hanyang
19	Adegoke.O	Badejo	Nigeria	Hanyang University
20	Sang-Wook	Yeh	Korea	Hanyang University
21	Philip	Wookey	UK	Heriot Watt University
22	Larry	Hinzman	USA	IARC
23	Trofim	Maximov	Russia	IBPC
24	Hoon	Choi	Korea	Incheon National University
25	Sreejith	Kottuparambil	Korea	Incheon National University
26	Haiyan	Chu	China	Institute of Soil Science
27	Young Jin	Joe	Korea	Jeju National University
28	Hyoung-Soo	Kim	Korea	Jungwon University
29	Kyung Sik	Woo	Korea	Kangwon National University
30	Sang-Yoon	Jun	Korea	KIAPS

31	Eun-Hyuk	Baek	Korea	KIOST
32	Sangmin	Hyun	Korea	KIOST
33	Yeon-Soo	Jang	Korea	KIOST
34	Jong-Seong	Kug	Korea	KIOST
35	Seung Kyeom	Lee	Korea	KIOST
36	Soonmi	Lee	Korea	KIOST
37	Kazuo	Ouchi	Japan	KIOST
38	Ho-Jeong	Shin	Korea	KIOST
39	Hye-Young	Son	Korea	KIOST
40	Young-Baek	Son	Korea	KIOST
41	Sung-Ho	Woo	Korea	KIOST
42	Chan-Su	Yang	Korea	KIOST
43	Dong-Won	Yi	Korea	KIOST
44	Bo Young	Yim	Korea	KIOST
45	Hai-Soo	Yoo	Korea	KIOST
46	Hitoshi	Shoji	Japan	Kitami Institute of Technology
47	Hyun-Suk	Kang	Korea	KMI
48	Su-Mi	Kang	Korea	KMI
49	Sung-Hwa	Park	Korea	KMI
50	Seonae	Kim	Korea	Kongju National University
51	Yeon-Hee	Kim	Korea	Kongju National University
52	Yung-Hun	Yang	Korea	Konkuk University
53	Soon-Keun	Chang	Korea	KOPRI
54	Moon Young	Choe	Korea	KOPRI
55	Han-Gu	Choi	Korea	KOPRI
56	Hyesun	Choi	Korea	KOPRI
57	Seonung Sunny	Choi	Korea	KOPRI
58	Taejin	Choi	Korea	KOPRI
59	Seolhee	Choi	Korea	KOPRI
60	Ho Kyung	Ha	Korea	KOPRI
61	Sun-Yong	Ha	Korea	KOPRI
62	Se Jong	Han	Korea	KOPRI
63	Jong Kuk	Hong	Korea	KOPRI

64	Soon do	Hur	Korea	KOPRI
65	Chung Yeon	Hwang	Korea	KOPRI
66	Geonhwa	Jee	Korea	KOPRI
67	Yong	Jiang	China	KOPRI
68	Dongmin	Jin	Korea	KOPRI
69	Young Keun	Jin	Korea	KOPRI
70	Hyoung Min	Joo	Korea	KOPRI
71	Ji Young	Jung	Korea	KOPRI
72	Pilsung	Kang	Korea	KOPRI
73	Sung-Ho	Kang	Korea	KOPRI
74	Dockyu	Kim	Korea	KOPRI
75	Hyemin	Kim	Korea	KOPRI
76	Hyerim	Kim	Korea	KOPRI
77	Hyun-cheol	Kim	Korea	KOPRI
78	Il-Chan	Kim	Korea	KOPRI
79	Jeong Han	Kim	Korea	KOPRI
80	Ji-Won	Kim	Korea	KOPRI
81	Joo-Hong	Kim	Korea	KOPRI
82	Minjeong	Kim	Korea	KOPRI
83	Seong-Joong	Kim	Korea	KOPRI
84	So-Young	Kim	Korea	KOPRI
85	Sung Jin	Kim	Korea	KOPRI
86	Tae Wan	Kim	Korea	KOPRI
87	Yea-Dong	Kim	Korea	KOPRI
88	BAEK MIN	Kim	Korea	KOPRI
89	Han-Woo	Kim	Korea	KOPRI
90	Hyeyoung	Kwon	Korea	KOPRI
91	Young Shin	Kwon	Korea	KOPRI
92	Heijin	Kyung	Korea	KOPRI
93	Bang Yong	Lee	Korea	KOPRI
94	Hyunjung	Lee	Korea	KOPRI
95	Yoo Kyung	Lee	Korea	KOPRI
96	Chi Won	Lim	Korea	KOPRI
97	Jun-Oh	Min	Korea	KOPRI

98	Joongho	Moon	Korea	KOPRI
99	Seung-Il	Nam	Korea	KOPRI
100	Sung Jin	Nam	Korea	KOPRI
101	jung	Ok	Korea	KOPRI
102	Byong-Kwon	Park	Korea	KOPRI
103	Haju	Park	Korea	KOPRI
104	Key Hong	Park	Korea	KOPRI
105	Ki Heon	Park	Korea	KOPRI
106	Sang-Jong	Park	Korea	KOPRI
107	Tae Siek	Rhee	Korea	KOPRI
108	Michael	Schreck	Germany	KOPRI
109	Hyunkyo	Seo	Korea	KOPRI
110	Hyunji	Seo	Korea	KOPRI
111	Taehyoun	Shim	Korea	KOPRI
112	Hyoung Chul	Shin	Korea	KOPRI
113	Jeong-ock	Son	Korea	KOPRI
114	Mi-Kyung	Sung	Korea	KOPRI
115	Ah-Ryeon	Yang	Korea	KOPRI
116	Jaeill	Yoo	Korea	KOPRI
117	Ju Eun	Yoo	Korea	KOPRI
118	Ho Il	Yoon	Korea	KOPRI
119	Young Jun	Yoon	Korea	KOPRI
120	Mi Sun	Yun	Korea	KOPRI
121	Sungchul	Hong	Korea	Korea Maritime and Ocean University
122	Young-sun	Kim	Korea	Korea Maritime and Ocean University
123	Mi Ok	Kwon	Korea	Korea Maritime and Ocean University
124	EunSun	Lee	Korea	Korea Maritime and Ocean University
125	Ho Jin	Lee	Korea	Korea Maritime and Ocean University

126	Minkyoung	Sung	Korea	Korea Maritime and Ocean University
127	Ah-ra	Kim	Korea	Kyunghee University
128	Eurico	D'Sa		Louisiana State University
129	Qigang	Wu	China	Nanjing University
130	David	Lawrence	USA	National Center for Atmospheric Research
131	Hanna	Lee	USA	National Center for Atmospheric Research
132	Masao	Uchida	Japan	National Institute for Environmental Studies
133	Jonghwa	Lee	Korea	NIMR
134	Mi-Lim	Ou	Korea	NIMR
135	Mats	Granskog	Norway	Norwegian Polar Institute
136	Stephen	Hudson	Norway	Norwegian Polar Institute
137	Yong	Cao	China	Ocean University of China
138	Fei	Huang	China	Ocean University of China
139	Guoliang	Jiang	China	Ocean University of China
140	Tao	Li	China	Ocean University of China
141	Gang	Liu	China	Ocean University of China
142	Yun	Liu	China	Ocean University of China
143	Min	Wang	China	Ocean University of China
144	Jinping	Zhao	China	Ocean University of China
145	Minkyoung	Kim	Korea	POSTECH
146	Seung-Ki	Min	Korea	POSTECH
147	Jai-Ho	Oh	Korea	Pukyong National University
148	Boo-Keun	Khim	Korea	Pusan National University
149	Sang Heon	Lee	Korea	Pusan National University
150	Jonathan	Adams		Seoul National University
151	Jeonghwan	Bang	Korea	Seoul National University
152	Eunji	Byun	Korea	Seoul National University
153	Donguk	Han	Korea	Seoul National University
154	JinWoo	Heo	Korea	Seoul National University
155	Sun-Kyong	Hur	Korea	Seoul National University

156	Euihyun	Jung	Korea	Seoul National University
157	Dorsaf	Kerfahi		Seoul National University
158	Sang-Woo	Kim	Korea	Seoul National University
159	Yoojin	Kim	Korea	Seoul National University
160	Euijae	Kim	Korea	Seoul National University
161	WooSung	Kim	Korea	Seoul National University
162	Eun Ju	Lee	Korea	Seoul National University
163	Hyohyemi	Lee	Korea	Seoul National university
164	Kyoo	Lee	Korea	Seoul National University
165	Yoon-Kyoung	Lee	Korea	Seoul National University
166	Junghyun	Lee	Korea	Seoul National University
167	Minjin	Lee	Korea	Seoul National University
168	HyoSeok	Park	Korea	Seoul National University
169	Jeong Soo	Park	Korea	Seoul National University
170	Jeong-Hyun	Park	Korea	Seoul National University
171	JungOk	Park	Korea	Seoul National University
172	Dharmesh	Singh		Seoul National University
173	Deokjoo	Son	Korea	Seoul National University
174	WooJin	Song		Seoul National University
175	Jiwoong	Yang	Korea	Seoul National University
176	Jae-Yul	Yun	Korea	Seoul National University
177	Itumeleng			Seoul National University
178	ChanJoong	Kim	Korea	Shinhan Tech
179	Deulre	Min	Korea	Shinhan Tech
180	Yun-Gon	Kim	Korea	Soongsil University
181	Hyesoon	Kang	Korea	Sungshin Women's University
182	Koji	Shimada	Japan	Tokyo University of MST
183	Yoo-jeong	Chae	Korea	Ulsan National Institute of Science and Technology
184	Daehyun	Kang	Korea	Ulsan National Institute of Science and Technology
185	Sarah	Kang	Korea	Ulsan National Institute of Science and Technology

186	jeongbin	Seo	Korea	Ulsan National Institute of Science and Technology
187	Yechul	Shin	Korea	Ulsan National Institute of Science and Technology
188	Jessica	Cherry	USA	University of Alaska Fairbanks
189	Andrew	Slater	USA	University of Colorado
190	Jacqueline	Grebmeier	USA	University of Maryland Center for Environmental Science
191	Hiroshi	Tanaka	Japan	University of Tsukuba
192	Soon-Il	An	Korea	Yonsei University
193	Namyi	Chae	Korea	Yonsei University
194	Chun-Sang	Hong	Korea	Yonsei University
195	Inyoung	Jang	Korea	Yonsei University
196	Jin Hyun	Kim	Korea	Yonsei University
197	Seung-Hoon	Lee	Korea	Yonsei University
198	JaeHong	Park	Korea	Yonsei University
199	Juyoung	Seo	Korea	Yonsei University

Contents of Table

PLENARY SPEECH	1
TOWARD BETTER UNDERSTANDING OF CLIMATE CHANGES IN THE ARCTIC <i>Mojib Latif</i>	3
BIOLOGICAL HOTSPOTS IN THE PACIFIC ARCTIC: PHYSICAL DRIVERS, ECOSYSTEM PRODUCTIVITY AND SENSITIVITY TO CLIMATE CHANGE <i>Jackie Grebmeier</i>	4
THE INTERACTION OF ATMOSPHERIC, HYDROLOGIC, GEOMORPHIC AND ECOSYSTEM PROCESSES ON THE ARCTIC COASTAL PLAIN <i>Larry Hinzman</i>	9
PROJECTIONS AND IMPLICATIONS OF 21ST CENTURY PERMAFROST THAW <i>David Lawrence</i>	10
REPEATED PLEISTOCENE GLACIATION OF THE EAST SIBERIAN CONTINENTAL MARGIN <i>Frank Niessen</i>	11
SESSION 1	13
RECENT ARCTIC CLIMATE CHANGE AND ITS IMPACT ON MID-LATITUDES <i>Seong-Joong Kim</i>	15
ASSOCIATION OF INDIAN OCEAN ITCZ VARIATIONS WITH THE ARCTIC OSCILLATION DURING BOREAL WINTER <i>Dao-Yi Gong</i>	16
STUDY ON THE INFLUENCE OF ARCTIC SEA-ICE LOSS ON THE TROPICAL PACIFIC SST VARIABILITY <i>Sang-Wook Yeh</i>	17
RELATIONSHIP BETWEEN THE ARCTIC OSCILLATION AND ARCTIC AMPLIFICATION <i>Hiroshi Tanaka</i>	18
ROLE OF BIOLOGICAL FEEDBACK IN ARCTIC AMPLIFICATION <i>Jong-Seong Kug</i>	21
INTERANNUAL VARIABILITY AND LONG-TERM CHANGES OF ATMOSPHERIC CIRCULATION OVER THE CHUKCHI AND BEAUFORT SEAS <i>Qigang Wu</i>	22
ARCTIC CLOUD MICROPHYSICAL CHARACTERISTICS FROM SPACE-BASED LIDAR CALIOP <i>Sang-Woo Kim</i>	23
CHANGING RELATION BETWEEN ARCTIC SEA ICE AND ASIAN DUST ASSOCIATED WITH GLOBAL WARMING <i>Jeong-Hyun Park</i>	27

SESSION 2.....	31
CARBON CONTRIBUTION OF SEA ICE FLOES IN THE ARCTIC OCEAN	
<i>Sang H Lee</i>	33
USING PELAGIC CILIATED MICROZOOPLANKTON COMMUNITIES AS AN INDICATOR FOR MONITORING ENVIRONMENTAL CONDITION UNDER IMPACT OF SUMMER SEA-ICE REDUCTION IN WESTERN ARCTIC OCEAN	
<i>Yong Jiang</i>	34
PROJECTION OF SHIP-ACCESSIBLE DAYS IN THE ARTIC SEA BASED ON IPCC CLIMATE CHANGE SCENARIOS	
<i>Jai-Ho Oh</i>	39
NO-REBOUND REDUCTION OF SEA ICE IN THE ARCTIC OCEAN: ROLE OF "INERTIA" EFFECT OF THE OCEAN	
<i>Koji Shimada</i>	43
OPTICAL PROPERTIES AROUND MENDELEEV RIDGERELATED TO THE PHYSICAL FEATURES OF WATER MASSES	
<i>Jinping Zhao</i>	44
SUBSEASONAL TO SEASONAL PREDICTION OF ARCTIC SEA-ICE CONCENTRATION BY SEASONAL EMPRICAL ORTHOGONAL FUNCTION (EOF) METHOD	
<i>Baek-Min Kim</i>	45
THE EFFECT OF POLEWARD MOISTURE FLUX ON ARCTIC WINTER SEA-ICE MELTING	
<i>Hyo-Seok Park</i>	46
ENERGY BUDGET OF FIRST-YEAR ARCTIC SEA ICE IN ADVANCED STAGES OF MELT	
<i>Stephan Hudson</i>	47
SOLAR ENERGY BUDGET OF FIRST-YEAR SEA ICE IN THE CENTRAL ARCTIC – AUTONOMOUS OBSERVATIONS FROM TWO SUMMER MELT SEASONS	
<i>M. A. Granskog</i>	50
SESSION 3.....	53
CLIMATE AND PERMAFROST CHANGE IN WESTERN ALASKA: 115 YEARS OF MEASUREMENTS ON THE SEWARD PENINSULA	
<i>Jessica Cherry</i>	55
GREENHOUSE GAS EXCHANGE AT AN ALASKA PERMAFROST REGION	
<i>Sang-Jong PARK</i>	56
THE PERMAFROST-DOMINATED ECOSYSTEMS IN A CHANGING CLIMATE	
<i>Trofim Maximov</i>	57
STRUCTURE OF THE ATMOSPHERIC BOUNDARY LAYER AT NY ALESUND: STATISTICS AND CASE STUDIES	
<i>Angelo P. Viola</i>	58

SIMULTANEOUS MEASUREMENTS OF CARBON EXCHANGE OVER THREE PERMAFROST SITES AT THE ARCTIC

Taejin Choi..... 63

SESSION 4..... 65

THE FUTURE TERRESTRIAL ARCTIC: PROJECTIONS FOR PERMAFROST AND SNOW

Andrew Slater..... 67

METHANE DYNAMICS UNDER MELTING EXCESS ICE AND PERMAFROST THAW IN THE COMMUNITY LAND MODEL 4.5

Hanna Lee 69

'DYNAMIC DISEQUILIBRIA' IN THE ARCTIC TERRESTRIAL REALM: LANDSCAPES AND ECOSYSTEMS IN TRANSITION

Philip A. Wookey..... 73

CIRCUM-POLAR VEGETATION AND ENVIRONMENTAL CONDITIONS

Eun Ju Lee 77

SOIL MICROBIAL COMMUNITIES IN ARCTIC AND OTHER COLD ECOSYSTEMS

Haiyan Chu 78

CLIMATE CHANGE AND SOIL ECOSYSTEM

Yoo Kyung Lee 79

SESSION 5..... 81

INTERPRETATION OF LIPIDS BIOMARKERS IN THE SEDIMENT OF WESTERN ARCTIC OCEAN: LAST 100YEARS RECORDS OF ORGANIC SOURCES, STORAGE AND SURFACE SEAWATER TEMPERATURE

Adegoke.O Badejo 83

STABLE ISOTOPE COMPOSITIONS OF AUTHIGENIC CARBONATES IN PELAGIC SEDIMENTS OF THE MENDELEEV RIDGE (ARCTIC OCEAN): THEIR IMPLICATIONS FOR PALEOCEANOGRAPHY

Kyung Sik Woo..... 84

PRELIMINARY RESULTS OF 3RD/4TH RV ARAON EXPEDITIONS (ARA04B/4C, 2013) INTO THE WESTERN ARCTIC OCEAN

Seung Il Nam 85

SESSION 6..... 87

SUMMER CDOM OPTICAL PROPERTIES IN THE WESTERN ARCTIC UNDER LOW SEA ICE CONDITIONS

Eurico D'Sa..... 89

CONCEPTUAL DESIGN OF A SATELLITE-BASED ICE NAVIGATION SUPPORTING SYSTEM FOR THE NORTHERN SEA ROUTE

Sun-Hwa Kim..... 94

**PRECONDITIONING EFFECT OF ABSORBED SHORTWAVE RADIATION ON
ARCTIC SEA-ICE VARIATION IN SUMMER**

Baek-Min Kim 98

POSTER SESSION 1	99
IMPACT OF ARCTIC SEA-ICE LOSS ON THE 2009/2010 EURASIAN COLD WINTER <i>Taehyoun Shim</i>	101
ARCTIC GREENING CAN CAUSE EARLIER SEASONALITY OF POLAR AMPLIFICATION <i>Yoo-jeong Chae</i>	102
THE ATMOSPHERIC MODE RELATED TO CLIMATE CHANGE IN ARCTIC REGION <i>Euihyun Jung.....</i>	103
ASYMMETRIC CHANGE OF GLOBAL RAINY SEASON PATTERN ON GLOBAL WARMING SCENARIOS <i>Yechul Shin</i>	105
THE RESPONSE OF THE ITCZ TO THERMAL FORCING WITH THE CHANGE OF PERTURBED LATITUDE <i>Jeongbin Seo</i>	106
THE HIGH HEAT FLUX EVENT IN THE BARENTS/KARA SEAS IN THE WINTER OF 2011/12 <i>Joo-Hong Kim</i>	107
CLIMATE IMPACT OF CHANGES IN EURASIAN ARCTIC VEGETATION ON THE EAST ASIAN SUMMER MONSOON <i>Ah-Ryeon Yang</i>	108
HOW MUCH WINTER STRATOSPHERIC POLAR-CAP WARMING IS EXPLAINED BY UPWARD-PROPAGATING PLANETARY WAVES IN CMIP5 MODELS?: PART 1. AN INDIRECT APPROACH USING A WAVE INTERFERENCE INDEX <i>Ji-Won Kim</i>	109
CHANGE IN WINTER SST OVER THE NORTH PACIFIC INDUCED BY SEA ICE LOSS IN BARENTS - KARA SEA <i>Hyerim Kim</i>	110
AGCM SIMULATIONS OF ATMOSPHERIC RESPONSES TO ARCTIC SEA ICE AND SST ANOMALY DURING BOREAL WINTER: IMPACTS OF CLOUD <i>Jung Ok</i>	111
PREDICTION OF THE ARCTIC OSCILLATION IN BOREAL WINTER BY SEASONAL FORECASTING SYSTEMS: STRATOSPHERIC CONNECTION <i>Daehyun Kang.....</i>	112
SHIP-BORNE LIDAR MEASUREMENTS OF AEROSOL VERTICAL DISTRIBUTION AND OPTICAL PROPERTIES IN ARCTIC AND ANTARCTIC REGION <i>Youngmin Noh</i>	116
IMPACT OF SEA ICE ON ARCTIC WARMING IN CMIP5 <i>Bo Young Yim</i>	117
TEMPERATURE VARIATION OVER EAST ASIA IN ASSOCIATION WITH STRATOSPHERIC POLAR VORTEX DURING THE BOREAL WINTER SEASON <i>Sung-Ho Woo.....</i>	120
INFLUENCES OF ARCTIC SEA ICE VARIABILITY ON THE SUMMER NORTH ATLANTIC OSCILLATION (SNAO) <i>Hans W Linderholm.....</i>	123

RECENT CHANGES IN WINTER ARCTIC CLOUD AND ITS RELATION TO ATMOSPHERIC STATES OVER THE SURROUNDING REGION	
<i>Sang-Yoon Jun</i>	124
UNDERSTANDING OF CIRCULATION CHARACTERISTICS IN DIFFERENT TYPES OF SUDDEN STRATOSPHERIC WARMING USING WACCM	
<i>Hyesun Choi</i>	125
INTERANNUAL VARIATION OF ARCTIC SEA ICE CONCENTRATION IN SUMMER IN RESPONSE TO PRECURSORY ABSORBED SHORTWAVE RADIATION	
<i>Yong-Sang Choi</i>	126
DETECTING HUMAN INFLUENCE ON ARCTIC SEA-ICE	
<i>Seung-Ki Min</i>	127
VARIATION OF ATMOSPHERIC CARBON MONOXIDE OVER THE ARCTIC OCEAN AND THE NORTHWESTERN PACIFIC DURING SUMMER 2012	
<i>Keyhong Park</i>	128
SPATIAL DISTRIBUTION OF TRACE GASES IN THE EAST SEA, NORTH PACIFIC, AND BERING SEA ALONG R/V ARAON'S CRUISE TRACK IN 2012	
<i>Tae Siek Rhee</i>	129
MARITIME BOUNDARY LAYER RESEARCH AT POLAR OCEANS BASED ON AARON	
<i>Sang Jong Park</i>	130
POSTER SESSION 2	131
DISTRIBUTION OF MICROBIAL POPULATIONS AND THEIR RELATIONSHIPS WITH ENVIRONMENTAL FACTORS IN THE PRYDZ BAY AND ITS ADJACENT SOUTHERN OCEAN, ANTARCTIC	
<i>Min Wang</i>	133
ASYMMETRY VARIABILITY BETWEEN THE ARCTIC AND ANTARCTIC SEA ICE	
<i>Fei Huang</i>	134
PYROSEQUENCING ASSESSMENT OF PROKARYOTIC COMMUNITY IN THE CHUKCHI SEA DURING SUMMER 2012	
<i>Chung Y. Hwang</i>	135
RAPID ROBOTIC TOXICITY BIOASSAY METHOD FOR BIOCIDES USING MALE GAMETOPHYTE OF POLAR BROWN ALGAE <i>SACCHARINA LATISSIMA</i>	
<i>Hoon Choi</i>	136
PHYTOPLANKTON COMMUNITIES IN THE WESTERN ARCTIC OCEAN DURING LATE SUMMER	
<i>Hyoung Min Joo</i>	137
UNDER-ICE MEASUREMENT OF SUSPENDED PARTICULATE MATTERS, CHUKCHI SEA	
<i>Hyun Jung Lee</i>	142
SINKING PARTICLE FLUX AND RADIOCARBON VALUES OF PARTICULATE ORGANIC CARBON IN THE DEEP CANADA BASIN	
<i>Minkyoung Kim</i>	143

POPULATION DYNAMICS OF BACTERIAL ASSEMBLAGES IN THE ARCTIC SEAFLOOR	
<i>Dukki Han</i>	144
STUDY ON THE DISTRIBUTION OF DISSOLVED ORGANIC CARBON (DOC) IN THE WESTERN ARCTIC	
<i>Jun-Oh Min</i>	145
DETERMINATION OF THE PRODUCTION RATE OF MYCOSPORINE-LIKE AMINO ACIDS THROUGH CARBON STABLE ISOTOPE ANALYSIS IN ARCTIC MELT PONDS	
<i>Sun-Yong Ha</i>	149
NUMERICAL STUDY ON THE ARCTIC SEA ICE VARIATION USING AN ICE-OCEAN COUPLED MODEL	
<i>Mi Ok Kwon</i>	153
TEMPORAL AND SPATIAL VARIATION OF PACIFIC-ORIGIN SUMMER WATER IN THE CHUKCHI BORDERLAND, ARCTIC OCEAN	
<i>T. W. Kim</i>	154
REGIONAL PRODUCTIVITY OF PHYTOPLANKTON IN THE NORTHEAST CHUKCHI SEA AND WESTERN CANADA BASIN DURING EARLY SUMMER IN 2010	
<i>Mi Sun Yun</i>	155
MACROMOLECULAR PRODUCTIVITY OF PHYTOPLANKTON IN THE AMUNDSEN SEA	
<i>HuiTae Joo</i>	156
MACROMOLECULAR COMPOSITIONS OF PHYTOPLANKTON IN THE ARCTIC OCEAN IN 2012	
<i>Jae Joong Kang</i>	157
LIPID CONCENTRATION OF PHYTOPLANKTON IN THE NORTHERN CHUKCHI SEA, ARCTIC	
<i>Su Min Kim</i>	158
STUDY ON RECENT INTERNATIONAL TREND IN BIPOLAR OCEANS AND KOREA'S FUTURE POLICY DIRECTION	
<i>Su jin Park</i>	159
COMPARATIVE RESPONSE OF ARCTIC AND TEMPERATE MICROALGAE TO TEMPERATURE ELEVATION	
<i>Sreejith Kottuparambil</i>	160
BIOCHEMICAL COMPOSITIONS OF PARTICULATE ORGANIC MATTER IN THE NORTHERN CHUKCHI SEA, 2011	
<i>Bo Kyung Kim</i>	161

POSTER SESSION 3163

GREENHOUSE GAS FLUX MEASUREMENT NETWORK OF KOPRI AT CIRCUM-POLAR PERMAFROST SITES

Jaeill Yoo 165

MEASUREMENTS OF ENVIRONMENTAL FACTORS IN POLAR REGIONS BASED ON A UBIQUITOUS SENSOR NETWORK

Namyi Chae 166

CARBON DIOXIDE EXCHANGE OVER THE ARCTIC TUNDRA IN COUNCIL, ALASKA: CONTROLLING FACTORS AND CONTRIBUTION OF VEGETATION TO CARBON CYCLE

Namyi Chae 167

GEOCHEMICAL ANALYSIS OF ALASKAN PERMAFROST SOIL: DEFINING GAS PERMEABLE LAYER AND QUANTIFYING GAS TRANSPORT

Eunji Byun 168

POSTER SESSION 4169

TEMPERATURE AND PRECIPITATION MANIPULATION EXPERIMENT IN CAMBRIDGE BAY, CANADIAN HIGH ARCTIC

Hyeyoung Kwon 171

GEOGRAPHICAL ANALYSIS OF MICROBIAL ACTIVITY IN ARCTIC SOILS

Inyoung Jang 172

COMPARISONS OF METABOLIC PROFILES OF *DRYAS INTEGRIFOLIA* IN RELATION WITH SOIL MICROBIAL COMMUNITY CHANGES FROM AN OPEN TOP CHAMBER EXPERIMENT IN CAMBRIDGE BAY, CANADA.

Dongwoo Yang 173

SPATIAL DISTRIBUTION OF BACTERIAL COMMUNITY STRUCTURE IN TUNDRA SOIL, ALASKA

Hye Min Kim 174

CHANGES IN COMMUNITY STRUCTURE AND DEGRADATIVE CAPACITY OF SOIL HUMIC SUBSTANCES-DEGRADING BACTERIA FROM COLD ENVIRONMENTS

Ha Ju Park 175

EFFECTS OF SVALBARD REINDEER (*RANGIFER TARANDUS PLATYRHYNCHUS*) GRAZING ON GAS CHROMATOGRAPHY-MASS SPECTROMETRY (GC-MS) METABOLIC PROFILES OF DWARF WILLOW (*SALIX POLARIS*) LEAVES IN AN ARCTIC REGION

Donguk Han 176

TURNOVER TIME OF SOIL ORGANIC CARBON IN PERMAFROST USING RADIOCARBON AND THEIR APPLICATION FOR DETERMINING LONG AND SHORT TERMS CARBON BALANCES: CASE STUDY IN ALASKAN TUNDRA AND BOREAL FOREST

Miyuki Kondo 177

**EFFECTS OF CLIMATE MANIPULATIONS ON SOIL ORGANIC MATTER UNDER
CASSIOPE TETRAGONA IN ZACKENBERG, GREENLAND**

Ji Young Jung 178

POSTER SESSION 5 181

**SEDIMENTARY FACIES ANALYSIS OF LATE PLEISTOCENE CORE SEDIMENTS
RECOVERED FROM THE CHUKCHI SEA, THE WESTERN ARCTIC OCEAN**

Young-Jin Joe 183

**PALEOCEANOGRAPHIC RECORDS IN THE CHUKCHI PLATEAU, WESTERN
ARCTIC OCEAN**

Boo-Keun Khim..... 185

**A HIGH PRECISION GAS EXTRACTION SYSTEM FOR MEASUREMENT OF
ATMOSPHERIC METHANE AND TOTAL AIR CONTENT IN POLAR ICE CORE**

Jiwoong Yang..... 186

**VEGETATION CHANGES IN THE WESTERN ARCTIC DURING THE HOLOCENE:
PRELIMINARY RESULTS FROM POLLEN AND SPORE RECORDS FROM THE
SHELF SEDIMENTS IN THE CHUKCHI SEA**

So-Young Kim 188

**SEDIMENTARY ORGANIC MATTER VARIATIONS IN THE CHUKCHI
BORDERLAND OVER THE LAST 155 KYR**

Masao Uchida 189

**MULTIBEAM BATHYMETRIC AND SEDIMENT PROFILER EVIDENCES FOR
POCKMARKS AND ICE GROUNDING SCOURS ON THE CHUKCHI BORDERLAND
AND BEAUFORT SEA**

Masao Uchida 190

**TERRESTRIAL N-ALKANES SIGNATURES IN SEDIMENT OF THE NORTH
ATLANTIC**

Sangmin Hyun 191

**NEOGENE BIOSTRATIGRAPHY AND PALAEOENVIRONMENT ACROSS THE FRAM
STRAIT GATEWAY**

Michael Shreck 192

PLENARY SPEECH

TOWARD BETTER UNDERSTANDING OF CLIMATE CHANGES IN THE ARCTIC

Mojib Latif

*Ocean Circulation and Climate Dynamics Division,
GEOMAR Helmholtz Centre for Ocean Research Kiel and University of Kiel
mlatif@geomar.de*

ABSTRACT

The Arctic featured the strongest surface warming over the globe during the recent decades, and the temperature increase was accompanied by a rapid decline in sea ice extent. However, little is known about Arctic sea ice change during the Early Twentieth Century Warming (ETCW) during 1920-1940, also a period of a strong surface warming, both globally and in the Arctic. We investigate the sensitivity of Arctic winter surface air temperature (SAT) to sea ice during 1875-2008 by means of simulations with an atmospheric general circulation model (AGCM) forced by estimates of the observed sea surface temperature (SST) and sea ice concentration. The Arctic warming trend since the 1960s is very well reproduced by the model. In contrast, ETCW in the Arctic is hardly captured. AGCM simulations with observed SST but fixed sea ice reveal a strong dependence of winter SAT on sea ice extent. In particular, the warming during the recent decades is strongly underestimated by the model, if the sea ice extent does not decline and varies only seasonally. This suggests by implication that a significant reduction of winter Arctic sea ice extent may have also accompanied the Early Twentieth Century Warming, exemplifying the importance of natural sea ice extent variability when assessing 20th century and early 21st century Arctic sea ice change.

Results from a set of simulations with coupled models further suggest that natural internal multidecadal climate variability in the North Atlantic-Arctic Sector could have considerably contributed to the Northern Hemisphere surface warming since 1980. Although covering only a few percent of the Earth's surface, the Arctic may have provided the largest share in this. It is hypothesized that a stronger Atlantic Meridional Overturning Circulation (AMOC) and the associated increase in northward heat transport enhanced the heat loss from the ocean to the atmosphere in the North Atlantic region, and especially in the North Atlantic portion of the Arctic due to anomalously strong sea ice melt.

In fact, compelling observational evidence is found that in the mid-latitude North Atlantic and at timescales longer than 10 years, surface turbulent heat fluxes are driven by the ocean and may force the atmosphere, while at shorter timescales the converse is true, thereby confirming the Bjerknes conjecture. This result, although strongest in boreal winter, is found in all seasons. In summary, climate models of varying complexity and surface observations suggest a prominent role of the North Atlantic-Arctic Sector in producing large-scale surface climate anomalies over the Northern Hemisphere on decadal timescales and longer.

BIOLOGICAL HOTSPOTS IN THE PACIFIC ARCTIC: PHYSICAL DRIVERS, ECOSYSTEM PRODUCTIVITY AND SENSITIVITY TO CLIMATE CHANGE

Jacqueline M. Grebmeier¹, Lee W. Cooper¹, Karen E. Frey², Sue E. Moore³, and Robert P. Pickart⁴

¹*University of Maryland Center for Environmental Science, Chesapeake Biological Laboratory, Solomons, Maryland 20688, USA; jgrebmei@umces.edu*

²*Graduate School of Geography, Clark University, Worcester, MA 01610, USA*

³*NOAA Fisheries, Office Science & Technology, Seattle, WA 98115, USA*

⁴*Department of Physical Oceanography MS 21, Woods Hole Oceanographic Institution, Woods Hole, MA 02543, USA*

ABSTRACT

Over the past decade the northern Bering and Chukchi seas in the Pacific Arctic region have experienced seasonal seawater warming, freshening and major reductions in seasonal sea ice cover. Seasonal sea ice duration and extent are critical factors driving biological processes and marine ecosystem structure. The seasonal ice zones directly influence sea ice algal biomass and productivity and also provide early stabilization of the water column following sea ice melt, which can lead to intense phytoplankton blooms. The timing and location of this primary production and associated grazing by zooplankton has a direct influence on the energy pathways connecting the water column to the underlying sediments. There are also indications of Arctic biological systems responding at different time and space scales to these environmental changes. Recent studies for example indicate that increasing seawater temperature can have a positive impact on zooplankton growth and grazing rates. These changes would have the potential to diminish export production of carbon that currently supports globally significant soft-bottom infaunal populations on the shallow shelves of many areas of the Pacific Arctic (citations in Grebmeier et al. 2012). Changes in the short food chains characteristic of Arctic continental shelf regions would have immediate cascading impacts on higher trophic organisms, including diving seabirds, seals, walrus, and whales.

Mature benthic infaunal communities respond to variable levels of export production, building up biomass over multiple years-to-decades and maintaining persistent community patches or “hotspots” that provide important prey to mobile epibenthic animals and upper trophic level animals, particularly marine mammals and diving seabirds. Benthic “hotspots” occur on the continental shelf in the northern Bering Sea between St. Lawrence Island and Bering Strait, in the southern Chukchi Sea, and in the northeast portion of the Chukchi Sea, including upper Barrow Canyon (Figure 1). Many of these biological features are annually persistent and seasonally consistent regions of high water column and benthic biomass. All of the continental shelf “hotspots” are directly tied to hydrographic processes that bring high nutrients onto the shelf and support high algal production, often where a reduction of current

speeds facilitate higher export production of particulate carbon to the benthos (Grebmeier et al. 2006a). In addition, cold, early season Pacific winter water temperatures limit zooplankton growth, thus minimizing the impact of the overall grazing capacity of zooplankton and resulting in high biomass benthic infaunal communities at the hotspot sites (Grebmeier et al. 2006a, 2009).

Satellite and field observations indicate the annual reoccurrence of high chlorophyll features at the benthic hotspot sites (Hill and Cota 2005, Lee et al. 2007), whereas annual shipboard sampling provides evidence of continued persistence of underlying non-motile, macroinfaunal organisms that benefit from the high carbon export to the underlying benthos at these sites (Grebmeier et al. 2006a,b, Grebmeier 2012). The benthic biomass hotspot sites support benthic feeding marine mammals, such as gray whales, walrus, and bearded seals (Moore et al. 2003, Jay et al. 2012, Moore et al. accepted), and in certain areas, diving seaducks (Lovvorn et al. 2009). By comparison, zooplankton hotspots are somewhat more ephemeral, but do indicate repeatable patterns of organic carbon transport. For example, sites with seasonal build up of water column biomass, such as the late spring-summer accumulations observed in the southern Chukchi Sea (Bluhm et al. 2007), water mass frontal zones, and shelf boundaries with wind- and current-induced concentrating mechanisms (e.g. upwelling at Barrow Canyon) and nearby shelf areas provide indicators of water-column or epibenthos biomass hotspots (Ashjian et al. 2010, Walkusz et al. 2012). Although we will focus on benthic biomass hotspots in this presentation, it is recognized that there are key locations for concentration of zooplankton used by pelagic-feeding, upper trophic species, including bowhead whales (feeding on copepods and euphausiids), belugas (feeding on forage fish, including arctic cod), and pelagic seabirds (feeding on copepods, small fish, and gelatinous zooplankton). Persistent advective sites, such as Barrow Canyon, which is located at the interface of Pacific-produced Bering Sea waters (winter and summer types) and upwelled Atlantic water, are important sites for pelagic-feeding upper trophic organisms (Moore et al. accepted). Understanding biological hotspots is important in evaluating the overall system as these sites track the status and change in physical forcing, sea ice retreat, and ecosystem response in a shallow water continental shelf system that is being stressed by both climate change and anthropogenic impacts (e.g., oil development, transportation) (see Wassmann et al. 2011).

Identifying and collecting key prey-predator biological data in the context of high priority physical and chemical measurements will allow for integration of these data into scientific community analyses and ecosystem modeling efforts. Some of the best-documented examples of biological response to physical forcing in the Pacific Arctic sector are prey-predator response to hydrographic shifts. For example, a reduction in sea ice provides access for migrating baleen whales to feed north of Bering Strait (Moore and Huntington 2008). Gray whales now feeding more prominently north of the Bering Strait are likely responding to declines in benthic amphipod populations in the historical northern Bering Sea feeding grounds (citations in Grebmeier et al. 2012). Another change is in dominant clam populations in the northern Bering Sea, which have declined in abundance and biomass, as have Spectacled Eiders that preferentially consume these clams as prey. Modeling by Lovvorn et al. (2009) indicates that these diving birds expend more energy resting in the water between feeding bouts than when standing on ice. Thus, both the shift to more open-water conditions and the observed clam population declines could be key factors creating energy stress for these diving seaducks. The recent observations of thousands of walrus coming ashore on both the US and Russia Chukchi coastlines are another indication of biological response to rapid sea ice retreat in the Chukchi Sea. In addition to the increased mortalities for young walrus on beaches in close proximity to much larger adults, all of these shore-based populations have increased energetic requirements to access offshore waters that have higher concentrations of benthic infaunal prey (Jay et al. 2012, citations in Grebmeier et al. 2012).

Data documenting the importance of these ecosystem "hotspots" provide a growing marine time-series from the northern Bering Sea to Barrow Canyon at the boundary of the Chukchi and Beaufort seas. Results from these studies show spatial changes in carbon production and export to the sediments as indicated by infaunal community composition and biomass, shifts in sediment grain size on a S-to-N latitudinal gradient, and range extensions for lower trophic levels and further northward migration of

higher trophic organisms, such as gray whales. There is also direct evidence of negative impacts on ice dependent species, such as walrus and polar bears. To more systematically track the broad biological response to sea ice retreat and associated environmental change, an international consortium of scientists are developing a coordinated Distributed Biological Observatory (DBO) that includes selected biological measurements at multiple trophic levels (Figure 2; Grebmeier et al. 2010). These measurements are being made simultaneously with hydrographic surveys and satellite observations. The DBO currently focuses on five regional biological "hotspot" locations along a latitudinal gradient. The spatially explicit DBO network is being organized through the Pacific Arctic Group (PAG), a consensus-driven, international collaboration sanctioned by the International Arctic Science Committee. This cooperative effort is based upon the assumption that in order to understand the ecosystem of the Pacific Arctic region, coordinated and international studies are needed. The PAG includes institute and individual representation from six countries (USA, Canada, Russia, Japan, the Republic of Korea, and the People's Republic of China). The framework facilitates regional science planning through partnerships that plan, coordinate, and collaborate on climate, structure and function of Arctic ecosystems, and contaminants. The DBO is a key examples of PAG activities that are improving scientific understanding of environmental change in the northern Bering and Chukchi Seas. For the past few years, the PAG has focused on collaborative, ship-based research in the northern Bering, Chukchi and Beaufort Seas and in the central Arctic Basins. Recently, the PAG developed a shared interest in studying physical variability and change and estimating the ecosystem response, including expanding the DBO-type observation system to the Beaufort Sea and Arctic Basin (Figure 2). Data sharing and publications from recent studies are ongoing. PAG is also developing plans for a coordinated sea ice/atmospheric sampling effort as well as continued synthesis activities, such as the Pacific Arctic region Springer synthesis volume, Deep-Sea Research II special issues, as well as other publications and products. Further information on time series changes and the DBO can be found at <http://www.arctic.noaa.gov/dbo> and further information on PAG activities can be found at: <http://pag.arcticportal.org>.

References

- Ashjian, C.J., Braund, S.R. Campbell, R.G., George, J.C. , Kruse, J., Maslowski, W., Moore, S.E., Nicolson, C.R., Okkonen, S.R., Sherr, B.R., Sherr, E.B., and Spitz, Y., 2010, Climate variability, oceanography, bowhead whale distribution and Inupiat subsistence whaling near Barrow, Alaska: Arctic, v. 63, p. 179-194.
- Bluhm, B.A., Coyle, K.O., Konar, B., and Highsmith, R., 2007, High gray whale relative abundances associated with an oceanographic front in the south-central Chukchi Sea: Deep Sea Research II, v. 54, p. 2919-2933.
- Grebmeier, J.M., Cooper, L.W., Feder, H.M., and Sirenko, B.I., 2006a, Ecosystem dynamics of the Pacific influenced Northern Bering and Chukchi Seas: Progress in Oceanography, v. 71, p. 331-361.
- Grebmeier, J.M., Overland, J.E., Moore, S.E., Farley, E.V., Carmack, E.C., Cooper, L.W., Frey, K.E., Helle J.H., McLaughlin, F.A., and L. McNutt, 2006b, A major ecosystem shift in the northern Bering Sea: Science, v. 311, p. 461-1464.
- Grebmeier, J.M., Harvey, H.R., and Stockwell, D.A., 2009, The Western Arctic Shelf-Basin Interactions (SBI) project, volume II: An overview: Deep-Sea Research II, v. 56, p. 1137-1143.
- Grebmeier, J.M, Moore, S.E., Overland, J.E., Frey, K.E., and Gradinger, R., 2010, Biological response to recent Pacific Arctic sea Ice retreats: Eos, Transactions of the American Geophysical Union, v. 91, p. 161-162.
- Grebmeier, J.M., 2012, Shifting patterns of life in the Pacific Arctic and Sub-Arctic seas: Annual Review of Marine Science, v. 4, p. 63-78.
- Hill, V.J., and Cota. G.F., 2005, Spatial patterns of primary production in the Chukchi Sea in the spring and summer of 2002: Deep-Sea Research II, v. 52, p. 3344–3354.
- Jay, C.V., Fischbach, A.S., and Kochnev, A.A., 2012, Walrus areas of use in the Chukchi Sea during sparse sea ice cover: Marine Ecology Progress Series, v. 468, p. 1-13.

- Lee, S.H., Whittledge, T., and Kang, S.-H., 2007, Recent carbon and nitrogen uptake rates of phytoplankton in Bering Strait and the Chukchi Sea: *Continental Shelf Research* v. 27, p. 2231-2249.
- Lovvorn, J.R., Grebmeier, J.M., Cooper, L.W., Bump, J.K., and Richman, S.E., 2009, Modeling marine protected areas for threatened eiders in a climatically changing Bering Sea: *Ecological Applications*, v. 19, p. 1596-1613.
- Moore, S.E., Grebmeier, J.M., and Davis, J.R., 2003, Gray whale distribution relative to forage habitat in the northern Bering Sea: current conditions and retrospective summary: *Canadian Journal of Zoology*, v. 81, p. 734-742.
- Moore, S.E., and Huntington, H.P., 2008, Arctic marine mammals and climate change: impacts and resilience: *Ecological Applications* 18(2) Supplement: S157-S186.
- Moore, S.E., Logerwell, E., Eisner, L., Farley, E., Harwood, L., Kuletz, K., Lovvorn, J., Murphy, J., and Quakenbush, L., Marine fishes, birds and mammals as sentinels of ecosystem variability and reorganization in the Pacific Arctic Region, in Grebmeier, J.M., and Maslowski, W., eds, *The Pacific Arctic region: Ecosystem status and trends in a rapidly changing environment*: Springer: Dordrecht (accepted).
- Walkusz, W., Williams, W.J., Harwood, L., Moore, S.E., Stewart, B., and Kwasniewski, S., 2012, Composition, biomass and energetic content of biota in the vicinity of feeding bowhead whales (*Balaena mysticetus*) in Cape Bathurst upwelling region (south eastern Beaufort sea): *Deep-Sea Research I*, v. 69, p. 25-35.
- Wassmann, P., Duarte, C.M., Agusti, S., and Sejr, M.K., 2011, Footprints of climate change in the Arctic marine ecosystem: *Global Change Biology*, v. 17, p. 1235-1249.

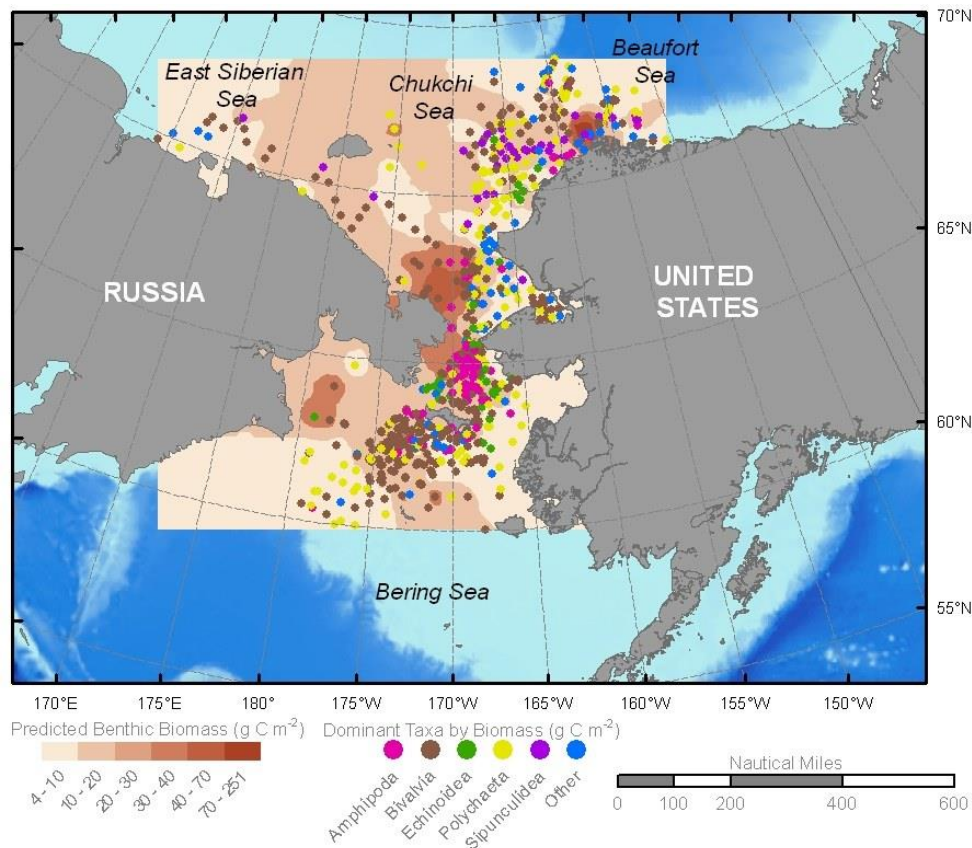


Figure 1. Macroinfaunal benthic hotspots by biomass, along with dominant infaunal type, in the Pacific Arctic region (data updated and modified from Grebmeier 2012).

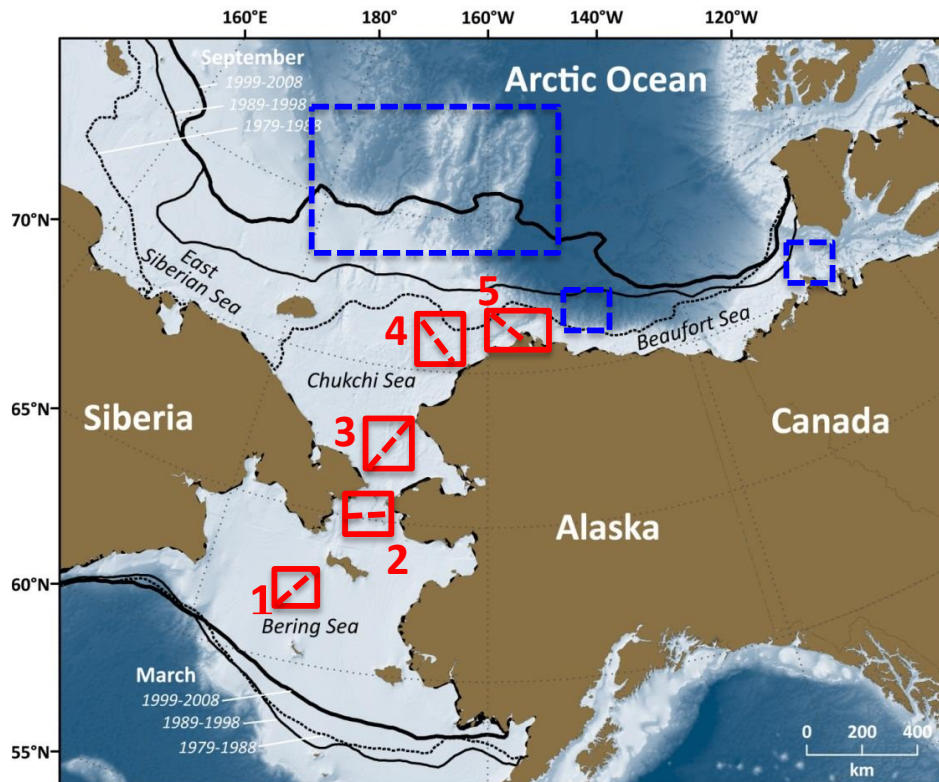


Figure 2. Location of current (red) and proposed future (blue) Distributed Biological Observatory (DBO) target sampling areas.

THE INTERACTION OF ATMOSPHERIC, HYDROLOGIC, GEOMORPHIC AND ECOSYSTEM PROCESSES ON THE ARCTIC COASTAL PLAIN

Larry Hinzman

*International Arctic Research Center
University of Alaska Fairbanks
lhinzman@iarc.uaf.edu*

ABSTRACT

The complex interplay of physical, chemical, and biological processes interact to such a degree that it is not possible to understand future trajectories without developing more fully holistic perspectives of the complete system. The components of the Arctic are inter-related through a complex network of linkages, feedbacks and multi-dependent interactions. Theoretically a change in one variable in a part of the system can initiate a cascade of effects throughout the system, and these connections need to be understood and quantified to achieve a level of predictability. In arctic regions, the interactions of surface mass and energy fluxes are complicated by the presence of permafrost and the important role of microtopography; these both affect and are mediated by dynamic atmospheric, geomorphological and ecosystem processes such as non uniform snow distribution, lake formation and drainage, wetland succession, thermokarst and erosion, and hydrological dynamics highly variable on different temporal and spatial scales.

Spatially distributed model simulations are being conducted across a range of scales. Preliminary results indicate macro-topographic gradients greatly impact the importance of lateral versus vertical fluxes. Micro-topographic differences affect the small spatial scale differences in snow distribution, soil moisture and runoff rates, but have less impact upon flux direction. Permafrost in arctic regions exerts a significant influence on soil moisture through controls on snow cover, vegetation and drainage and through differential degradation due to inhomogeneous ground ice distribution. In relatively flat areas where the frozen layer is near the surface, the soil moisture contents are usually quite high. These areas have relatively high evapotranspiration and sensible heat transfer, but quite low conductive heat transfers due to the insulative properties of thick organic soils. As in more temperate regions, watershed morphology exerts strong controls on hydrological processes; however unique to arctic watersheds are complications arising from the short-term active layer dynamics and longer-term permafrost dynamics. In permafrost lowlands, degradation of near-surface regularly and irregularly distributed ground ice may substantially enhance microtopographic gradients impacting hydrologic flow. In addition, hydrologic flow patterns are seasonally highly variable due to strongly varying water supply and connectivity throughout the thaw season.

PROJECTIONS AND IMPLICATIONS OF 21ST CENTURY PERMAFROST THAW

David Lawrence

National Center for Atmospheric Research, USA

ABSTRACT

The Arctic is currently experiencing strong warming and associated environmental change. Threshold and non-linear responses associated with phase change between ice and water leave the terrestrial Arctic particularly susceptible to swift and disruptive transitions. The projected warmer and wetter climate in the northern high-latitudes has the potential to amplify and accelerate the environmental changes that are already being observed. A large-scale thawing of permafrost could initiate a diverse array of changes to Arctic vegetation, hydrology, and carbon cycling (e.g., shifts in lake and wetland distribution, shifts in vegetation community composition, decomposition of previously frozen organic matter and release as CO₂ or CH₄) that can feedback onto the global climate system both positively and negatively. The magnitude of these potential terrestrial Arctic feedbacks remains difficult to quantify and the extent to which they might interact with each other is even less well-understood.

The tools with which we can assess the strength of these anticipated Arctic terrestrial feedbacks have been imperfect, partly because most land models that are used in global Earth system models were not specifically developed to address the permafrost thaw and associated feedbacks problem. Here, we will describe targeted improvements in the representation of permafrost in the Community Land Model (CLM) including improvements in soil hydrology and thermodynamics, snow, and biogeochemical cycling. In particular, we will focus on the impact of an improved representation of cold region hydrology, which in CLM4 was insufficiently realistic to enable a holistic study of the Arctic permafrost carbon problem.

We will show projections of 21st century permafrost thaw with the latest version of CESM/CLM and also projections from other global earth system models. We will then synthesize our current understanding, based in part on the improved CLM, of the integrated impact of projected permafrost thaw on the global climate system. Finally, scientific priorities from the observational, experimental, and modeling perspectives that are needed to better understand the permafrost carbon feedback will be outlined.

REPEATED PLEISTOCENE GLACIATION OF THE EAST SIBERIAN CONTINENTAL MARGIN

Niessen, F

*Alfred Wegener Institute, Helmholtz Centre for Polar and Marine Research,
Bremerhaven, Germany
frank.niessen@awi.de*

ABSTRACT

Based on swath bathymetry, sediment echosounding, seismic profiling and sediment coring we present results of the RV „Polarstern“ cruise ARK-XIII/3 (2008) and RV "Araon" cruise ARA02B (2012), which investigated an area between the Chukchi Borderland and the East Siberian Sea between 165°W and 170°E. At the southern end of the Mendeleev Ridge, close to the Chukchi and East Siberian shelves, evidence is found for the existence of Pleistocene ice sheets/ice shelves, which have grounded several times in up to 1200 m present water depth. We found mega-scale glacial lineations associated with deposition of glaciogenic wedges and debris-flow deposits indicative of sub-glacial erosion and deposition close to the former grounding lines. Glacially lineated areas are associated with large-scale erosion, accentuated by a conspicuous truncation of pre-glacial strata typically capped with mostly thin layers of diamicton draped by pelagic sediments. So far there is no robust age model for these glaciations. In the area, where glaciogenic bedforms are found, sedimentation rates of the final hemipelagic drape suggest that glaciations on the East Siberian continental margin predate the Last Glacial Maximum (LGM). According to our results, ice sheets of more than one km in thickness continued onto, and likely centered over, the East Siberian Shelf. They were possibly linked to previously suggested ice sheets on the Chukchi Borderland and the New Siberian Islands. We propose that the ice sheets extended northward as thick ice shelves, which grounded on the Mendeleev Ridge to an area up to 78°N. These results have important implications for the former distribution of thick ice masses in the Arctic Ocean during the Pleistocene. They are relevant for global sea-level variations, albedo, ocean-atmosphere heat exchange, freshwater export from the Arctic Ocean at glacial terminations and the formation of submarine permafrost. The existence of km-thick Pleistocene ice sheets in the western Arctic Ocean during glacial times predating that of the LGM also implies significantly different atmospheric circulation patterns, in particular availability and distribution of moisture during pre-LGM glaciations.

SESSION 1

ATMOSPHERE

RECENT ARCTIC CLIMATE CHANGE AND ITS IMPACT ON MID-LATITUDES

*Seong-Joong Kim, Hyesun Choi, Baek-Min Kim, Sang-Jong Park,
Taehyoun Shim, Joo-Hong Kim*

*Division of Polar Climate Research,
Korea Polar Research Institute
seongkim@kopri.re.kr*

ABSTRACT

This study investigates the climate change over the Arctic and its linkage to midlatitude using the ERA-Interim reanalysis data from European Center for Medium-range Weather Forecast (ECMWF). Since 1979, the substantial surface warming has occurred over the Arctic with the biggest warming in winter offshore of the Kara-Barents Sea, associated with the increase in turbulent heat fluxes from the marginal ice zone. In contrast to the marked warming over the Arctic Ocean in winter, a substantial cooling appears over the entire Eurasia, linked to the reduction of sea ice over the Arctic during the freezing season (September-March). However, in summer, very little change is observed in surface air-temperature over the Arctic because the increased radiative heat is used to melt the sea ice and the turbulent heat gain from the ocean is relatively small. Overall, the heat stored in the upper ocean mixed layer in summer by the opening of the Arctic Ocean associated with the increase in anthropogenic greenhouse gas seems to releases back to atmosphere in autumn through next spring as turbulent heat fluxes and warms up the Arctic and the reduced sea ice leads to the surface cooling over Siberia and east Asia in winter.

ASSOCIATION OF INDIAN OCEAN ITCZ VARIATIONS WITH THE ARCTIC OSCILLATION DURING BOREAL WINTER

Dao-Yi GONG¹, Yong-Qi GAO^{2,3}, Miao HU¹, and Dong GUO²

¹ *State Key Laboratory of Earth Surface Processes and Resource Ecology, Beijing Normal University, Beijing 100875, China*

² *Nansen-Zhu International Research Center, Institute of Atmospheric Physics, Chinese Academy of Sciences, Beijing 100029, China*

³ *Nansen Environmental and Remote Sensing Center/Bjerknes Center for Climate Research, Bergen, Norway*
gdy@bnu.edu.cn

ABSTRACT

In this study, the authors analyzed the associations between the Arctic Oscillation (AO) and the tropical Indian Ocean (TIO) intertropical convergence zone (ITCZ) in boreal winter for the period 1979–2009. A statistically significant AO-TIO ITCZ linkage was found. The ITCZ vertical air motion is significantly associated with the AO, with upward (downward) air motion corresponding to the positive (negative) AO phase. The Arabian Sea anticyclone plays a crucial role in linking the AO and the TIO ITCZ. The Arabian Sea vorticity is strongly linked to high-latitude disturbances in conjunction with jet stream waveguide effects of disturbance trapping and energy dispersion. During positive (negative) AO years, the Arabian Sea anticyclone tends to be stronger (weaker). The mean vorticity over the Arabian Sea, averaged from 850 hPa to 200 hPa, has a significant negative correlation with AO ($r = -0.63$). The anomalous anticyclone over the Arabian Sea brings stronger northeastern winds, which enhance the ITCZ after crossing the equator and result in greater-than-normal precipitation and minimum outgoing long-wave radiation.

STUDY ON THE INFLUENCE OF ARCTIC SEA-ICE LOSS ON THE TROPICAL PACIFIC SST VARIABILITY

Sang-Wook Yeh, Baek-Min Kim, and Herim Kim

*Department of Marine Sciences and Convergent Technology Hanyang University and
Korea Polar Research Institute
swyeh@hanyang.ac.kr*

ABSTRACT

In this study, we examine how the changes in the sea-ice loss over the polar region influence the sea surface temperature (SST) variability in the tropical Pacific. By conducting idealized experiments based on the CAM3, it is found that the atmospheric circulation due to sea-ice melting over the Barents/Kara Sea is able to modify the Aleutian low pressure system over the North Pacific via Rossby wave propagations. We speculate that these changes are associated with the changes in the Aleutian low pressure on the low frequency timescales, which is associated with the variability of North Pacific Oscillation (NPO). Our further analysis indicates that the NPO plays a role to modify the SST variability in the tropical Pacific through air-sea interactions in the subtropical Oceans.

RELATIONSHIP BETWEEN THE ARCTIC OSCILLATION AND ARCTIC AMPLIFICATION

Hiroshi L. Tanaka

*Center for Computational Sciences,
University of Tsukuba
tanaka@ccs.tsukuba.ac.jp*

ABSTRACT

1. Introduction

It is well known that the global warming occurs most prominently in the Arctic. When the global warming is 4 deg. C, the Arctic warms 12 deg. C; three times of the mean. This characteristic warming pattern is called Arctic amplification. When global cooling occurs, the cooling is also amplified in the Arctic. When the warming in both poles are concerned, we call it polar amplification, although the Arctic warms more than Antarctic.

The Arctic amplification (referred to as AA) becomes evident after the year 2000, but the warming pattern was characterized by the Arctic Oscillation (hereafter called AO) during 1970 to 1990. When the cause of the AA is argued, the ice-albedo feedback is apparently most responsible. Yet, other factors, such as meridional heat transport by the atmosphere and ocean, intensified long-wave radiation from clouds and vapor, from sea ice and open water, and increased black carbon aerosols are all responsible for the AA. These factors are mutually interacting to cause the AA. According to a model experiment, the AA occurs even when the ice-albedo feedback is fixed. In that case the increased meridional heat transport causes the AA. Therefore, we can understand that the AA is essentially produced by the general circulation of the atmosphere and ocean, and the ice-albedo feedback acts to enhance the AA.

The AA occurs mostly in fall and winter at the lower troposphere. From this observational fact, it is inferred that the short wave radiation is unimportant in a direct sense. In summer to fall when sea ice melts, the solar energy is accumulated in the open water, and that energy will come out to the atmosphere in winter through the lead or polynia. It is realized that the AA occurs at the low level in the atmospheric boundary layer, and it is reduced at high land such as Greenland. In addition to the warming at the lower troposphere we can find another warming in the upper troposphere. This part of warming may be caused by the meridional heat transport by the internal variability of the atmosphere.

2. Model of the Arctic Amplification

In order to study the mechanism of the AA, a simple two-box energy balance model is proposed by Alexeev and Jackson (2012). The entire atmosphere and oceanic mixed layer, separated by higher and lower latitudes at 30 N are considered as the two control volumes for the energy balance model. The annual mean temperature T_1 and T_2 for the lower and higher latitudes averaged over the control volumes are governed by short wave radiation, long wave radiation, and

meridional heat flux across the boundary, in addition of the anthropogenic radiative forcing (namely CO₂). The variation of the sea-ice concentration is included in the high latitude box. When AA occurs, the meridional sensible heat flux decreases by the reduced temperature difference. However, the meridional latent heat flux increases by the warming. As a result, the total meridional heat flux in the model changes little by the global warming as observed in a real atmosphere.

3. Results of the AA and AO

Using this simple energy balance model, we first demonstrate the local equilibrium temperature by eliminating all factors but the radiation. It is known that the temperature difference between the pole and equator would be 100 K for such a local radiative equilibrium. According to the result of the model, the temperature difference $T_1 - T_2$ becomes 60 K. This strong baroclinicity causes the amplification of Hadley circulation in the tropics and baroclinic instability waves in the extra-tropics, initiating the meridional heat flux to relax $T_1 - T_2$ to 20 K. By this heat flux, temperature at the high latitudes becomes well above the radiative equilibrium temperature that causes the enhanced radiative cooling in the Arctic. After introducing the sea ice in the Arctic to accomplish the reasonable present climate, we introduce the doubling CO₂. Then the ice-albedo feedback operates to increase temperature ΔT_1 by 2K in low latitudes, while ΔT_2 by 4K in high latitudes. Namely, Arctic warms twice than tropics. This is the mechanism of the Arctic amplification in response to the uniform radiative forcing by the doubling CO₂. In order to deal with the AA more quantitatively, we define the Arctic amplification by $\alpha = \Delta T_2 / \Delta T_1 = 2$ in the present result. According to the theoretical derivation of the model, the AA is caused solely by the ice-albedo feedback. Moreover, when we define the global warming by $(\Delta T_1 + \Delta T_2) / 2$ we can find that the global warming is a function of the AA as $(1 + \alpha) / 2$ time the climate sensitivity. The outgoing long wave radiation (OLR) also becomes a function of the AA as $(1 + \alpha) / 2$ time the radiative forcing. Namely, when global warming occurs, warmed arctic efficiently cools the earth by the intensified AA.

When the AA did not occur, $\alpha = \Delta T_2 / \Delta T_1 = 1$. The global warming occurs uniformly, and the radiative cooling against the anthropogenic warming is uniform too. But, when AA occurs, global warming is amplified as a function of α , consequently the climate system is cooled by the enhanced AA. In other word, the climate system prefers to respond in a pattern of the AA against the uniform anthropogenic forcing so as to most efficiently cool the climate system.

Lastly, we can investigate the effect of the Arctic Oscillation (AO) using the fact of warmer Arctic and colder lower-latitudes when the AO index is negative. Although the global mean temperature remains the same, sea-ice fraction should shrink by the AO negative. It is found that the reduced sea ice fraction intensifies the AA and the global mean temperature remains the same by the AO negative, demonstrating the hiatus of global warming due to the combination of the AO and AA.

4. Summary

The objective of this study is to understand the dynamics of the Arctic amplification (AA) in relation to the variability of the Arctic Oscillation (AO). The dynamical interpretation of the AA and its connection to the AO are investigated using a simple energy balance model for the low- and high-latitudinal boxes, developed originally by Alexeev and Jackson (2012). We find that the global warming is a function of the AA, defined by the warming ratio for the low- and high-latitudinal boxes in response to the uniform anthropogenic heating. Total cooling by the OLR is also a function of the AA. It may be important to realize that the AA is the most efficient cooling pattern of the climate system in response to the uniform anthropogenic warming.

The AA results in the AO negative, causing warm Arctic and cold low-latitudes, and the AA-AO system induces the rapid melt of the Arctic sea ice but the global mean temperature remains the same. We attempted to confirm this hypothesis using the energy balance model of the AA by implementing the AO in that model. It is found by this study that the global mean temperature is controlled both by the natural variability of the AO and the anthropogenic radiative forcing by the doubling CO₂.

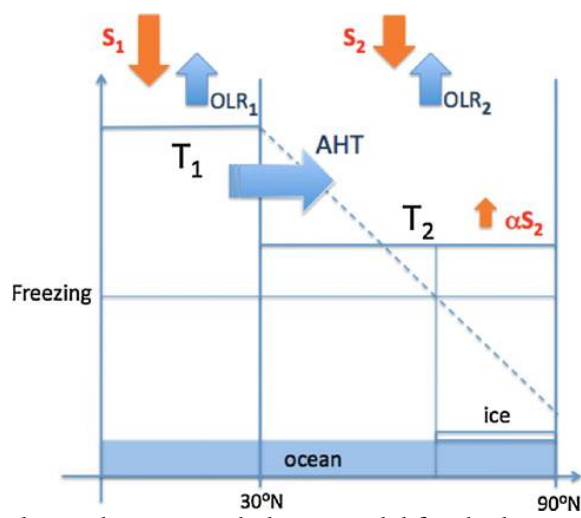


Figure 1. A simple two box energy balance model for the low and high latitudes (by Alexeev and Jackson 2012, *Clim. Dyn.*).

ROLE OF BIOLOGICAL FEEDBACK IN ARCTIC AMPLIFICATION

Jong-Seong Kug

Korea Institute of Ocean Science and Technology

ABSTRACT

The Arctic and northern high-latitude region have experienced substantial climate warming in recent decades, and its degree and pace is much larger and faster than the global average, indicating Arctic amplification. Here, we examine dynamical processes of the Arctic amplification. In particular, it is demonstrated that the earth system interaction is a critical for the Arctic amplification.

It is well known that the sea ice-albedo feedback and strong surface stability over the Arctic, which are strong positive feedback, provide strong sensitivity to the anthropogenic radiative forcing, leading to the Arctic amplification. However, it has been recognized that these are not enough to fully explain the observed arctic amplification. For example, the state-of-the-art climate system models have failed to simulate the recent rapid decline of the Arctic sea ice. We found that earth system interaction, such as vegetation feedback, ocean biological feedback, and aerosol feedback, can contribute significantly to the Arctic amplification. Furthermore, the effect of these feedbacks is amplified by coupling with the sea ice-albedo feedback and the strong stability. In addition, it is suggested that the atmospheric heat transport plays a role in adjusting the extent of the Arctic amplification. Our findings suggest that earth system interaction is indispensable to understanding and predicting the Arctic amplification.

INTERANNUAL VARIABILITY AND LONG-TERM CHANGES OF ATMOSPHERIC CIRCULATION OVER THE CHUKCHI AND BEAUFORT SEAS

Qigang Wu 1 Jing Zhang 2,3 Xiangdong Zhang 4*

¹School of Atmospheric Sciences, Nanjing University

²Department of Physics, North Carolina A&T State University

³Department of Energy and Environmental Systems, North Carolina A&T State University

⁴International Arctic Research center, University of Alaska Fairbanks

qigangwu@nju.edu.cn

ABSTRACT

The Beaufort Sea High (BSH) plays an important role in forcing Arctic sea ice and the Beaufort Gyre. In this study, we examine the variability and long-term trends of atmospheric circulation over the Chukchi and Beaufort Seas using the ERA-Interim Reanalysis for the period 1979–2012. Due to the mobility of the BSH through the year, EOF analysis is applied to the sea level pressure (SLP) field in order to investigate the principal patterns of BSH variability. In each season, the three leading EOF modes explain nearly 90% of the total variance, and reflect a wintertime-like strengthened or weakened BSH centered over the western Arctic Ocean (EOF1), a north-south dipole-like SLP anomaly (EOF2), and a west-east dipole-like SLP anomaly (EOF3), respectively. These three EOF modes offer distinct influences on local climate in each season and have different connections with the large-scale climate variability modes in winter. In particular, PC2, associated with EOF2 in the autumn, exhibits a tendency toward high-index polarity significant at the 5% level for the period 1979–2012, and is related to strongly reduced sea ice extent.

Further, we have detected both significant anticyclonic trends among surface wind fields associated with a strengthened BSH during summer and autumn, and significant cyclonic trends within surface wind fields associated with a weakened BSH during early-mid winter. Such changes in atmospheric circulation for the summer through mid-winter seasons over the Chukchi-Beaufort Seas and northern Alaska cannot be explained by natural variability at the 5% significance level, and may instead be attributable to external anthropogenic forcing.

ARCTIC CLOUD MICROPHYSICAL CHARACTERISTICS FROM SPACE-BASED LIDAR CALIOP

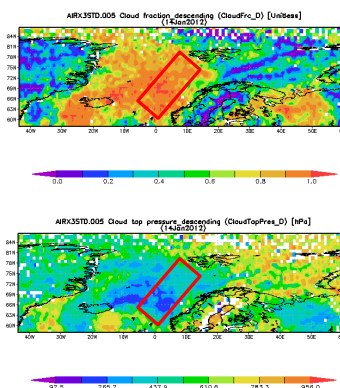
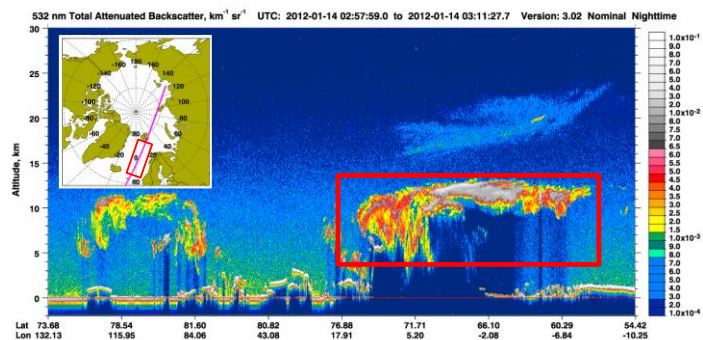
Sang-Woo Kim, Man-Hae Kim, Seok-Woo Son and Huidong Yeo

*School of Earth and Environmental Sciences,
Seoul National University
sangwookim@snu.ac.kr*

ABSTRACT

An accurate determination of cloud amount, height and associated optical properties is critical to studying the Arctic climate system and its changes. Arctic clouds are a key factor in determining the energy budget both at the top of the atmosphere and at the surface by modulating the long-wave and short-wave radiative fluxes, which affect the surface temperature and may effect on the growth or retreat of sea ice extent and thickness. In this work, we examine three-dimensional geometric and microphysical properties of Arctic clouds from multi-year space-borne passive and active sensor observations. Cloud data from the Cloud-Aerosol Lidar with Orthogonal Polarization (CALIOP) onboard Cloud-Aerosol Lidar and Infrared Pathfinder Satellite Observations (CALIPSO) and the Moderate Resolution Imaging Spectroradiometer (MODIS) are studied over the Arctic region. Space-based active sensor, CALIOP, utilizes the return signal from light pulses to identify cloud height and associated optical and microphysical properties, and is generally known to perform well even on cloud and highly reflective surfaces [Winker et al., 2007]. Figure 1 is an example of CALIOP and MODIS observations over the Kara Sea on January 14-15, 2012. CALIOP 532 nm lidar attenuated backscatter profiles on January 14, 2012 over the Kara Sea show the presence of low-level clouds near 1 km altitude and high-level clouds, as indicated by red box. The cloud top height is estimated to be about 14 ~ 15 km above mean sea level. The MODIS observation shows high cloud fraction (> 0.9) over the Kara Sea and 200~300 hPa of cloud top pressure. On January 15, 2012, we observed the same cloud features over the eastern part of Kara Sea. Cloud frequency over the Arctic region on January 2012 and December 2006, as an example, is shown in Figures 2 and 3. Compared to other regions, high cloud frequency for a whole atmospheric column is apparent over the Kara Sea, Scandinavian Peninsula, and northern parts of Russia (Figures 2a and 3a). This high fraction of clouds, especially over the Kara Sea, is contributed by high-level clouds (Figures 2e and 3e) rather than low-level (Figures 2b and 3b) or middle-level (Figures 2c-2d and 3c-3d) clouds. To characterize the vertical distribution and further quantify the presence of cloud top occurrences, we present the frequency distribution of cloud top height over the Kara Sea (30-60E, 70-80N) during winter of 2006-2012 (Figure 4). High occurrences of cloud top height are found around 1~2 km and above 9 km altitude. This suggests that high-level clouds may largely influence on the long-wave radiation budget, with low-latitude clouds. Detailed investigations on the vertical distribution of Arctic clouds (i.e., cloud top and bottom height, cloud thickness, etc.) and cloud droplet type (i.e., ice or water droplet) and microphysical properties (e.g., effective cloud droplet size) and their seasonal and inter-annual characteristics also will be presented.

(a) 2012.01.14



(b) 2012.01.15

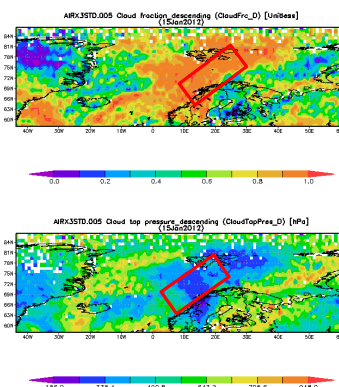
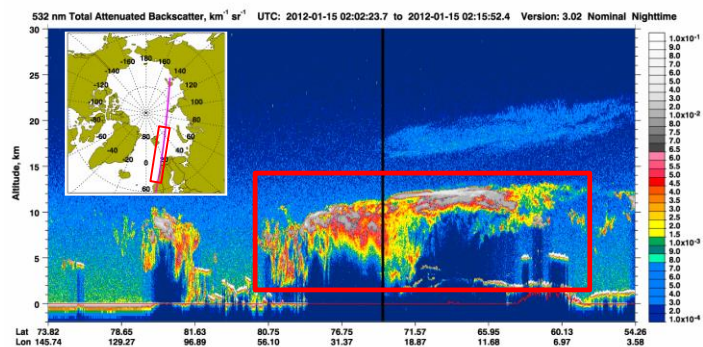


Figure 1. An example of CALIOP and MODIS observations of clouds over the Kara Sea on (a) January 14 and (b) January 15, 2012. Left panel shows CALIOP 532 nm lidar attenuated backscatter and right panels show cloud fraction and cloud top pressure (hPa) from MODIS. The red box indicates the presence of high-altitude clouds.

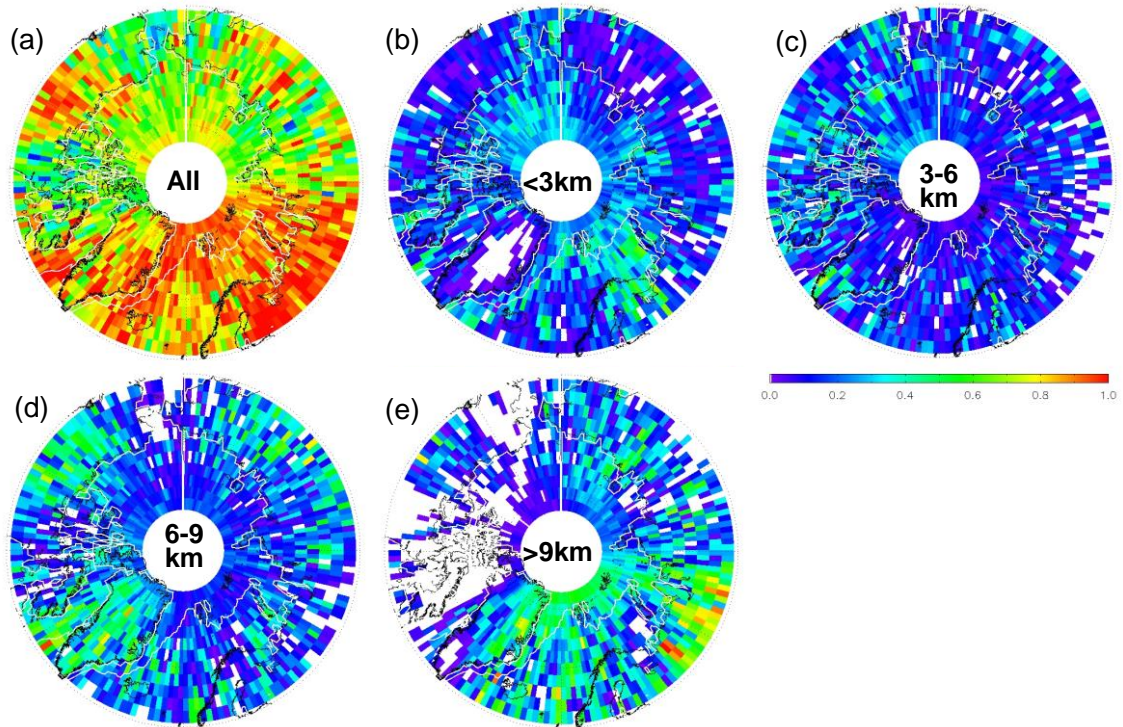


Figure 2. CALIOP cloud frequencies on January, 2012 for (a) whole atmospheric column, (b) below 3 km altitude, (c) between 3 and 6 km altitude, (d) between 6 and 9 km and (e) above 9 km altitude. The white solid line represents the edge of sea ice.

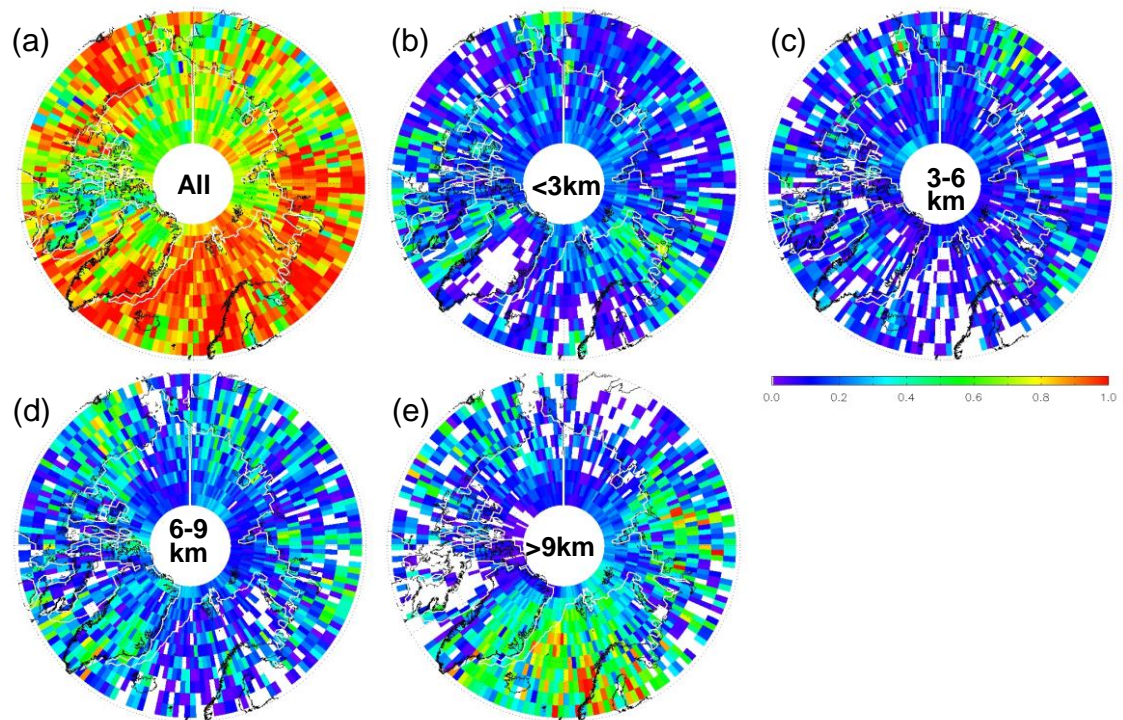


Figure 3. Same as Figure 2, except for December 2006.

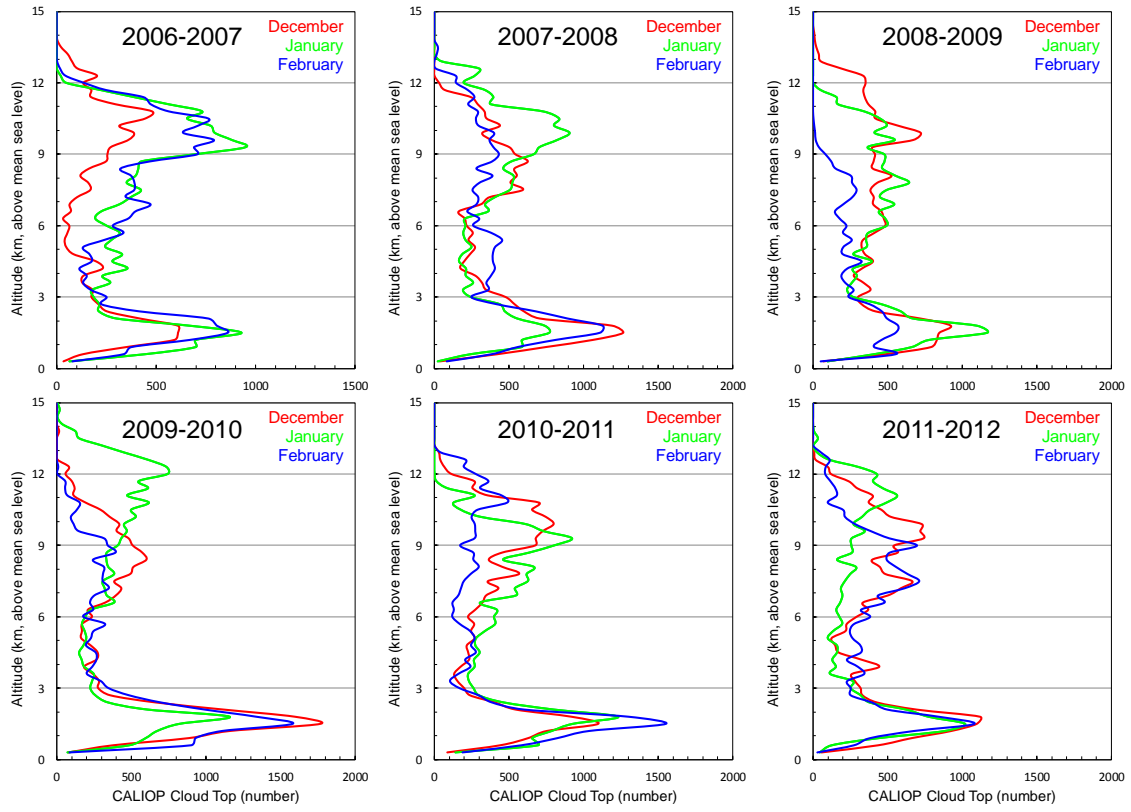


Figure 4. Frequency distribution of cloud top height from winter-time CALIOP measurements over the Kara Sea (30-60E, 70-80N).

CHANGING RELATION BETWEEN ARCTIC SEA ICE AND ASIAN DUST ASSOCIATED WITH GLOBAL WARMING

J-H Park¹, C-H Ho¹, J-H Kim², Y.G. Lee¹

¹*School of Earth and Environment Sciences,
Seoul National University*

²*Division of Polar Climate Research,
Korea Polar Research Institute
pjh21@cpl.snu.ac.kr*

ABSTRACTS

The dust storm occurs in arid and semiarid regions over the globe and makes an impact on human activities and biogeochemical cycles among atmosphere, land and ocean (Martin and Gordon, 1988; Bergametti, 1998). Asian dust from desert regions and Loess Plateau in China and Mongolia arises frequently in springtime and is influenced by varying weather and climate conditions (Chun et al., 2001). Sea ice cover is a critical component of the Arctic climate and its variation makes a significant impact on Asian climate (Honda et al., 2009; Zhang et al., 2006). This study has investigated the relationship between Asian dust and Arctic sea ice in a recent decade (2003–2012) and suggested possible physical mechanisms. Considering spring season, there is a strong negative correlation (~ -0.85 , significant at the 99% confidence level) between dust frequency over northeast Asia and sea ice extent (SIE) over the Arctic Sea. The reduction of Arctic SIE is accompanied by a dipole structure of temperature anomaly in the lower troposphere on interannual timescale: strong warm anomaly over the Arctic and adjacent high latitudes including eastern Russia versus weak cold anomaly over northeast Asia. These temperature distributions induce trough to deepen and jet stream to intensify over northeast Asia. Hence, dust storm generates frequently over source regions and dust transportation activates to downstream regions. It is noted that this distinctive negative correlation was not found in earlier two decades (1979–2002) based on dust observations in 11 stations of South Korea. The diverse dust-SIE relation on decadal timescale would be related to interdecadal changes in large-scale environments associated with substantial decrease of Arctic SIE; about 33% reduction for spring in the recent decade (2003–2012) compared to the earlier decades (1979–2002). These results demonstrate that the reduced spring SIE over Arctic, especially in the Barents Sea, due to global warming has altered large-scale environments in eastern Russia and northeast Asia. Therefore, it could provide a new connection to dust activity over northeast Asia.

References

- Bergametti G., 1998: Mineral aerosols: Renewed interest for climate forcing and tropospheric chemistry studies. *IGACtivities Newsletter*, No. 1, IGAC Core Project Office, 13–17.
- Chun Y., K. O. Boo, J. Kim, S. U. Park, and M. Lee, 2001: Synopsis, transport, and physical

characteristics of Asian dust in Korea. *J. Geophys. Res.* **106** (D16): 18461-18469, doi:10.1029/2001JD900184

Honda M., J. Inoue, and S. Yamane, 2009: Influence of low Arctic sea-ice minima on anomalously cold Eurasian winters. *Geophys. Res. Lett.* **36**, L08707, doi:10.1029/2008GL037079

Martin J. H. and R. M. Gordon, 1988: Northeast Pacific iron distributions in relation to phytoplankton productivity. *Deep-Sea Res.* **35**, 177–196.

Zhang J., G. Peng, M. Huan, and S. Zhang, 2006: Are dust storms activities in North China related to Arctic ice-snow cover? *Global and Planetary Change* **52**, 225–230, doi:10.1016/j.gloplacha.2006.02.007

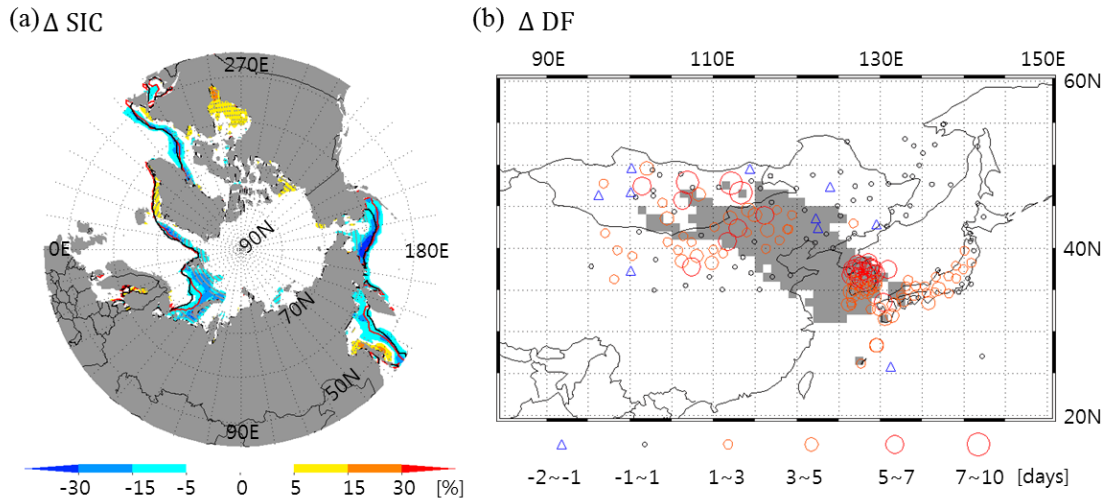


Figure. 1. (a) Composite differences of the Arctic sea ice concentration (SIC) between SIE- and SIE+ years (SIE- minus SIE+) for the springs of 2003–2012. (b) Same as (a), but for the dust frequency. Solid line in (a) indicates mean sea ice coverage for the springs of 2003–2012. Shaded area in (b) is the dust transport routes. SIE- years include 2006, 2007, 2011 and SIE+ years are 2003, 2008, 2009, 2010, 2012.

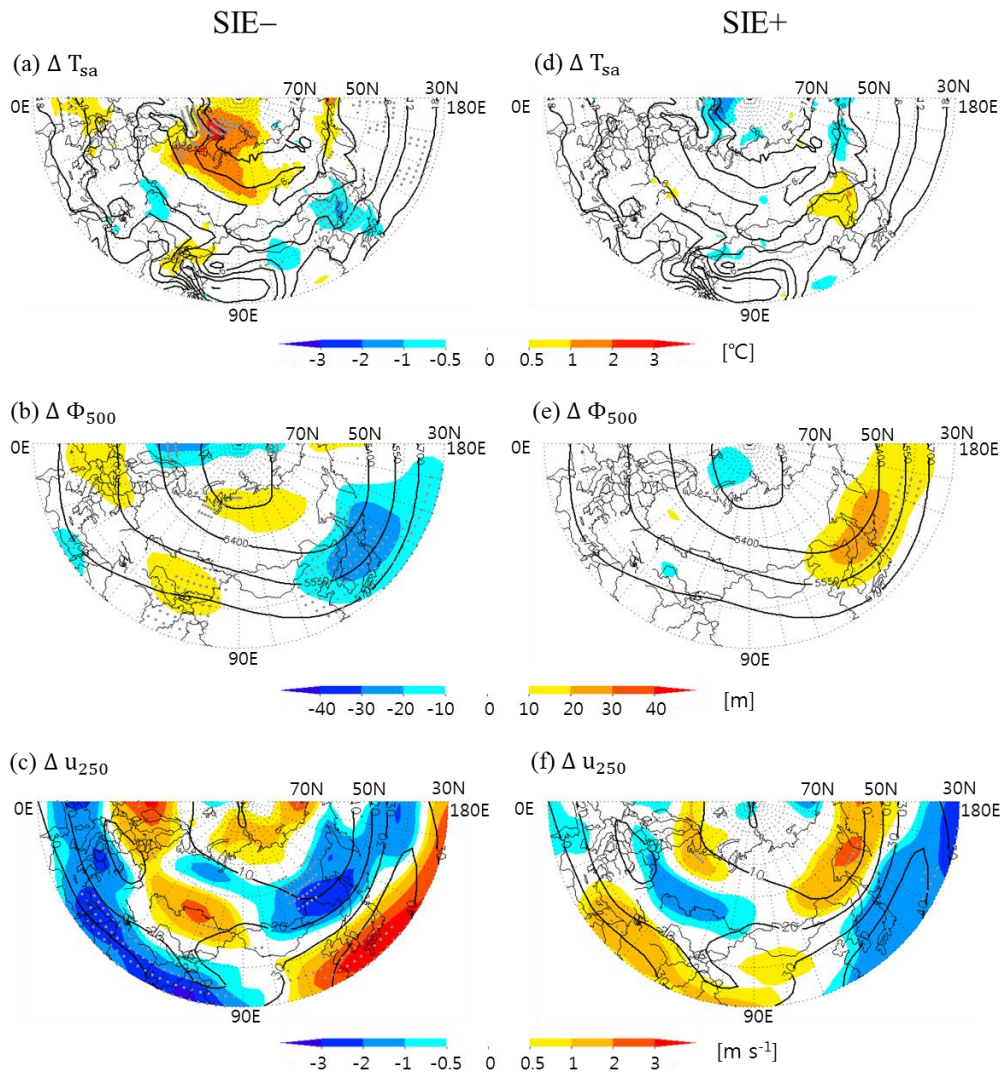


Figure. 2. Composite anomalies (shaded colors) in SIE- years (left figures) and SIE+ years (right figures) and mean fields (contour lines) for the springs of 2003–2012: (a), (d) surface air temperature ($^{\circ}\text{C}$), (b), (e) geopotential height at 500 hPa (m), and (c), (f) zonal wind at 250 hPa (m s^{-1}). The dots denote the areas where the composite anomalies are significant at the 90% confidence level using a t-test.

SESSION 2

ICE AND OCEAN

CARBON CONTRIBUTION OF SEA ICE FLOES IN THE ARCTIC OCEAN

Sang H Lee¹, Bo Kyung Kim¹, Hui-Tae Joo¹, Jung Woo Park¹, Ho Jung Song¹
Hyoung-Min Joo², Doo Byoul Lee², Sung-Ho Kang²

¹*Department of Oceanography,
Pusan National University*

²*Korea Polar Research Institute
sanglee@pusan.ac.kr*

ABSTRACT

Detail contributions of particulate organic carbon (POC) in various environments of the Arctic sea ice floes were executed at two different types of sea-ice stations (ST 1 and ST 2) in the northern Chukchi Sea, 2011. The surface ice of melt ponds at ST 1 had the highest POC concentration, followed by sea-ice cores at ST 2. The POC concentrations in melt ponds ranged between 90.0 mg C m⁻³ (S.D. = ± 12.7 mg C m⁻³) and 103.9 mg C m⁻³ (S.D. = ± 47.7 mg C m⁻³) at ST 1 and ST 2, respectively with major POC contributors were diatoms (48.7%). The total POC concentration of sea-ice floes ranged from 2.8% to 5.3% of the POC concentration of the euphotic water column at the study locations, which could be important to higher trophic levels because of relatively much higher POC concentration than the community of the water column.

USING PELAGIC CILIATED MICROZOOPLANKTON COMMUNITIES AS AN INDICATOR FOR MONITORING ENVIRONMENTAL CONDITION UNDER IMPACT OF SUMMER SEA-ICE REDUCTION IN WESTERN ARCTIC OCEAN

Yong Jiang, Eun Jin Yang*, Jun-Oh Min, Sung-Ho Kang and SangHoon Lee

Division of Polar Climate Research,
Korea Polar Research Institute
yjiangeco@gmail.com

ABSTRACT

The Arctic Ocean may be a sensitive indicator of global climate changes (Shimada et al., 2006). In the last decade, the extent of summer Arctic sea ice has decreased dramatically (Perovich, 2011) and in 2012, the summer catastrophic reduction reached its lowest ever recorded sea ice extent (Jiang et al., 2013) (Fig. 1).

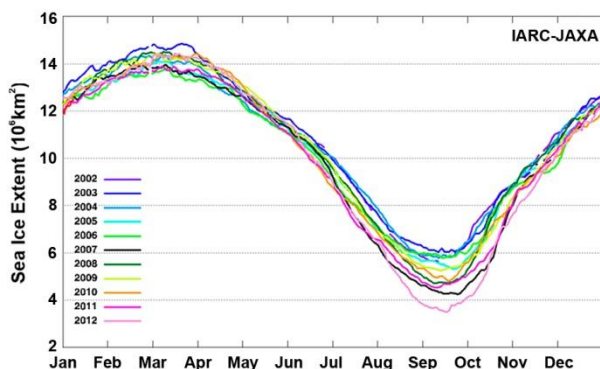


Fig. 1. Time-series results for Sea Ice Extent in Arctic from 2002-2012 (http://www.ijis.iarc.uaf.edu/en/home/seaice_extent.htm).

Increasing numbers of studies have shown the strong relationship between ciliate communities and environmental conditions and ciliates could be used as a bioindicator (e.g., Kchaou et al., 2009; Jiang et al., 2011, 2012). The limnological and physiochemical variability could be measured easily by modern technique, however, the instantaneous measurement could not give enough information to understand how the environmental changes influence the living creatures' habitat condition, and we still cannot predict whether ongoing climate changes will affect ciliated microzooplankton in Arctic regions because community-level observations are scarce. Thus, we examined ciliate species distribution, community structure variation, and its relationship to environmental conditions at 32 stations onboard the Korean icebreaker Araon in the Chukchi Sea of the

western Arctic Ocean during summer sea-ice reduction period from August 1 to September 10, 2012 (Fig. 2).

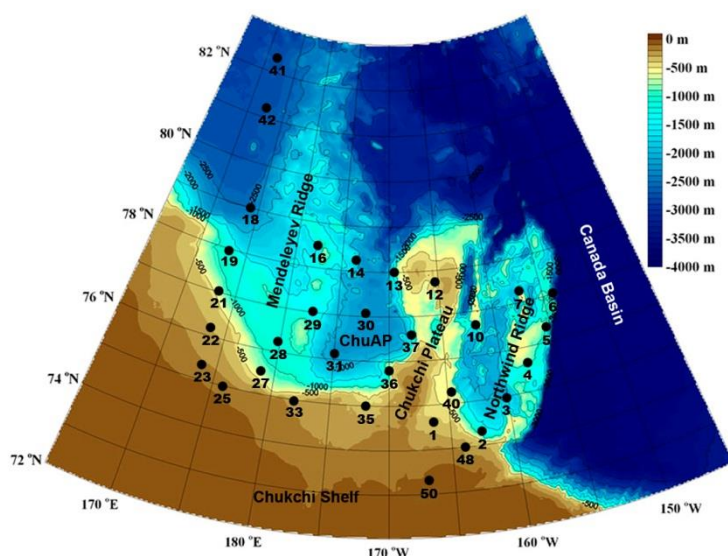


Fig. 2. 32 Sampling stations in western Arctic Ocean from August 1 to September 10, 2012. ChuAP, Chukchi Abyssal Plain.

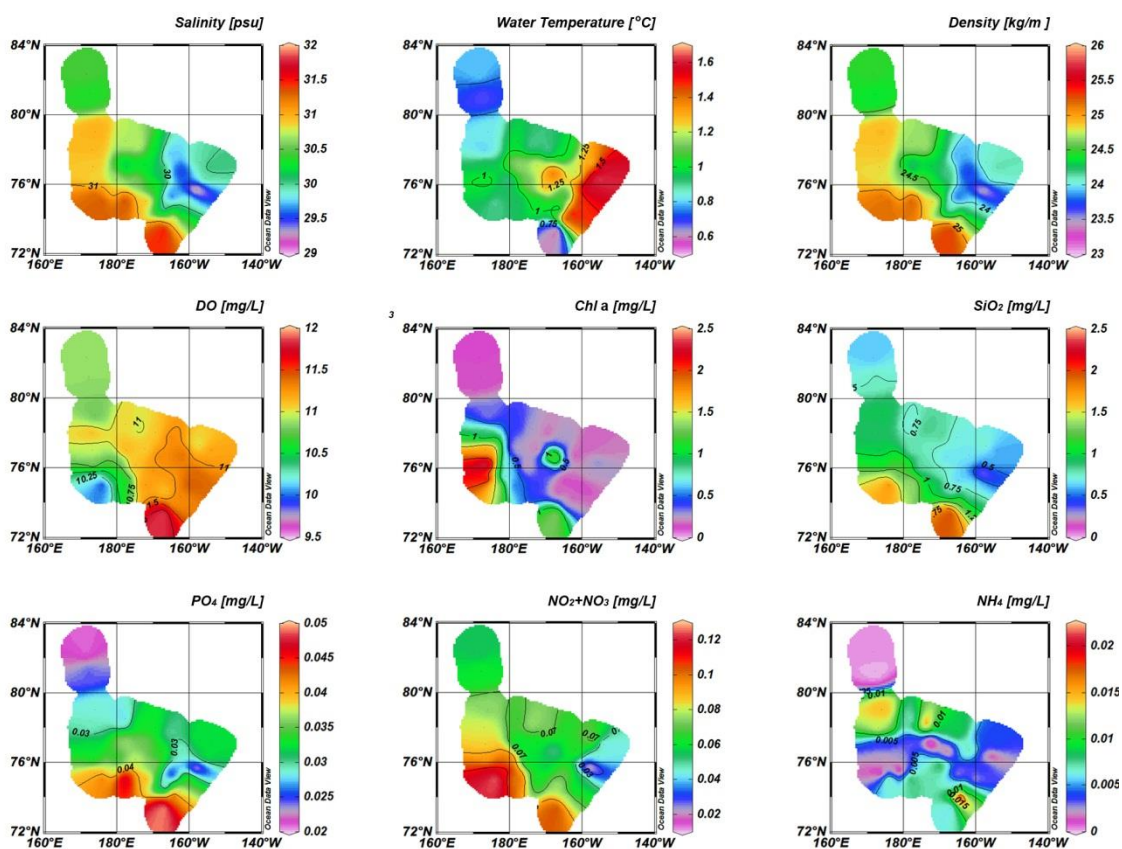


Fig. 3. Spatial distribution of nine environmental variables monitored at 32 sampling stations in western Arctic sea from August 1 to September 10, 2012 (depth mean values for each sampling station).

Based on our physicochemical measurements from 32 stations, the sampled area could be

basically divided into the western part (Mendeleyev Ridge and Chukchi Abyssal Plain) and eastern part (Chukchi Plateau and Northwind Ridge), with the western edge of the Chukchi Plateau as a dividing line (Fig. 2 and 3).

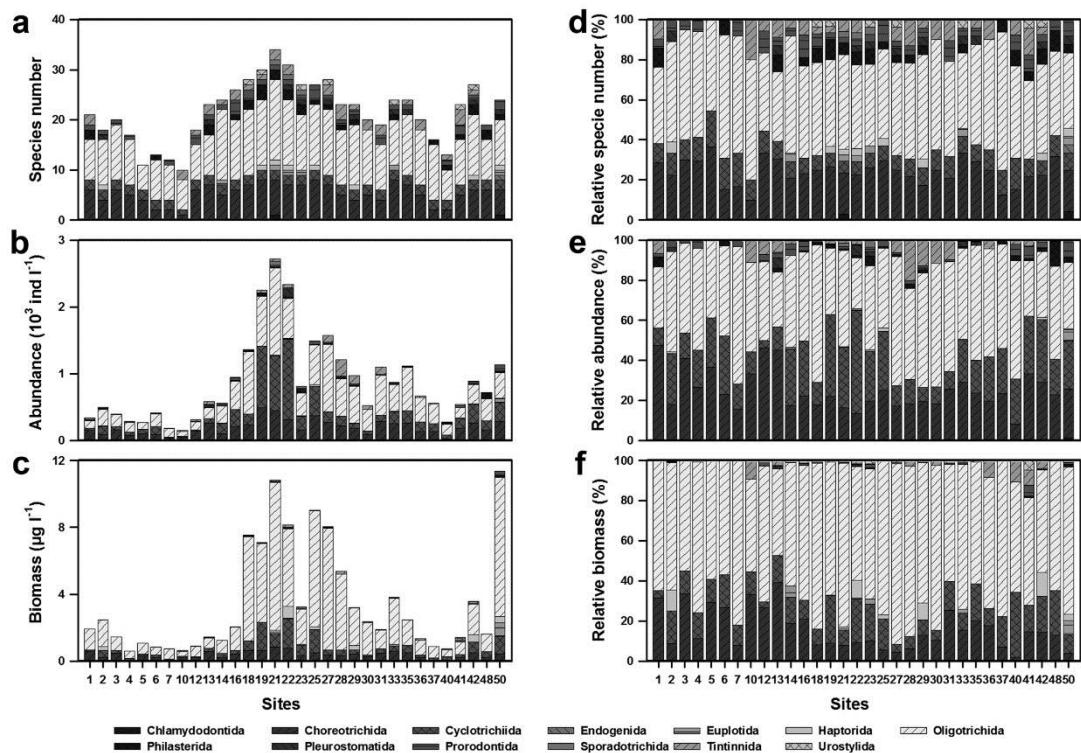


Fig. 4. Taxonomic compositions and variations in species number (a), abundance (b), biomass (c), relative species number (d), relative abundance (e) and relative biomass (f) of planktonic ciliates from 32 stations.

The ciliate community in this region was diverse with total 55 species identified representing 32 genera and 13 orders. Top 16 ranked contributing species provided a cumulative contribution of 90.73% to communities were defined as “dominant”. Species number, abundance and biomass all exhibited the similar east–west distribution pattern like the case in environment condition with higher values in the western stations and lower in the eastern ones (Fig. 4). Aloricate species including oligotrichids, cyclotrichiids and choreotrichids were major contributors to dominate the communities (Fig. 4).

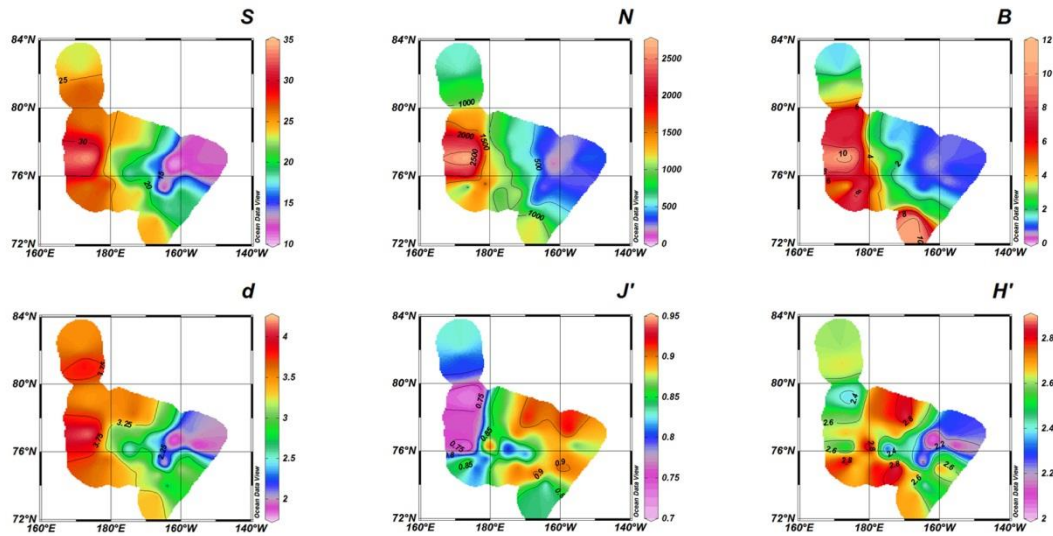


Fig. 5. Spatial pattern of species number (S), abundance (N), biomass (B), richness (Margalef d), diversity (Shannon-Wiener H') and evenness (Pielou's J') of ciliated microzooplankton communities.

The horizontal variations of species number, abundance, biomass, and three species diversity indices all showed the same east–west distribution pattern as above (Fig. 5). 16 dominant species abundance and species diversity indices were significantly correlated (spearman correlations) with physicochemical variables, especially with nitrates and phosphates.

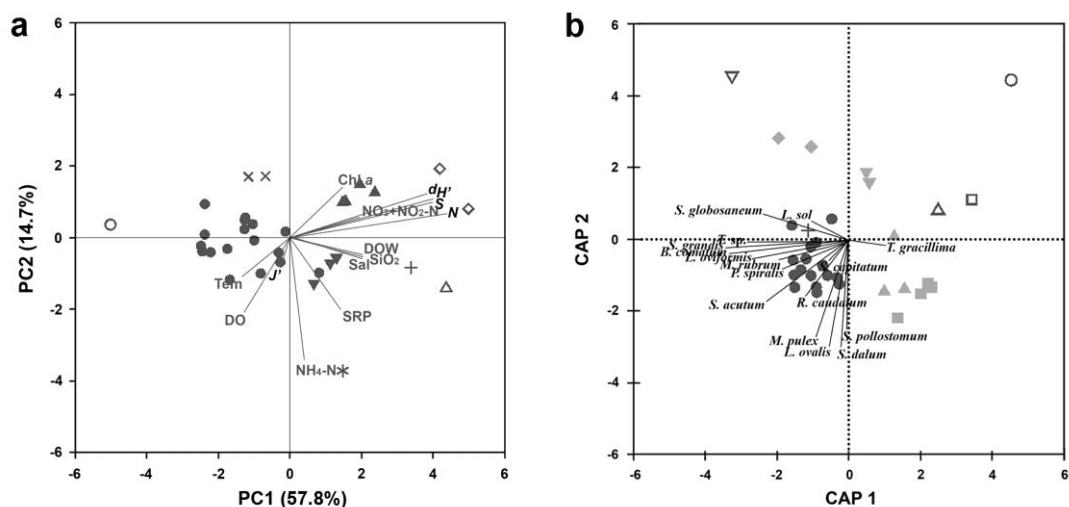


Fig. 6. Principal component analysis (PCA) plot (a) for spatial changes of environmental conditions based on abiotic data and Canonical analysis of principal (CAP) coordinates (b) on Bray-Curtis similarities from log-transformed species-abundance data, and correlations of 16 dominant species with the two CAP axes. PCA Axes 1 and 2 respectively accounted for 57.8% and 14.7% of the variation present.

Multivariate analyses demonstrated that ciliated microzooplankton community structures (Fig. 6b) showed significant differences between the western (round symbols) and eastern (other icons) parts of the sampling region; consistent with east–west differences in environmental conditions (Fig. 6a); and the significantly association between spatial patterns of community structure and of environmental condition was found by Mantel test ($r = 0.818$; $p = 0.001$). Multivariate biota–environment analysis showed that the best match with the ciliates occurred with the combination of

$\text{NO}_3 + \text{NO}_2\text{-N}$ and SRP ($p = 0.01$). These results suggest that the summer sea-ice reduction has affected ciliate biodiversity seriously and the pelagic ciliate communities may be useful as robust bioindicators for studying climate change effects under increasing sea-ice melting in the Arctic Ocean.

Reference

- Jiang, Y., Xu, H., Hu, X., Zhu, M., Al-Rasheid, K.A.S., Warren, A., 2011. An approach to analyzing spatial patterns of planktonic ciliate communities for monitoring water quality in Jiaozhou Bay, northern China. *Mar. Pollut. Bull.* 62, 227–235.
- Jiang, Y., Xu, H., Zhang, W., Zhu, M., Al-Rasheid, K.A.S., 2012. Can body-size patterns of ciliated zooplankton be used for assessing marine water quality? A case study on bioassessment in Jiaozhou Bay, northern Yellow Sea. *Environ. Sci. Pollut. Res.* 19, 1747–1754.
- Jiang, Y., Yang, E.J., Min, J.O., Kang, S.H., Lee, S.H., 2013. Using pelagic ciliated microzooplankton communities as an indicator for monitoring environmental condition under impact of summer sea-ice reduction in western Arctic Ocean. *Ecol. Indic.* 34, 380-390.
- Kchaou, N., Elloumi, J., Drira, Z., Hamza, A., Ayadi, H., Bouain, A., Aleya, L., 2009. Distribution of ciliates in relation to environmental factors along the coastline of the Gulf of Gabes, Tunisia. *Estuar. Coast. Shelf Sci.* 83, 414–424.
- Perovich, D.K., 2011. The changing Arctic sea ice cover. *Oceanography* 24, 162–173.
- Shimada, K., Kamoshida, T., Itoh, M., Nishino, S., Carmack, E., McLaughlin, F., Zimmermann, S., Proshutinsky, A., 2006. Pacific Ocean inflow: Influence on catastrophic reduction of sea ice cover in the Arctic Ocean. *Geophys. Res. Lett.* 33, L08605, doi: 10.1029/2005GL025624

Acknowledgments

This work was supported by the Korea Polar Research Institute projects (PM12020).

PROJECTION OF SHIP-ACCESSIBLE DAYS IN THE ARTIC SEA BASED ON IPCC CLIMATE CHANGE SCENARIOS

Jai-Ho Oh^{1}, Sumin Woo¹, Hyeon-kun Jin¹, Jin-woo Kim¹, and Kyoung-Min Lee²*

*¹ Department of Environmental and Atmospheric Sciences,
Pukyong National University,*

*² CRAY Korea Inc.,
jhoh@pknu.ac.kr*

ABSTRACT

A high-resolution AGCM has been used to estimate future sea ice extent and thickness in the Arctic and to provide future projection of marine access in Arctic Sea due to the global warming caused from greenhouse gas emission. For computational efficiency, we have used GME model, a high-resolution GCM, which is based on uniform icosahedral-hexagonal grid. To demonstrate the capability of GME GCM to reproduce the past climate in detail the present-day climate has been simulated for the period of 1979-2009 with the use of the AMIP observed SST and Sea Ice Concentration. Subsequently the future climate until the end of 21st century has been simulated by adopting the SST simulated by 4 CMIP5 models for the two RCP scenarios (RCP 8.5 and RCP 4.5) in the IPCC AR5.

As one of the simulation results it shows the decreasing trend in sea ice extent and increasing trend in ship-accessible days estimated by three vessel classes. The year to year variation of ship-accessible days is an important information to make a decision to operate The Arctic shipping routes.

Keywords : IPCC, Climate Change, Sea Ice Extent, Sea Ice Thickness, Ship-accessible days

1. Introduction

Climate change has caused the increase of temperature, rise of sea level and reduced arctic sea ice. Especially, change of arctic sea ice extent is so important issue to decide the accessing area, navigation season length and economic viability with regarding to shipping potential. Recently, sea ice extent and thickness in September 2007 and 2012 were recorded the robust downward trends observed since 1979 and the extent of older, thicker multiyear ice (MYI) has decreased ~15% per decade (Stephenson et al. 2013).

In this study, we have simulated the future climate change with the use of an ultra-high resolution atmospheric global climate model with 40 km horizontal grid resolution based on the coarse IPCC climate model simulations. With this high resolution climate model may provide a regional information on the changes in arctic sea ice extent as well as thickness in detail.

2. Materials and Methods

The atmospheric GCM used is an operational global numerical weather prediction model GME (Majewski et al., 2002) of German Weather service. It is based on uniform icosahedral–hexagonal grid. In this study, we adopted the high resolution of GME with 40-km/40 layers. In 40-km mesh size, the number of gridpoints is 368,642 and transformed grid uses 900 X 451 grid cells. Detailed description of the model is given in Majewski et al. (2002). We have performed the present-day climate simulation from 1979 to 2009 with the historical sea surface temperature (SST) and Sea Ice concentration observation data of AMIP. And for the future climate simulations sequentially, the model was integrated to 2100 with future SST and Sea Ice boundary data. This is the multi-model ensemble from four models of Coupled Model Intercomparison Project phase 5 (CMIP5) participating models based on the Representative Concentration Pathway scenario (RCP 8.5 and RCP 4.5) by IPCC AR5. The specification of models is summarized in Table 1. And we forced the change of CO2 concentration and other greenhouse gases yearly from the Goddard Institute for Space Studies (GISS) National Aeronautics and Space Administration (NASA) for present-day climate simulation and the RCP database for future climate simulation.

Table1. Specification of 4 models in CMIP5

No.	Model	Resolution Lon. ×Lat.	Institution	Country
1	CanESM2	2.8125°×2.8125°	Canadian Centre for Climate Modelling and Analysis (CCCma)	Canada
2	GISS-E2-R	2.5°×2°	NASA Goddard Institute for Space Studies (NASA GISS)	USA
3	HadGEM2-CC	1.875°×1.24°	Met Office Hadley Centre (MOHC)	UK
4	HadGME2-ES	1.875°×1.24°		UK

Sea ice simulation during present-day climate is compared with observation of the Hadley Centre sea-ice and sea surface temperature (HadISST) dataset on the 1 degree from 1979 to 2009 (Rayner et al., 2003). For the projection of the future ship-accessible days, we used the three vessel classes [Polar Class 3 (PC3), Polar Class 6 (PC6), Open-water (OW)] by ‘Supplementary Methods’ and detail are summarized in Stephenson et al. (2013)

3. Results and discussion

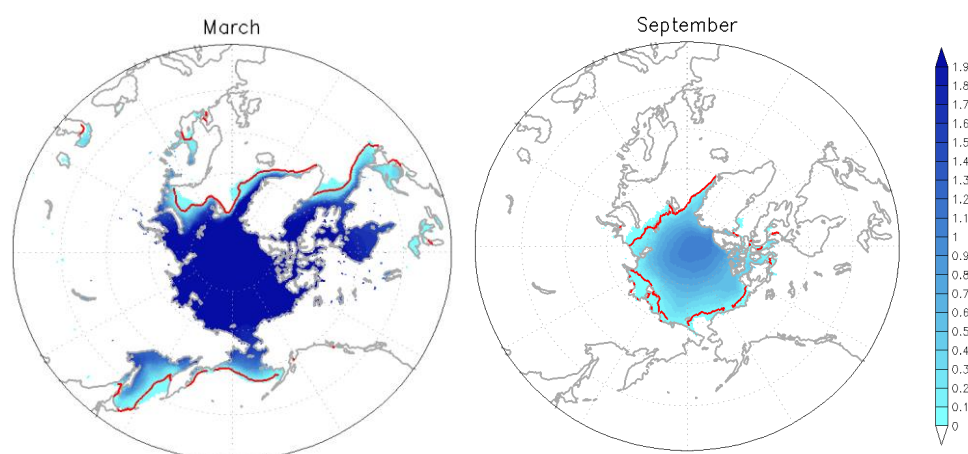


Fig. 1. Spatial distribution of Sea ice thickness (unit: m) of present-day climate simulation during 1979-2009 in the Northern Hemisphere for March (left) and September (right). The red line is observed 15% concentration boundary of HadISST.

The simulated spatial distributions of sea ice thickness for March and September 1979-2009 are shown in Fig. 1 together with the ice extent of HadISST in the Arctic region. As illustrated in Fig.1 the simulated sea ice thickness is in good agreement with observed.

The seasonal variation of the monthly averaged sea ice extent, as shown in Fig. 2, is also in good agreement with observed data with the maximum in February or March and the minimum in August or September. The model over estimates the sea ice extent compared to observation for all months monotonically. It might be caused of the design of sea ice model in the GME AGCM, in which there is no wind driven sea ice movement. The mechanism of sea ice change is only by radiative heating or cooling and by heat exchange with the atmosphere at the upper surface of sea ice and with sea water at the bottom in the model. Accordingly the model may overestimate the sea ice without weather related sea ice movement.

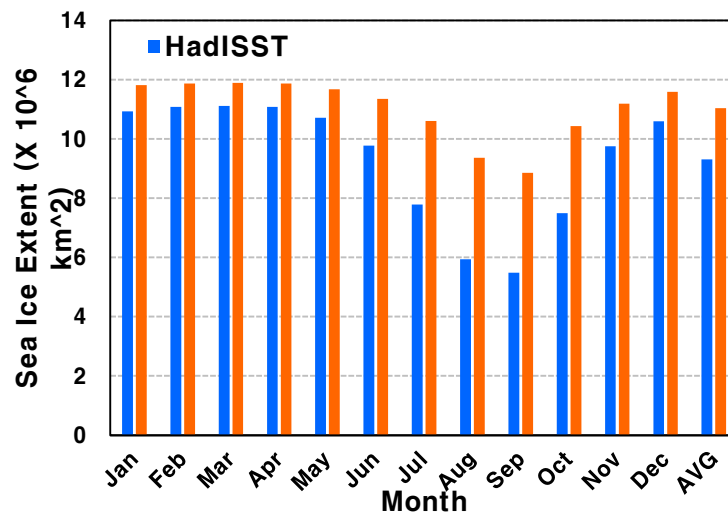


Fig. 2. Seasonal Cycle of Sea ice Extent climate simulation during 1979-2009 in the Arctic Circle by the GME model (red) and HadISST (blue).

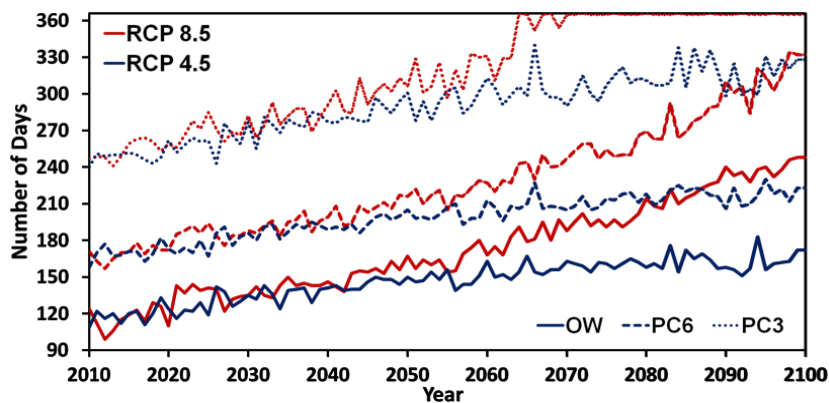


Fig. 3. The numbers of ship-accessible days for RCP 4.5 and RCP 8.5 by the vessel classes (PC3, PC6 and OW).

Based on the validation of present-day climate simulation, the numbers of ship-accessible days for each year are shown for both scenarios until 2100 by the three vessel classes (Fig. 3). It is shown that the number of ship-accessible days typically increases. In the comparison between both scenarios, the rate of increase in RCP 8.5 appears higher than RCP 4.5 in all vessel classes. Especially, the difference in the rate of increase is noticeable since 2050s.

4. Conclusion

The high-resolution GCM was used for the change of future sea ice extent and ship-accessible days due to the RCP scenario. In validation, it captures the detailed monthly sea ice distributions in the

Northern Hemisphere with observation. Based on the GME-projected future simulation by RCP scenarios, the number of ship-accessible days shows the increase patterns. Between both scenarios, the RCP 8.5 shows the greater increases in marine access than RCP 4.5. In all vessel classes, RCP 8.5 shows the higher marine access than RCP 4.5.

Although the future climate projection by the AGCM is not able to capture accurately the response of climate change, the results may provide an essential data to estimate regionally spatial and temporal ranges of arctic marine operations in future.

5. Acknowledgements

This work was funded by the Korea Meteorological Administration Research and Development Program under Grant CATER 2012-7015 and it was also supported the computing resources by GSDC Project in KISTI.

6. References

- Majewski D, D. Liermann, P. Prohl, B. Ritter, M. Buchhold, T. Hanisch, G. Paul, W. Wergen, and J. Baumgardner (2002), The Operational Global Icosahedral–Hexagonal Gridpoint Model GME: Description and High-Resolution Tests, *Monthly Weather Review*, 130, 319–338
- Rayner, N. A., D. E. Parker, E. B. Horton, C. K. Folland, L. V. Alexander, D. P. Rowell, E. C. Kent, A. Kaplan, (2003), Global analyses of sea surface temperature, sea ice, and night marine air temperature since the late nineteenth century *J. Geophys. Res.* Vol. 108, No. D14, 4407 10.1029/2002JD002670
- Stephenson, S. R., L. C. Smith, L. W. Brigham and J. A. Agnew (2013), Projected 21st-century changes to Arctic marine access. *Climatic Change*, 118, 885-899.

NO-REBOUND REDUCTION OF SEA ICE IN THE ARCTIC OCEAN: ROLE OF "INERTIA" EFFECT OF THE OCEAN

Koji Shimada, Eri Yoshizawa,

Tokyo University of Marine Science and Technology
koji@kaiyodai.ac.jp

Tae Wan Kim, Ho Kyung Ha, Hyun Jung Lee, Ho Jin Lee, Sung-Ho Kang,
and Kyung Ho Chung

Korea Polar Research Institute

ABSTRACT

Sea ice area in the Arctic Ocean in 2007-2008 recorded anomalous yearly minimums from the value on the reduction trend after late 1990s. During this period, both clockwise circulation in both atmosphere (Beaufort High: BH) and sea ice (Beaufort Gyre of the sea ice: BGI) were enhanced in the Pacific sector of the Arctic Ocean. After that, both BH and BGI rebounded to the value before 2007. The underlying ocean circulation (Beaufort Gyre of the ocean: BGO), however, sustained its strength and delivered substantial heat into the Arctic basin. These observational evidences imply that the strength of upper ocean circulation was not easily changed synchronized with the changes in the surface forcings such as wind and sea ice motion. The "inertia" of the ocean would be a key to understand no-rebounded reduction of sea ice. The time scale of the "inertia" effect of the ocean was evaluated as about four years.

OPTICAL PROPERTIES AROUND MENDELEEV RIDGERELATED TO THE PHYSICAL FEATURES OF WATER MASSES

Jinping Zhao, Weibo Wang, Sung-Ho Kang, and Tae-Wan KIM

1. Physical Oceanography Lab, Ocean University of China

2. Korea Polar Research Institute

jpzhao@ouc.edu.cn

ABSTRACT

Irradiance profiles was measured with the Korean 2012 summer cruise and the optical property was studied. The optical attenuation features are described. The attenuation coefficient in all top levels was low. The high attenuation zone appeared at about 40-60 m. The attenuation properties are sorted to five types. Type-3 water has an intense maximum of attenuation coefficient up to 0.56/m located on west flank of Mendeleev Ridge. Type-4 is with weaker maximum attenuation coefficient located at the north margin of the observed region. The difference between Type-3 and Type-4 waters indicated two water masses: one is the shelf water massively mixed with river water and transported to the east by the East Siberian Slope Current. The other is the water from Pacific with less nutrient and transported to the west along the north margin of the observed region. The two integral parameters, attenuation depth and optical thickness, are given to show the spatial distribution. The attenuation depth is basically smaller (40m) at the west and larger at the east(100m). The averaged optical thickness at the level of 30-60m is the main high attenuation zone, showing the strong attenuation and high productivity. From both the optical attenuation property and the physical feature of water masses, it is suggested that the Pacific Water spread to the north and west over the Chukchi Plateau, and than circulated back through Mendeleev Abyssal Plain and the Chukchi slope.

SUBSEASONAL TO SEASONAL PREDICTION OF ARCTIC SEA-ICE CONCENTRATION BY SEASONAL EMPIRICAL ORTHOGONAL FUNCTION (EOF) METHOD

Baek Min Kim

*Division of Climate Change
Korea Polar Research Institute
bmkim@kopri.re.kr*

ABSTRACTS

A statistical method for short-term (up-to 12 months) prediction of Arctic sea-ice concentration (SIC) is developed based on season-reliant Empirical Orthogonal Function (S-EOF) technique. This method provides the prediction of monthly sea-ice concentrations for all local grid-points over the Arctic region with up-to 12-month lead. Since Arctic SIC exhibits a strong seasonality and its anomaly also has preferred spatio-temporal evolution patterns that are influenced by the seasonality of the Arctic climate, we use the S-EOF technique to extract the dominant spatio-temporal evolution patterns (S-EOFs of 12-month length) of the Arctic SIC from a historical observation. Using the recent 12 months data, coefficients for the S-EOF modes representing the present state (recent 12 months) of the Arctic SIC are obtained by projecting the observed sea-ice anomalies for the last 12 months onto the identified S-EOFs. Assuming that the space-time evolution of each S-EOF mode during the last 12 months persists, the future evolution of the Arctic SIC anomalies is reconstructed by multiplying the projection coefficients with the corresponding S-EOFs and taking summation. Predictability of the devised method is assessed by the hindcasts of 12-month prediction starting from every month for the period 1980-2012. Comparing with forecasts from a dynamical prediction model (NCEP CFSv2) this method shows better skill in predicting both the total sea ice extent and local concentration anomalies. This method has limited skills for spring to summer predictions, but shows excellent skill (>0.8 in correlation coefficient with respect to observation for 4-5 months lead) for autumn and winter predictions.

THE EFFECT OF POLEWARD MOISTURE FLUX ON ARCTIC WINTER SEA-ICE MELTING

Hyo-Seok Park^{1}, Sukyoung Lee^{1,2}, Seok-Woo Son¹, Yu Kosaka³ and Bruno Tremblay⁴*

¹School of Earth and Environmental Sciences, Seoul National University, South Korea

²Department of Meteorology, Pennsylvania state university, State College, USA

³Scripps Institution of Oceanography, University of California, San Diego, USA

⁴Department of Earth System Science, McGill University, Montreal, Canada

ABSTRACTS

Even without the ice-albedo feedback, the wintertime intraseasonal variability of Arctic Sea ice cover is as large as the variability of other seasons. Strengthening of south-westerlies associated with the North Atlantic Oscillation is a well-known factor for changing the Arctic sea ice cover. Here, using reanalyses and satellite observation data, the authors show that the poleward moisture transport across 70N plays a key role in melting the Barents-Kara sea ice by increasing downward infrared radiation (IR) flux. The pentad-mean correlation between the poleward moisture flux and Arctic downward IR is quite significant and the moisture flux leads the downward IR by 1-3 days.

These strong downward IR events in the Arctic Ocean are often led by localized diabatic heating in the Indonesian and western Pacific warm pool, suggesting that tropical SST pattern or the Madden-Julian Oscillation (MJO) phase is a potential predictor of Arctic sea ice concentration.

ENERGY BUDGET OF FIRST-YEAR ARCTIC SEA ICE IN ADVANCED STAGES OF MELT

*S. R. Hudson, M. A. Granskog, A. Sundfjord, A. Randelhoff,
A. H. H. Renner, and D. V. Divine*

Norwegian Polar Institute, Tromsø, Norway
hudson@npolar.no

ABSTRACTS

The Arctic Ocean, once the domain of old, thick multiyear ice, is now largely covered by younger sea ice, much of it first-year ice. This transition affects many of the processes acting on the Arctic ice since first-year ice is thinner than and has many physical differences from multiyear ice. A clear example that affects the energy budget and resulting melt rate of the Arctic is that first-year ice generally has less topography, which leads to more extensive melt pond coverage. These ponds, underlain by thin ice, are dark, allowing much more sunlight to be absorbed by the ice or transmitted to the ocean than white ice, or even melt ponds on thicker ice. The transmitted light is absorbed by the ocean, providing an added source of turbulent heating from below.

To gain a better understanding of the energy budget of first-year sea ice in the high Arctic in summer, we observed the radiative and turbulent fluxes of energy both above and below an ice floe. The floe was typical for the region, between 82° and 82.5°N and 20° and 22.5°E, during the observation period of 26 July to 3 August 2012. Turbulent heat fluxes from the atmosphere to the surface and from the ocean to the underside were observed during the period at fixed locations 2 m above and 1 m below the ice. All components of the radiation budget were monitored continuously at one site. In addition, extensive surveys were carried out to measure the spatial variability of spectral and broadband albedo and spectral transmittance.

Combining the typical albedo and transmittance of various surface types from the transect data and a categorized aerial photograph of the floe, we were able to determine the floe-scale albedo and transmittance and combine this with the other fluxes to get an overview of the floe's energy budget. The study area of approximately 0.4 km² was 96% ice covered, of which 77% was white (bare) ice, 16% was dark melt pond, and 7% was bright melt pond. The ice-covered area had an overall albedo of 0.47 and transmittance of 0.16, under the prevailing cloudy sky. Figure 1 shows that absorbed shortwave radiation (10–30 W m⁻² at midnight, 80–150 W m⁻² at noon) was generally the largest source of energy to the ice, though oceanic heat fluxes to the ice (–10 to +70 W m⁻²) were similar to, and in one case much larger than, nighttime solar heating. Atmospheric turbulent heating was negligible.

Average fluxes for the 7-day period are summarized in Table 1. Longwave emission worked to slightly offset the heating driven by solar absorption and oceanic turbulent heat transfer, but the net result was

significant energy absorption by the ice, which drove ice melt at an average rate of about 3 cm day⁻¹.

The observations were made away from the continental slope, at depths greater than 3000 m, where Atlantic water inflow is unlikely to have contributed to the oceanic heat flux. It is therefore likely that the source of the oceanic heat was the transmitted solar radiation, which had resulted in a layer of warm water (0.3 to 0.4 K above local freezing temperature) between 10 and 30 m depth. During the observation period, fairly late in summer, the transmitted solar radiation was still about twice the oceanic heat flux, indicating this layer was continuing to accumulate heat. The heating of this near surface water layer represents a potentially significant feedback resulting from the transition to thinner, first-year ice, which allows more sunlight to reach the ocean beneath. The higher transmittance provides for an oceanic heat source to melt ice from below, but the fact that much of it is stored in the layer also provides significant potential to delay autumn freezing.

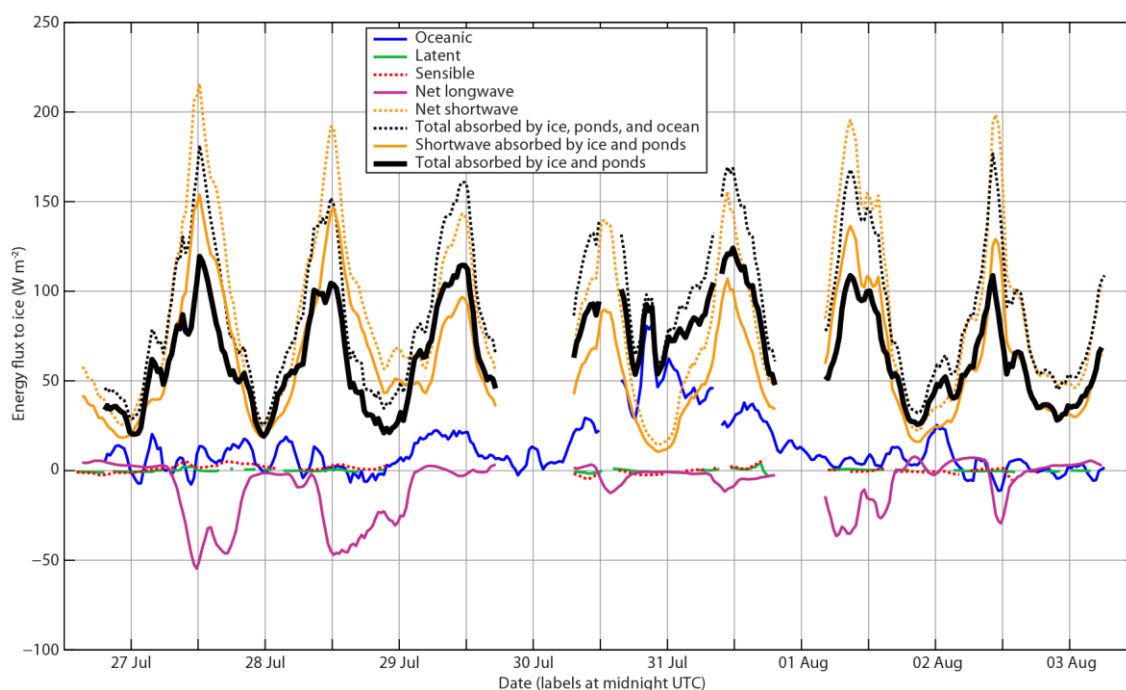


Figure 1. Time series of observed oceanic and atmospheric (sensible and latent) turbulent heat fluxes to the ice and net shortwave and longwave radiative fluxes. Also shown is the shortwave radiative flux absorbed by the ice and ponds in the ice-covered area (after removing the solar energy transmitted to the ocean). Turbulent fluxes are positive when they are providing heat to the ice; negative longwave fluxes indicate the ice is losing more heat to surface emission than it is gaining from atmospheric emission. All fluxes have been smoothed with a 2 h running mean. Totals are calculated for both the amount of energy absorbed by the ice (thick line) and by the ice-ocean system. In calculating the totals, missing atmospheric turbulent fluxes were assumed to be zero.

	Average (W m^{-2})	Contribution (%)
Shortwave	60.2	92.9
Longwave	-9.0	-13.8
Oceanic	13.1	20.3
Sensible	0.4	0.6
Latent	0.1	0.1
Total absorbed	64.8	100
Transmitted shortwave	26.0	-

Table 1. Average of the Observed Fluxes Absorbed by the Ice and Ponds. The shortwave value excludes that which was reflected or transmitted. The values are also presented as relative contributions to the total energy absorbed by the ice and ponds during the period. The bottom line shows the solar energy transmitted through the ice and ponds to the underlying ocean water.

REFERENCE

Hudson, S. R., M. A. Granskog, A. Sundfjord, A. Randelhoff, A. H. H. Renner, and D. V. Divine (2013). Energy budget of first-year Arctic sea ice in advanced stages of melt, *Geophys. Res. Lett.*, 40, doi:10.1002/grl.50517.

SOLAR ENERGY BUDGET OF FIRST-YEAR SEA ICE IN THE CENTRAL ARCTIC – AUTONOMOUS OBSERVATIONS FROM TWO SUMMER MELT SEASONS

C. Wang¹, M. A. Granskog¹, S. Gerland¹, S. R. Hudson¹, D. K. Perovich², M. Nicolaus³, T. I. Karlsen¹, K. Fossan¹, and M. Bratrein¹

¹Norwegian Polar Institute, Tromsø, Norway

granskog@npolar.no

²Cold Regions Research and Engineering Laboratory, Hanover, NH, USA

³Alfred-Wegener-Institut, Helmholtz-Zentrum für Polar- und Meeresforschung, Bremerhaven, Germany

ABSTRACTS

A Spectral Radiation Buoy (SRB) was developed to autonomously measure the spectral incident, reflected, and transmitted solar radiation (350 to 800 nm) above and below sea ice. It was deployed on drifting first-year sea ice near the North Pole prior to melt onset in April 2012, recovered in October 2012, and redeployed near the North Pole in April 2013, both times co-located with Ice Mass Balance (IMB) buoys. The buoys drifted southward, reaching the Fram Strait in early autumn, covering the complete melt season in both summers.

In 2012, albedo was high and transmittance was very low until snow melt onset, on 10 June. Figure 1 shows the seasonal progression of the individual spectral radiative fluxes and of the spectral albedo and transmittance. The decrease in snow depth after melt onset was accompanied by a decrease in albedo and an increase in transmittance. The greatest transmission of solar radiation to the ocean occurred in July (average 20 W m^{-2}), following the disappearance of snow and formation of melt ponds, which resulted in low albedo and high transmittance. The solar heat that accumulated in the ocean was enough to cause two thirds of the observed ice bottom melt; the remaining bottom melt may be explained by radiation entering through open water or melt ponds. Estimates of the energy absorbed in snow and ice corresponded well with observed surface melt, demonstrating that solar heating played an important role in the ice melt in the Arctic basin in 2012.

Recent data from 2013 indicate that snow melt onset was later than in 2012, and it took longer for the snow to melt completely, even though there was less snow in 2013. This may be due in part to lower temperatures in 2013. Thus albedo was higher and transmittance was lower than in summer 2012; however, this may also be due to the difference in the extent of melt ponds that were in the field of view of the SRB. All these factors likely had significant consequences for the energy available for ice melt. In this presentation we will examine in detail the partitioning of solar energy during these two contrasting summers, and showcase the importance of the surface conditions, especially snow cover, in the summer melt of Arctic sea ice.

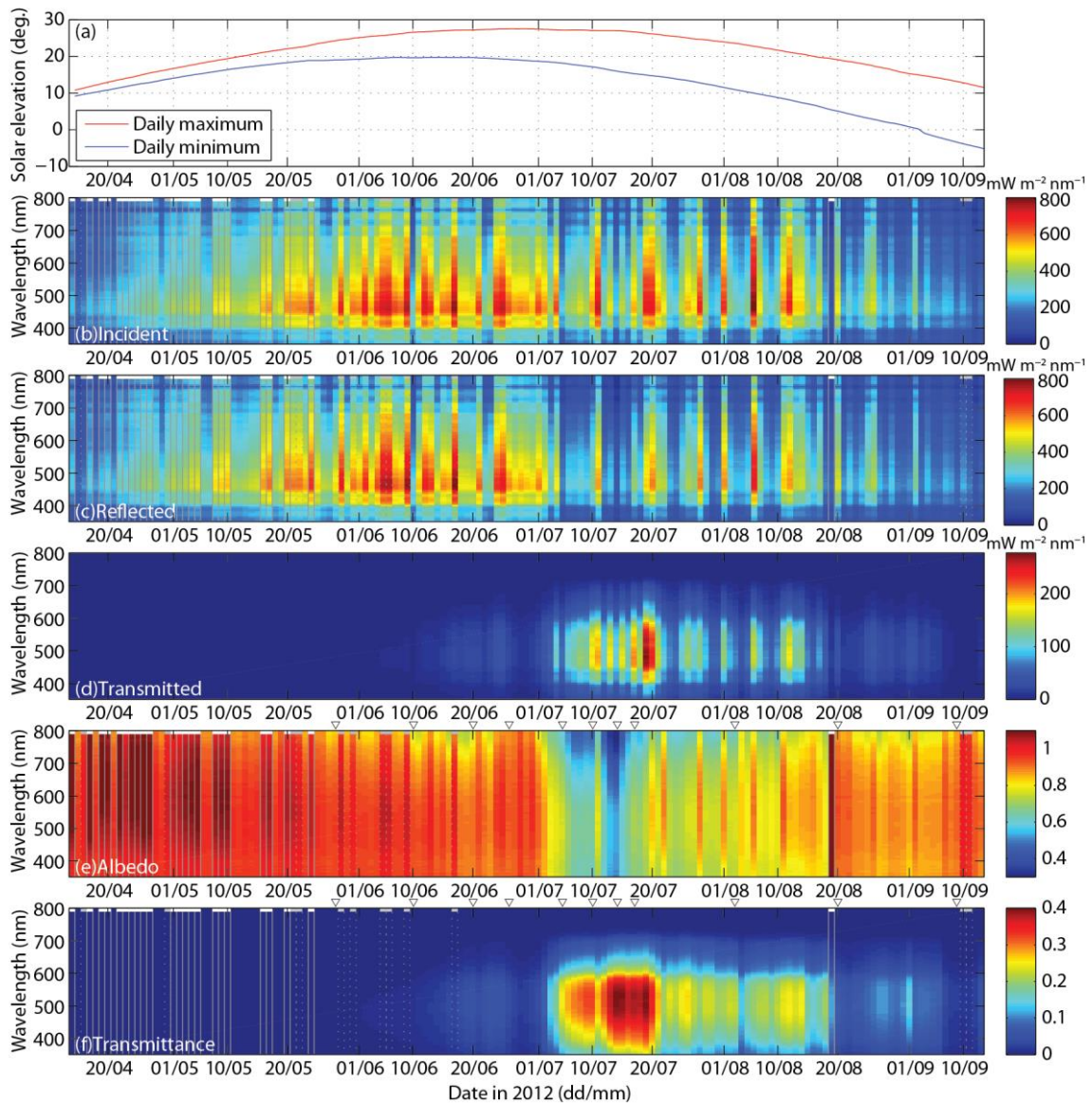


Figure 1. Daily maximum and minimum solar elevation at the SRB location during the drift (a). Spectral incident (b), reflected (c), and transmitted (d) solar flux and spectral albedo (e) and transmittance (f), observed at noon on each day during the drift. Observations made when the incident sensor was partially covered by precipitation, resulting in apparent albedo greater than 1 at any wavelength, are outlined in gray.

SESSION 3

PERMAFROST

CLIMATE AND PERMAFROST CHANGE IN WESTERN ALASKA: 115 YEARS OF MEASUREMENTS ON THE SEWARD PENINSULA

Jessica Cherry

*The International Arctic Research Center and the Institute of Northern Engineering,
University of Alaska Fairbanks
jessica.cherry@alaska.edu*

ABSTRACTS

This presentation explores the climate change and variability of Alaska's Seward Peninsula, as well as the impacts on permafrost distributions in this vulnerable part of the Arctic's cryosphere. Our group has maintained a network of meteorological sites throughout the Peninsula since 1999. We have also engaged in a major effort to rescue and digitize climate data from this region, which dates back to the late 19th Century. Mechanisms for change are discussed, as well as the role of the observational network coverage, and other human dimensions in our understanding of change. Finally, implications for climate system feedbacks such as biogeochemical fluxes, being studied by our KOPRI colleagues, will also be considered.

GREENHOUSE GAS EXCHANGE AT AN ALASKA PERMAFROST REGION

Sang-Jong Park*, Tae-Jin Choi, Jae-Il Yoo, Jung-Ok Son, and Namyi Chae¹

Korea Polar Research Institute, Songdomirae-ro 26, Yeonsu-gu, Incheon, 406-840 Korea

¹Yonsei University

sangjong@kopri.re.kr

ABSTRACT

Recent Arctic warming is thought to introduce environmental change over circum-arctic permafrost area in many ways. Warming of permafrost layer would increase the depth of active layer, where organic material has long been frozen in the past. Consequent massive release of greenhouse gases (i.e. carbon dioxide and methane) would then presumably enhance global warming. To monitor and understand physical and biological behavior of Arctic permafrost in a warming climate, we have operated an environmental monitoring site at Council, Alaska, USA since July 2012. In this presentation, we will show carbon dioxide flux as well as energy and water fluxes obtained from eddy-covariance system during summertime of 2012. Surface characteristics such as albedo, roughness length are also analyzed. Beside the eddy-covariance system, automatic chamber system was installed on typical vegetation around the site to investigate carbon flux variation more specifically. These results would be used to improve permafrost vegetation components in climate models. The observed carbon flux shows clear diurnal variation playing as a sink during summer days, which is changed to a source almost all day from October. Daytime sensible heat flux was shown to be as much as 250 Wm^{-2} in July and gradually decrease to be less than 50 Wm^{-2} by the late October. During nighttime, strong downward sensible heat flux greater than 50 Wm^{-2} is often observed from September. Latent heat flux shows as much as 150 Wm^{-2} in July but is decreased to be negligible from October.

THE PERMAFROST-DOMINATED ECOSYSTEMS IN A CHANGING CLIMATE

Trofim Chr. MAXIMOV, Dr.

Institute for Biological Problems of Cryolithozone of SB RAS, Yakutsk, Russia
BEST Center of BioGeographical Faculty of North Eastern Federal University, Yakutsk, Russia

ABSTRACTS

Almost 65% of Siberian forests and 23% of tundra vegetation grow in permafrost zone. According to our estimate, carbon stocks in the soils of forest and tundra ecosystems of Yakutia (Eastern Siberia, Russia) amount to 17 billion tons (125.5 million hectares of forest and 37 million hectares of tundra in total) that is about 25% of total carbon resource in forest soils of the Russian Federation.

Since the end of XIX century winter air temperatures in Arctic Siberia have risen by 10°C, and average annual ones – by 2.0-3.5°C. For the last 50 years in Eastern Siberia the average air temperature in January has grown by 7°C, i.e. it was increasing 1.5-2 times faster compared to the first half of the century. Mean annual air temperature has increased by 1.0-2°C. An increase in annual air temperature in the zone of permafrost development is able to cause the activation of biogeochemical processes, and speed up the release of greenhouse gases conserved in permafrost. Along with, the contribution of permafrost ecosystems to global and continental balances of carbon are still little-studied.

For the first time in the conditions of Eastern Siberia an attempt has been made to ground the photosynthetic productivity of plants in terms of physiology, and quantitative parameters of the productive process were obtained. Original data on sink-source relations of plants are stated at the levels of whole plant organism and community. A number of specific results have been got: 1) conclusion was made about high depositing role of the root system of high latitude plants; 2) micrometeorological estimates of carbon balance were done; 3) quantitative dependence of CO₂ concentration on the season period, weather condition and forest fire intensity was shown; 4) carbon parameters of forest and tundra ecosystems were investigated; 5) attention was drawn to short growing season of plant development – this feature contributes to enrichment of the atmosphere of high latitudes by carbon dioxide.

Permafrost forest and tundra ecosystems at present are estimated by carbon budget as areas of significant carbon sink. However, under predicted climate warming, their functions as carbon absorbers will essentially depend on the result of coordination of antagonistic processes: 1) increasing of carbon accumulation owing to prolonged growing season and elevated summer air temperatures; 2) frequency raise of forest fires that result in increased carbon dioxide emission into the atmosphere.

STRUCTURE OF THE ATMOSPHERIC BOUNDARY LAYER AT NY ALESUND: STATISTICS AND CASE STUDIES

*Angelo P. Viola⁽¹⁾, Francesco Tampieri⁽¹⁾, Mauro Mazzola⁽¹⁾, Taejin Choi⁽²⁾,
Christian Lanconelli⁽¹⁾, Angelo Lupi⁽¹⁾, Marion Maturilli⁽³⁾, Armando Pelliccioni^(1,4)*

⁽¹⁾ CNR Institute of Atmospheric Sciences and Climate, Bologna and Roma, Italy

⁽²⁾ Korean Polar Research Institute, Incheon, Korea

*⁽³⁾ Alfred Wegener Institute Helmholtz Centre for Polar and Marine Research, Potsdam,
Germany*

⁽⁴⁾ INAIL, Roma, Italy

ABSTRACTS

The Amundsen-Nobile Climate Change Tower (CCT) at Ny Ålesund - Svalbard is a 33 m high observation platform particularly suited for investigating the thermodynamic characteristics the planetary boundary layer (PBL) at multiple levels using fast and slow response instruments. A set of four conventional meteorological sensors positioned at 2, 5, 10 and 33 m and three sonic anemometers at 3.7, 7.5 and 21 m of height is the main atmospheric equipment. Radiation and snow height sensors are also installed as well as instruments to estimate the heat flux into the snow and to measure the radiation fluxes and balance at the surface. For some periods a tethered balloon equipped with meteorological sensors was operational to provide temperature, humidity and wind up to 600-700 m. Selected period with optimal data coverage, for different seasons, have been investigated to test the literature profiles based on the Monin-Obukhov Similarity Theory (MOST). The shape of the similarity function is evaluated in different stability conditions. By using the set of three sonic anemometers, the vertical structure of the boundary layer above the surface layer is also investigated.

Introduction

Climate, weather and air quality are themes of overwhelming importance for society. The understanding of fundamental processes of the atmosphere is a key aspect to forecast and to develop reliable scenarios. Among these processes, the exchange of momentum, heat and tracers plays a relevant role. The increase of mean temperature of the atmosphere leads to modify the climatological fluxes at the various latitudes. The urbanization process (remember that today more than half of the world population lives in cities) and the development of industrial activities in new countries affect and are affected by the changing atmospheric composition at regional and global scales.

The Arctic land areas are subject to warming faster than other region on earth. The “Arctic amplification” may be due to feedback mechanisms from loss of sea ice or changes in atmospheric and oceanic circulations. To deepen the knowledge of such mechanisms a 32 m high platform named Amundsen-Nobile Climate Change Tower (CCT) has been set up at Ny Ålesund - Svalbard on 2009 by Italian CNR. Multiple levels of fast and slow response instruments are provided to investigate the processes related to the energy balance and to the mean and the turbulent characteristics of the planetary boundary layer (PBL) under different conditions. Purpose of this research is to exploit the in-depth use of measurements

in the atmospheric boundary layer made with different kind of instruments to understand its dynamic features and to develop parameterizations necessary for improved weather forecasts, air quality assessment and climatic simulations.

Site and measurements

The Amundsen-Nobile Climate Change Tower is located at the confluence zone of two glacier (78 55 20 N, 11 52 8 E , 50 m asl), 1.2 km apart from the village of Ny Å lesund. It faces the main wind flow from southeast and the closest (1.5 km) relief is Mount Zeppelin (475 m) in south direction (Fig 1). The set of conventional sensors includes four Vaisala thermo-hygrometer and four Young propeller anemometer positioned 2, 5, 10 and 33 m respectively. The fast response sensors set includes two Gill Solent and a Campbell CSAT3 sonic anemometers at 3.7 m 7.5 m and 21 m of height, respectively. The last one has been installed on May 2012 by KOPRI in the frame of the collaboration between Italy and Korea. Radiation measurements are available and sensors to estimate the heat flux into the snow are also installed on the ground. For some periods a tethered balloon equipped with meteorological sensors is operated by AWI (Germany) to provide temperature, humidity and wind up to 600 - 700 m.

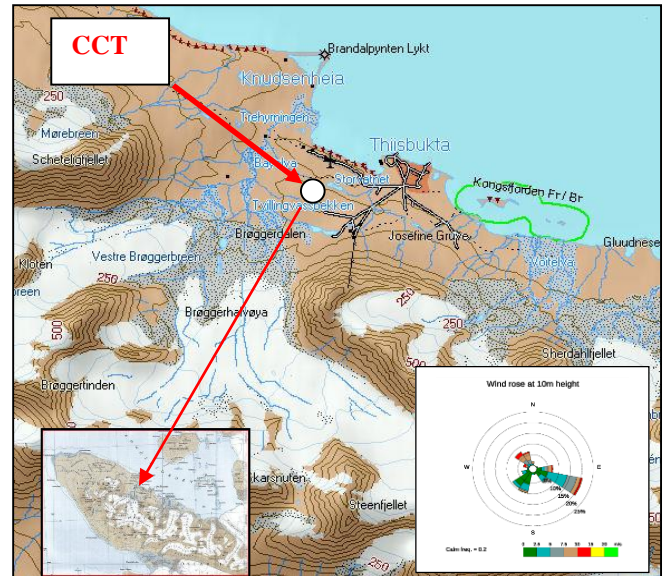


Fig 1: map of the area and location of the CCT.

The structure of the surface layer

Based on a selected set of periods with optimal coverage of data and referring to different seasons (and thus to different radiative and large scale meteorological forcing) the wind in the surface layer has been investigated to test surface layer literature profiles based on the widely used Monin-Obukhov Similarity Theory (MOST).

The dependence of the roughness length z_0 on the snow coverage and on the wind direction has been retrieved using almost neutral profiles, fitted by the logarithmic law $u(z)=u_*k \log(z/z_0)$ and using quite selective criteria (neutral conditions $|z/L| \leq 0.01$; vertical alignment of the wind direction ($R = (\frac{WD}{WD}) \leq 0.03$); strong correlation ($r^2 \geq 0.90$) of the measured profiles with logarithmic law and correcting of the measurement heights by to the snow height data (Fig. 2).

	WD (304- 311)	WD (196-216)	WD (116-123)	z_0 (monthly mean)
Jan	0.06764	0.28941	0.12859	0.162
May	0.01080	1.00258	0.18215	0.399
Jun-Jul	0.52087	2.43620	-	1.479
z_0 (WD mean)	0.200	1.243	0.155	

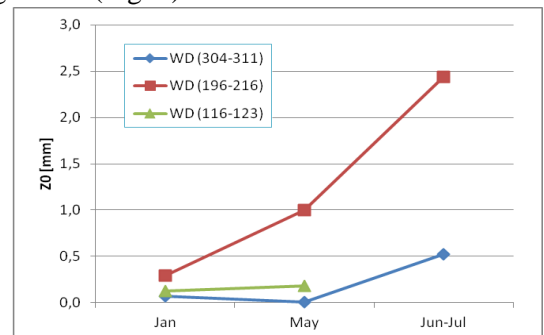


Fig 2: roughness length for different seasons and different wind directions.

The shape of the similarity function has been evaluated in different stability conditions, expressed as

function of z/L , being L the Obukhov length determined from the turbulent fluxes measured by a sonic anemometer placed at 7.5 m height.

For the unstable case, the formulas for the non dimensional gradient by Kader and Yaglom (1990) and by Hogstrom (1996) have been used.

$$\Phi_m = 1 \text{ for } z/|L| < 0.1 \quad \Phi_m = \alpha_{KY} \left(\frac{z}{|L|} \right)^{1/3} \text{ for } z/|L| > 1$$

$$\Phi_m = (1 - \beta_m z/|L|)^{-1/4} \text{ for } z/|L| < 2$$

The results are shown in Fig. 3 (left) where KY formula seems better describe the data (with a proper coefficient, different from the original one).

For the stable case, the Högström (1996) log-linear law and the Beljaars-Hotslag (1991) formulations have been used

$$\Phi_m = 1 + \alpha_{m3} z/L$$

$$\Phi_m = 1 + a z/L + b z/L (1 + c - d z/L) \exp(-d z/L)$$

The results are shown in Fig. 3 (right) and indicate a good agreement.

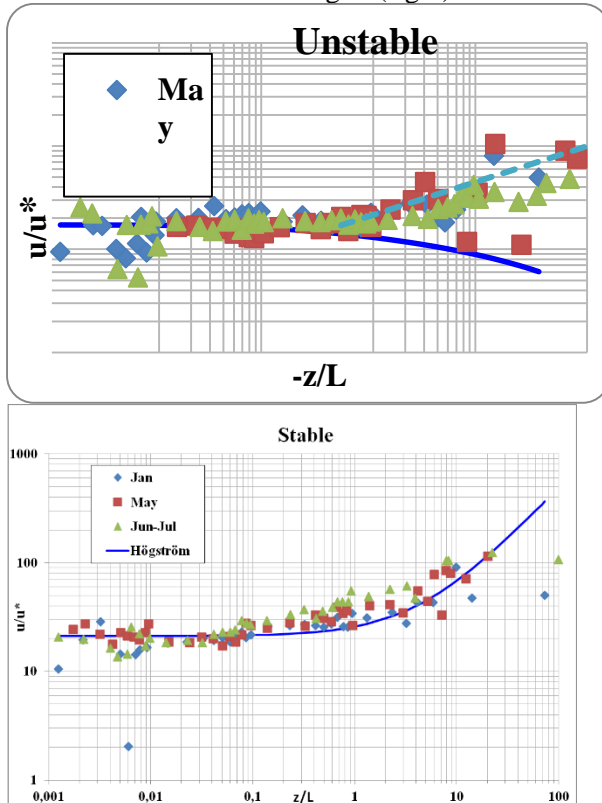


Fig. 3: u/u^* for unstable cases (left) and for stable cases (right). Symbols refer to data for different time periods, each symbol reports the mean value for suitably chosen bins in z/L .

For some particular periods, selected analyzing CCT profiles as those shown in Fig. 4, simultaneous tethered balloon vertical profiles of wind and temperature have been merged with the CCT data, in order to extend the investigation to the vertical structure of the entire boundary layer.

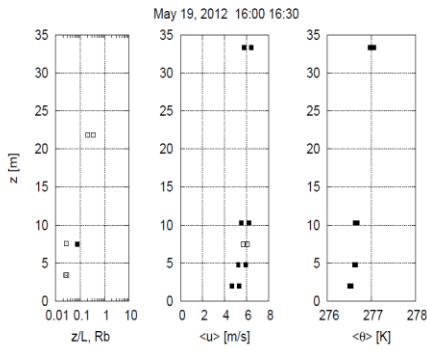


Fig 4: vertical profiles of z/L (fill square) and Richardson number (open squares), wind speed and potential temperature at CCT for a stable case.

The vertical structure of planetary boundary layer

The set of three sonic anemometers data has been used to investigate the vertical structure of the PBL above the surface layer. Although the boundary layer height may be quite larger than the tower height, cases of small positive forcing and cases of moderately stable conditions occur, in which the tower spans most of the PBL itself. In particular the turbulent kinetic energy and the sensible heat flux profiles can be studied as function of height and of the stability of the layer, expressed in terms of bulk Richardson number, and a possible estimation of the PBL height related to the level where the fluxes become zero can be given. A case study for SBL (stable) and one for CBL (convective) are illustrated in Figs. 5 and 6 respectively.

For SBL, the decrease of fluxes and of variances with height is evident, consistent with boundary layer height of about 30 m, estimated from the heights at which the fitted curves go to zero. The profiles are consistent with Nieuwstadt (1984) but with different heights at variance with the theory. The equilibrium formula by Zilitinkevich and Esau (2007) suggests the correct order of magnitude (and can be tuned properly).

For CBL the stability conditions lead to evidence the free-convection increase of $\langle w^2 \rangle$ and the corresponding decrease of $\langle \tau^2 \rangle$, compatible with a PBL height of about 200m. Heat fluxes decay quite rapidly, more than can be seen from LES (Canuto et al., 1994) or field observations (Hartmann, pers. comm.).

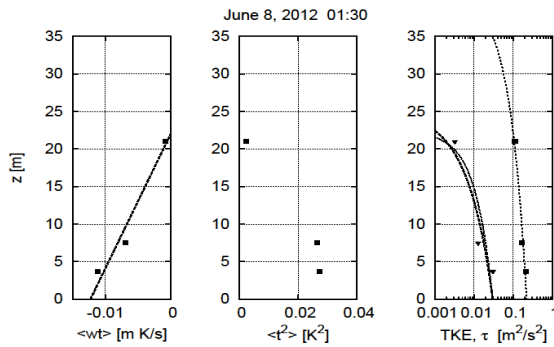


Fig. 5: profiles of heat flux, temperature variance, and turbulent kinetic energy (TKE, squares), momentum flux (triangles) for SBL. The dashed lines correspond to the linear fits. For momentum flux, also a power law fit is shown.

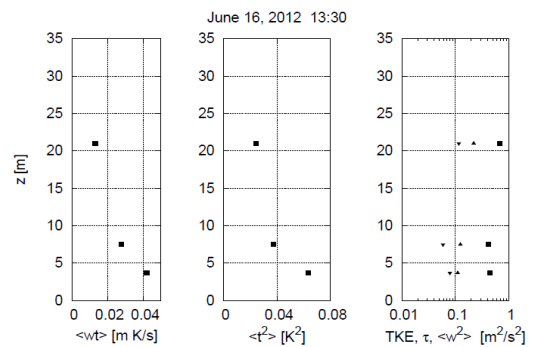
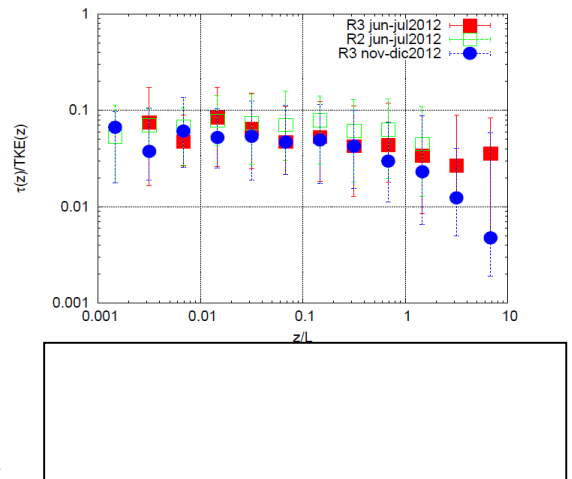


Fig.6: profiles of heat flux, temperature variance, and turbulent kinetic energy (squares), momentum flux (pointing down triangle) and vertical velocity variance (pointing up triangle) for CBL.

The similarity dimensionless rules (used in the PBL parameterization for NWF and atmospheric composition models) relating momentum and heat fluxes, velocity and temperature variances to turbulent kinetic energy are evaluated and literature results also validated under different stability conditions. An example is reported in Fig. 7. The different symbols refer to R2 and R3 and to different time periods (only for R3). A general decrease of u_*^2/TKE is depicted, as stability increases according to literature results (see for instance Mauritsen and Svensson, 2007). Note that all the values are quite smaller than the literature ones.



Conclusions

The experimental setup and the long term measurements allow investigating the dynamic features of PBL at CCT, partially confirming well accepted results and partially posing new questions. The study has shown that the values of z_0 are coherent with the literature for this soil type, presenting a dependence on wind conditions and a seasonal variability.

For instance, the literature profiles for non-dimensional wind are quite confirmed in stable cases, whereas in unstable cases the predictions of Kader and Yaglom (1990) fit the data trend much better than the Högström, (1996) law, but with a different numerical coefficient.

The vertical profile of turbulence allows to new estimates of the PBL height in stable conditions, to be compared with literature formulations. The study of the non-dimensional ratios of turbulent quantities (here the momentum flux over turbulent kinetic energy is shown) shows the well known decrease with stability, but with numerical values smaller than those currently accepted.

References

- Högström, U., 1996: Review of some basic characteristics of the atmospheric surface layer. *Boundary-Layer Meteorology*, 78, 215–246.
- Beljaars, A. and A. A. M. Holtslag, 1991: Flux parameterization over land surfaces for atmospheric models. *J. Appl. Meteorol.*, 30, 327–341.
- Kader, B. A. and A. M. Yaglom, 1990: Mean fields and fluctuation moments in unstably stratified turbulent boundary layers. *J. Fluid Mech.*, 212, 637– 662.
- Nieuwstadt, F. T. M., 1984: The turbulent structure of the stable, nocturnal boundary layer. *J. Atmos. Sci.*, 41, 2202–2216.
- Canuto, V. M., F. Minotti, C. Ronchi, and R. Ypma, 1994: Second-order closure PBL model with new third-order moments: comparison with LES data. *Journal of the Atmospheric Sciences*, 51, 1605–1618.
- Mauritsen, T. and G. Svensson, 2007: Observations of stably stratified shear-driven atmospheric turbulence at low and high richardson numbers. *Journal of Atmospheric Sciences*, 64, 645–655.
- Zilitinkevich, S. S. and I. N. Esau, 2007: Similarity theory and calculation of turbulent fluxes at the surface for the stably stratified atmospheric boundary layer. *Boundary-Layer Meteorology*, 125, 193–205.

Acknowledgements

This work was supported by National Research Foundation of Korea-Grant funded by the Korean Government (Ministry of Science, ICT and Future Planning)-2013-2012K1A3A1A25038619 and by the Italian Ministry of Foreign Affairs in the frame of bilateral project Italy- Korea 2013-2015.

SIMULTANEOUS MEASUREMENTS OF CARBON EXCHANGE OVER THREE PERMAFROST SITES AT THE ARCTIC

Taejin Choi, Sang Jong Park, Jaeill Yoo, Bang Yong Lee, Young Jun Yoon

*Division of Polar Climate Research,
Korea Polar Research Institute
ctjin@kopri.re.kr*

ABSTRACTS

To better understand carbon cycle over the Arctic is very important in prognosing future climate change. Despite of its importance, studies on carbon cycle based on in situ measurement are limited, especially permafrost area. In addition, recent interest of climate change science in arctic region goes to multidisciplinary studies, integrating atmospheric and biological monitoring at an atmosphere-biosphere interface, and modeling to expand understanding of its process. Carbon flux measurements have been simultaneously performed at permafrost sites of the Arctic, located at Council, Alaska, USA (64°N/165°W), Cambridge Bay, Canada (69°N/105°W) and Ny-Alesund, Norway (79°N/12°E) led by KOPRI's CAMP program through collaboration with IARC, USA(Council), Nunavut Research Institute, Canada(Cambridge Bay) and CNR, Italy(Ny-Alesund). The purpose of the measurements are to evaluate whether the current permafrost sites at high Arctic region are a sink or source for the atmospheric carbon, and how the sinks or sources are affected by the Arctic warming, especially permafrost degrade and to contribute to the better understanding of carbon cycle over the Arctic. Since the sites have different climate, vegetation, soil properties and so on, in situ measurement data can be used at various fields such as process study, linkage with satellite and ecosystem models. Air temperature ranges from -30 to 10 °C and annual precipitation is in the range of 100 to 400 mm. Based on the circumpolar arctic vegetation map (<http://www.geobotany.uaf.edu/cavm/>), three site are classified as P1 (prostrate dwarf-shrub, Cambridge Bay and Ny-Alesund) and W3 (sedge, moss, low-shrub wetland, Council). Open- and closed- path eddy covariance system, measuring directly the exchanges of CO₂, CH₄, energy and momentum between the atmosphere and permafrost were used. Especially, at the site in Ny-Alesund with a 30m walk-up tower(the Amundsen Nobile Climate Change Tower established in 2009 by National Research Council(CNR), Italy), where electric power and the internet are available, closed-path CRDS has been operated to measure methane flux together with open-path CH₄ analyser since May of 2012. In this presentation, we will present preliminary results on greenhouse gas fluxes in 2012 in terms of different climate, vegetation type and soil properties. *This research was supported by the National Research Foundation of Korea Grant funded by the Korean Government (MEST) (NRF-CIABA001-2011-0021063, PN13081).*

SESSION 4

ARCTIC TERRESTRIAL ECOSYSTEMS

THE FUTURE TERRESTRIAL ARCTIC: PROJECTIONS FOR PERMAFROST AND SNOW

Andrew G. Slater¹ and David M. Lawrence²

1 National Snow and Ice Data Center, University of Colorado, USA
2 National Center for Atmospheric Research, Boulder, Colorado, USA
[*aslater@kryos.colorado.edu*](mailto:aslater@kryos.colorado.edu)

ABSTRACT

The terrestrial Arctic is experiencing considerable change in many aspects of the climate system, from altered vegetation patterns to shrinking glaciers. Permafrost is a characteristic aspect of the terrestrial Arctic and the fate of near-surface permafrost over the next century is likely to exert strong controls on Arctic hydrology and biogeochemistry. Using output from the fifth phase of the Coupled Model Intercomparison Project (CMIP5), the authors assess its ability to simulate present-day and future permafrost. Permafrost extent diagnosed directly from each climate model's soil temperature is a function of the modeled surface climate as well as the ability of the land surface model to represent permafrost physics. For each CMIP5 model these two effects are separated by using indirect estimators of permafrost driven by climatic indices and compared to permafrost extent directly diagnosed via soil temperatures. Several robust conclusions can be drawn from this analysis. Significant air temperature and snow depth biases exist in some model's climates, which degrade both directly and indirectly diagnosed permafrost conditions. The range of directly calculated present-day (1986–2005) permafrost area is extremely large ($\sim 4\text{--}25 \times 10^6 \text{ km}^2$). Several land models contain structural weaknesses that limit their skill in simulating cold region subsurface processes. Because of sizable differences in future climates for the representative concentration pathway (RCP) emission scenarios, a wide variety of future permafrost states is predicted by 2100 [Figure 1]. Conservatively, the models suggest that for RCP4.5, permafrost will retreat from the present-day discontinuous zone. Under RCP8.5, sustainable permafrost will be most probable only in the Canadian Archipelago, Russian Arctic coast, and east Siberian uplands.

Snow produces the most variable surface condition on a global scale and it impacts the terrestrial system through its ability to insulate the ground, act as a moisture store and reflect shortwave radiation. Present-day simulations of snow mass across the Arctic by CMIP5 models are compared to various observational data sets; large uncertainties exist in both observations and models. Future regimes of Arctic snow suggest deeper mid-winter snow, but an earlier melt. Satellite observations since the 1960's show a noticeable seasonal cycle in northern hemisphere snow extent trends, with earlier spring melt being an obvious feature. Indeed, the largest retreat in northern hemisphere snow extent over a one- to two-month period was observed in 2013 [Figure 2]. However, models have had difficulty reproducing the extent trend of the past 45 years.

Permafrost Area (via Surface Frost Index with CMIP5 Climate Change from Present Day)

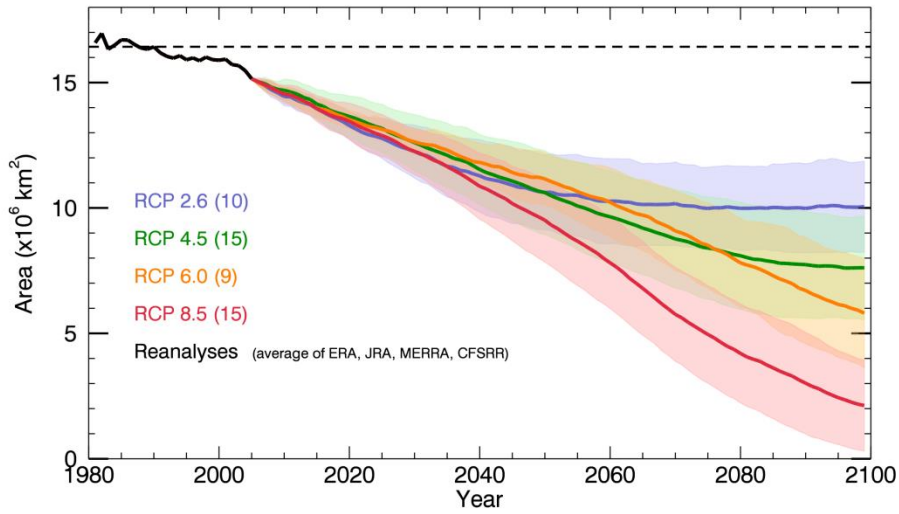


Figure 1: Projected extent of sustainable permafrost over the 21st Century, based on surface climate trajectories from numerous CMIP5 climate models. (Figure is copyright of the American Meteorological Society: Slater and Lawrence [2013]: Diagnosing Present and Future Permafrost from Climate Models. *J. Climate*, **26**, 5608–5623.)

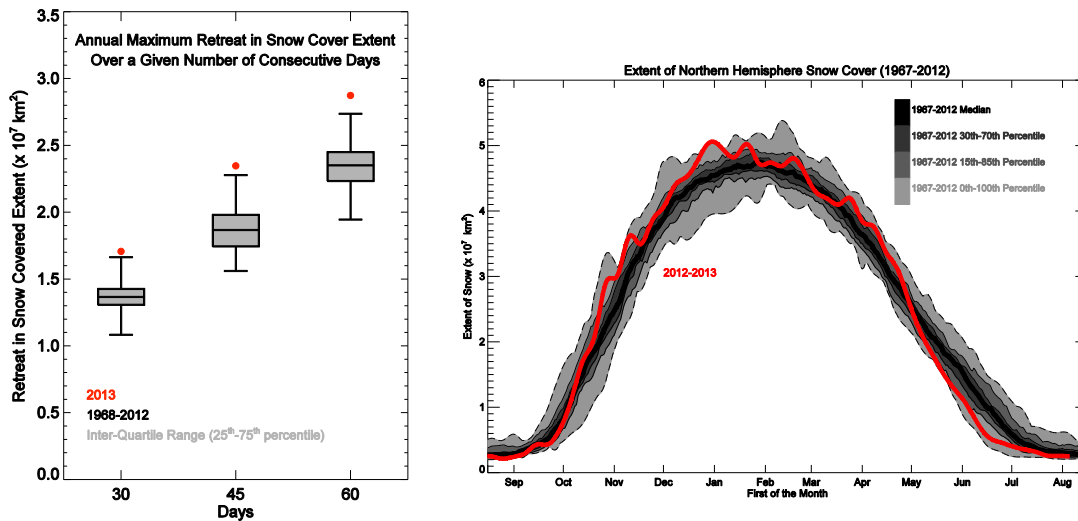


Figure 2: Left panel shows the large and rapid retreat of snow cover extent seen in 2013 compared to all prior years on record. Snow extent rapidly changed from near record high extent in April to one of the lowest extents ever in May (right panel).

METHANE DYNAMICS UNDER MELTING EXCESS ICE AND PERMAFROST THAW IN THE COMMUNITY LAND MODEL 4.5

Hanna Lee, Sean C. Swenson, David M. Lawrence

*Climate and Global Dynamics Division,
National Center for Atmospheric Research,
Boulder, Colorado, USA
hannal@ucar.edu*

Andrew G. Slater

*National Snow and Ice Data Center,
Boulder, Colorado, USA*

ABSTRACTS

Permafrost soils characterize the Arctic landscape and are known to contain massive soil carbon (C) pools that are vulnerable to changing climate. The response of permafrost soils to Arctic warming represents a major source of uncertainty in projecting C-cycle climate feedbacks. Permafrost soils are highly heterogeneous, especially related to oxygen availability and redox conditions that govern the C-cycle response to changing soil conditions and the production and consumption of methane (CH₄) and carbon dioxide (CO₂). Uncertainty in the mechanisms controlling C mineralization is compounded by concurrent changes in soil hydrology associated with permafrost thaw. Until recently, the ESMs that incorporate global C cycle-climate feedbacks lacked sufficient structural completeness to realistically represent permafrost-C feedbacks. Developments in the most recent version of the Community Land Model (CLM4.5, released in June 2013, <http://www.cesm.ucar.edu/models/cesm1.2/clm/>) target a more complete representation of permafrost soil biogeophysical and biogeochemical processes and provide an exciting tool with which we can scale our understanding of hydrological influences on the C dynamics of thawing Arctic soils. Recent developments in CLM4.5BGC (the biogeochemistry subcomponent of the CLM4.5 that includes simulations of CH₄ production and oxidation) aimed to improve representation of the complex biogeophysical and biogeochemical interactions characteristic of permafrost soils. These model development efforts, however, have outpaced collection of data in permafrost systems. To date, model validation efforts have largely relied on surface flux measurements of CO₂ and CH₄. These surface measurements alone cannot properly evaluate the processes represented in the vertically resolved structure of the model because they represent the net sum of CH₄ production and oxidation throughout the soil column and are not directly linked to subsurface drivers that vary across steep vertical gradients. The objective of this study was to present the model structure related to aerobic and anaerobic CO₂ and CH₄ production and oxidation within the new version of CLM4.5BGC and suggest the types of observations that are necessary to evaluate and enhance the model. In addition, the newly developed excess ice features in the CLM4.5 was tested to show how permafrost-thaw associated land surface subsidence influences future simulations of CH₄ from thawing permafrost.

In this study, we integrated a new module including excess ice in permafrost regions into the CLM4.5 (Oleson *et al.*, 2013). The CLM is the land component of the Community Earth System Model. It is a process-based model that includes modules to simulate photosynthesis, energy balance, soil heat and biogeochemistry, surface runoff and groundwater, and snow and soil ice dynamics. The thermal and hydrological properties of the soil are determined by a weighted combination of mineral and organic soil content (Lawrence *et al.*, 2008). Heat conduction through the soil is dependent on the thermal and hydrological properties of each soil layer and is a function of soil liquid and ice water content, soil texture (sand, silt, clay, organic), and soil temperature. A comprehensive technical description of CLM4 is provided in Oleson *et al.* (2013).

We include several changes to the default CLM4 cold region hydrology parameterization, including the introduction of a stronger ice impedance function, which alleviates the cold bias and generates more realistic active layer hydrological conditions (Swenson *et al.*, 2012)

We incorporated excess ice in the CLM soil layers. For the amount of excess ice, we used information from the Circum-Arctic Map of Permafrost and Ground-Ice Conditions archived in the National Snow and Ice Data Center (<http://nsidc.org/data/ggd318.html>; Brown *et al.* 1997). The circumpolar permafrost and ground ice data contribute to a unified international data set that depicts the distribution and properties of permafrost and ground ice in the Northern Hemisphere (20°N to 90°N). The re-gridded data set shows discontinuous, sporadic, or isolated permafrost boundaries. Permafrost extent is estimated in percent area (90-100%, 50-90%, 10-50%, <10%, and no permafrost). Relative abundance of ground ice in the upper 20 m is estimated in percent volume (>20%, 10-20%, <10%, and 0%). The data set also contains the location of subsea and relict permafrost. The gridded data are gridded at 12.5 km, 25 km, and 0.5 degree resolution. We merged these data into 1-degree resolution and percent area of low, medium, and high values into percent of ground ice in the upper 20m within the grid cell. In this study, we used mean values to understand vulnerability of permafrost under future climate with and without the presence of excess ice.

Incorporating excess ice allowed simulation of land surface subsidence at a gridcell mean level. However, incorporating excess ice did not influence the extent of permafrost over time of current day and future simulations using the RCP8.5 climate scenario. Instead, structure of soil temperature and moisture profiles have changed due to excess ice incorporation. As a result, the magnitude and structure of CH₄ production and oxidation both in saturated and unsaturated areas were influenced with excess ice (Figure 1 and 2) as CH₄ dynamics highly depend on soil temperature and oxidation availability, which is sensitive to soil moisture (Riley *et al.*, 2011).

References

- Brown J, Ferrans Jr. OJ, Heginbottom JA, Melnikov ES (1997) Circum-Arctic Map of Permafrost and Ground-Ice Conditions. Version 2. . pp Page, Boulder, Colorado USA: National Snow and Ice Data Center.
- Lawrence DM, Slater AG, Romanovsky VE, Nicolsky DJ (2008) Sensitivity of a model projection of near-surface permafrost degradation to soil column depth and representation of soil organic matter. *Journal of Geophysical Research-Earth Surface*, **113**.
- Oleson KW, Lawrence DM, Bonan GB *et al.* (2013) Technical Description of version 4.5 of the Community Land Model (CLM). In: *NCAR Technical Note NCAR/TN-478+STR*. pp Page, National Center for Atmospheric Research, Boulder, CO.
- Riley WJ, Subin ZM, Lawrence DM *et al.* (2011) Barriers to predicting changes in global terrestrial methane fluxes: analyses using CLM4Me, a methane biogeochemistry model integrated in CESM. *Biogeosciences*, **8**, 1925-1953.
- Swenson SC, Lawrence DM, Lee H (2012) Improved simulation of the terrestrial hydrological cycle in permafrost regions by the Community Land Model. *Journal of Advances in Modeling Earth Systems*, **4**.

Figure 1. Model simulations showing the capabilities of vertically resolved CH₄ production and oxidation (mg CH₄ m⁻² d⁻¹) at saturated and unsaturated part of the gridcell, soil temperature, and soil moisture using CLM4.5BGC (July monthly average at a gridcell representing Fairbanks, AK).

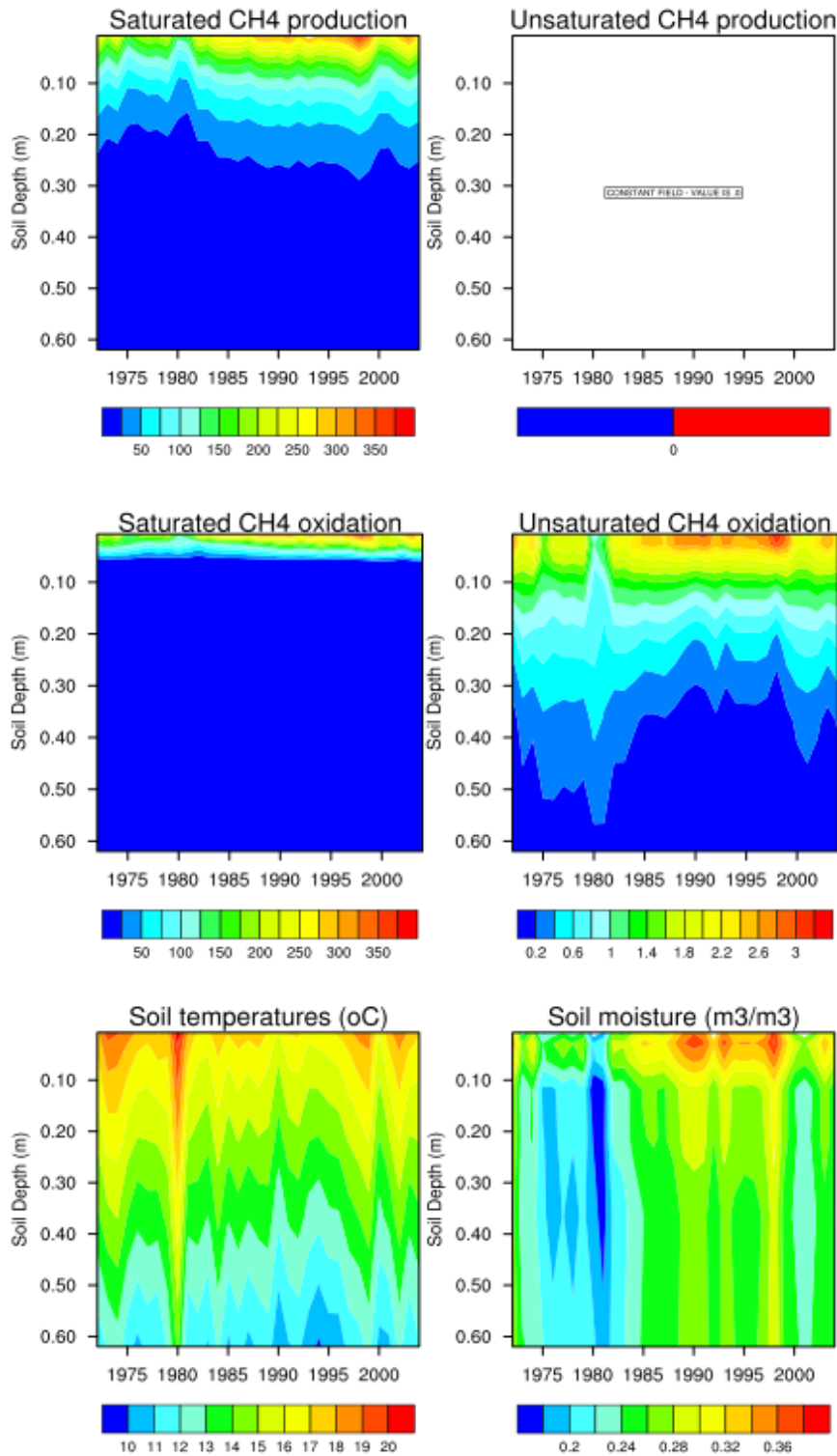
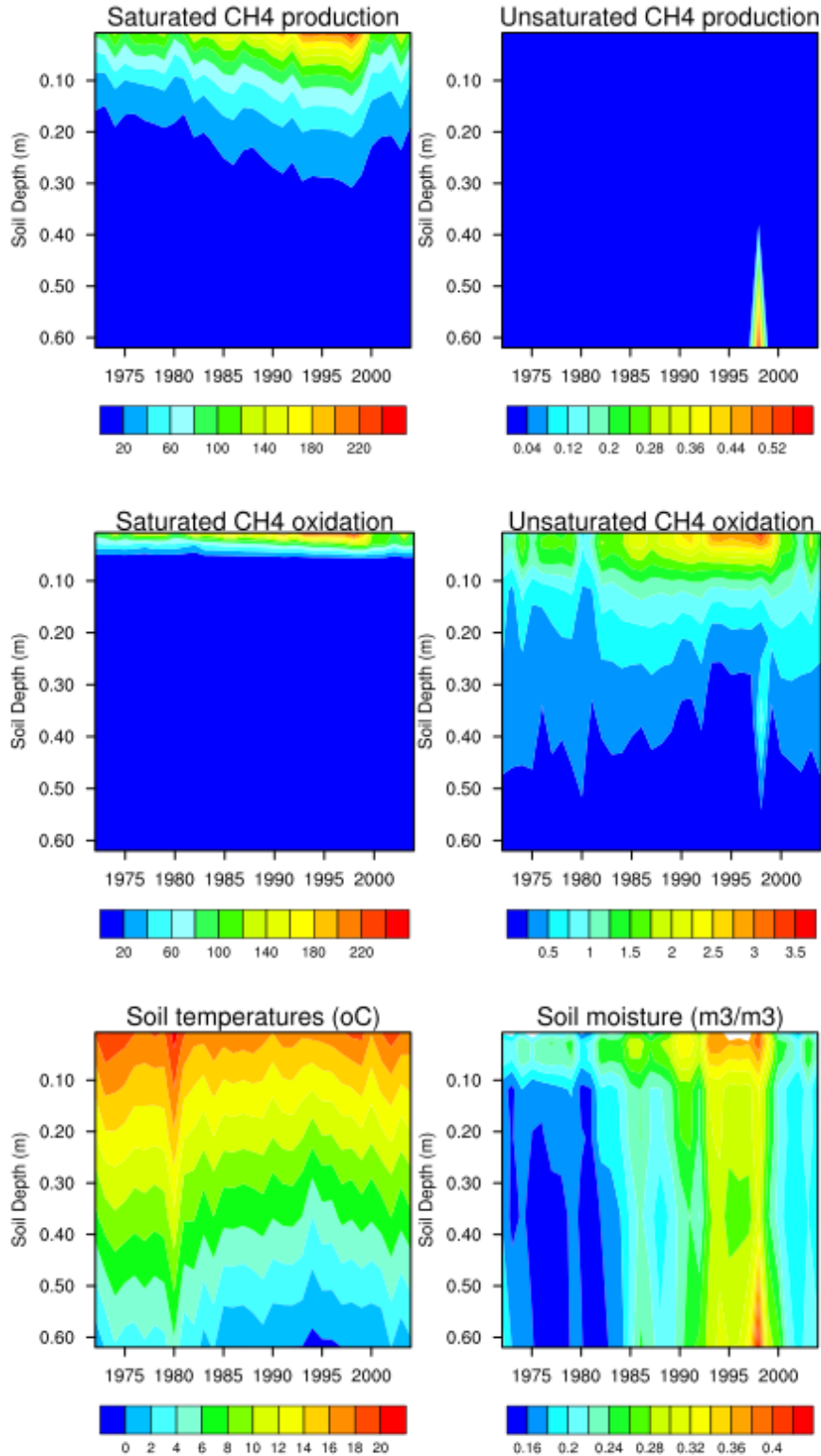


Figure 2. Model simulations with excess ice incorporation showing the capabilities of vertically resolved CH₄ production and oxidation (mg CH₄ m⁻² d⁻¹) at saturated and unsaturated part of the gridcell, soil temperature, and soil moisture using CLM4.5BGC (July monthly average at a gridcell representing Fairbanks, AK).



'DYNAMIC DISEQUILIBRIA' IN THE ARCTIC TERRESTRIAL REALM: LANDSCAPES AND ECOSYSTEMS IN TRANSITION

Philip A Wookey

*School of Life Sciences, Biological Sciences
Heriot Watt University
Edinburgh, EH14 4AS
Scotland, UK
p.a.wookey@hw.ac.uk*

ABSTRACTS

Rapid warming in the Arctic terrestrial realm, linked with the 'Arctic Amplification' (Hansen et al. 2006; Serreze & Francis, 2006) and changes in sea ice extent and distribution, is prompting biotic responses at the organismal, community and ecosystem scale (Chapin et al. 2005; Tape et al. 2006; Post et al. 2009; Myers-Smith et al. 2011; Epstein et al. 2012). Lines of evidence from long-term monitoring, experimental studies and remote sensing (Callaghan et al. 2009; Elmendorf et al. 2011; Epstein et al. 2012; Marcia-Faurias et al. 2013) are converging; significant biotic responses to climate change are strongly underway in the Arctic. These direct responses to climate forcing are also superimposed upon, and modulated by, changes in the cryosphere (e.g. active-layer deepening; thermokarst slumping and collapse of peat plateaus, and changes in the depth, duration, distribution and physical properties of snow in the landscape) (Flanner et al. 2011; AMAP 2012). The combined biospheric and cryospheric changes in the Arctic have substantial implications (through physical, biophysical and biogeochemical feedback processes) for the Earth System (McGuire et al. 2006; Schuur et al. 2008; Flanner et al. 2011; Koven et al. 2011; AMAP 2012), as well as for the provision of ecosystem goods and services in the Arctic and further south (Forbes et al. 2009; Marcia-Faurias et al. 2013).

Under climate forcing, different ecosystem components and processes have inherently contrasting timescales of response (Shaver et al. 2000); photosynthesis, for example, will respond within seconds to changes in light availability, while soil respiration will respond within minutes to hours to changes in soil temperature and/or moisture. By contrast, plant phenological shifts might be measured in timescales of days to weeks, while community change, or adjustments in soil organic matter pools and nutrient status, will take years through millennia (Pearson et al. 2013). The consequence of these contrasting response dynamics is that components of ecosystems and landscapes, across large regions of the circumpolar north, will increasingly be at disequilibrium both with the prevailing climate and with their own internal components (i.e. contrasting trophic levels, or above- and below-ground parts). This raises the prospect of substantial changes in ecosystem structure and function, including altered carbon (C) and water budgets (i.e. changes in the magnitude, and even direction, of net fluxes of radiatively-forcing 'greenhouse' gases), surface energy budgets, trophic interactions, biodiversity and ecosystem service provision.

With 'dynamic disequilibria' (Luo & Weng, 2011) intensifying in the coming decades ecosystems will increasingly be operating in 'catch-up' mode, but with no clear end-point. It is crucial to recognize that these responses will co-occur with dramatic change in the cryosphere. For example, C stocks in permafrost soils are massive (Hugelius et al. 2013); 1,672 Pg C, based on current best estimates, which is more than is currently stored in the atmosphere and living vegetation on earth, combined (Fig. 1).

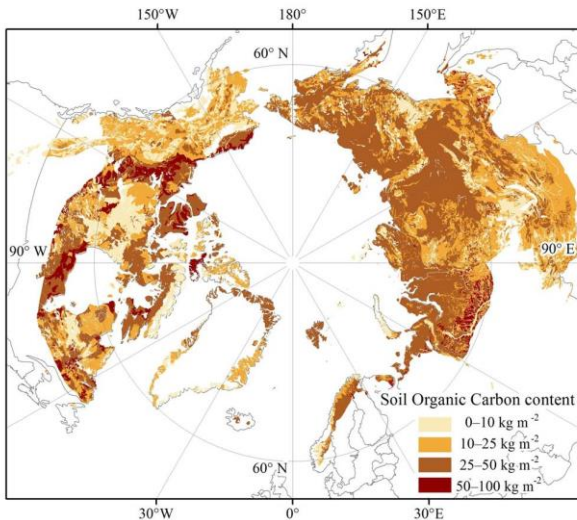


Figure 1. The map shows the extent of the northern circumpolar permafrost region and soil organic carbon content to a depth of 1 m, estimated using the Northern Circumpolar Soil Carbon Database (NCSCD): <http://bolin.su.se/data/ncscd/> Gustav Hugelius and the NCSCD Scientific Steering Committee are gratefully acknowledged.

tree-dominated communities. This transformation is well underway (Tape et al. 2006; Wookey et al. 2009; Myers-Smith, 2011; Macias-Fauria et al. 2012), as part of the so-called pan-arctic 'shrubification' (Zhang et al. 2013), and coupled C cycle-climate models predict that increased productivity will result in increased C sequestration in ecosystems (or a net negative feedback on climate change) (Qian et al., 2010). This modeled increase in C sequestration is thought to reflect a greater increase in net primary production (NPP) in response to climate change compared with soil organic matter (SOM) decomposition. With shifts from heath to shrub tundra, or forest, however, there are supplemental processes at work, not currently incorporated into modeling efforts: The mycorrhizal status of heaths (largely ericoid mycorrhizas; ERMs) and forests (largely ecto-mycorrhizas; ECMs), for example, may play a central role in controlling C stocks above- and below-ground (Clemmensen et al. 2013). There is growing evidence from field studies and experimentation that ECMs act as 'decomposers in disguise' (Talbot et al. 2008) and have the potential to accelerate decomposition of older soil organic matter (Hartley et al. 2012). This, together with ongoing shifts in plant functional composition,

Once thawed, this C is vulnerable to degradation by microorganisms in soils and sediments (Zimov et al. 2006; Schuur et al. 2008, 2009), with potential net release of the biogenic greenhouse gases carbon dioxide (CO₂) and methane (CH₄), in proportions reflecting redox status and the balance of aerobic metabolism to anaerobic fermentation reactions. These processes have the potential to feed-back significantly on atmospheric CO₂ and CH₄ concentrations (Koven et al. 2011) yet they are poorly incorporated into coupled C cycle-climate and ecosystem models.

This presentation will outline the above issues in the circumpolar north, but will then present a particular case study where shifts in plant functional composition have counterintuitive consequences for net ecosystem carbon stocks and fluxes; namely, the shift from tundra heath communities dominated by ericaceous dwarf shrubs, to taller, more productive, low shrub or



Figure 2. Arctic 'treeline' site, Trail Valley Creek, Northwest Territories, Canada. Green alder (*Alnus crispa*) foreground; black spruce (*Picea mariana*) middle distance, and low shrub tundra (*Betula nana* and *Salix* spp.) in the middle foreground. Where vegetation characteristic of these 'low shrub' tundras (sub-zone 5 of the CAVM; see Walker et al. (2005)) colonizes colder subzones 3-4 a shift in mycorrhizal status of the dominant plants might have counterintuitive consequences for net ecosystem C sequestration.

superimposed upon the massive stocks of 'old' C in permafrost soils, hints at some looming and unwelcome 'surprises' in the global greenhouse, and challenges the validity of some of the basic logic underpinning key models of the global carbon cycle and climate system.

References

- AMAP, 2012, Arctic Climate Issues 2011: Changes in Arctic Snow, Water, Ice and Permafrost: SWIPA 2011 Overview Report. Arctic Monitoring and Assessment Programme (AMAP), Oslo. xi + 97pp.
- Callaghan, T.V. et al., 2011, Multi-Decadal Changes in Tundra Environments and Ecosystems: Synthesis of the International Polar Year-Back to the Future Project (IPY-BTF): *Ambio*, v. 40, p. 705-716. doi 10.1007/s13280-011-0179-8
- Chapin, III F.S. et al., 2005, Role of land surface changes in Arctic summer warming: *Science*, v. 310, p. 657-660.
- Clemmensen, K.E. et al., 2013, Roots and associated fungi drive long-term carbon sequestration in boreal forest: *Science*, v. 339, p. 1615-1618.
- Deslippe, J.R. et al., 2011, Long-term experimental manipulation of climate alters the ectomycorrhizal community of *Betula nana* in Arctic tundra: *Global Change Biology*, v. 17, p. 1625-1636.
- Epstein, H.E. et al., 2012, Dynamics of aboveground phytomass of the circumpolar Arctic tundra during the past three decades: *Environmental Research Letters* v. 7 015506. doi: 10.1088/1748-9326/7/1/015506
- Elmendorf, S.C. et al., 2011, Global assessment of experimental climate warming on tundra vegetation: heterogeneity over space and time: *Ecology Letters*, doi: 10.1111/j.1461-0248.2011.01716.x
- Flanner, M.G. et al., 2011, Radiative forcing and albedo feedback from the Northern Hemisphere cryosphere between 1979 and 2008: *Nature Geoscience*, v. 4, p. 151-155. doi: 10.1038/NCEO1062
- Forbes, B.C. et al., 2009, High resilience in the Yamal-Nenets social-ecological system, West Siberian Arctic, Russia: *Proceedings of the National Academy of Sciences (PNAS)* v. 106, p. 22041-22048.
- Hansen, J. et al., 2006, Global temperature change: *PNAS*, v. 103, p. 14288-14293.
- Hartley, I.P. et al., 2012, A potential loss of carbon associated with greater plant growth in the European Arctic: *Nature Climate Change*. doi: 10.1038/NCLIMATE1575
- Hugelius, G. et al., 2013, The Northern Circumpolar Soil Carbon Database: spatially distributed datasets of soil coverage and soil carbon storage in the northern permafrost regions: *Earth System Science Data*, v. 5, p. 3-13, doi:10.5194/essd-5-3-2013
- Koven, C.D. et al., 2011, Permafrost carbon-climate feedbacks accelerate global warming: *PNAS* v. 108, p. 14769-14774. doi: 10.1073/pnas.1103910108
- Luo, Y. and Weng, E., 2011, Dynamic disequilibrium of the terrestrial carbon cycle under global change: *Trends in Ecology and Evolution (TREE)* v. 26, p. 96-104.
- Macias-Fauria, M. et al., 2012, Eurasian Arctic greening reveals teleconnections and the potential for novel ecosystems: *Nature Climate Change*, v. 2, p. 613-618. doi: 10.1038/NCLIMATE1558
- McGuire, A.D. et al., 2006, Integrated regional changes in arctic climate feedbacks: Implications for the global climate system: *Annual Review of Environment and Resources*, v. 31, p. 61 -91.
- Myers-Smith, I.H., 2011, Shrub expansion in tundra ecosystems: dynamics, impacts and research priorities: *Environmental Research Letters*, v. 6, 045509. doi:10.1088/1748-9326/6/4/045509
- Pearson, R.G. et al., 2013, Shifts in Arctic vegetation and associated feedbacks under climate change: *Nature Climate Change*, v. 3, p. 673-677. doi:10.1038/NCLIMATE1858
- Post, E. et al., 2009, Ecological Dynamics Across the Arctic Associated with Recent Climate Change: *Science*, v. 325, p. 1355-1358.
- Qian, H. et al., 2010, Enhanced terrestrial carbon uptake in the Northern High Latitudes in the 21st century from the Coupled Carbon Cycle Climate Model Intercomparison Project model projections: *Global Change Biology*, v. 16, p. 641-656. doi: 10.1111/j.1365-2486.2009.01989.x
- Serreze, M.C. and Francis, J.A., 2006, The Arctic Amplification Debate: *Climatic Change*, v. 76, p. 241-264.
- Schuur, E.A.G. et al., 2008, Vulnerability of Permafrost Carbon to Climate Change: Implications for the Global Carbon Cycle: *BioScience*, v. 58(8), p. 701-714.
- Schuur, E.A.G. et al., 2009, The effect of permafrost thaw on old carbon release and net carbon

- exchange from tundra: *Nature*, v. 459, p. 556-559.
- Schuur, E.A.G. et al., 2011, High risk of permafrost thaw: *Nature*, v. 480, p. 32-33.
- Shaver, G.R. et al., 2000, Global warming and terrestrial ecosystems: A conceptual framework for analysis: *Bioscience*, v. 50, p. 871-882. doi: 10.1641/0006-3568(2000)050[0871:GWATEA]2.0.CO;2
- Talbot, J.M. et al., 2008, Decomposers in disguise: mycorrhizal fungi as regulators of soil C dynamics in ecosystems under global change: *Functional Ecology*, v. 22, p. 955-963.
- Tape, K. et al., 2006, The evidence for shrub expansion in Northern Alaska and the Pan-Arctic: *Global Change Biology*, v. 12, p. 686-702.
- Walker, D.A. et al., 2005, The Circumpolar Arctic Vegetation Map: *Journal of Vegetation Science*, v. 16, p. 267–282.
- Wookey, P.A. et al., 2009, Ecosystem feedbacks and cascade processes: understanding their role in the responses of arctic and alpine ecosystems to environmental change: *Global Change Biology*, v. 15, p. 1153-1172.
- Zhang, W. et al., 2013, Tundra shrubification and tree-line advance amplify arctic climate warming: results from an individual-based dynamic vegetation model: *Environmental Research Letters*, 8 034023.
- Zimov, S.A. et al., 2006, Permafrost and the global carbon budget: *Science* v. 312, p. 1612–1613.

CIRCUM-POLAR VEGETATION AND ENVIRONMENTAL CONDITIONS

Eun Ju Lee, Kyoo Lee, Jeong Soo Park, Hyo Hye Mi Lee

School of Biological Sciences,
Seoul National University
ejlee@snu.ac.kr

ABSTRACTS

To predict future vegetational ecosystem by environmental changes, understanding the present patterns in plants species distribution characteristics along environmental gradients is necessary. To find suitable methods in arctic tundra vegetation ecosystems, we used grid sampling method and applied geostatistics, semi-variogram and block kriging analysis, to analyze vegetation spatial variability and pattern within the two dimensional space, and calculated the Moran's *I* statistics to find out the spatial autocorrelation of vegetation. Dominant species were *Vaccinium uliginosum*, *Ledum palustre* and Lichens at site of Council in Alaska. In spatial distribution analysis, interpolation maps and cross-correlograms revealed the strong negative spatial correlation between *Carex aquatilis* and *Eriophorum vaginatum* and the strong positive result between moss and *Rubus chamaemorus*. At study site of Ny-Å lesund in Svalbard archipelago, dominant species were different by habitats. Moss and genus Saxifraga were dominated in costal habitat from shoreline to the foot of a slope. In other site on the head of a slope, dominant species were perennial shrubs, *Dryas octopetala* and *Casiope teragona*. We thought that was difference from intensity of disturbance, freezing and thawing of seawater, sea level change, salt and nutrient, melting of snow and glacial et al. We are performing experiments about physical and chemical characters of soil samples to analyzing of spatial relationships between vegetation and habitats. We have some plans for future study. We will apply same methods at other circumpolar research place, Zackenberg in Greenland and Cambridge Bay in Canada. Second, to study of potential changes in vegetation due to climate change, we are going to research the seed bank at Arctic permafrost soil.

SOIL MICROBIAL COMMUNITIES IN ARCTIC AND OTHER COLD ECOSYSTEMS

Haiyan Chu

Institute of Soil Science, Chinese Academy of Sciences, Nanjing 210008, China.

ABSTRACTS

Climate warming is widely predicted to be largest and most rapid at high latitudes and high altitudes like Arctic tundra, Tibetan plateau, etc. The impacts of climate change on these ecosystems are critical for the global C cycle because of the large amount of C stored in these cold regions due to long-term low microbial decomposition. Microbial communities in cold ecosystems are exposed to particularly severe environmental stresses and thus these soils may be expected to harbor relatively unique bacterial communities. However, few spatially-comprehensive surveys of soil bacterial communities have been conducted, and it is not known if soils in cold ecosystems harbor bacterial communities that are generally distinct from those found in more temperate environments. We investigate soil microbial community composition and spatial distributions in cold ecosystems, and microbial community responses to climatic warming. Our studies will provide scientific base to characterize the impacts of future warming in cold terrestrial ecosystems.

CLIMATE CHANGE AND SOIL ECOSYSTEM

*Yoo Kyung Lee*¹, Ok-Sun Kim, Joohan Lee², Ji Young Jung¹, Sungjin Nam, Hyemin Kim,
Hyeyoung Kwon,*

¹ Division of Life Sciences, Korea Polar Research Institute

² Department of New Antarctic Station, Korea Polar Research Institute

ABSTRACT

Recent rapid climate change accelerates the changes in the Arctic ecosystem, and greenhouse gases evolved from the permafrost soil could feedback to the climate change. Therefore, we aim to understand the characteristics of soil microorganisms, soil properties, their changes in response to the climate change, the relationship between CO₂ from microbial respiration and other environmental factors, etc. from four different circumpolar areas (Ny-Å lesund, Svalbard; Council Alaska, USA; Zackenberg, Greenland, Cambridge Bay, Canada).

We are focusing on microbial succession and soil development along a chronosequence from a glacier retreat area in Ny-Å lesund (N 78°). From the Council area (N 66°), Alaska, the soil contains lots of accumulated organic matter, and the average depth of the active layer is about 50-70 cm in summer. We have collected several 1-m depth of soil cores in Council and are analyzing the microbial community in both active and permafrost layers. In Zackenberg, Greenland (N 74°) and Cambridge Bay, Canada (N 69°), we are conducting a climate manipulation experiment (increase in temperature or precipitation) to predict the responses of soil ecosystem to climate change in the Arctic.

SESSION 5

ARCTIC PALEOCEANOGRAPHY

INTERPRETATION OF LIPIDS BIOMARKERS IN THE SEDIMENT OF WESTERN ARCTIC OCEAN: LAST 100YEARS RECORDS OF ORGANIC SOURCES, STORAGE AND SURFACE SEAWATER TEMPERATURE

Adegoke Olugboyega Badejo^a, Sooa Jeon^a, Jong-ku Gal^a, Seung-Il Nam^b, Kyung-Hoon Shin^{a*}

^a *Department of Environmental Marine Sciences, Hanyang University, Ansan 426-791, Republic of Korea*

^b *Division of Polar Climate Research, Korea Polar Research Institute, Incheon 406-840, Republic of Korea*
shinkh@hanyang.ac.kr

ABSTRACT

Lipid biomarkers from cores sediments in the Western Arctic Ocean were identified to determine the source and transport of organic matter from the Chukchi shelf and Canada Basin. Hydrocarbon and fatty acid molecular markers showed higher contribution from marine organisms in the Chukchi shelf than in the Canada Basin with minor contributions of terrestrial organic matter. In order to reconstruct the recent change of paleo-sea surface temperature (SST) in the Chukchi shelf and the Canada Basin, we investigated alkenone temperature ($U^{K'_{37}}$ temperature) and alkyl diol temperature indices in bulk sediments. Apparent variations in alkenone and alkyl diol concentrations are related to the production of haptophyte algae and diatom species respectively. There was a significant change in diol compound composition between Chukchi shelf and the Canada Basin, probably reflecting the differences in the water mass. An offset ($\sim 1^\circ\text{C}$) seen between the inferred alkenone and alkyl diol temperatures in the Canada Basin, might be due to production of both organisms (haptophytealgae and diatom species) at different seasons or depths affected by sea-ice distribution and seawater stratification related to changing climatic conditions. These results thus indicate that alkenone temperature ($U^{K'_{37}}$ temperature) and diol temperature (LDI temperature) can be useful tools for tracing past sea surface temperature in the western Arctic. However the seasonality of both paleo temperatures should be further studied in reconstructing past sea surface temperature.

STABLE ISOTOPE COMPOSITIONS OF AUTHIGENIC CARBONATES IN PELAGIC SEDIMENTS OF THE MENDELEEV RIDGE (ARCTIC OCEAN): THEIR IMPLICATIONS FOR PALEOCEANOGRAPHY

K.S. Woo¹, H. S. Ji¹, S.-I. Nam², R. Stein³, A. Mackensen³ and J. Matthiessen³

*¹Department of Geology, Kangwon National University
wooks@kangwon.ac.kr*

²Division of Polar Climate Research, Korea Polar Research Institute

³Alfred Wegener Institute for Polar and Marine Research

ABSTRACTS

Carbonate minerals were discovered from the giant box core (PS72/410-1) of the pelagic sediments recovered from the Canadian Arctic across the central Mendeleev Ridge (Station location= Lat. 80°30.37"N, Long. 175°44.38"W) during the Arctic cruise by Polarstern in 2008. The core was 39 cm long and was collected from the water depth of 1802 meters. The sediments include planktonic foraminifers together with carbonate minerals. The contents of planktonic foraminifers and carbonate minerals vary with core depth, however these carbonate minerals are present through the whole sequence except for a few centimeters. The carbonates are composed of high Mg-calcite, low Mg-calcite and aragonite with a variety types of textures. Various crystal shapes of aragonite and calcite together with clear growth shapes of the crystals suggest that they are inorganic in origin. Highly enriched carbon isotope compositions ($\delta^{13}\text{C} = 0.5 \sim +5.8\text{‰}$ vs. PDB) strongly indicate that they formed in methanogenic zone below sediment/water interface by the reaction between anoxic pore fluids and host sediments induced by methanogenic bacteria. However, a wide range of oxygen isotope values ($\delta^{18}\text{O} = -5.0 \sim +6.4\text{‰}$ vs. PDB) indicate that porewater has been changed due to reaction between residual seawater and volcanoclastic sediments. Because the core sediments are not organic-rich, the presence of the authigenic carbonates may be related to paleoceanographic conditions of the Arctic Ocean which resulted in anoxic pore water conditions just a few centimetres below the sediment/water interface. Trace elemental compositions show clear divisions at the boundary of ca. 10 cm in core depth. Authigenic carbonates found shallower than this depth (Interval A) show higher Mg, Mn, Fe and Sr compositions which may imply paleoenvironmental changes with time. Averaged oxygen isotope compositions of authigenic carbonates at the Interval A (+3‰) in core depth show more positive values than those from 20 to 26cm (Interval B; -1.7‰), showing the distinctive increase between two intervals. Geochemical analysis of detrital muddy sediments also show two distinctively different trace element compositions. Also, the increase in $\delta^{18}\text{O}$ value of authigenic carbonates also support the 'freshwater discharge event story' during the Last Glacial Period. However, the presence of negative oxygen isotope values of authigenic carbonates throughout the whole sequence implies continuous supply of volcanoclastic sediments.

PRELIMINARY RESULTS OF 3RD/4TH RV ARAON EXPEDITIONS (ARA04B/4C, 2013) INTO THE WESTERN ARCTIC OCEAN

*S.-I. Nam¹ · L. Polyak² · F. Niessen³ · S.-Y. Kim¹ · B.R. Lee¹ ·
Y.S. Sim¹ · M. Schreck¹ · S.K. Kim¹ · H.J. Kim¹ · Y.J. Joe⁴ · G.B. Goh⁴ ·
A.H. Quantmann-Hensen³ · M. Yamamoto⁵ · F. Ohira⁵ · D.K. Han⁶*

¹*Division of Polar Climate Research, Korea Polar Research Institute, Incheon, Korea*

²*Byrd Polar Research Center, Ohio State University, Ohio, USA*

³*Alfred-Wegener-Institute for Polar- & Marine Research, Bremerhaven, Germany*

⁴*Jeju National University, Jeju, Korea*

⁵*Hokkaido University, Hokkaido, Japan*

⁶*Gwangju Institute of Science & Technology, Gwangju, Korea*

ABSTRACT

The 3rd/4th RV Araon Arctic expeditions (ARA04B/4C) were conducted from 21st Aug. to 28th Sep. 2013. to acquire SBP and multi-beam data along the selected survey lines and to take new sediment cores from the western Arctic Ocean where current sea-ice extent has been reducing dramatically. A total of 15 scientists from 4 countries were participated in marine geology program.

The main objectives of the marine geology program in the East Siberian-Chukchi Sea region-the northern Alaskan continental margin of the western Arctic were:

- (1) to characterize paleoceanographic conditions during warm (low ice) periods of the past, exemplified by the Holocene;
- (2) to investigate the western Arctic Pleistocene glaciation history: extent and timing of glaciations, ice provenance and flow patterns, interaction of ice sheets and ice shelves;
- (3) to understand sedimentation systems in front of the major cross-shelf canyons (Herald, Hanna, and Barrow canyons) and their relationship to circulation;
- (4) to Identify potential sites for future coring with a long piston core and ocean drilling.

The data collected significantly improve our understanding of sedimentary environments and late Quaternary glacial history of the Chukchi-East Siberian region and the northern Alaskan margin, which is only sparsely covered with quality marine geological/geophysical data. A combination of MB bathymetry and SBP records allowed identification of glacial deposits and glacial sea floor features as well as depocenters of undisturbed marine/glacimarine sediments. Sediment cores were taken at carefully selected locations to ground-truth geophysical records and to add the age control. As absolute age determinations will be performed later using AMS ¹⁴C dating and marine stable isotope stratigraphy (MIS), relative ages were estimated onboard based on correlation between the new cores and earlier investigated sedimentary records. Correlation was primarily based on core descriptions and MSCL logs, combined with seismo-stratigraphy, where possible.

SESSION 6

NORTHERN ROUTE

SUMMER CDOM OPTICAL PROPERTIES IN THE WESTERN ARCTIC UNDER LOW SEA ICE CONDITIONS

Eurico D'Sa and Hyun-cheol Kim

*Department of Oceanography and Coastal Sciences
Louisiana State University, Baton Rouge, LA, USA*

*Division of Polar Climate Research
Department of International Cooperation,
Korea Polar Research Institute
kimhc@kopri.re.kr*

ABSTRACT

Background: Dissolved organic matter (DOM) constitutes the largest pool of reduced organic carbon in the ocean and plays an important part in the global carbon cycle. The Arctic Ocean, with about 1% of the global ocean volume receives about 10% of the global river discharge. Under climate change, increased discharge from the Arctic rivers could significantly affect the carbon cycle in the Arctic Ocean. The colored or chromophoric DOM or CDOM is the fraction of DOM that absorbs light in the ultraviolet and visible wavelength and is a major light absorbing constituent in the ocean that influences light penetration and thus biological productivity. Through its influence on the water leaving radiance or the light field it also affects satellite ocean color chlorophyll algorithms. CDOM also fluoresces and its fluorescence properties have been studied using excitation-emission matrix spectroscopy (EEMs). The fluorescent constituents of DOM can include humic and protein substances (Coble 1996; 1997; Mopper and Schultz 1993). Humic substances are mostly of terrestrial origin, but humic-like fluorescent material of marine origin is also present in aquatic systems (Coble 2007).

CDOM is produced in situ by biological production (autochthonous) or transported from terrestrial sources (allochthonous), and removed by photochemical degradation or physical processes such as circulation and mixing (Hansell and Carlson 2002; Blough and Del Vecchio 2002; D'Sa and DiMarco 2009; D'Sa 2008; Nelson and Siegel 2013). CDOM absorption properties including spectral slopes have been used to gain insights into CDOM source, and photooxidative state (Blough and Del Vecchio 2002; Helms et al. 2008). Studies have reported on the DOM/CDOM absorption properties in the Arctic (Wheeler et al. 1997; Gueguen et al. 2005; 2011) and the rivers have been found to be an important source of DOM/CDOM to the Arctic Ocean. Fluorescence measurements have also been reported for the Arctic and both humic-like and protein like substances have been detected (Gueguen et al. 2005). Only limited studies have been reported for the Western Arctic (Gueguen et al. 2005). In this study we report on the DOC and CDOM optical properties of absorption and fluorescence in the Western Arctic region during summer of 2012 when the extent of Arctic sea ice was the lowest recorded.

Data and Methods: Field samples were obtained during a field campaign in the Western Arctic onboard the Korean Ice Breaker Araon between 31st July – 10th August 2012. Hydrographic data were collected using a Sea-Bird CTD and water samples were collected at every station during the CTD casts from Niskin bottles attached to a Carousel rosette sampler. Samples were obtained at three depths – surface, at chlorophyll fluorescence maximum and at depths below the maximum where chlorophyll fluorescence signals were low. Samples were filtered immediately through 0.2 μm nylon membrane filters under low vacuum and stored at 4°C in acid cleaned, pre-combusted amber colored bottles until processed for DOC concentrations and CDOM absorption in the laboratory. Absorbance measurements of CDOM were obtained on a Perkin-Elmer Lambda 850 spectrophotometer and the absorption coefficients were calculated using the standard equation (D'Sa et al. 2006) after correction of the absorbance data at 700 nm over a 10 nm interval. CDOM absorption coefficient at 355 nm ($a_{g,355}$) (m^{-1}) was used as a quantitative parameter of CDOM and the spectral slope for the interval of 275-295 nm ($S_{275-295}$) (μm^{-1}) was calculated according to Helms et al. (2008). EEMs were obtained using a Fluoromax 4 Jobin Yvon fluorometer by scanning emission spectra from 290 to 550 nm at 5 nm intervals while exciting every 5 nm between 250 to 450 nm. Instrument corrections and normalization were carried out according to method described in Singh et al. 2010. DOC measurements were made on a Shimadzu TOC 5000A (with ASI-5000A autosampler).

Preliminary results and discussion: Surface chlorophyll concentrations were generally low with some elevated concentrations off the Alaska coast and the Antarctic Basin (Fig. 1a). Mean DOC concentrations for the average three depths for all the stations sampled were $133.24 \pm 32.50 \mu\text{Mol}$ and varied over the range 47.91-248.10 μMol (Fig. 1b). Although, high concentrations of DOC in the northern-western stations in the Arctic Basin were coincident with elevated levels of phytoplankton chlorophyll concentrations (Fig. 1a, b), patterns differed at most other locations.

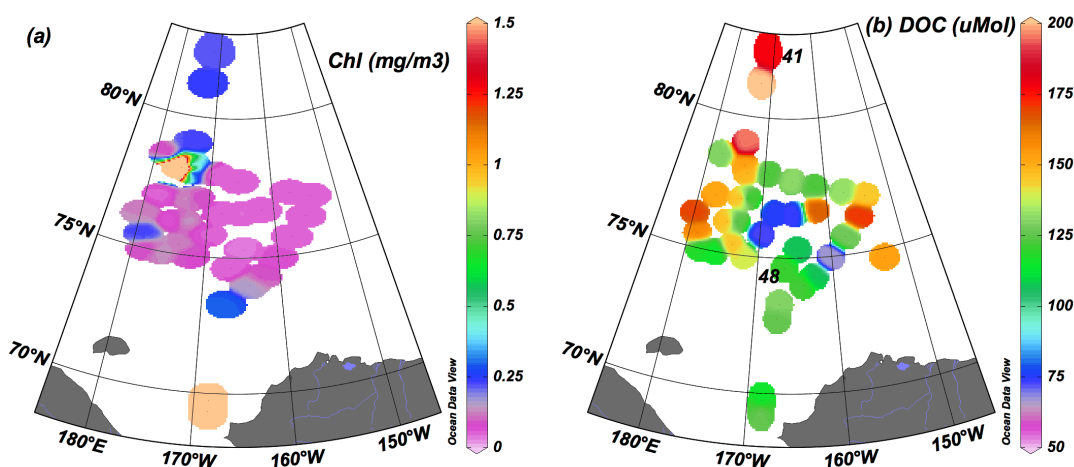


Figure 1. (a) Surface spatial distribution of phytoplankton chlorophyll (mg m^{-3}), (b) DOC concentrations ($\mu\text{Mol L}^{-1}$).

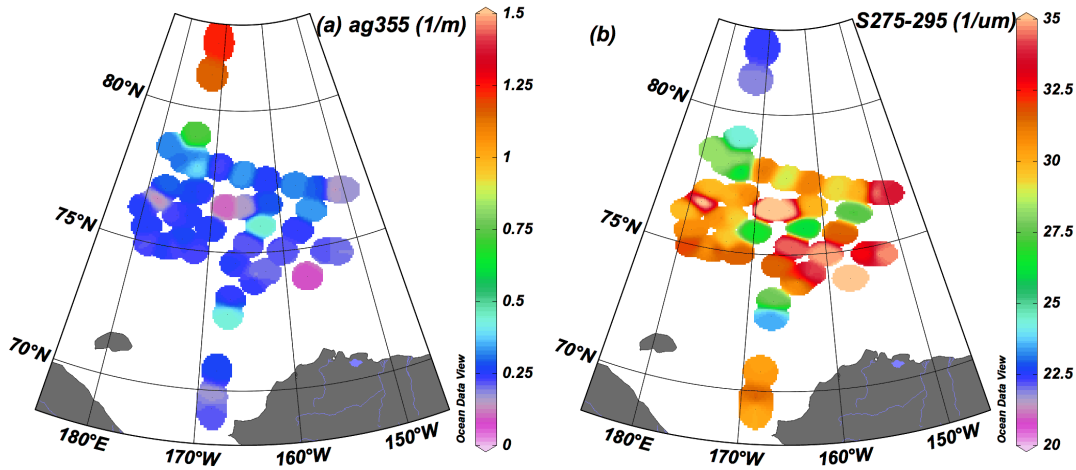


Figure 2. Surface spatial distribution of (a) CDOM absorption coefficient at 355 nm, $a_g(355) \text{ m}^{-1}$, (b) spectral slope $S_{275-295} (\mu\text{m}^{-1})$.

The mean absorption coefficient at 355, $a_g(355)$ was $0.361 \pm 0.282 \text{ m}^{-1}$, and varied from 0.053 to 2.03 m^{-1} . Most values of $a_g(355)$ were $< 0.6 \text{ m}^{-1}$ with the northern stations having relatively high amount of CDOM. The spectral slope $S_{275-295}$ in the surface waters of the western Arctic was relatively high suggesting the photodegradation of CDOM (Fig. 2b). However, the low $S_{275-295}$ at the northern stations (e.g., station 41) in the Arctic Basin suggested that surface waters at these high latitudes were not photooxidized likely due to reduced solar radiation or recent melt of the sea ice. $a_g(355)$ increased with increasing DOC concentrations however the relationship appeared non-linear (Fig. 3a). The relationship between $a_g(355)$ and the spectral slope $S_{275-295}$ revealed two trends (Fig. 3b). One trend was for $a_g(355)$ values $< 0.5 \text{ m}^{-1}$, and the other was for higher absorption values. These will be examined together with salinity and temperature for linkages to water masses in the western Arctic Ocean.

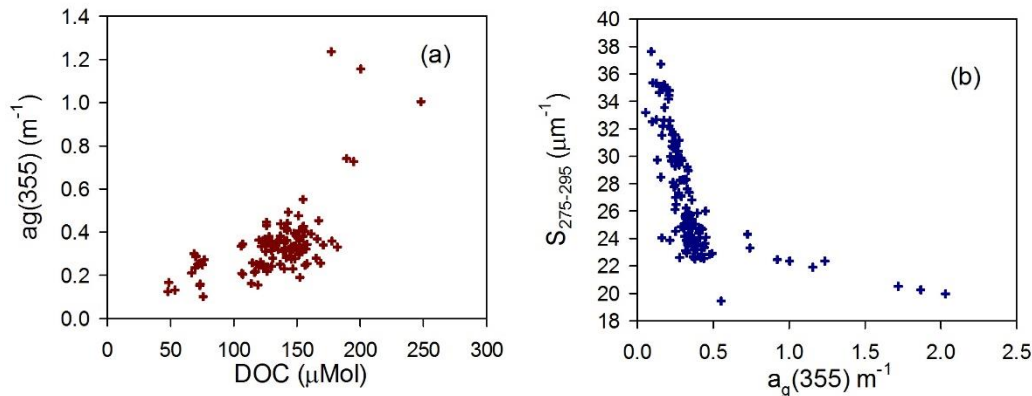
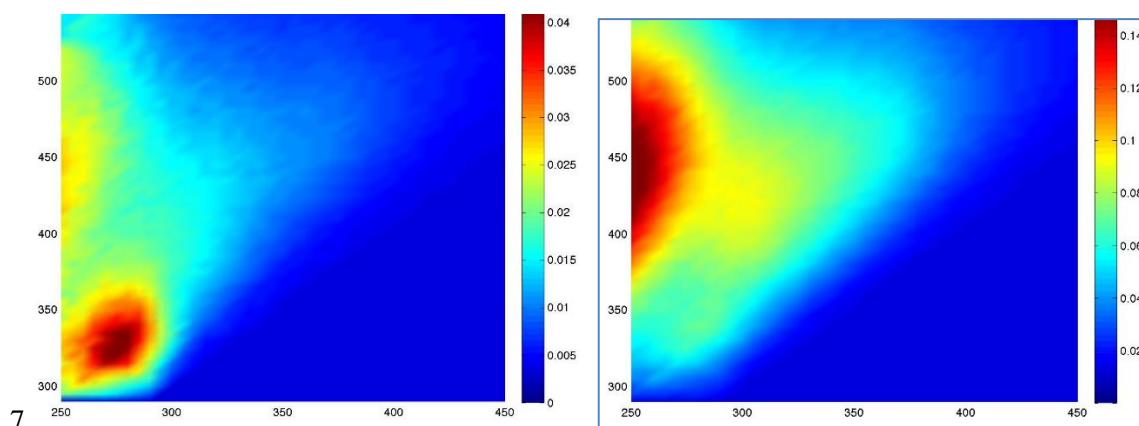


Fig. 3. Relationship between (a) DOC and $a_g(355)$, (b) $a_g(355)$ and spectral slope S

EEMs plots for two end members are shown as examples of typical fluorescence observed for the various stations sampled during the cruise (Fig. 4). The EEMs plot shown in Figure 4-left corresponds to station 48 that is located in the Chukchi shelf (station location shown in Figure 1b). At this location the EEMs spectra shows maximum emission fluorescence intensity corresponding to peak 'T' or protein-like tyrosine amino acids, and is due to relatively fresh DOM (Coble 1996; Stedmon et al. 2003). There are also peaks of smaller intensities corresponding to the humic-like 'A' peak that can be related to terrestrial source of humic material. Other two lower fluorescence intensity peaks that can be observed are the 'C' and the 'M' peaks. These peaks correspond to terrestrial 'C' and marine 'M' source of humic-like material (Coble 1996; Singh et al. 2010).



7 Fig. 4. Plots of EEM spectra for surface samples at station 48 (Chukchi shelf) and station 41 (Arctic Basin). Locations of these two stations are shown in Figure 1b.

In contrast, the EEMs fluorescence at a station in the Arctic Basin (Fig. 4-right; station 41) is almost four times as intense as that at station 48 in the Chukchi shelf. The Arctic Basin surface water appears to be dominated by the 'A' and 'M' peaks. A strong terrestrial influence is observed in the most northern station 41. The EEMs data set will be further analyzed using parallel factor analysis (PARAFAC), which allows for the chemical identification of the CDOM fluorophores (Stedmon et al. 2003).

Acknowledgement: The authors would like to acknowledge project support from "Korea-Polar Ocean Rapid Transition (K-PORT): PM12020" for the Arctic survey and the project "Optimum Utilization of Satellite data for Polar Research: PG13020" for travel support. E. D'Sa also acknowledges support from NASA grant NNX10AP10G.

References:

- Blough, N. V., and Del Vecchio, R., 2002, Chromophoric DOM in the coastal environment, in: Hansell, D. A., Carlson, C. A. (Eds.), *Biogeochemistry of Marine Dissolved Organic Matter*: Academic Press, San Diego, p. 509-578.
- Coble, P.G., 1996, Characterization of marine and terrestrial DOM in seawater using excitation-emission matrix spectroscopy: *Marine Chemistry*: v. 51, p. 325-346.
- Coble, P. G., 2007, Marine optical biogeochemistry: the chemistry of ocean color: *Chemical Review*, v. 107, p. 402-418.
- D'Sa E. J., and DiMarco, S., 2009, Seasonal variability and controls on chromophoric dissolved organic matter in a large river-dominated coastal margin: *Limnology and Oceanography*, v. 54, p. 2233-2242.
- D'Sa, E. J., 2008, Colored dissolved organic matter in coastal waters influenced by the Atchafalaya River, USA: effects of an algal bloom: *Journal of Applied Remote Sensing*, v. 2, p. 023502.
- Hansell, D. A., Carlson, C. A., 2002, *Biogeochemistry of Marine Dissolved Organic Matter*: Academic Press, San Diego.
- Helms, J. R., Stubbins, A., Ritchie, J. D., and Minor, E. C., 2008, Absorption spectral slopes and slope ratios as indicators of molecular weight, source, and photobleaching of chromophoric dissolved organic matter: *Limnology and Oceanography*, v. 53, p. 955-969.
- Gueguen, C., Guo, L., Tanaka, N., 2005, Distributions and characteristics of colored dissolved organic matter in the Western Arctic Ocean: *Continental Shelf Research*, v. 25, p. 1195-1207.
- Gueguen, C., McLaughlin, F. A., Carmack, E. C., Itoh, M., Narita, H., Nishino, S., 2011, The nature of colored dissolved organic matter in the southern Canada Basin and East Siberian Sea: *Deep-Sea Research, Part II*, doi:10.1016/j.dsr2.2011.05.004.
- Mopper, K., Schultz, C. A., 1993, Fluorescence as a possible tool for studying the nature and water column distribution of DOC components: *Marine Chemistry*, v. 41, p. 229-238.
- Nelson, N. B., Siegel, D. A., 2013, The global distribution and dynamics of chromophoric dissolved organic matter: *Annual Review of Marine Science*, v. 5, p. 447-476.

- Stedmon, C.A., Markager, S., Bro, R., 2003, Tracing dissolved organic matter in aquatic environments using a new approach to fluorescence spectroscopy: *Marine Chemistry*, v. 82, p. 239-254.
- Singh, S., D'Sa, E.J., and Swenson, E.M., 2010, Chromophoric dissolved organic matter (CDOM) variability in Barataria Basin using excitation-emission matrix (EEM) fluorescence and parallel factor analysis (PARAFAC): *Science of Total Environment*, v. 408, p. 3211-3222.
- Wheeler, P.A., Watkins, J.M., Hansing, R.L., 1997, Nutrients, organic carbon and organic nitrogen in the upper water column of the Arctic Ocean: implications for the sources of dissolved organic carbon: *Deep-Sea Research II*, v. 44, p. 1571-1592.

CONCEPTUAL DESIGN OF A SATELLITE-BASED ICE NAVIGATION SUPPORTING SYSTEM FOR THE NORTHERN SEA ROUTE

Sungchul Hong¹, Sun-Hwa Kim¹, Chan-Su Yang^{1,2} and Kazuo Ouchi²

¹ Korea Maritime and Ocean University

² Korea Institute of Ocean Science & Technology

sungchul@hotmail.com

scorpio96@hhu.ac.kr

yangcs@kiost.ac

ouchi_sar@yahoo.ac.kr

ABSTRACT

IPCC (International Panel on Climate Change) reported that the arctic sea-ice extent has been decreased by 2.7% per decades since satellite observations in 1978. The decreased sea-ice extent has gained an international attention due to its economical benefits from the NSR (Northern Sea Route). The NSR - not a clearly defined single route, but a number of alternative routes across the top of Russia- has a 37% reduction in sailing distance, comparing to the SSR (Southern Sea Route) passing through the Suez Canal. Sailing days are consequently reduced from 30 days to 20 days. Also, it is estimated that the Northern Sea has 20 to 25% of world's oil resources and occupies 40% of the world's fishery production. As Republic of Korea was admitted as an observer to the Arctic Council on May 15, 2013, there has been increasing needs to explore new route in the Northern Sea. Republic of Korea have the long-term satellite plan as figure 1, three or more satellites will be launched soon.

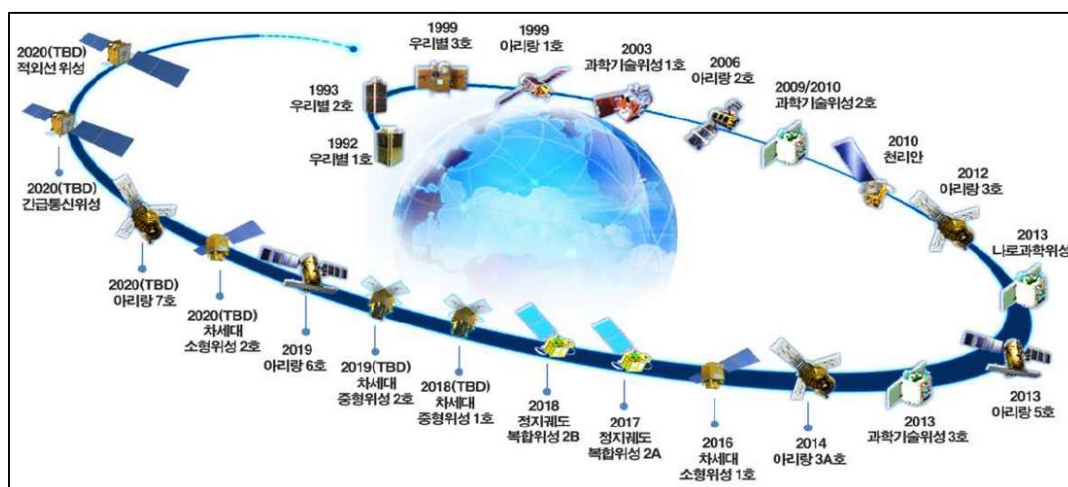


Figure 1. The long-term satellite launching plan of South Korea

KOSC (Korea Ocean Satellite Center) in KIOST (Korea Institute of Ocean Science & Technology) receives many satellite data including GOCI (Geostationary Ocean Color Imager) loaded on COMS (Communication, Ocean, and Meteorological Satellite) that was launched into a geostationary orbit at 36,000 km from the Kourou Space Center, French Guiana, on June 27, 2010. Its sensor acquires eight channels of multispectral images that provide hourly coverage of a 2500 km² area at 500 m resolution. KIOST also developed the KOOS (Korea Operational Oceanographic System) that provides the ocean environment information based satellite data and ocean-weather numerical models. As the concept that KOOS extend to Arctic sea, we conceptually design a satellite-based ice navigation supporting system for the Northern Sea.

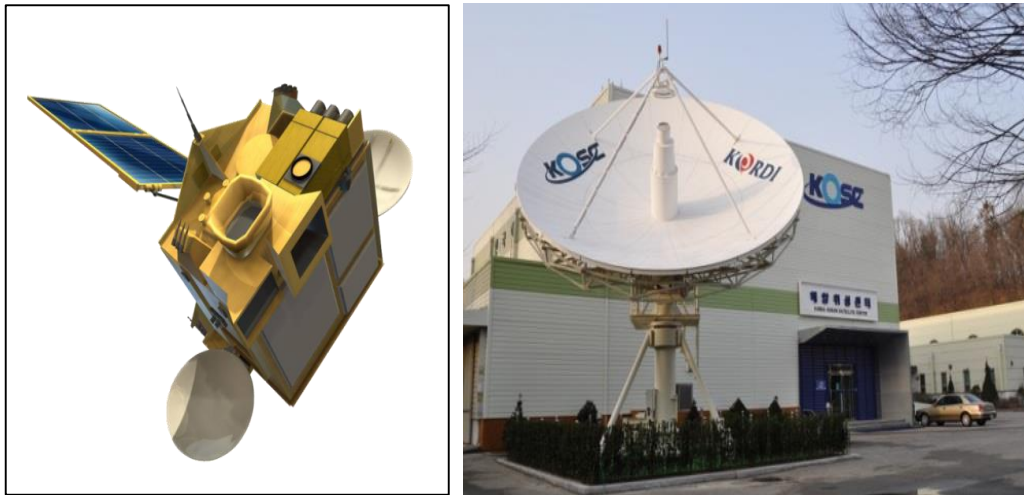


Figure 2. The COMS (Communication, Ocean, and Meteorological Satellite) launched successfully in 2010 (left) and KOSC (Korea Ocean Satellite Center) in KIOST (Korea Institute of Ocean Science and Technology) (right)

Figure 3 shows the expected basic NRS considering real ship route and vessel traffic density data. The NRS begins Busan to Rotterdam, total length is about 20,827,000km. The route needed the sea-ice monitoring is consisted of three steps which 1st-step route is from **Kamchatka Peninsula** to Sannilkov Strait, 2nd-step route is to Polarstrtor Heiberg Islands, and 3rd-step route is to Bergen harbor in Norway. 2nd-step route is splite two routes from Wrangel Island and 3rd-step route is divided with two routes which the one route passed up Sannilkov Strait, the other route passes by Sannilkov Strait. In this study, the system is designed to support the safe operation of the ship which passes near this route using various satellite data. In Figure 3, there is also KOOS boundary. In this boundary, all environmental information for supporting the Northern Sea route is provided from KOOS.

To support safe NSR, this study conceptually designs a satellite-based ice navigation supporting system for the Northern Sea (Figure 4). The system is designed for minimizing vessels' sailing risks to sea-ices and weather conditions in the Northern Sea, for which the arctic sea environmental information center will be developd based upon a sea-ice monitoring module, a sea-ice/iceberg modeling module, and an arctic KOOS.

Among many environmental factors, the sea-ice is an important factor for safe ship navigation in that the sea-ice is continuously moving and changing location. In this regard, the sea-ice monitoring module, consisting of receiving, processing, and service sub-systems, is designed to provide satellite data in near real-time. The sea-ice monitoring module aims to provide the sea-ice information such as a sea-ice extent, a sea-ice concentration, a sea-ice type, and a sea-ice motion. Also, the sea-ice modeling module is designed to forecast the sea-ice information for scheduling vessels' routes. The KOOS provides marine meteorological observations on the sea surrounding the Korean Peninsula. The arctic

KOOS module will be developed to extend KOOS to the Arctic Ocean. The Arctic KOOS provides the various marine weather information including SST (Sea Surface Temperature), wind, ocean currents, and wave, which are generated from various satellite and marine meteorological model.

The risk assessment method in the ice navigation supporting system then computes safe-economical sea routes related to sea-ice and weather conditions in the Northern Sea. An acceptable sailing risk indicates that vessels can be operated due to low cost or difficulty of sailing in given sea-ice conditions. Sea routes with moderate sailing risk can suggest ice-breaker's assistance to continue their voyages to destination. However, for a high sailing risk, vessels need to find other alternative routes to avoid unfavourable effects to ships' structures and marine environments in the Northern Sea.

< Reference >

Choi K.S., Park M. K., Lee J.H., and Park G.I., 2007. A study on the optimum navigation route safety assessment system using real time weather forecasting, *Journal of the Korean Society of Marine Environment & Safety*, 13(2), pp. 133-140.

Choi M., Chung H., Yamaguchi H., Silva L., 2013. Application of Genetic Algorithm to ship route optimization in ice navigation, *Proceedings of the 22nd International Conference on Port and Ocean Engineering under Arctic Conditions*.

IPCC (Intergovernmental Panel on Climate Change), 2007. *Climate change 2007: The physical science basis. Contribution of working group I to the fourth assessment report of the Intergovernmental Panel on Climate Change*. Cambridge University Press, New York.

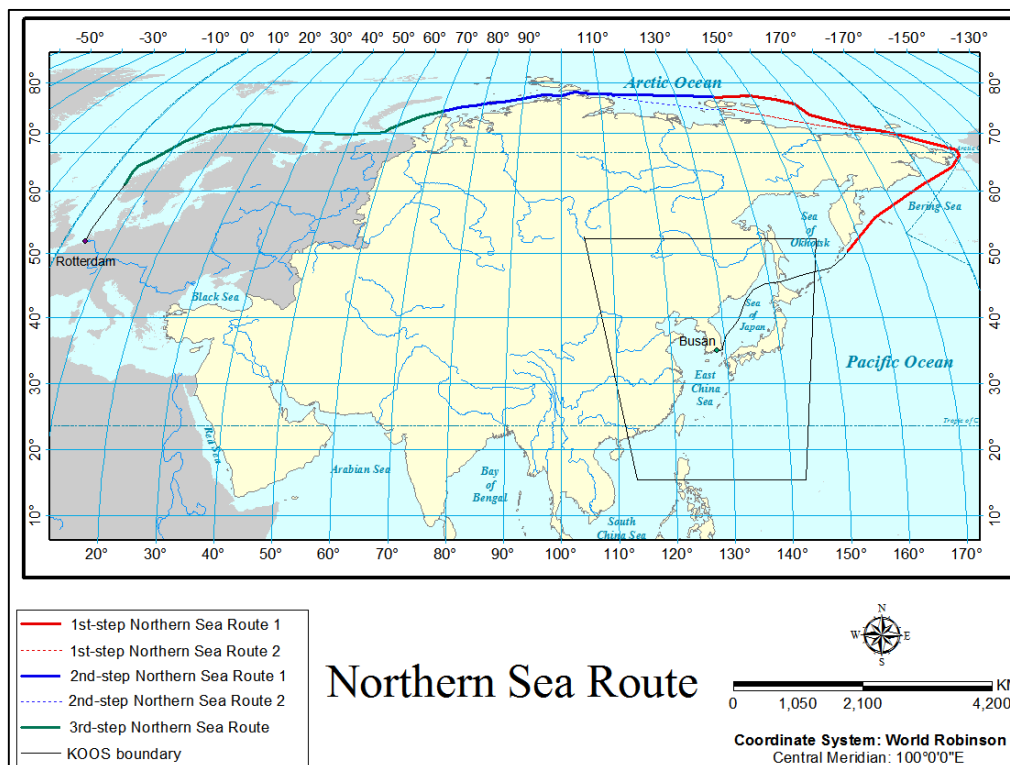


Figure 3. The NSR (Northern Sea Route) map designed for the satellite-based ice navigation supporting system

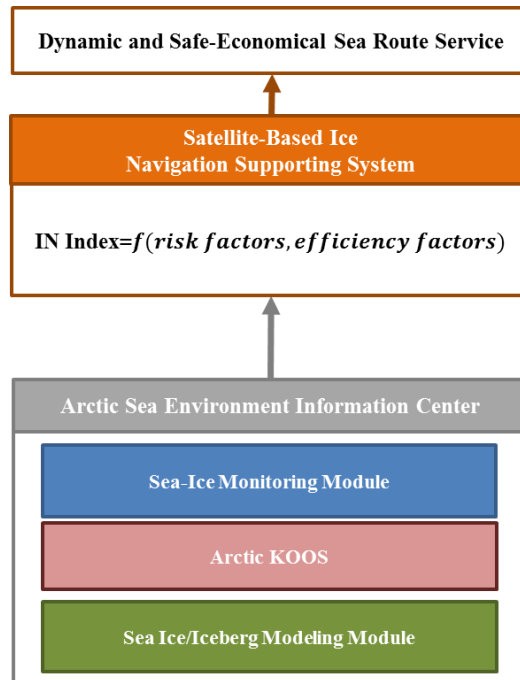


Figure 4. A satellite-based ice navigation supporting system for the NSR (Northern Sea Route)

PRECONDITIONING EFFECT OF ABSORBED SHORTWAVE RADIATION ON ARCTIC SEA-ICE VARIATION IN SUMMER

Baek Min Kim

*Division of Climate Change
Korea Polar Research Institute
bmkim@kopri.re.kr*

ABSTRACTS

Influence of cloud-controlled absorbed solar radiation on Arctic sea ice is crucial, but the underlying mechanism remains unclear [REFERENCE]. Here we demonstrate that for the Arctic region (north of 65°N) the absorbed solar radiation in early-summer months (May-June-July), is primarily altered by cloud variations and plays a dominant role for the determination of Arctic sea ice extent at the late-summer months (August- September-October). Satellite data show that anomalously high absorbed solar radiation coincides with anomalously low cloud albedo, low surface albedo, and low Arctic sea ice concentration for Junes of 2007, 2011, and 2012 when summer sea ice concentrations had record-breaking small values during the last few decades. In the 13-year (2000–2012) anomaly records, the increase (decrease) in the absorbed solar radiation in the early-summer months is consistently followed by the decrease (increase) in sea ice concentration in the late-summer months. Especially, sea ice concentration in October strongly responds to the absorbed solar radiation in June, and considerably changes the absorbed solar radiation in the following spring months (March-April-May). Current state-of-the-art climate models seem to underestimate this observed strong solar energy-sea ice connection.

POSTER SESSION 1

ATMOSPHERE

IMPACT OF ARCTIC SEA-ICE LOSS ON THE 2009/2010 EURASIAN COLD WINTER

TaeHyouon Shim, Baek-Min Kim and Sung-Joong Kim

Korea Polar Research Institute
thshim@gmail.com

ABSTRACTS

In 2009/2010 winter, a few extreme cold events and heavy snowfall occurred over central North America, north western Europe, and East Asia exerting a severe social and economic impacts. In this study, we performed modeling experiments to examine the role of substantially reduced Arctic sea-ice over Barents/Kara Sea on the 2009/2010 cold winters. To investigate the influence from the Arctic, we designed two model runs using Community Atmosphere Model Version 3 (CAM3) with different prescribed surface boundary conditions: (a) Climatological seasonal cycle of sea surface temperature (SST) and sea ice concentration (SIC) prescribed everywhere (CLIM) and (b) Same with CLIM except for SST and SIC inside the Arctic circle replaced by 2009/2010 values. Model results successfully captured local surface warming and thickened geopotential height at the upper-level in the Arctic. They also reproduced the downstream wave propagation toward mid-latitude. This is a typical feature of Barents Oscillation (BO) defined by previous study. We also show that the BO pattern can easily propagate upward and play a role for the weakening of polar vortex that causes a subsequent cold winter for late winter by downward coupling. Also, model captures observed the abrupt increase of snow depth anomaly over Siberian region in early winter, which is an important precondition of stratospheric polar vortex weakening. Therefore, given the successful reproduction of key observed features of cold winter 2009/2010 by numerical experiments, we conclude that the Arctic sea-ice of 2009 for early winter played a key role for the subsequent development of cold winter 2009/2010 and was not the only role of the autumn Siberia snow-cover.

ARCTIC GREENING CAN CAUSE EARLIER SEASONALITY OF POLAR AMPLIFICATION

*Yoo-jeong Chae*¹, *Sarah Kang*¹, *Dargan M. W. Frierson*², *Beakmin Kim*³
*, and Su-jong Jeong*⁴

¹*School of Urban and Environmental Engineering, UNIST, Ulsan, Korea*

²*Department of Atmospheric Sciences, University of Washington, Seattle, Washington*

³*Division of Climate Change, Korea Polar Research Institute*

⁴*Program in Atmospheric and Oceanic Sciences, Princeton University, USA*

chae@unist.ac.kr

ABSTRACTS

As global temperatures rise, it is expected that vegetation may also change, particularly in the Northern Hemisphere high latitudes. This study examines the impact of a vegetation change poleward of 60°N on polar amplification. Three experiments are performed with the NCAR Community Atmosphere Model 3.0 (CAM3.0) coupled to a slab ocean and perturbed by 1) vegetation change from grass and shrub to boreal forest, 2) doubling of CO₂, and 3) vegetation change with doubling of CO₂. When the vegetation is changed poleward of 60°N, warming over the Arctic region in boreal summer driven by the albedo change. The doubled CO₂ with vegetation change experiment suggests that if large vegetation change occur in the high latitudes in the future, polar amplification may be appear earlier in the seasonal cycle.

THE ATMOSPHERIC MODE RELATED TO CLIMATE CHANGE IN ARCTIC REGION

Euihyun Jung¹⁾, Baek-min Kim²⁾ and Gyu-ho Lim¹⁾

*¹⁾School of Earth and Environmental Sciences
Seoul National University
aster042@snu.ac.kr*

²⁾Division of polar climate research, Korea Polar Research Institute

ABSTRACTS

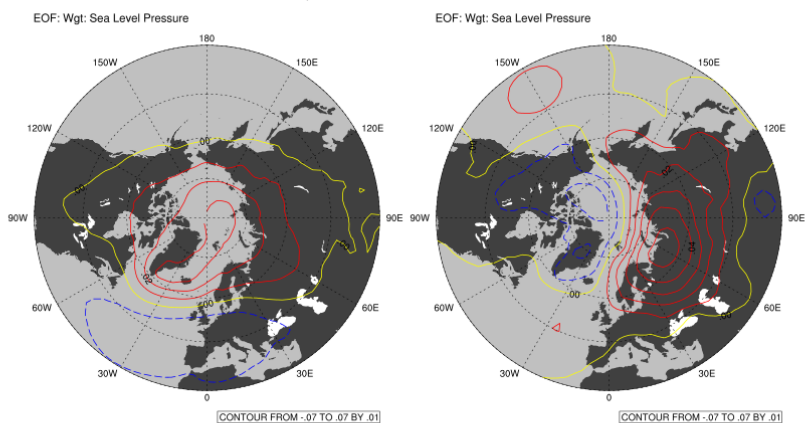
One of the major atmospheric modes governing the atmospheric motion on the Arctic region in boreal winter is Arctic Oscillation. This zonally symmetric pattern is first identified by Lorenz(1951) and named in 1887 by Thompson and Wallace. After its discovery many researchers have explained variability of winter climate over the northern hemisphere using intensity of Arctic oscillation and its relationship have been well shown.

In the last decade, Arctic oscillation has trended to a more neutral state. However, in the same period Arctic warming has been faster than any other region and strong cold surge events over Eurasia have occurred. Strong relationship between Arctic oscillation and these phenomena is not well explained

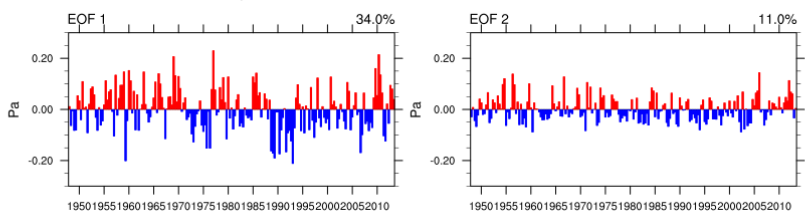
Skeie(2000) called second EOF mode of sea level pressure Barents oscillation. Using this index, the relationship between recent cold events over Eurasia and Barents oscillation can be shown. Briefly, recent changes over the Arctic region are well associated with this mode.

Some of studies consider Barents oscillation as a non-real mode and artificially made from statistical error. In this study, difference between Barents oscillation and Arctic oscillation is shown according to its statistical relationship with other variables and dynamical structure.

a) SLP:1948-2013 DJF



b) PC time serieses :1948-2013 DJF



ASYMMETRIC CHANGE OF GLOBAL RAINY SEASON PATTERN ON GLOBAL WARMING SCENARIOS

Yechul Shin ¹, Sarah Kang ¹, Dargan M. W. Frierson ²

¹School of Urban and Environmental Engineering, UNIST, Ulsan, Korea

²Department of Atmospheric Sciences, University of Washington, Seattle, Washington

[*yechul@unist.ac.kr*](mailto:yechul@unist.ac.kr)

ABSTRACTS

The climatology and trend of spatial and temporal characteristics of rainy season are analyzed over 40°S to 40°N using CMIP3 and CMIP5 (Coupled model inter-comparison project, phase3, 5) model archive. The results are expected to help agricultural planning with climate change. We define the onset, offset, and length of rainy season based on precipitation anomaly from the annual-mean at each grid. The rainy season of the semi-arid African Sahel, Amazon, and South Africa is projected to start later and becomes shorter. Over most continent region in the Southern Hemisphere, the rainy season starts later and becomes shorter, whereas the response is relatively noisy in the Northern Hemisphere, with the moistening trend over India due to earlier onset and later offset. Over most ocean, the rainy season is projected to start later and end earlier, leading to a significant shortening of rainy season.

THE RESPONSE OF THE ITCZ TO THERMAL FORCING WITH THE CHANGE OF PERTURBED LATITUDE

Jeongbin. Seo ¹, Sarah M. Kang ¹, and Dargan M. W. Frierson ²

¹ School of Urban and Environmental Engineering, UNIST, Ulsan, Korea

² Department of Atmospheric Sciences, University of Washington, Seattle, Washington
sjbin1218@unist.ac.kr

ABSTRACTS

Previous studies have shown that the position of the ITCZ(Inter-tropical Convergence Zone) is altered by external thermal forcing not only in the tropics but also in the extratropics. To examine whether the ITCZ is shifted more effectively by the tropical forcing or the extratropical forcing, we perform experiments with an idealized moist atmospheric GCM that has no water vapor or cloud feedbacks and a comprehensive atmospheric GCM, both coupled to a slab mixed layer ocean. The control climate with no flux adjustment is perturbed by prescribing heating of the mixed layer in the Northern Hemisphere and cooling of equal magnitude in the Southern Hemisphere, equivalent to imposing northward cross-equatorial flux. The meridional position of thermal forcing with 10 degree latitudinal width is systematically varied, holding the cross-equatorial flux fixed by adjusting the amplitude. In an idealized GCM, the tropical forcing is more efficient in shifting the ITCZ, whereas in a comprehensive GCM the extratropical forcing is more effective due to positive cloud radiative feedbacks over the high latitudes.

THE HIGH HEAT FLUX EVENT IN THE BARENTS/KARA SEAS IN THE WINTER OF 2011/12

Joo-Hong Kim, Baek-Min Kim, Jeong-Ock Son, Sang-Jong Park, and Seong-Joong Kim

*Division of Polar Climate Research,
Korea Polar Research Institute
joo-hong.kim@kopri.re.kr*

ABSTRACTS

With recent rapid decline of Arctic sea-ice, the air-sea interaction over the marginal ice zone (MIZ) is expected to be much vigorous, which is considered to contribute to Arctic amplification. The intense heat exchange events, high heat flux events (HHFEs) during a cold air outbreak in the MIZ are of particular interest, because it may actively warm the atmosphere through the cloud-radiation feedback. Here we show such a possible case during the winter of 2011/12 when the Arctic region was anomalously warm; for example, the near-surface temperature over the MIZ of the northern Barents/Kara Seas was about 10°C warmer than the 1979–2012 climatology. Two major HHFEs were detected during the mid-November and the year-end of 2011, during which the intense cold-core cyclone traversed over the Barents/Kara Seas. Without such intense synoptic systems, the large dump of turbulent heat fluxes from the ocean to the atmosphere would not be realized. The turbulent heat fluxes that we use here are the forecast products from the ERA-interim reanalysis data, whose uncertainty is relatively larger because it is dependent on model formulation (e.g., resolution, parameterizations, etc.). To evaluate the magnitude of ERA-interim heat fluxes, we conducted the triply nested simulations of the Polar WRF over the Barents/Kara domain. The ERA-interim heat fluxes are then compared with those simulated by the high-resolution WRF.

CLIMATE IMPACT OF CHANGES IN EURASIAN ARCTIC VEGETATION ON THE EAST ASIAN SUMMER MONSOON

Ah-Ryeon Yang¹, Baek-Min Kim¹, Su-Jong Jung² and Sa-Ra Kang³

*¹Division of Polar Climate Research,
Korea Polar Research Institute, Incheon 406-840, Korea*

²Atmospheric and Oceanic Sciences, Princeton University, Princeton, USA

*³Ulsan National Institute of Science and Technology, Ulsan, Korea
ahryeon@kopri.re.kr, bmkim@kopri.re.kr*

ABSTRACTS

Climate impact of changes in Eurasian Arctic vegetation on the East Asian summer monsoon has been investigated using general circulation model (GCM). In the model simulation, shrub and grass of the Eurasian Arctic have been changed by boreal forest needle leaf to assess climatic impact induced by future vegetation changes in high-latitude. Direct consequence of the changes in arctic vegetation is large decrease in surface albedo and the local energy budget at the high-latitude composed of latent heat flux, sensible flux, longwave radiation and shortwave radiation has been changed significantly. Along with the surface warming associated with the energy budget result, circulation also changes. Geopotential height and upper-level wind have been changed and the resulting large-scale disturbance has propagated toward lower latitude along the downstream of climatological jetstream. We show that this large-scale teleconnection initiated by the Arctic vegetation is sufficiently strong that eventually influences the East Asian summer monsoon (the North Pacific summer monsoon) circulation, which is a climate system fairly far from the Arctic region.

Keyword: the Arctic vegetation, vegetation change, East Asian summer monsoon.

HOW MUCH WINTER STRATOSPHERIC POLAR-CAP WARMING IS EXPLAINED BY UPWARD-PROPAGATING PLANETARY WAVES IN CMIP5 MODELS?: PART 1. AN INDIRECT APPROACH USING A WAVE INTERFERENCE INDEX

Joo-Hong Kim, Ji-Won Kim, and Baek-Min Kim*

Korea Polar Research Institute, Incheon, Korea

ABSTRACTS

The breaking of upward-propagating planetary (typically characterized by the combination of zonal wave number 1 and 2) waves in the stratosphere is regarded as one of the factors that provoke the sudden stratospheric warming (SSW) and the accompanying collapse of stratospheric polar vortex during winter. It is also known that if the anomalous stationary wave pattern is in phase with that of the climatology during a certain period, this period is dynamically favorable for the upward propagation and amplification of planetary waves. This kind of phenomenon that amplitude of resultant wave increases by combining two or more waves in phase is called the constructive interference. Our research evaluates whether and to what degree the Coupled Model Intercomparison Project Phase 5 (CMIP5) models simulate such a relation between tropospheric wave interference and Northern polar stratosphere temperature anomaly during winter. Here the 500-hPa wave interference index (WII500) is defined as the coefficient that is obtained by projecting the anomaly of wave number 1 and 2 components of 500-hPa geopotential height onto its climatology. Using monthly outputs of the CMIP5 historical runs currently available to us, we examine the lagged relationship (R-square) between the WII500 during November-December-January (NDJ) and the polar-cap temperature anomaly at 50 hPa (PCT50) during December-January-February (DJF) on an interannual timescale. By sampling uncertainty in R-squares of 33-yr samples (chosen fit with the modern reanalysis period, 1980-2012) with bootstrap resampling, we obtain the sampled medians for all models. The observed relations are then calculated using six reanalyses (ERA-40, ERA-Interim, JRA-25, MERRA, NCEP-R1, and NCEP-R2), and the 5-95% confidence interval of their observed R-square is obtained again with bootstrap resampling of all six reanalyses blended. Then we evaluate which CMIP5 model simulates the WII500-PCT50 relation within the probable range of observed R-squares. It is found that R-squares for 16 (8) of 21 (19) high-top (low-top) models are within the probable range. Our results seemingly suggest that high-top models simulate the WII500-PCT50 relation better than low-top models. Furthermore, it is found that the finer version within a same model suite tends to have the WII500-PCT50 relationship closer to that in the observation.

CHANGE IN WINTER SST OVER THE NORTH PACIFIC INDUCED BY SEA ICE LOSS IN BARENTS - KARA SEA

Hyerim Kim, Sang-Wook Yeh, and Baek-Min Kim

*Korea Polar Research Institute
Department of Marine Sciences and Convergent Technologym Hanyang University
hyerimkim@kopri.re.kr*

ABSTRACTS

Satellite data since 1979 reveals that sea ice concentration over the Arctic decreases sharply especially over the Barents-Kara sea. Experiments using a slab ocean model (SOM) have been conducted in order to investigate how much sea surface temperature (SST) change over the North Pacific can be explained in associated with reduction of sea ice concentration (SIC) over the Arctic. Annual cycle of SIC and SST calculated using the composite years of minimum SIC over Barents-Kara sea for November and December when solar radiation merely exists so that heat flux over uncovered ocean is important is forced over polarcap region during simulation, while they are freely evolved elsewhere. Cooling over the western Pacific in the mid-latitude and warming over the eastern Pacific around the cooling region in winter is shown, which is basically driven by change in air circulation and winds thus sensible and latent heat flux.

AGCM SIMULATIONS OF ATMOSPHERIC RESPONSES TO ARCTIC SEA ICE AND SST ANOMALY DURING BOREAL WINTER: IMPACTS OF CLOUD

Jung Ok¹, Baek-Min Kim¹, Dae-Hyun Kim², and Joo-Hong Kim¹

¹*Department of International Cooperation, Korea Polar Research Institute*
²*Lamont-Doherty Earth Observatory, Columbia University, Palisades, New York*
okjung@kopri.re.kr

ABSTRACTS

Recent warming of sea surface temperature (SST) and associated reduction of sea ice over the Arctic is believed to cause the negative phase of the Arctic Oscillation (AO). In this study, two versions of an atmospheric general circulation model (AGCM) are used to simulate the response of atmospheric circulation to the Arctic sea ice and SST anomalies of 2000's. The revised version differs from the control version only in the treatment of low cloud: generation of low cloud is suppressed in cold condition following the work of Vavrus and Waliser (2008). Ensemble simulations were conducted using the two versions of the AGCM by prescribing climatological and recent condition of SST and sea ice over the Arctic.

Results show that the capability of the AGCM to reproduce the observed atmospheric circulation response to the recent Arctic sea ice and SST anomaly strongly depends on the treatment of low cloud. The revised version is able to capture a negative phase of the AO when forced with the recent SST and sea ice anomalies, while the control version simulates a positive phase of the AO.

Surface turbulent flux is suggested as a key process that differentiates the revised version from the control version. In the revised version, positive surface turbulent flux anomalies are confined to the area with negative sea ice anomalies over the Kara-Barents sea, while surface turbulent flux is suppressed over the Greenland Sea. This dipole pattern of surface turbulent flux resembles that of negative AO simulated with the climatological SST and sea ice condition. On the other hand, the control version simulates enhanced surface turbulent flux over the both areas. The longwave radiative feedback of low cloud is much stronger in the revised version due to a lower mean low cloud fraction. The stronger longwave radiative feedback of low cloud enhances surface air temperature effectively, thereby reducing surface turbulent flux over the Greenland Sea.

PREDICTION OF THE ARCTIC OSCILLATION IN BOREAL WINTER BY SEASONAL FORECASTING SYSTEMS: STRATOSPHERIC CONNECTION

Daehyun Kang and Myong-In Lee

*School of Urban and Environmental Engineering,
Ulsan National Institute of Science and Technology
milee@unist.ac.kr*

ABSTRACTS

Prediction skills of the Arctic Oscillation (AO) are compared by the state-of-the-art seasonal prediction systems. UK Met Office Global Seasonal Forecasting System version 4 (GloSea4), the National Center for Environmental Prediction (NCEP) Climate Forecast System version 2 (CFSv2) and The National Aeronautics and Space Administration (NASA) Goddard Earth Observing System Model, Version 5 (GEOS-5) were examined to understand current skills of coupled prediction systems. The systems have ability to reproduce observed large-scale AO phenomenon. Prediction skill of each system shows difference depending on system, and this implies a potential to improve AO prediction and associated climate anomalies in sub-seasonal to seasonal time scale during boreal winter.

INTRODUCTION

The Arctic Oscillation (AO) is the dominant natural climate variability in the Northern Hemisphere winter (Thompson and Wallace, 1998). The AO has dipole structure of sea level pressure (SLP) which has centered mass over the Arctic and mid-latitude with opposite sign. Observational aspects and physical mechanisms of AO have been studied extensively to establish better understandings respect to AO. For example, some studies suggest connection between winter AO and Siberian snow cover and wave propagation in preceding season (Baldwin and Dunkerton, 2001; Cohen et al., 2010).

However, prediction skills of AO (or North Atlantic Oscillation) were not much precise in dynamical seasonal prediction in previous studies (Kim et al., 2012; Arribas et al., 2011). Riddle et al. (2013) found higher correlation of wintertime AO, and source of the prediction skill difference is not precise. This study examines the uncertain aspects of AO by state-of-the-art dynamical seasonal prediction systems.

DATA

Data from following coupled prediction system are used in this research, UK Met Office Global Seasonal forecasting system version 4 (GloSea4) and NCEP coupled forecast system model version 2 (CFSv2) for 14 years (1996-2009). GloSea4 uses Met Office Unified Model (UM) for atmosphere with spatial resolution of 1.25° latitude × 1.875° longitude, with coupled model. Hindcast data initialized in each year are used in this study. The CFSv2 based on forecast from the 126L64

NCEP's Global Forecast System (GFS) with half-hourly coupling to the ocean. CFSv2 9-month hindcasts initiated from every 5th day and run from all 4 cycles of that day, beginning from Jan 1 of each year. The output atmospheric data have horizontal resolution of 1° latitude \times 1° longitude. Seasonal coupled forecasts from GEOS-5 AOGCM uses GEOS-5 AGCM for atmosphere, MOM4 for ocean, the Catchment Land Surface Model for land, and CICE version 4.0 model for sea ice model. Prediction results of winter from November initialization data are used in this study to compare boreal winter AO. Each system has different number of ensemble members in November initialization (12 for GloSea4, 24 for CFSv2, and 15 for GEOS-5).

RESULT AND CONCLUDING REMARKS

Averaged sea level pressure for 1997-2010 winter is shown in Fig. 1. SLP have dipole structure of high pressure over continent and low pressure over the ocean. Each system shows analogous pattern, but amplitude of the pattern varies with system. This implies that the model bias of SLP, and it may correlated to prediction skill of AO. The AO pattern, which is leading EOF of SLP north of 20°N , is shown in Fig. 2. The variability centered over the Arctic and mid-latitude with opposite sign. The AO index of each system result is calculated by the same EOF pattern in Fig. 2. The normalized leading PCs from the EOF are shown in Fig. 3 (i.e. AO index). Each system seems that have marginal prediction skill of AO. GloSea4 and CFSv2 show strong negative AO in 2010 same as MERRA, while GEOS-5 show almost neutral AO state. The source of the relatively lower prediction skill of GEOS-5 may be related to high pressure and cold bias over high-latitude of the system (not shown). Prediction skills of stratospheric coupling process of dynamical prediction systems are also regarded as contributing process to AO (Baldwin and Dunkerton, 2001). Stratospheric prediction skill and physical understanding will be a marginal source to improve prediction skill of AO.

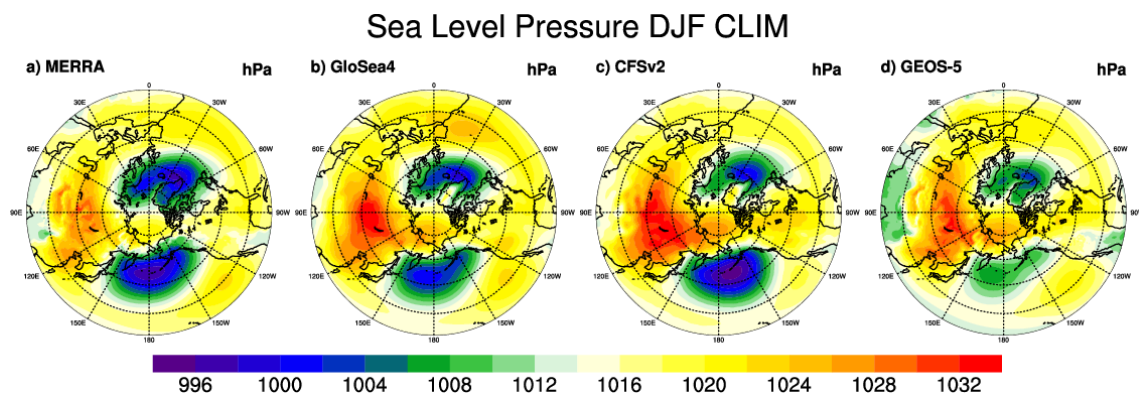


Figure 1. Averaged sea level pressure for 1997-2010 winter (DJF). Each subplot indicates MERRA (a), GloSea4 (b), CFSv2 (c), and GEOS-5 (d).

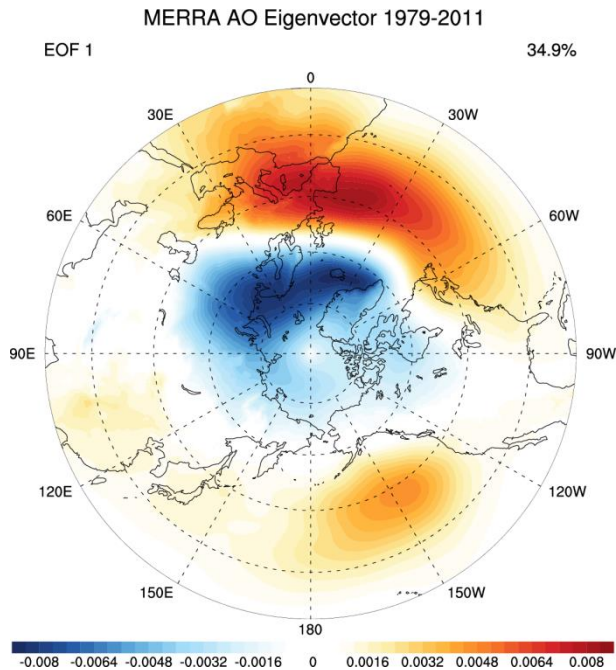


Figure 2. Leading EOF of SLP anomaly north of 20°N from MERRA.

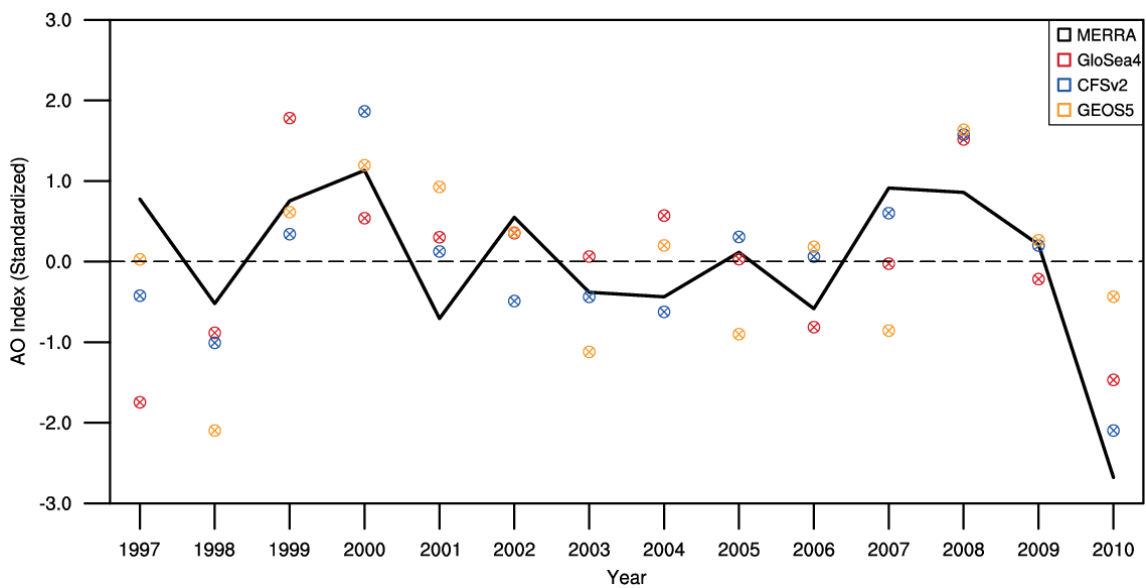


Figure 3. AO index time series from each data. Line indicate MERRA and markers indicate GloSea4 (red), CFSv2 (blue), and GEOS-5 (orange).

REFERENCES

- Arribas A., et al., 2011, The GloSea4 ensemble prediction system for seasonal forecasting, *Mon. Wea. Rev.*, 139, 1891–1910.
- Baldwin, M. P., and T. J. Dunkerton, 2001, Stratospheric harbingers of anomalous weather regimes, *Science*, V. 294, 581-584.
- Cohen J, Foster J, Barlow M, Saito K, and Jones J. (2010), Winter 2009–2010: A case study of an extreme Arctic Oscillation event, *Geophys. Res. Lett.*, 37:L17707.
- Kim, H. M., P. J. Webster, and J. A. Curry, 2012, Seasonal prediction skill of ECMWF System 4 and NCEP CFSv2 retrospective forecast for the Northern Hemisphere Winter, *Clim. Dyn.*, 39, 2957–2973, doi:10.1007/s00382-012-1364-6.
- Riddle, E. E., A. H. Butler, J. C. Furtado, J. L. Cohen, A. Kumar, 2013, CFSv2 ensemble prediction of the

wintertime Arctic Oscillation. *Clim. Dyn.*, 41:3-4, 1099-1116.
Thompson, D. W. J., and J. M. Wallace, 1998, The Arctic Oscillation signature in the wintertime geopotential height and temperature fields, *Geophys. Res. Lett.*, 25, 1297–1300.

SHIP-BORNE LIDAR MEASUREMENTS OF AEROSOL VERTICAL DISTRIBUTION AND OPTICAL PROPERTIES IN ARCTIC AND ANTARCTIC REGION

Youngmin Noh, ^aDongho Shin, ^aSungkyun Shin, ^bTaejin Choi, ^bYoungjun Yoon

*International Environmental Research Center, Gwangju Institute of Science and Technology,
nym@gist.ac.kr*

*^a School of Environmental Science & Engineering, Gwangju Institute of Science and
Technology*

^b Korea Polar Research Institute

ABSTRACTS

Shipboard measurements of vertical distribution and optical properties of atmospheric aerosols in polar regions were performed with a DePolarization Lidar (DPL). The DPL system developed by KOPRI between March 2007 and April 2008 is the first ship-borne lidar of Korea. The DPL was installed aboard the research icebreaking Araon. Araon is operated by the Korea Polar Research Institute (KOPRI). The measurements were performed around the Arctic region from 31 July to 15 August 2011 and 7 July to 9 October 2012 and the Antarctic region from 10 February to 19 March 2012. The DPL system measures profiles of the linear depolarization ratio and backscatter and extinction coefficients of atmospheric particles at 532 nm wavelength. The aerosol optical depth (AOD) was retrieved by integrating extinction coefficient. Among 102 days measurement data, only 28 days data can be analyzed because of weather conditions. The number of analyzed day is 7, 10, and 9 days on 2011 Arctic, 2012 Antarctic, and 2012 Arctic region, respectively. The aerosol was only observed below 2 km altitude except cloud. A low value of AOD less than 0.05 was observed through the whole analyzed days at the Arctic measurement period in 2011. But comparably higher values of AOD were observed at the Antarctic region in 2012 as the value of AOD from 0.08 to 0.18. Since only three days of data were analyzed on Arctic measurement data in 2012, it is hard to explain the overall trend during the measurement period. However, higher values were observed in this period as the highest value of 0.32. The average values of each observation period were 0.045 ± 0.01 , 0.113 ± 0.028 , and 0.177 ± 0.127 on 2011 Arctic, 2012 Antarctic and 2012 Arctic, respectively. Through the whole observation period, volume depolarization ratio was less than 4.0 % except the high altitude cloud. It means that the sea-salt particle was not observed in this measurement period.

IMPACT OF SEA ICE ON ARCTIC WARMING IN CMIP5

Bo Young Yim and Jong-Seong Kug

Korea Institute of Ocean Science & Technology
byyim@kiost.ac

ABSTRACTS

The Arctic warming trends are analyzed using newly archived the Coupled Model Intercomparison Project Phase 5 (CMIP5) dataset. In order to examine how Arctic amplification (AA) is related to the simulated climatological mean sea ice, the dataset of historical and RCP4.5 scenario runs (1960 – 2060) from twenty-eight CGCMs are used. We find that annual AA trends depend on climatological ASO season mean sea ice concentration (SIC_{ASO}) and the nonlinear relationship between them exists from the selected models (Fig. 1). Here, the models are selected based on the ability to reproduce the observed sea ice climatology during 1960 - 2012 (Fig. 2). It indicates that until the SIC_{ASO} reaches at a certain range (i.e., $10 \leq SIC_{ASO} < 20$), AA trends increase, which is probably associated with surface Albedo feedback. After that, however, AA trends decrease slightly for nearly sea ice free condition (i.e., $0 \leq SIC_{ASO} < 10$). To compare the difference of the warming trends for the climatological mean SIC_{ASO} , the global distributions of temperature trends for the highest and lowest SIC_{ASO} in Fig. 1 are shown in Fig. 3. It is found that Arctic warming trends for the highest SIC_{ASO} is more than twice that for the lowest SIC_{ASO} . This also reveals that the remarkable warming is confined to the Arctic for the highest SIC_{ASO} , whereas it tends to extend over the globe for the lowest SIC_{ASO} . Finally, dynamical understanding of the relationship between the Arctic warming and SIC is further discussed.

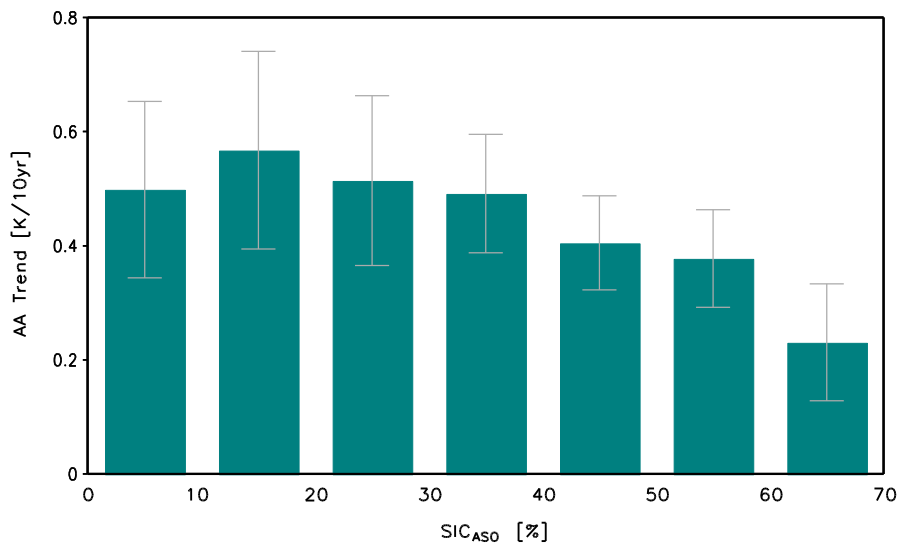


Fig. 1 Annual Arctic amplification (AA) trends for climatological mean SIC_{ASO} for the 14 selected models. Here AA is defined by subtracting global temperature trends from Arctic (> 70°N) temperature trends. Both the mean and trend are calculated on moving over consecutive 30-yr periods from 1960 to 2060.

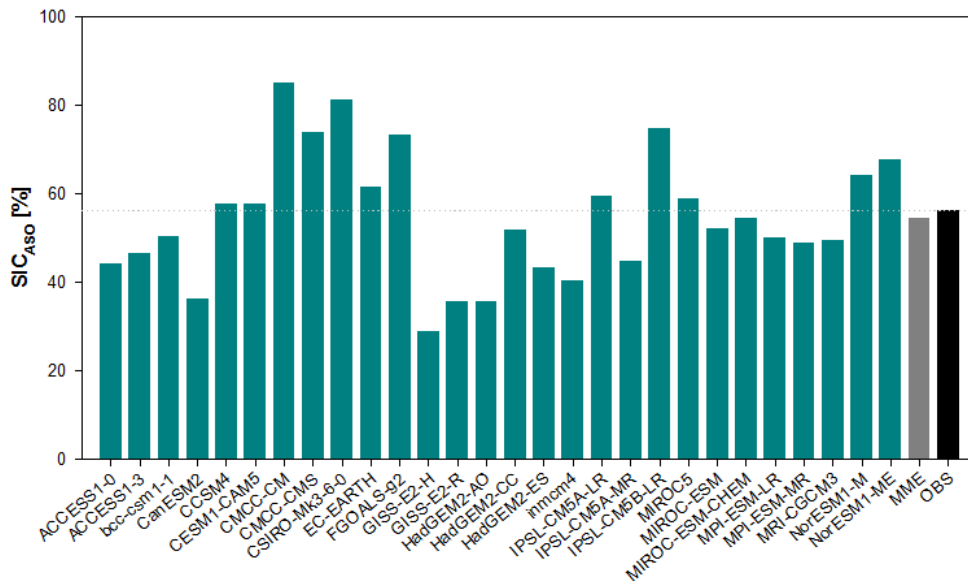


Fig. 2 Climatological mean Arctic SIC_{ASO} for each CMIP5 model, its multi-model ensemble mean (MME), and the observation (HadISST) during 1960 - 2012. The models in which the simulated SIC_{ASO} falls within 20% of the observation are selected in Fig. 1, as in Wang and Overland (2012).

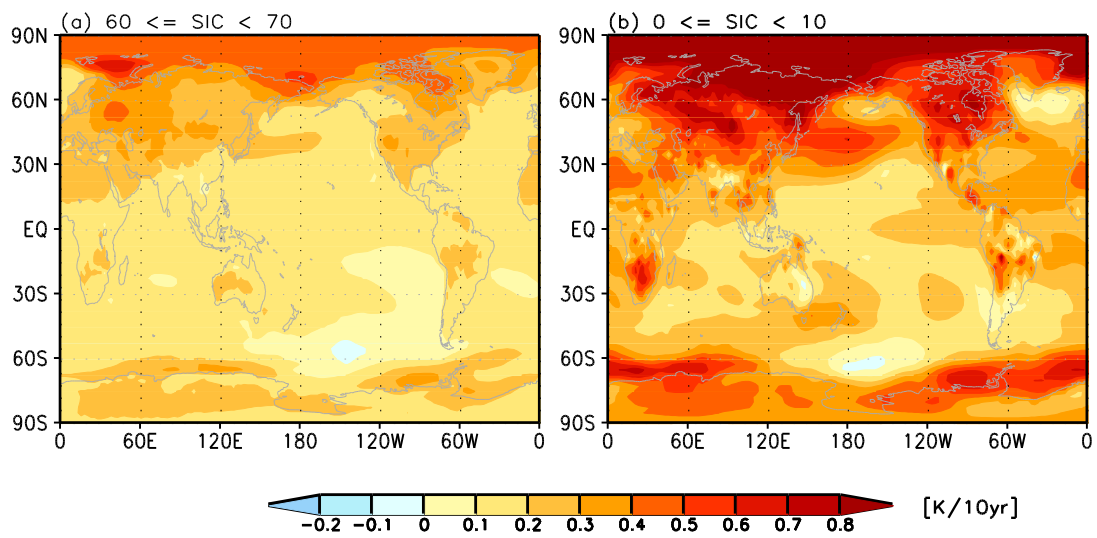


Fig. 3 The global distributions of temperature trends for the highest and lowest SIC_{ASO}.

Wang, M., and Overland J. E., 2012, A sea ice free summer Arctic within 30 years: An update from CMIP5 models, *Geophysical Research Letter*, 39, L18501, doi:10.1029/2012GL052868.

TEMPERATURE VARIATION OVER EAST ASIA IN ASSOCIATION WITH STRATOSPHERIC POLAR VORTEX DURING THE BOREAL WINTER SEASON

¹Sung-Ho Woo, ¹Jong-Seong Kug and ²Baek-Min Kim

¹Korea Institute of Ocean Science and Technology

²Korea Polar Research Institute

oxmanse@gmail.com

ABSTRACTS

In this study, we investigated the tropospheric circulation and temperature variation related with the weakening of stratospheric polar vortex. During the stratospheric weak vortex (SWV) period, the cold condition is dominant over East Asia. A notable feature is the fluctuation of temperature with longer timescale than 10 days during the SWV event while stratospheric circulation varies slowly (Figure 1). The temperature fluctuation in the lower-troposphere over East Asia is mainly forced by the variation of climatological trough located in the upper-troposphere over the East Asian coast during the SWV event. The trough varies in a close connection with the evolution of the SWV. Particularly, in the beginning period of the SWV event (Peak period, -5 - +5 days) when East Asia shows extreme coldness, the trough is deepened exceptionally by wave forcing from the upstream side over the area of Ural Mountain as well as the direct impact related to the decrease of stratospheric geopotential height (Z) over East Asia. In the subsequent period (Decay 1 period, +6 - +16 days), we detected the weakening of the upper-tropospheric trough over East Asia, which mitigates the coldness over the region. The weakening of the trough is caused by the westward migration of strong positive Z anomaly from the North Pacific. The westward positive anomaly comes from the clockwise rotation of stratospheric positive Z anomaly. After about 20 days since the SWV occurrence (Decay 2 period, +17 - +27), the coldness over East Asia gains its strength again. This coldness is induced by the re-developing of the trough over East Asia, which is related to the negative AO-like type pattern associated with the SWV.

The circulation change and temperature variation over East Asia related with the SWV influence the cold surge (CS) characteristics such as its frequency, duration and strength. In comparison of the characteristics of cold surge for the SWV and the stratospheric strong vortex (SSV), the cold surges occurred more frequently in the SWV than in the SSV. Moreover, they are stronger and longer-lasting in SWV than in SSV (Figure 2). The differences between these cold surge characteristics are originated by the impact of anomalous tropospheric circulation (long-lasting and deepening of East Asian trough in the upper-troposphere), which has a close relationship with the SWV.

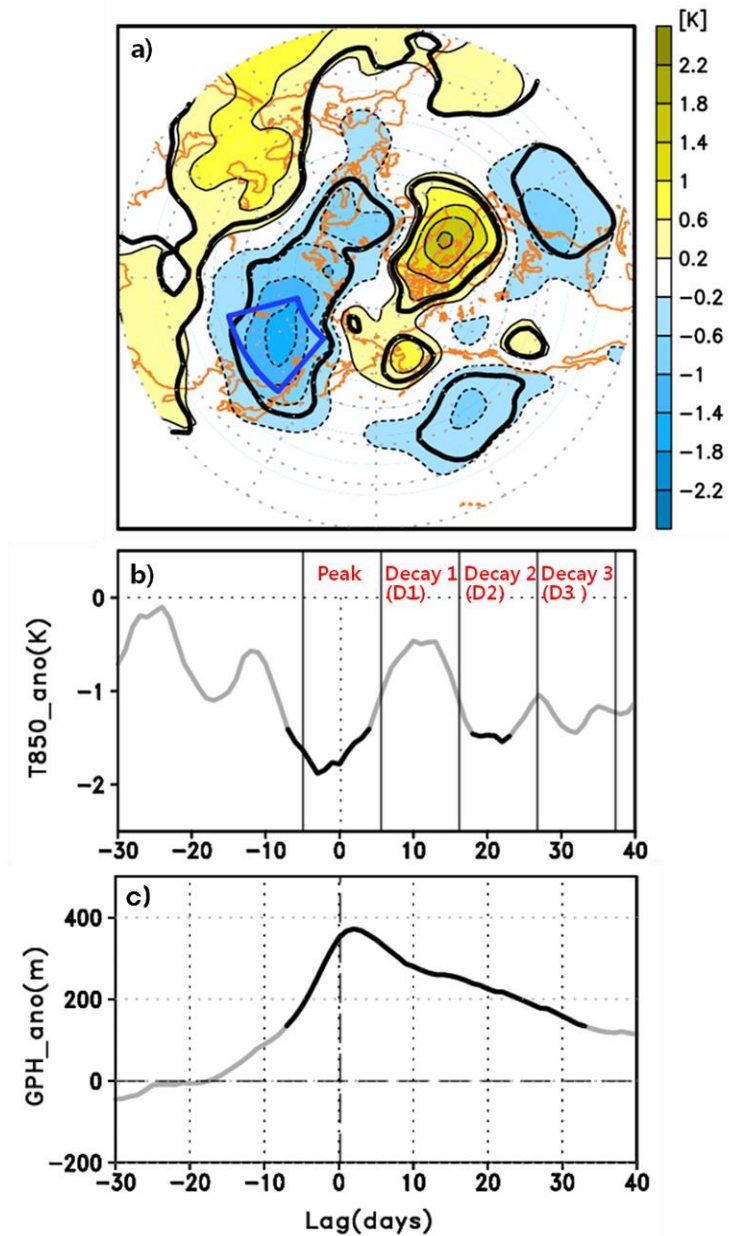


Figure 1. (a) Composite map of mean temperature anomaly ($^{\circ}\text{C}$) at 850 hPa during the SWV event. (b) Lag composite of temperature ($^{\circ}\text{C}$) at 850 hPa averaged over East Asia (blue box in (a)) before and after the starting date of SWV event (0 lag day). The red words represent the sub-periods defined and used in this study. (c) Lag composite of Z anomaly (m) averaged over the poleward region of 65°N at the 50 hPa level. In all the three figures, the thick black lines represent the area and periods satisfying the 95% confidence level.

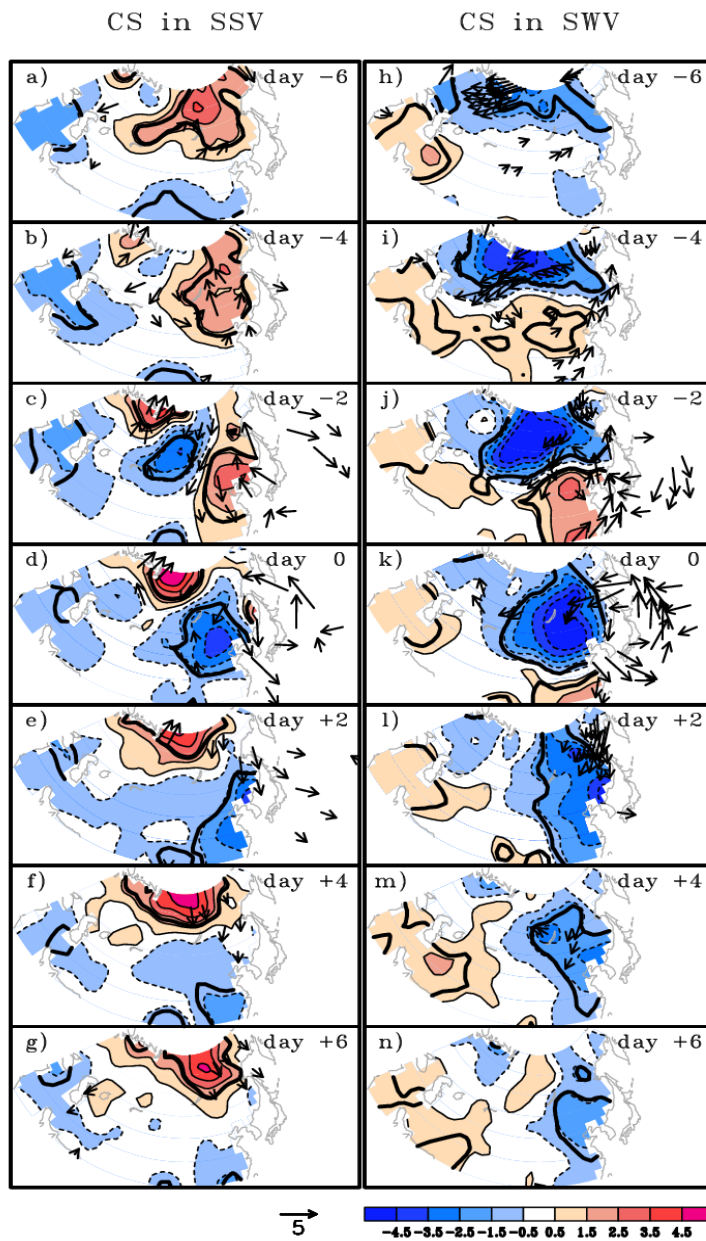


Figure 2. Composite maps of the anomalies of SAT ($^{\circ}\text{C}$) at 850 hPa with thin contour and shading and wind ($\text{m}\cdot\text{s}^{-1}$) for the cold surge period from lag -6 days to lag +6 in the SSV (a–g) and SWV event (h–n) over the East Asian domain. The thick black line represents the boundary of area satisfying the 95% confidence level.

INFLUENCES OF ARCTIC SEA ICE VARIABILITY ON THE SUMMER NORTH ATLANTIC OSCILLATION (SNAO)

Hans W Linderholm^{1}, Tinghai Ou^{1,2}, Jee-Hoon Jeong², Deliang Chen¹, Baek-Min Kim³ and
Chris Folland⁴*

*¹Department of Earth Sciences, University of Gothenburg, Sweden; ²Department of
Oceanography, Chonnam National University, Korea; ³ Korea Polar Research Institute,
Korea; ⁴Met Office Hadley Centre for Climate Change, UK*

**hansl@gvc.gu.se*

ABSTRACT

The influence of the north Atlantic oscillation (NAO) on climate across the North Atlantic region has been highlighted over the past few decades. So far, most research has focused on the winter season, but recently conclusive evidence of strong links of the NAO to climate variability over Europe, especially Northern Europe, also in summer has been presented. The summer NAO (SNAO) exerts a strong influence on rainfall, temperature, and cloudiness and is related to summer extremes, such as droughts and floods and related phenomena (e.g. forest fires), mainly in Europe but also elsewhere. In its positive phase, the SNAO is associated with anticyclonic conditions over Northern Europe, yielding sunny, warm and dry conditions due to a northerly position of the main storm track. In the negative SNAO phase, the storm track moves ~10 degrees (latitude) further south, giving cloudy, wet and cooler conditions over the same region. Moreover, it has been demonstrated that the SNAO is related through teleconnections with climate outside Europe e.g. eastern USA, North Africa and East Asia. Thus, this weather pattern is associated with climate variability in both heavily populated, but also sensitive regions.

A number of possible physical factors affecting NAO variability have been identified, but mainly during winter, and it has been suggested that the melting of Arctic sea ice causes changes in the large-scale atmospheric circulation over the Northern Hemisphere. For instance, recent cold winters, associated with extreme negative phases of the NAO, have been linked to the strong reduction in Arctic sea ice. Here we present the results from a recent study of possible influences of Arctic sea Ice extent (SIE) variability on the SNAO. Analyses over the period 1979-2012 suggest significant links between March-April SIE in the northernmost Pacific (negative) and west of Greenland (positive), and SNAO. These relationships can tentatively be linked to the variability in latent and sensible heat flux related to SIE variability inducing the atmospheric warming and cooling over the two regions. The associated atmospheric circulation, a dipole pattern in sea level pressure anomalies, persists to early summer by strong atmosphere-ocean coupling. A new SEI index, depicting the dipole relation between the two regions, corresponds well with SNAO variability in most years. However, in some extreme SIE years, the two records disagree. It is suggested that this is due to the effect of extremely positive/negative winter Arctic Oscillation years, which will have a stronger effect on the SNAO than SIE. Finally, we take a look at the long-term (multidecadal) relationship between Arctic SIE and the SNAO for the last

few centuries using proxy data.

The 19th International Symposium on Polar Sciences (ISPS)

Korea Polar Research Institute, Incheon, Republic of Korea, October 16-18, 2013

RECENT CHANGES IN WINTER ARCTIC CLOUD AND ITS RELATION TO ATMOSPHERIC STATES OVER THE SURROUNDING REGION

Sang-Yoon Jun^{1,2}, Chang-Hoi Ho², Jee-Hoon Jeong³, and Yong-Sang Choi⁴

¹Systems Development Team, Korea Institute of Atmospheric Prediction Systems

²School of the Earth and Environmental Sciences, Seoul National University

³Faculty of Earth Systems & Environmental Sciences, Chonnam National University

⁴Department of Environmental Engineering, Ewha Womans University

ABSTRACTS

Change in Arctic cloud amount during winter (December to February) in recent three decades is examined with satellite and reanalysis datasets. All datasets present that cloud amount decreases gradually during late 20th century, and both reanalyses show that cloud amount increases largely in the 21st century. In addition, the early gradual decrease and late large increase in three decades are also found in the change in wintertime surface air temperature (SAT) over the Arctic. These coherent changes in cloud amount and SAT are affected by change in relationship between cloud and environmental temperature (moisture); a interannual variation of low level cloud over the Arctic is linked to temperature and humidity at near surface over the marginal Arctic region in the late 20th century, and become to be linked to those over the central Arctic region in the 21st century. Surface condition change due to reduced sea-ice cover is a major cause for the relationship change between two periods. Reduced sea-ice cover leads to near surface warming, decrease in lower-tropospheric static stability, and deepening of planetary boundary layer, which induce a moistening of lower troposphere. Low-level cloud, in turn, increases in the closer relation to surface conditions. In addition, the increase in cloud affects surface through cloud radiative forcing, which further enhances near surface warming. The atmospheric general circulation model experiments also support that reduced sea-ice cover plays a crucial role on the relationship change between cloud and temperature (moisture) and an increase in the Arctic cloud. This study emphasizes that the cloud can enhance the surface warming in recent decade over the winter Arctic, under sea ice retreat condition.

UNDERSTANDING OF CIRCULATION CHARACTERISTICS IN DIFFERENT TYPES OF SUDDEN STRATOSPHERIC WARMING USING WACCM

Hyesun Choi, Baek-Min Kim, and Seong-Joong Kim

*Division of Polar Climate Research
Korea Polar Research Institute
hschoi@kopri.re.kr*

ABSTRACTS

The differences in atmospheric circulation according to the types of sudden stratospheric warming (SSW) are addressed in Northern Hemisphere high-latitude region during boreal winter seasons using Whole Atmosphere Community Climate Model (WACCM) version 4. The identification of SSWs is based on zonal-mean zonal wind at 10 hPa and 60°N. The SSWs are subdivided into two different events that stratospheric polar vortex splits or displacements. To verify the results from WACCM, Modern Era Retrospective-analysis for Research and Applications (MERRA) assimilation products and European Centre for Medium-Range Weather Forecasts (ECMWF) ERA-Interim reanalysis data are used. In order to exclude the influences due to SST and sea-ice forcing, prescribed climatological sea surface temperature (SST) and sea-ice annual cycle are used as boundary conditions every year in the model experiments. The model results show the SSW frequency per year and the ratio of vortex displacements to vortex splits in reasonable ranges. We note that the prominent temperature differences in stratosphere and mesosphere depending on the SSWs types. In the case of split events, the polar temperatures after SSWs are colder in stratosphere and warmer in mesosphere, respectively, than the case of SSW displacement events. Zonal-mean zonal wind is closely related with the differences in temperature since strong westerly anomaly in stratosphere and strong easterly anomaly in mesosphere appear in the split events. It is also interesting that tropospheric temperature is warmer prior to SSWs in the split events. We attempt to explain the dynamical reasons of the temperature differences in polar region by showing the changes in geopotential height, meridional heat flux, residual circulation, etc.

INTERANNUAL VARIATION OF ARCTIC SEA ICE CONCENTRATION IN SUMMER IN RESPONSE TO PRECURSORY ABSORBED SHORTWAVE RADIATION

¹Yong-Sang Choi, ²Baek-Min Kim, ³Sun-Kyong Hur and ⁴Ha-Rim Kim*

¹Department of Environmental Science and Engineering, Ewha Womans University, Seoul, Korea

²Korea Polar Research Institute, Incheon, Korea

³School of Earth and Environmental Sciences, Seoul National University, Seoul, Korea

⁴Department of Atmospheric Science and Engineering, Ewha Womans University, Seoul, Korea

ysc@ewha.ac.kr

ABSTRACTS

Solar radiation in the Arctic region is a main source in the thermodynamic process of sea ice. How much the Arctic sea ice is varied in association with solar radiation absorbed and reflected with highly variable clouds remains to be investigated. Here we used recent satellite observations from the Clouds and the Earth's Radiant Energy System (CERES) to argue that interannual variability in sea ice concentration (SIC) for the north of 65°N is largely explained by 2-3 months preceding absorbed shortwave radiation (ASR), and that ASR is primarily altered by clouds. We first correlated monthly SIC from Hadley center with monthly ASR data for 2000-2012. Results show that decrease in SIC in summer (August-September-October) was followed by the increase in ASR in a few months prior to SIC. The covariance of SIC and ASR was negatively maximized at 2 to 4-month lags. The correlation of ASR and SIC after 4 months remains significant (>95%), whereas the autocorrelation of SIC is trivial for the same lag. This suggests that ASR can be a major predictor of SIC, instead of SIC per se as a predictor. Regionally, thinner sea ice distributed over lower latitudes is generally found to respond faster to ASR. The summer SIC is highly sensitive to ASR ($\delta\text{SIC}/\delta\text{ASR} < -1\% (\text{W m}^{-2})^{-1}$) especially for the transition zone between firstyear ice and multi-year ice. Finally, the ASR was decomposed into cloud albedo and amount, surface albedo, and TOA solar incident flux; among them, contribution of cloud albedo to ASR is predominant during the period from April to September. Therefore the significant correlation between ASR and summer SIC can be mainly due to cloud albedo variations occurred before the summer. However, in our analysis, the opposite effect that the prior SIC affects ASR was not clearly observed. This may suggest that Arctic SIC in summer more likely responds to, but not leads to cloud variations. Considering the aforementioned findings, we will also present a detailed method for a seasonal forecast model where change in SIC throughout the year is determined stochastically. This model consists in two parts, dynamics and thermodynamics, and combines the two parts using Markov method. The performance of this model will be discussed in comparison with previous models.

DETECTING HUMAN INFLUENCE ON ARCTIC SEA-ICE

Seung-Ki Min

*School of Environmental Science and Engineering,
Pohang University of Science and Technology (POSTECH)*
skmin@postech.ac.kr

ABSTRACTS

Identifying and quantifying human influence on the observed climate changes is critical to more reliable projection of future climate changes as well as to better assessment of climate change impacts on human society and ecosystem. Understanding past changes also helps to evaluate climate models in terms of physical mechanisms associated with model responses to anthropogenic (increases in greenhouse gases and sulfate aerosols) and natural (changes in solar and volcanic activities) external forcing factors. During the recent two decades, the Arctic and subarctic regions have been experiencing the impact of global change much earlier and/or more strongly than other regions, which is known as Arctic amplification, and provide a unique opportunity for climate change researches. In the context of detection and attribution, an increasing number of studies have been able to identify human fingerprints on Arctic changes such as surface warming, moistening, and sea-ice decrease. This presentation will introduce our detection study of the Arctic sea-ice change. We have compared observed changes in Arctic sea-ice extent for 1953-2006 with multi-model simulations (CMIP3) integrated under anthropogenic-only forcing and under natural-plus-anthropogenic forcing using a statistical technique (optimal fingerprinting technique). Results suggest that human influence on Arctic sea-ice could have been detected from early 1990s onwards. It is also demonstrated that the detected anthropogenic signal is strongest in summer and extending into colder seasons. We are now conducting an updated attribution analysis by extending the analysis period up to 2012 and using recent multi-model simulations (CMIP5).

Reference: Min, S.-K., X. Zhang, F. W. Zwiers, and T. Agnew (2008), Human influence on Arctic sea ice detectable from early 1990s onwards, *Geophys. Res. Lett.*, 35, L21701, doi:10.1029/2008GL035725.

VARIATION OF ATMOSPHERIC CARBON MONOXIDE OVER THE ARCTIC OCEAN AND THE NORTHWESTERN PACIFIC DURING SUMMER 2012

Keyhong Park¹, Tae Siek Rhee¹, and Louisa Emmons²

¹. Korea Polar Research Institute, Incheon, Korea

². National Center for Atmospheric Research, Boulder, CO, U.S.A.

ABSTRACTS

Atmospheric carbon monoxide (CO) plays an important role in ozone-related chemistry in the troposphere, especially under low-NO_x conditions like the open ocean.

During summer 2012, we performed continuous shipboard measurement of atmospheric CO in the Arctic Ocean and the northwestern Pacific.

Also, for further analyses of the observation, we ran the Model for OZone And Related chemical Tracers-4 (MOZART-4) which is a 3-D global chemical transport model. In the model, we applied tags for each sources and emission regions of CO and this enables us to see the source contribution of the observations.

We found large (± 20 ppbv) variation of CO concentration in both the Arctic Ocean and the north western Pacific which is mostly influenced by the variation of biomass burning CO. Along with the observed variation of CO concentration during the research cruise, we will present in detailed analysis of the variation of source components and change of regional contributions.

SPATIAL DISTRIBUTION OF TRACE GASES IN THE EAST SEA, NORTH PACIFIC, AND BERING SEA ALONG R/V ARAON'S CRUISE TRACK IN 2012

*Tae Siek Rhee¹, Keyhong Park¹, Young-Shin Kwon¹, Kyoung-Ah Park¹, Hyun-Duck Jeon¹,
Doshik Hahm¹, Brian Seok², Dasol Song³, Gangwung Lee³, Hyunjee Kim⁴, and Seunghee
Han⁴*

- 1. Korea Polar Research Institute, Incheon, Korea*
- 2. University of Colorado, Boulder, U.S.A.*
- 3. Hankuk University of Foreign Studies, Youngin, Korea*
- 4. Gwangju Institute of Science and Technology, Gwangju, Korea*

ABSTRACTS

The ocean is an important reservoir of trace gases that are closely related to the climate change on Earth. About 30% of the CO₂ emitted to the atmosphere is taken up by the ocean every year. Other greenhouse gases, CH₄ and N₂O, are adversely emitted to the atmosphere from the ocean. Beside these important greenhouse gases, many trace gases are produced in the ocean associated with biological activities occurring in the ocean. SHIPPO (SHIP-borne Pole-to-Pole Observations) project aims to investigate the distribution of trace gases in the marine boundary layer (MBL), impact of the physical, biological, and chemical processes to the trace gas distribution above, and photochemistry in the MBL, which are ultimately related to the climate in the marine environment. In July 2012, the first SHIPPO campaign took place between Korean peninsula and Alaska, U.S.A., in the North Pacific along the regular track of R/V Araon. The campaign had lasted for two weeks covering west and south coast of Korean peninsula, the East Sea, western limb of the North Pacific, and the Bering Sea. Here we will present the spatial distribution of trace gases that are related to the climate directly or indirectly via photochemistry in the MBL. Included are CO₂, CH₄, N₂O, CO, H₂, O₃, NO_x, PAN, gaseous elemental Hg (GEM), reactive gaseous Hg (RGM), particle bounded Hg (PBM). Along the cruise track, we encountered several air masses coming from South Asia, East Siberia, the North Pacific, and the Arctic Ocean as she straddled between the two large air systems, East Asian Low and North Pacific High. In addition, west-east stark contrast of air quality along the track, most trace gas concentration shows a similar spatial trend from Korean peninsular to Alaska. We also measured trace gases dissolved in the mixed layer, which allows us to determine their fluxes across the air-sea interface. Most of the surface waters were under-saturated with respect to the atmospheric CO₂ above, in particular the continental shelf zone of the Bering Sea appear to be the strongest. Anomalously high CH₄ was observed south of the Hokkaido right after passing the Tsugaru Strait. N₂O was supersaturated everywhere, particularly strongest to the East of the Kuril archipelago. CO showed typical diurnal pattern, although the degree of saturation was not so high as expected that in the open ocean, likely due to overcast during the campaign.

MARITIME BOUNDARY LAYER RESEARCH AT POLAR OCEANS BASED ON AARON

Sang Jong Park, Jaill Yoo, Taejin Choi, Sung Ho Kang, Seoung Joon Kim

*Division of Polar Climate Research,
Korea Polar Research Institute
ctjin@kopri.re.kr*

ABSTRACTS

As the Arctic sea ice shows the pronounced decreases in its area in summer season since 1997, in-situ measurements of meteorological variables, greenhouse gases and aerosol are needed at the higher latitude to better understand the effect of decreased sea ice on the atmosphere and the climate. Especially evaluation of cycles of greenhouse gases and aerosol and their distribution of sink/source is important in understanding the Arctic environment change. Even though some monitoring stations are located in the high latitude Arctic area such as the GAW station at Barrow, Alaska(71.3°), melting of sea ice in summer allows measurements of greenhouse gases and aerosol at higher latitude area at Chucki Sea or Beaufort Sea. Such measurements are possible when ice-breaking research vessels are available. For observation of atmospheric environment variables including fluxes of energy and greenhouse gases, eddy covariance system, consisting of 3-D sonic anemometer (CAST3, Campbell Scientific Inc, USA), wave-scanned cavity ring-down (G2301-f, Picarro Inc., USA) analyzer, open-path gas analyzer (LI7500, Licor, USA), an elastic LIDAR (DPL3020, EN3, Korea) together with meteorological instruments are operated at Korean Icebreaking Research Vessel, ARAON during the research cruise. In this presentation, we will present preliminary results from the Arctic ocean cruise by ARAON in 2012 and 2013. This research was supported by grants from KOPRI (PM12020). This research was also partly supported by grants from KOPRI(PE13010).

POSTER SESSION 2

ICE AND OCEAN

DISTRIBUTION OF MICROBIAL POPULATIONS AND THEIR RELATIONSHIPS WITH ENVIRONMENTAL FACTORS IN THE PRYDZ BAY AND ITS ADJACENT SOUTHERN OCEAN, ANTARCTIC

Min WANG

Ocean University of China, Qingdao, China

ABSTRACTS

During the Austral summer of 2009/2010, flow cytometry was used to analyze samples collected from the waters of 30 stations from two cruises during December 24 - 26, 2009 and February 14 – 25, 2010 in the Prydz Bay and its adjacent Southern Ocean, Antarctic (70° E-76°E, 61° S-69°S). Three groups of microbes were detected and counted in this study, including picoeukaryotes, heterotrophic bacteria and virus. Viral variability mainly depends on their host cell abundance and on different host groups in different water depths (bacteria and chlorophyll a in the epipelagic waters, picoeukaryotes and bacteria in the mesopelagic waters, and bacteria in the bathypelagic waters). For the horizontal distribution, picoeukaryotes and heterotrophic bacteria abundances were higher in the offshore open ocean waters, while virus and chlorophyll a concentration were abundant in the nearshore continental shelf waters. For the vertical distribution, when the surface chlorophyll a concentration was higher than 0.1 µg l⁻¹, the highest values of virus always coincided with the maximum values of chlorophyll a in the surface or the sub-surface water layers (25 m). In the open ocean waters, the highest values of virus usually agreed with the maximum values of bacteria abundance in the deeper water depth (50m, 300m and 500m) when the surface chlorophyll a concentration was lower than 0.1µg l⁻¹. Virus and bacteria abundances decreased with increasing water depth below the maximum value layer and increased a little near the seafloor. Picoeukaryotes were abundant in the surface and subsurface waters in the nearshore IS transect and abundant from surface to 75/100m in the P2, P3 and P4 transects. Principle component analysis and Pearson correlation analyses results indicated that virus had an intimate relationship with chlorophyll a and bacteria, and nutrients (NO₂+NO₃, phosphate and silicate) and possible water masses (water depth, salinity) were the major control factors of the variation of picoeukaryotes in the Prydz Bay and its adjacent Southern Ocean, Antarctic.

ASYMMETRY VARIABILITY BETWEEN THE ARCTIC AND ANTARCTIC SEA ICE

Fei HUANG, Xiao ZHOU and Hui DI

*Department of International Cooperation,
Korea Polar Research Institute
Physical Oceanography Laboratory and Ocean-Atmosphere Interaction and Climate
Laboratory, Ocean University of China, Qingdao, China*

ABSTRACTS

It is known that the Arctic sea ice extent (SIE) reduced dramatically during the past 30 years, while the Antarctic sea ice extent appeared a slightly rising trend under the global warming background. Besides the linear trend difference of total SIE in Arctic and Antarctic, dominant modes on seasonal and interannual and decadal timescales also shows different features between Arctic and Antarctic. On the seasonal timescale, asymmetry variability between the Arctic and Antarctic sea ice mainly appears in semi-annual variation. On the interannual and decadal timescales, the Arctic total SIE is dominant by a descending trend, while the Antarctic total SIE appears significant interannual and decadal variabilities. In order to investigate the detailed spatial and temporal asymmetry variability between the Arctic and Antarctic sea ice and their season-dependent evolving process, a season-reliant empirical orthogonal function (S-EOF) analysis onto the sea ice concentration (SIC) from 1979 to 2007 was performed. It is found that the first leading mode, accounts for 12.1% of total variance, shows a descending trend in principal component (PC) in the past 30 years, especially in the latest decade, mostly reflecting the declining of the Arctic sea ice trend. The Arctic appears consistent sea ice melting while in most regions around the Antarctic continent except for the Bellingshausen Sea and Amundsen Sea around western Antarctic, the SIC shows an increasing trend. The second significant mode, which account for 10.1% of total variance, mostly indicates the interannual and decadal oscillation of the Antarctic sea ice with a seesaw pattern between the northwest part and other sectors around the Antarctic. This mode may relevant to an out-of-phase oscillation of joint annular mode between two hemispheres in the atmosphere, which links the two hemispheres by a wave-train-like "atmosphere bridge" through the central Pacific across Equator in transition seasons.

Acknowledgement: The work was supported by the Global Change Research Program of China (2010CB951403) and the special scientific research fund of the State Oceanic Administration (201005017-6).

PYROSEQUENCING ASSESSMENT OF PROKARYOTIC COMMUNITY IN THE CHUKCHI SEA DURING SUMMER 2012

Chung Y. Hwang¹, Yoon Y. Yang¹, Yoo K. Lee¹, Sung-H. Kang², Hong K. Lee¹

¹Division of Polar Life Sciences, ²Division of Polar Climate Research,
Korea Polar Research Institute
cylwang@kopri.re.kr

ABSTRACTS

Prokaryotes (i.e. *Bacteria* and *Archaea*) play important roles in biogeochemical cycles in marine environments. During a summer season in the Chukchi Sea, it usually exhibits 4 distinct water bodies based on hydrographical properties; surface mixed layer water, Pacific summer water, Pacific winter water and Atlantic water. During the icebreaker R/V Araon expedition in summer 2012, Arctic sea ice extent was lowest ever recored, enabling us to investigate large spatial distribution of prokaryotic community structures along a latitudinal transect between 75.3°N and 82.3°N in the Chukchi Sea. Prokaryotic community was examined using 454 pyrosequencing of the V5-V8 region of the 16S rRNA gene for epi- and mesopelagic seawater samples at 7 stations covering from the continental shelf to deep basin. We obtained 237,329 sequence reads falling into 2,800 operational taxonomic units (OTUs) at the 97 % identity level. In the surface water, *Proteobacteria* were most dominant and increased from 53 to 75% toward higher latitudes. *Bacteroidetes* were abundant in either the surface or the subsurface chlorophyll maximum (SCM; 31-46%) at 5 stations located in < 80 usually eather decreased to 12-20% at the 2 northmost stations where chlorophyll *a* concentrations were relatively low. *Bacteroidetes* showed a steep decline to 2-5% below the 100 m depth at all stations. *Planctomycetes* were unexpectedly abundant (5-11%) between SCM and 100 m at most stations. Interestingly, *Archaea* were abundant (35 abundant (5-11%) between SCM and 100 m at most stations. Interestingly, 5 stations located in < 80 usually eather decreased to 12-20% at the 2 northmos
This research was supported by the Korea Polar Research Institute (Grant No. PM12020).

RAPID ROBOTIC TOXICITY BIOASSAY METHOD FOR BIOCIDES USING MALE GAMETOPHYTE OF POLAR BROWN ALGAE *SACCHARINA LATISSIMA*

Hoon Choi^{1,2}, *Gyo-Sun Jin*³, *In-Young Ahn*³, *Eun Jin Park*⁴, *Youn-Jung Kim*^{4,5} and *Taejun Han*^{2,4,5*}

¹*Division of Life Science, Incheon National University, 12-1 Songdo-dong, Yeonsu-gu, Incheon, Korea 406-772*

²*Institute of Green Environmental Research Center, 7-46 Songdo-dong, Yeonsu-gu, Incheon, Korea 406-772*

³*Korea Polar Research Institute (KOPRI), 7-50, Songdo-dong, Yeonsu-gu, Incheon 406-840, Republic of Korea*

⁴*Greenpioneer, 2nd floor, R&D center, Incheon National University, 7-46 Songdo-dong, Yeonsu-gu, Incheon, Korea 406-772*

⁵*Department of Marine Sciences, Incheon National University, 12-1 Songdo-dong, Yeonsu-gu, 406-840, Incheon, Korea*
hanalgae@incheon.ac.kr

ABSTRACTS

The sensitivity on chlorophyll *a* fluorescence of male gametophyte of the Arctic brown seaweed *Saccharina latissima* to four PSII damaging herbicides (atrazine, hexazinone, diuron and simazine) and bis-tributyltin were investigated and a new toxicity bioassay method was developed. *S. latissima* was collected from Kongsfjorden, an inlet in the Arctic's Svalbard archipelago. The endpoint used was the effective quantum yield (F_v'/F_m') and exposure time was 30 min. Optimal test conditions determined for irradiance, pH, salinity and temperature were darkness, 7, 35 ‰ and 5 °C, respectively. Effect of aforesaid PSII damaging toxicants were evaluated in terms of Effective Concentration (EC₅₀). For the tested toxicants, the magnitude of the effect was as follows: diuron (EC₅₀ of 0.003 mgL⁻¹) > hexazinone (0.006 mgL⁻¹) > atrazine (0.011 mgL⁻¹) > simazine (> 2.5 mgL⁻¹) and the EC₅₀ for TBT was 0.007 mgL⁻¹. The CV (%) range for F_v'/F_m' was 1.47 - 6.31, indicating high levels of precision of the tests. Gametophytes of *S. latissima* can be preserved for several years in the laboratory. Likewise, high growth rate, wide range of temperature tolerance and easiness to culture are their unique characteristics. The robotic assessment using PAM fluorometry allows easy and fast detection. The data presented here proclaim the advantages of early life stages of polar brown algae for sensitive, easy and fast toxicity assessment on various toxicants could be change in Arctic environment.

PHYTOPLANKTON COMMUNITIES IN THE WESTERN ARCTIC OCEAN DURING LATE SUMMER

Hyoungh Min Joo^{1}, Hans-Uwe Dahms², Jun Oh Min¹, Sang Heon Lee³,
Kyung Ho Chung¹, Seung Won Jung⁴, Jin Hwan Lee², Sung-Ho Kang¹,*

¹ Korea Polar Research Institute, KIOST, Korea

² Sangmyung University, Korea

³ Pusan National University, Korea

⁴ Library of Marine Samples, KIOST, Korea

hmjoo77@kopri.re.kr

ABSTRACTS

The Arctic Sea has not been studied as intensively as the other oceans because of difficulties imposed by severe temperatures and ice conditions. Biological oceanographic research has been particularly limited at these high latitudes. The combination of low temperature, occurrence of sea ice, and extreme seasonal variations in the light regimen strongly influences the growth of phytoplankton and regulates their spatial and temporal patterns of distribution in polar oceans. Phytoplankton assemblage structure varies over large spatial scales in the Arctic Ocean and subarctic waters due to geographic variation in environmental conditions. It is important to assess this variability for improved understanding of the responses of marine ecosystems to current and future climate changes in high northern latitudes. We therefore investigated the structure of phytoplankton communities and environmental conditions in the Canada Basin, the northern Bering Sea, and the Chukchi Sea. The Canada Basin is mostly covered by multi-year and first-year ice. The northern Bering and Chukchi Seas are shallow shelf regions (20–60 m deep) that are covered by ice for about six months of each year. The Chukchi Sea lies near the eastern boundary of the great polar continental shelf system; it functions as a conduit connecting the waters of the north Pacific and Arctic Oceans. The specific objectives of our study were (1) to develop an overview phytoplankton communities structures in different sectors (Bering Sea, Chukchi Sea, and Canada Basin) of the western Arctic Ocean in the periods 2006–2009, (2) to determine the distribution of phytoplankton assemblages along latitudinal gradients in the western Arctic Ocean, and (3) to improve understanding of the relationships between phytoplankton assemblages and environmental factors.

To determine the spatial distributions of phytoplankton communities in these three sectors of the western Arctic Ocean, We analyzed algal samples in each sector during summer using light microscopic examinations of slides prepared by the HPMA method. The data for the period 2006–2009 were collected during the course of five research surveys aboard diverse research vessels. In this time period, there was variation in algal species richness. Across all sectors, 116 taxa were compiled for seven algal classes: Dinophyceae (23 species), Bacillariophyceae (76 species), Cryptophyceae (1 species), Chrysophyceae (1 species), Dictyochophyceae (3 species), Prasinophyceae (2 species), and Prymnesiophyceae (1 species). The Bering and Chukchi Seas had high species richness in the summer period, but waters of the Canada Basin were less diverse, likely because of differences in

physicochemical factors that determine the structure of phytoplankton assemblages. The predominant taxa in the Bering and Chukchi Seas were diatoms, whereas prasinophyceae were predominant in the Canada Basin. Differentiation in phytoplankton assemblages among regions may be explained by the large-scale spatial distributions of ocean currents and by recently observed changes in environmental factors within the sea ice substratum.

Photosynthetic eukaryotes are widely considered to be an active and often predominant component of high-latitude phytoplankton assemblages. To examine this premise over large spatial scales, we collected samples to determine assemblage structure and biovolumes of phytoplankton taxa along an ocean transect in western Arctic waters. The transect included 37 stations where samples were collected at the surface and in subsurface chlorophyll a maximum (SCM) depths of the Bering Sea, Chukchi Sea, and Canada Basin from July 19 to September 5, 2008. Phytoplankton ($>2 \mu\text{m}$) were identified and counted. A cluster analysis of abundance and biovolume data revealed different assemblages in waters of the shelf, slope, and basin regions. Phytoplankton assemblages comprised 71 taxa in the following algal classes: Dinophyceae, Cryptophyceae, Bacillariophyceae, Chrysophyceae, Dictyochophyceae, Prasinophyceae, and Prymnesiophyceae. The most abundant species were pico-/nano-sized at both SCM depths at most stations. Nano- and pico-sized phytoplankton appeared predominant in the Bering Sea, whereas diatoms and nano-sized cells were responsible for most of the taxon diversity in the Bering Strait and in the Chukchi Sea. From the western Bering Sea to the Bering Strait, the abundance, biovolume, and species diversity of phytoplankton tracked marked latitudinal gradients toward the central Arctic. Although pico- and nano-sized phytoplankton contributed most to cell abundance, their chlorophyll a contents and biovolumes were smaller than those of the larger algal taxa. Micro-sized phytoplankton contributed most to the biovolume in the largely ice-free waters of the western Arctic Ocean during summer 2008.

Finally, to detect changes in phytoplankton community traits correlated with nutrients at the surface and at chlorophyll a maximum depths in the western Arctic Ocean, we measured phytoplankton assemblage parameters and selected environmental factors in the Chukchi Sea during summer 2012 and performed correlation analyses. Phytoplankton assemblages comprised 53 taxa in the following algal classes: Dinophyceae, Cryptophyceae, Bacillariophyceae, Chrysophyceae, Dictyochophyceae, Prasinophyceae, and Prymnesiophyceae. The most abundant species were nano-/pico-sized phytoplankton at both depths at most stations. These small cells are likely predominant at high latitudes, whereas diatoms were predominant near the western and eastern boundaries of the study area. From an analysis of MDS plots derived from additive trees clustering, we detected four (surface) and three (SCM) clusters of collection stations. This differentiation of stations into clusters according to their phytoplankton assemblage structures may relate to the water flow circulation pathways in the Arctic Ocean. The correlation between phytoplankton assemblages and environmental factors demonstrated that salinity and nutrients (especially nitrate+nitrite) influenced phytoplankton assemblages. The results predict that phytoplankton assemblages are differentiated by water mass identity (e.g., Pacific Winter Water, East Siberian Water, and Northern Sea Ice Melting Water), salinity, and nutrients (especially nitrogen) in high-latitude currents of the western Arctic Ocean.

The significant contributions of this study are as follows. First, although there have been previous Arctic Ocean studies of phytoplankton using satellite data, chlorophyll determinations, and pigment analysis, our microscopic analyses of algal assemblages are novel. Second, we demonstrated that phytoplankton communities are more strongly affected by ocean currents than by other environmental factors during late summer.

This study was limited to collections made in summer. This short temporal window did not allow investigations of seasonal successional changes in the assemblages. Seasonal successional changes contribute substantially to the intra-annual variability of assemblage structure and biomass in high-latitude waters. As sea ice melts during spring and summer, phytoplankton tend to bloom farther north toward the Chukchi Sea where biomass accumulates into September. A better understanding of the ecology of phytoplankton assemblages in the Chukchi Sea will require multi-season and multi-year analyses.

Table 1. Region-specific taxa in the western Arctic Ocean during summer

Subarctic Ocean		Arctic Ocean	
Bering Sea		Chukchi Sea	Canada Basin
<i>Prorocentrum gracile</i>			<i>Chaetoceros socialis</i>
<i>Protoperidinium pellucidum</i>	<i>Ceratium pentagonum</i>		<i>Ceratium carriense</i>
<i>Chaetoceros furcellatus</i>	<i>Chaetoceros danicus</i>		
<i>Corethron criophilum</i>	<i>Stephanopyxis nipponica</i>		
<i>Detonula confervacea</i>	<i>Thalassionema frauenfeldii</i>		
<i>Fragilaria striatula</i>	<i>Thalassiosira hyaline</i>		
<i>Skeletonema costatum</i>			
<i>Thalassionema javanicum</i>			
<i>Thalassiosira australiensis</i>			
<i>Thalassiosira baltica</i>			
<i>Thalassiothrix longgissima</i>			

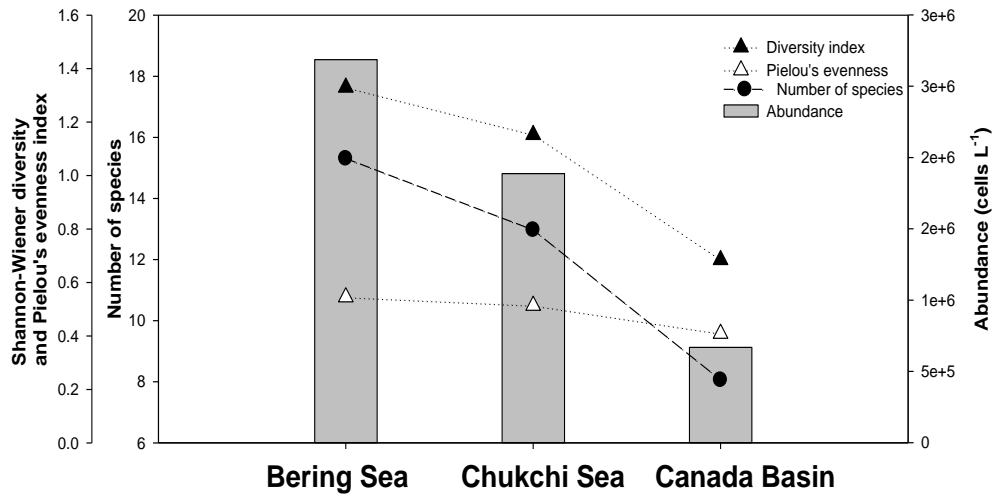


Figure 1. Average values of Shannon-Wiener diversity, evenness, number of species, and abundance of phytoplankton (other than pico- and nanophytoplankton) in three regions.

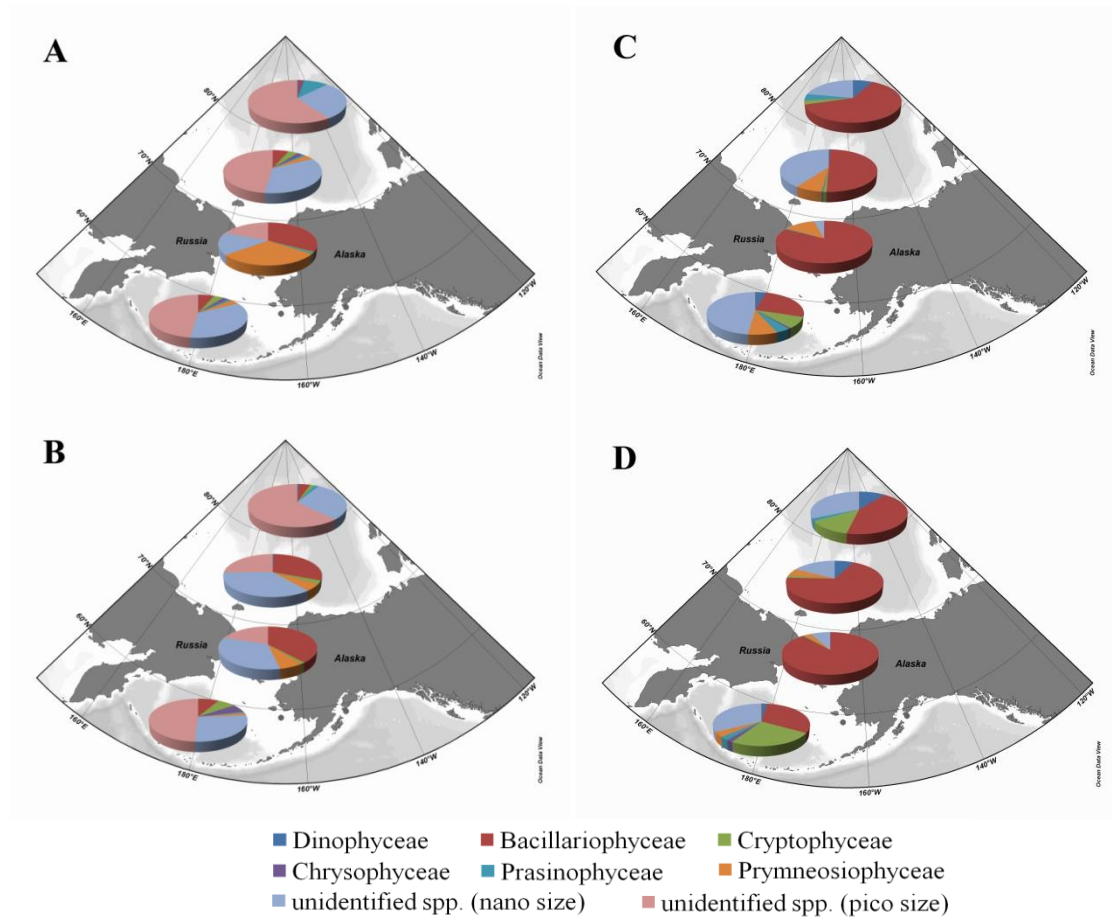


Figure 2. Composition of phytoplankton communities by abundance (A: surface, B: SCM depth) and biomass (C: surface, D: SCM depth) in the study area.

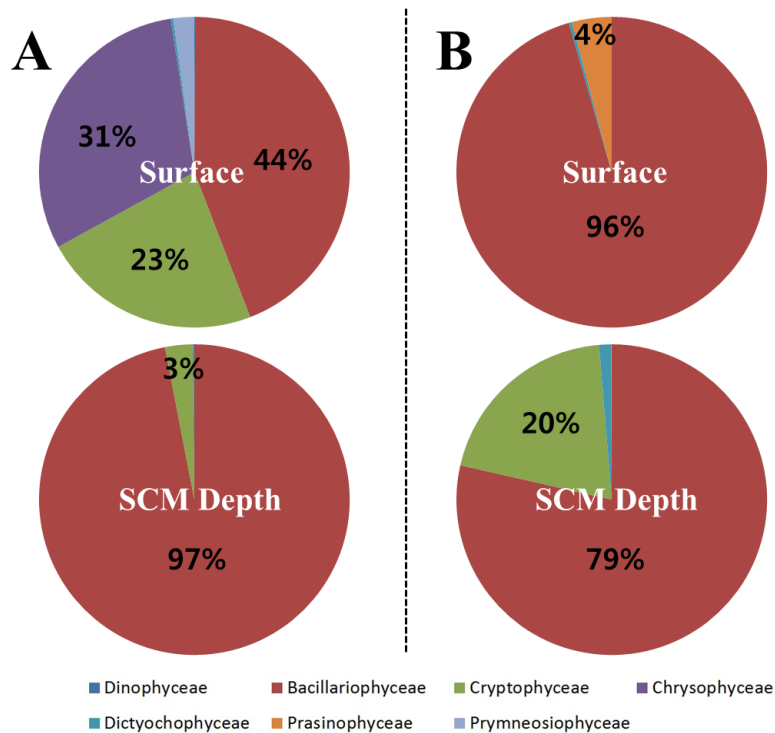


Figure 3. Proportional contributions by seven algal classes (excluding nano- and pico-sized taxa) to total cell densities in the western (A) and eastern (B) sectors of the study area during late summer 2012. The differences in proportions between sectors within depths were significant (t-tests, $p < 0.05$).

* This research was supported by grants from KOPRI (PM1 2020)

UNDER-ICE MEASUREMENT OF SUSPENDED PARTICULATE MATTERS, CHUKCHI SEA

Hyun Jung Lee^{1}, Ho Kyung Ha¹, Yong Hoon Kim², Hyoung Min Joo¹*

¹Korea Polar Research Institute, Incheon 406-840, South Korea,

²RPS ASA, South Kingstown, RI 02879, USA

*[*hyunjung@kopri.re.kr](mailto:hyunjung@kopri.re.kr)*

ABSTRACTS

Due to a high melt rate, a large amount of particulate matters existed in the Arctic sea ice are released into the underlying water column. Understanding the characteristics of particulate matters is important to determine the settling velocity and mass flux in water column. Using an acoustic Doppler current profiler and a submersible digital holographic camera (Sequoia, LISST-HOLO), an in-situ experiment was conducted on the drifting sea ice to estimate spatial and temporal variation in suspended particulate matters (SPM) distribution under the sea ice in the northern part of Chukchi Plateau, Arctic Ocean. The sediment captured in the sea ice might be released into the underlying water by melt out through the melt pond. The peak in size range of sediment measured by LISST-HOLO was in the range of 40-50 μ m, which corresponded with the dominant size of phytoplankton under the sea ice. SPM concentration under the sea ice increased up to about 100 mg/l. The increased biomass associated with a phytoplankton bloom contributed significantly to the increase in SPM. Particulate materials and ice algal communities contained in sea ice also contributed to the increase in SPM.

This study was supported by KOPRI grants (PE10260, PM12020)

SINKING PARTICLE FLUX AND RADIOCARBON VALUES OF PARTICULATE ORGANIC CARBON IN THE DEEP CANADA BASIN

*Minkyoung Kim¹, Jeomshik Hwang¹, Daniel B. Montluçon²,
Cameron P. McIntyre², Negar Haghipour², S. J. Manganini³, Timothy I. Eglinton²*

¹*Pohang University of Science and Technology, Pohang, South Korea*

²*ETH Zürich, Zürich, Switzerland*

³*Woods Hole Oceanographic Institution, Woods Hole, USA*

mini324@postech.ac.kr

ABSTRACTS

Canada Basin of the Arctic Ocean is experiencing drastic environmental changes such as increasing sea-ice retreat in summer and deepening chlorophyll maximum depth. Understanding how particulate organic carbon (POC) production and its transfer to the deep interior will respond to the current environment change is one of the main research topics in this critical region. We have been collecting sinking particles at three stations in the central Canada Basin from 2004.

It has been previously reported that POC supply into the basin interior from resuspended particles on the continental margin accounted for the major fraction of sinking POC (Hwang et al., 2008). We have expanded spatial and temporal coverage of sinking particle sample collection compared to the previous 2004-2005 study.

We will present particle flux and radiocarbon content and discuss the POC cycling and its potential change in the face of the current environmental change.

POPULATION DYNAMICS OF BACTERIAL ASSEMBLAGES IN THE ARCTIC SEAFLOOR

Dukki Han¹, Seung Il Nam², and Hor-Gil Hur¹

¹*School of Environmental Science and Engineering, Gwangju Institute of Science and
Technology* ²*Division of Polar Climate Research,
Korea Polar Research Institute*
hghur@gist.ac.kr

ABSTRACTS

The expedition for the IBRV *ARAON* to the western Arctic Ocean was progressed during summer season from 2011 to 2012. Total 22 sampling sites were selected to monitor benthic bacterial assemblages in the Arctic seafloor. From these sampling sites, 22 sediment cores were collected by the box corer or multicorer equipped in the *ARAON*, and their surface layers were respectively transferred into sterile tubes for the further analyses of pyrosequencing and sediment properties. In this study, a pyrosequencing approach using 454 GS FLX Titanium Sequencing System (Roche) is applied for bacterial diversity, taxonomic classification and phylogenetic analysis. The bacterial assemblage structure of 22 samples was determined using a pyrosequencing approach, and categorized into five groups (Group I to V). The primary aim of this study is to understand the abundance and composition of bacterial assemblages in the Arctic benthic ecosystem, and further to search the effects of environmental factors on the population dynamics of benthic bacterial assemblages by monitoring distributions of major taxa of the bacterial assemblages. Bacterial assemblages in the samples were mostly represented by *Proteobacteria* (47.9%), and followed by *Actinobacteria* (12.0%) and *Acidobacteria* (9.3%). Their relative abundance seemed to be influenced by dispersal limitation from continental shelf to seafloor. Our results suggest that there is a factor to affect population dynamics of bacterial communities in the seafloor although the collected samples showed the local community pattern.

STUDY ON THE DISTRIBUTION OF DISSOLVED ORGANIC CARBON (DOC) IN THE WESTERN ARCTIC

Jun-Oh Min¹, Kyung Ho Chung¹, Sun-Yong Ha¹, Hyun Min Joo¹, Kyung-Hoon Shin², Sung-Ho Kang^{1*}

¹Korea Polar Research Institute (KOPRI), Division of Polar Climate Research, 26 Songdomirae-ro, Yeonsu-Gu, Incheon, 406-840, South Korea

²Hanyang University, Marine Environmental Science department, 1271 Sa-3 dong, Sangnok-gu, Ansan, Kyeonggi-do, 425-791, Korea

jomin@kopri.re.kr

ABSTRACTS

The distribution of Dissolved Organic Carbon (DOC) in the Chukchi Sea was investigated on the Western Arctic using research vessel Araon from 1 August to 10 September 2012. DOC samples were collected at total 32 sampling stations, and contour distribution of DOC on seven stations at East Siberian Sea (ESS)/Mendeleev (MR) and Northwind Ridge (NWR) were sampled through depths.

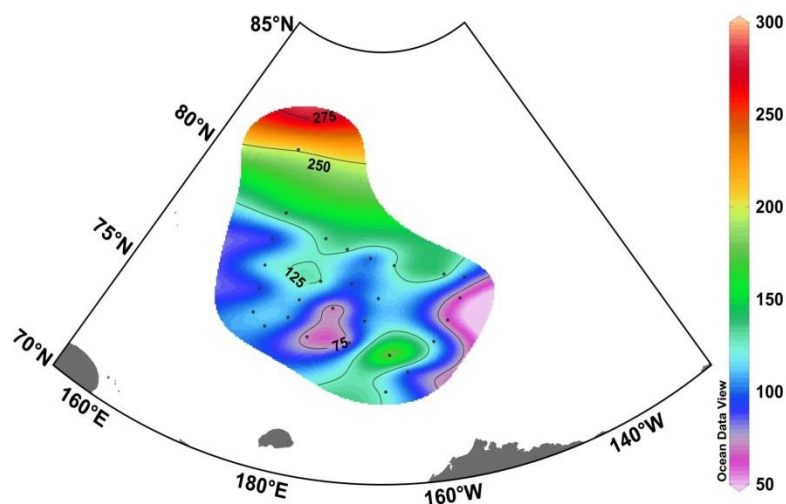


Fig. 1. Surface distribution of DOC concentration.

Surface distribution of DOC concentration was shown an increase trend toward higher latitude stations rather than lower latitude ones. Higher latitude stations (82° 32 N, 171° 62 E – 82° 20 N, 172° 27 E) which were affected by Sea Ice, were represented the highest values of DOC concentration (200 ~ 278 $\mu\text{M L}^{-1}$) (Fig. 1). Besides the DOC concentration obtained higher values (104 ~ 145 $\mu\text{M L}^{-1}$) in the eastern part (75° 33 N, 173° 76 E ~ 78° 99 N, 174° 00 E) than those (50~90 $\mu\text{M L}^{-1}$) in the western (74° 00 N, 163° 99 W ~ 76° 99 N, 153° 98 W) of Chukchi sea (Fig. 2 and Fig. 3).

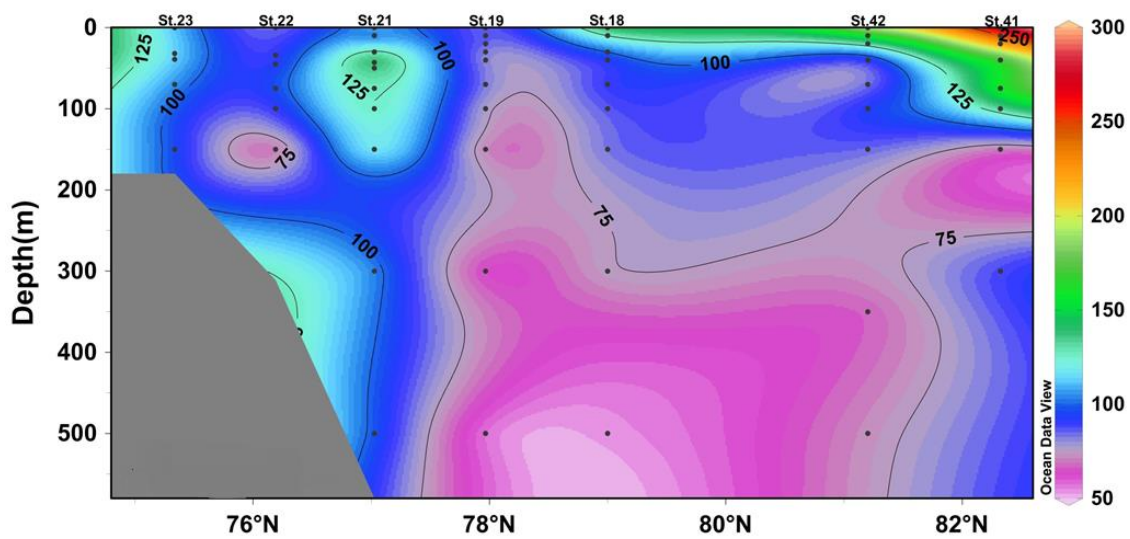


Fig. 2. Contour distribution of DOC concentration in each station (East Siberian Sea/Mendleyev)

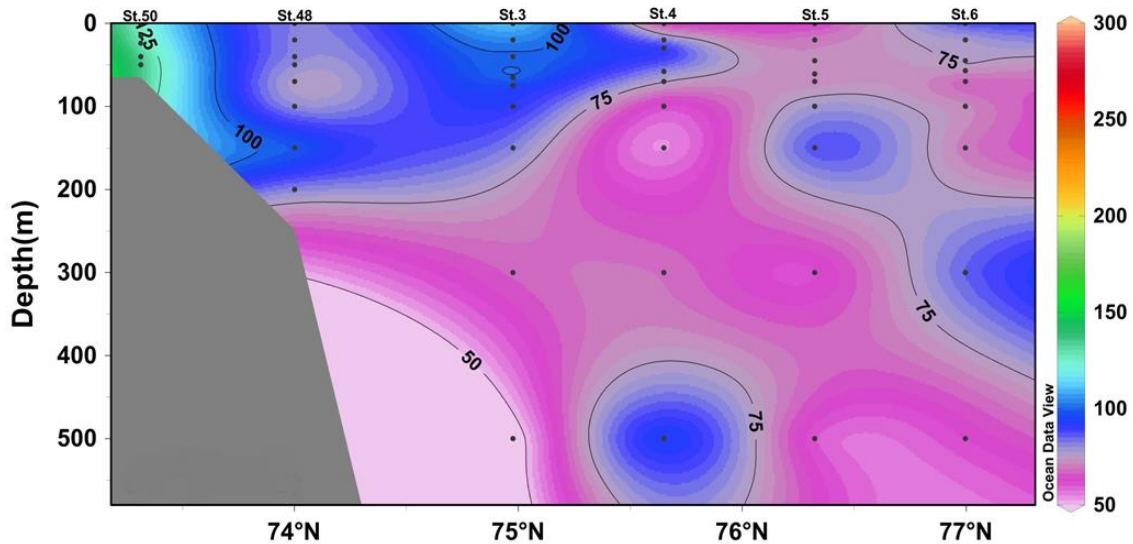


Fig. 3. Contour distribution of DOC concentration in each station (Norhwind Rige/Canada Basin)

Table 1. Comparison of DOC concentration in each area

Study area	Water mass	DOC(μ M)	References
Canada Basin	SML	100	Melnikov(1997);Wheeler et al.(1997); Mean of Opsahl et al.(1999)and Bussmann and kattner(2000)
	HL	75	
	AWL	53	
	AODW	55	
Chukchi Shelf/Canada Basin	-	45-85	Wang et al.(2006)
Northwind Ridge/Canada Basin	SML(0-50m)	74-114	This Study 2012
	UHL(~50-120m)	57-93	
	LHL(~150-220m)	51-101	
	AWL(>250-800m)	43-86	
	AODW(>800m Deep)	46-55	
East Siberian Sea/Mendeleyev	-	50-278	

* Surface mix layer(SML), Halocline Layer(HL), Atlantic Water Layer(AWL), Arctic Deep Ocean Water(ADOW),Upper Halocline Layer(UHL), Lower Halocline Layer(LHL)

DOC concentration also showed higher values in ESS/MR areas than these in NWR area, relatively. Especially, high latitude surface seawater had the above two high concentration of DOC (Table 1 and Fig. 1). High latitude areas were influenced by the sea ice melting and East Siberian current which had the high DOC concentration but we need to interpret the current characteristic and source of organic carbon by further biogeochemical analysis.

Reference

- Kattner, G., Lobbes, J. M., Fitznar, H. R., Engbrodt, R., Nöthig, E.-M., Lara, R.J., 1999. Tracing dissolved organic substances and nutrients from the Lena River through Laptev Sea (Arctic). *Mar. Chem.* 65, 25-39.
- Melnikov, I. A. ,1997. "The Arctic Ice Ecosystem." Gordon and Breach Science Publisher, The Netherlands.
- Opsahl, S., Benner, R., 1997. Distribution and cycling of terrigenous dissolved organic matter in the ocean. *Nature.* 386, 480-482.

- Wang, D., Henrichs, S. M., Guo, L., 2006. Distributions of nutrients, dissolved organic carbon and carbohydrates in the western Arctic Ocean. *Cont. Shelf Res.* 26, 1654-1667.
- Wheeler, P. A., Watkins, J. M., Hansing, R. L., 1997. Nutrients, organic carbon and organic nitrogen in the upper water column of the Arctic Ocean: implications for the sources of dissolved organic carbon. *Deep-Sea Res. II* 44, 1571-1592.

Acknowledgments

This work was supported by the Korea Polar Research Institute projects (PM12020).

DETERMINATION OF THE PRODUCTION RATE OF MYCOSPORINE-LIKE AMINO ACIDS THROUGH CARBON STABLE ISOTOPE ANALYSIS IN ARCTIC MELT PONDS

Sun-Yong Ha¹, Kyung Ho Chung¹, Jun-Oh Min¹, Hyun Min Joo¹, Kyung-Hoon Shin², Sung-Ho Kang^{1}*

¹ Korea Polar Research Institute (KOPRI), Division of Polar Climate Research, 26 Songdomirae-ro, Yeonsu-Gu, Incheon, 406-840, South Korea

² Hanyang University, Marine Environmental Science department, 1271 Sa-3 dong, Sangnok-gu, Ansan, Kyeonggi-do, 425-791, Korea

sundragon@kopri.re.kr

ABSTRACTS

In the Arctic, meltwater can be partitioned within different habitats in the sea ice environment (Mundy et al. 2011). Two different types of MPs can be visually distinguish by their color in a sea ice field. MPs connected to seawater either via holes in ice floes or channels (open MPs) are deep blue in color, showing salinities of approximately 29.0, while freshwater habitats (closed MPs) exhibit a salinity of approximately 0.1 and are light sky blue in color (Gradinger 2002; Lee et al. 2011; 2012). The active photoprotective strategies of marine microbes include the production of screening and quenching compounds (Kirk 1994; Roy 2000) and the production of carotenoids in ice algae in response to increasing light levels (Kudoh et al. 2003; Leu et al. 2010). Furthermore, Uusikivi et al. (2010) reported that mycosporine-like amino acids (MAAs) occur in relatively high quantities in the Baltic Sea. The objectives of the present study were to measure the carbon uptake rate and the production rate of MAAs in phytoplankton in both types of Arctic MPs and the Chukchi Sea.

The average carbon uptake rates of phytoplankton in the two MPs were $3.24 \text{ mg C m}^{-3} \text{ h}^{-1}$ ($\text{SD} = \pm(\text{SD} = \text{mg C m}^{-3} \text{ h}^{-1})$) in MP1 (closed MP) and $1.3 \text{ mg C m}^{-3} \text{ h}^{-1}$ ($\text{SD} = \pm(\text{SD} = \text{mg C m}^{-3} \text{ h}^{-1})$) in MP2 (open MP) under PC incubation. Under quartz incubation, the average uptake rates were $1.71 \text{ mg C m}^{-3} \text{ h}^{-1}$ ($\text{SD} = \pm(\text{SD} = \text{g C m}^{-3} \text{ h}^{-1})$) in MP1 and $1.21 \text{ mg C m}^{-3} \text{ h}^{-1}$ ($\text{SD} = \pm(\text{SD} = \text{mg C m}^{-3} \text{ h}^{-1})$) in MP2, which were lower compared to the PC incubations. The carbon uptake rates at the open seawater sites ranged from $0.01 \text{ mg C m}^{-3} \text{ h}^{-1}$ ($\text{SD} = \pm(\text{SD} = 2, \text{g C m}^{-3} \text{ h}^{-1})$) to $0.02 \text{ mg C m}^{-3} \text{ h}^{-1}$ ($\text{SD} = \pm(\text{SD} = 02 \text{ g C m}^{-3} \text{ h}^{-1})$) in the PC incubations and from $0.02 \text{ mg C m}^{-3} \text{ h}^{-1}$ ($\text{SD} = \pm(\text{SD} = \text{e Pg C m}^{-3} \text{ h}^{-1})$) to $0.03 \text{ mg C m}^{-3} \text{ h}^{-1}$ ($\text{SD} = \pm(\text{SD} = 03 \text{ g C m}^{-3} \text{ h}^{-1})$) in the quartz incubations (Fig. 1).

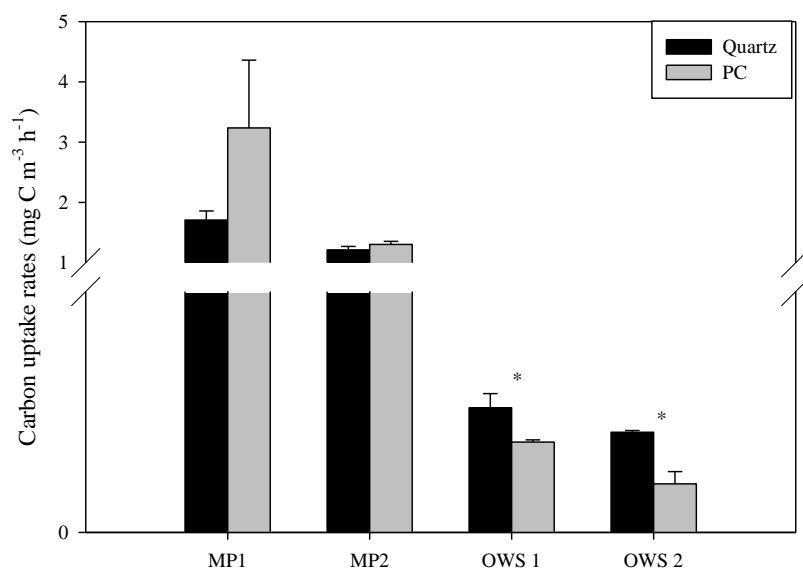


Fig. 1. Carbon uptake rates in *in situ* incubations performed at the melt ponds and open seawater stations. OWS: open seawater surface. *: $p < 0.05$

The *in situ* MAA analysis of the MP samples revealed four different types of MAAs (Shinorine, Palytine, Asterina-330, and Mycosporine-glycine). However, the MAA composition in the open seawater displayed a different trend, being characterized by Shinorine, Palytine, Asterina-330, and Mycosporine-glycine). The average total MAA concentration in the closed MP was $1.9 \mu\text{g } \mu\text{g}^{-1} \text{ Chl a}$ ($\text{SD} = \pm 0.6 \text{ a}$ ($\text{S}^{-1} \text{ Chl a}$), whereas that in the open MP was $10.8 \text{ diffe}^{-1} \text{ Chl a}$ ($\text{SD} = \pm 0.08 \text{ a}$ ($\text{SD}^{-1} \text{ Chl a}$) (Fig. 2). This study measured the MAA production rate, and the modulation of this parameter represents a survival strategy of phytoplankton in new habitats (MPs) in the Arctic. The phytoplankton in the MPs showed higher carbon uptake rates and higher MAA production rates than the phytoplankton in the open seawater. The phytoplankton in open MP, experiencing UV radiation and osmotic stress simultaneously, appear to exhibit higher UV-absorbing compound production compared to other seawater areas. The strategy of the phytoplankton for adapting to the new environment and surviving could be verified.

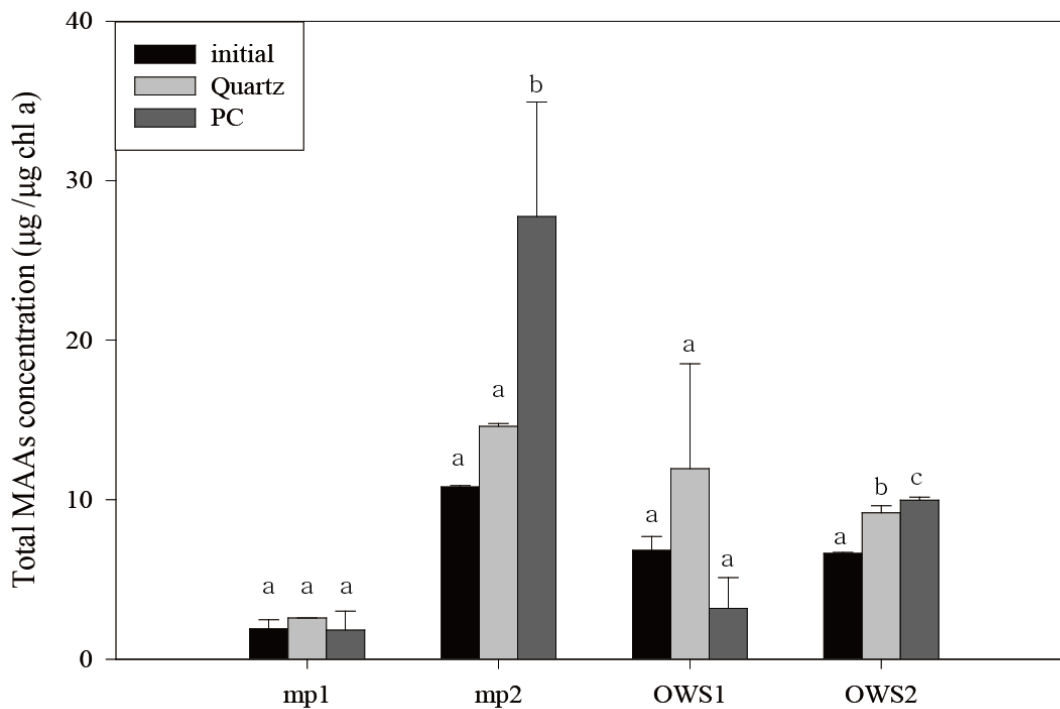


Fig. 2. Total MAA concentrations in melt ponds and open seawater stations. Values (mean \pm SD) with different letters (a, b, and c) indicate significant differences over initial values ($p < 0.05$).

Reference

- Mundy, C.J., Gosselin, M., Ehn, J.K., Belzile, C., Poulin, M., Alou, E., Roy, Su., Hop, H., Lessard, S., Papakyriakou, T. N., Barber, D. G., Stewart, J., 2011. Characteristics of two distinct high-light acclimated algal communities during advanced stages of sea ice melt. *Polar Biol.* 34, 1869-1886.
- Gradinger, R., 2002. Sea ice microorganisms. In: Bitton, G. (Ed.), *Encyclopedia of Environmental Microbiology*, John Wiley, New York, pp. 2833-2844.
- Lee, S.H., McRoy, C.P., Joo, H., Gradinger, R., Cui, X., Yun, M.S., Chung, K.H., Kang, S., Kang, C., Choy, E.J., Son, S., Carmack, E., Whitledge, T.E., 2011. Holes in progressively thinning Arctic sea ice lead to new ice algae habitat. *Oceanography* 24, 302-308.
- Lee, S.H., Stockwell, D.A., Joo, H., Son, Y.B., Kang, C., Whitledge, T.E., 2012. Phytoplankton production from melting ponds on Arctic sea ice. *J. Geophys. Res.* 117, C04030. doi:10.1029/2011JC007717.
- Kirk, J.T.O., 1994. *Light and photosynthesis in aquatic ecosystems*, 2nd edn. Cambridge University Press, Cambridge.
- Roy, S., 2000. Strategies for the minimization of UV-induced damage. In: de Mora, S.j., Demers, S., Vernet, M. (eds) *The effects of UV radiation in the marine environment*. Cambridge University Press, Cambridge, pp. 177-205.
- Kudoh, S., Imura, S., Kashino, Y., 2003. Xanthophyll-cycle of ice algae on the sea ice bottom in Saroma Ko lagoon, Hokkaido, Japan. *Polar Biosci.* 16, 86-97.
- Leu, E., Wiktor, J., Søreide, J.E., Brge, J., Falk-Petersen, S., 2010. Increased irradiance reduces food quality of sea ice algae. *Mar. Ecol. Prog. Ser.* 411, 49-60.
- Uusikivi, J., Vähätalo, A.V., Granskog, M. A., Sommaruga, R., 2010. Contribution of mycosporine-like amino acids and colored dissolved and particulate matter to sea ice optical properties and

ultraviolet attenuation. *Limnol. Oceanogr.* 55, 703-713.

Acknowledgments

This work was supported by the Korea Polar Research Institute projects (PM12020).

NUMERICAL STUDY ON THE ARCTIC SEA ICE VARIATION USING AN ICE-OCEAN COUPLED MODEL

*Mi Ok Kwon, Ho Jin Lee**

*Korea Maritime and Ocean University,
Dongsam-Dong, Youngdo-Gu, Busan, 606-791, Korea
hjlee@hhu.ac.kr*

ABSTRACTS

We here simulate the interannual variation of sea-ice in the Arctic Sea during the period 1979-2012 using an ice-coupled Ocean General Circulation Model (OGCM) and investigate a possible sources influencing the rapid declination of Arctic sea ice extent. The OGCM used in this study is the Regional Ocean Modeling System (ROMS) version 3.6, which is a three dimensional, s-coordinate, primitive equation ocean model with a free surface. The model covers the Arctic Sea with the Bering Sea and the part of North Atlantic Ocean. The horizontal grid size ranges from 11 to 13 km. A total of 50 s-coordinate levels are adopted along the vertical direction with enhanced resolution near the surface.

A set of 3-hourly atmospheric fields obtained from ERA (European center of medium range weather forecasting Re-Analysis)-Interim during the period from 1979 to 2012 is used to calculate heat and salt fluxes as well as wind stress at the sea surface. We used PHC (Polar science center Hydrographic Climatology) data for temperature and salinity along inflow open boundaries. To assess model performance, model results are compared with other model results and observations.

Sponsor : supported by the Korea Polar Research Institute, Grant No. PM12020.

TEMPORAL AND SPATIAL VARIATION OF PACIFIC-ORIGIN SUMMER WATER IN THE CHUKCHI BORDERLAND, ARCTIC OCEAN

T.W. Kim¹, H.K. Ha¹, K. Shimada², S.H. Kang¹

¹Korea Polar Research Institute, Incheon 406-840, Korea

²Tokyo University of Marine Science and Technology, Tokyo 108-8477, Japan
twkim@kopri.re.kr

ABSTRACTS

The Arctic Ocean may be a sensitive indicator of global climate changes. During 2012 summer, the extent of Arctic sea ice has reduced dramatically. These changes affect both the Arctic and global climate system by altering the heat exchanges between the ocean and atmosphere. The warm water inflow from the Bering Sea is recognized as an important driving force for rapid reduction of sea ice associated with an increase in the horizontal and vertical flux of heat, salt and momentum (Shimada et al., 2006; Carmack and Melling, 2011). The Pacific-origin Summer Water (PSW) reaches the mouth of the Barrow Canyon along the Alaskan Coast in the Chukchi Sea. After that PSW changes its advective direction toward northwest along the northern slope of the Chukchi Sea and is delivered in the Chukchi Borderland (CBL) region consisting of the Northwind Ridge and Chukchi Plateau. In 2012, the major pathway of PSW located on the Northwind Ridge. And, the PSW has been gradually extended toward the west direction as compared with previous investigations. This suggests that some changes in ice and ocean circulation regime occurred in 2011/2012 winter. The salinity of PWW at minimum potential temperature layer has decreased slightly in 2012. Also, the potential temperature of PWW on the Northwind Ridge was relatively colder than that on Chukchi Plateau. The water mass stratification is classified into two categories according to the bottom depths in the East Siberian Sea and Makarov Basin. In the region shallower than 1000m, volumetric cold water with its minimum temperature around $S=32.3-32.5$ spread from shelf region to the shelf slope about 1000m iso-bathymetry. In the deep Makarov Basin deeper than 1000m, oxygen rich lower halocline water dominated.

**REGIONAL PRODUCTIVITY OF PHYTOPLANKTON
IN THE NORTHEAST CHUKCHI SEA AND WESTERN CANADA
BASIN DURING EARLY SUMMER IN 2010**

*Mi Sun Yun^a, Bo Kyung Kim^a, Hui Tae Joo^a, Eun Jin Yang^b, Shigeto Nishino^c,
Kyung Ho Chung^b, Sung-Ho Kang^b, Sang H. Lee^{a,*}*

^a *Department Oceanography,
Pusan National University*

^b *Division of Polar Climate Research,
Korea Polar Research Institute,*

^c *Research Institute for Global Change,
Japan Agency for Marine-Earth Science and Technology*
misunyun@kopri.re.kr

ABSTRACTS

Phytoplankton production measurements were conducted in the northeast Chukchi Sea and western Canada Basin in the early summer season, from 20 July to 10 August 2010, using a ¹³C¹⁵N dual tracer technique. The daily carbon uptake rate in the northeast Chukchi Sea in 2010 was extremely low, with a mean of 29.8 mg C m⁻² d⁻¹ (SD = 17.6 mg C m⁻² d⁻¹). Regional and temporal differences might cause the low production rate compared to previous studies in the northeast Chukchi Sea. In the western Canada Basin, the mean daily carbon uptake rate from this study was 20.6 mg C m⁻² d⁻¹, which is affected by large dominance of small phytoplankton resulting in low carbon uptake rate in the region. Regionally high nitrate uptake rates compared to ammonium uptake rates in the western Canada Basin could be caused by warm-core eddies, which supplied high nitrate to the euphotic zone. Warm-core eddies in the Canada Basin largely enhanced locally phytoplankton production and contribution of large phytoplankton.

MACROMOLECULAR PRODUCTIVITY OF PHYTOPLANKTON IN THE AMUNDSEN SEA

HuiTae Joo and Sang Heon Lee

*Department of Oceanography,
Pusan National University
huitae@pusan.ac.kr*

ABSTRACTS

Using ¹³C isotope tracer technique, the productivity experiments for photosynthetic carbon allocations were conducted at three light depths (100%, 30%, and 1%) for total eleven different stations to understand physiological status of phytoplankton in the Amundsen Sea, 2012. The different macromolecular classes (low-molecular-weight metabolites (LMWM), lipids, polysaccharides, and proteins) of phytoplankton were extracted based on the method of Li et al. (1980). The overall average allocations were 18.1% (S.D. =) of phytoplankton were extracted based on the method of Li et al. (1980). The overall average allocations were epths (100%, 30%, and 1%) for tot The high incorporation of carbon into proteins was a genral pattern of the photosynthetic allocations of phytoplankton throughout the euphotic zone in this study. Based on previous studies, high protein incorporation reflects physiologically healthy phytoplankton with high major nutrient concentrations (especially nitrogen) in the Amumdsen Sea during the cruise period from early Febuary to March in 2012.

MACROMOLECULAR COMPOSITIONS OF PHYTOPLANKTON IN THE ARCTIC OCEAN IN 2012

Jae Joong Kang, Sang H. Lee

*Department of Oceanography,
Pusan National University, Pusan, Korea
jaejung@pusan.ac.kr*

ABSTRACTS

Macromolecular compositions (carbohydrates, proteins, lipids) of primary producers were investigated in the Chukchi Sea from August to early September in 2012. The proportion of lipids, proteins, and carbohydrates of phytoplankton in the water column were a mean of 57.6% (S.D. = 7.1%), and 26.0% (S.D. = 8.6%), respectively. Lipids (57.6% of total compositions) were predominant in the macromolecular compositions of phytoplankton during the cruise period. According to earlier studies, high incorporation into proteins is to be expected that physiologically healthy phytoplankton with high relative growth rates, while high incorporation into lipids indicates physiologically nitrogen-deficient phytoplankton. Based on this, high lipid contents among different macromolecular compositions indicate that were phytoplankton were nitrogen-deficient conditions.

LIPID CONCENTRATION OF PHYTOPLANKTON IN THE NORTEHRN CHUKCHI SEA, ARCTIC

Su Min Kim, Da Som Lee, Sang Heon Lee

*Department of Oceanography,
Pusan National University
show0hello@naver.com*

ABSTRACTS

The lipid concentrations of phytoplankton were studied in the northern Chukchi Sea, Arctic during summer in August to September, 2011. Water samples were obtained from 3 light depths (100, 30, and 1%) at 14 stations. Samples were filtered on 0.7 μ m Whatman GF/F filters (47mm) and the filters were immediately frozen and preserved for colorimetric measurements. Extraction of lipids was performed using the methods in Marsh and Weinstein (1966) and the concentration was determined by the optical density measured with a spectrophotometer. In this study, the phytoplankton biomass varied with depth, with a maximum of ca. 8.1 μ g L⁻¹ (chl-a) occurring at 1% light depth. The average chlorophyll-a (chl-a) concentration was 31.9 mg m⁻² (S.D. = occurring a⁻²), and small phytoplankton (0.7-5 th. The average chlorophyll-a (chl-a) concentration was 31.9 mg mummer in August to September, 20d large cells (> 20 μ m; 16.6 \pm 13.8%). The lipid concentration ranged from 50.2 to 105.0 μ g L⁻¹ with mean of 71.4 lankton (0.⁻¹. There was no significant relationship among the environmental factors (light and nutrients except for NH₄) (p > 0.05).

STUDY ON RECENT INTERNATIONAL TREND IN BIPOLAR OCEANS AND KOREA'S FUTURE POLICY DIRECTION

Jin hoi Hwang, Su jin Park

*Maritime Industry&Logistics Division, Marine Policy Research Division
Korea Maritime Institute*

jhhwang@kmi.re.kr, forest21@kmi.re.kr

ABSTRACTS

Bipolar oceans hold great value as a rich repository of natural resources and a significant place for research on and preparation for changes of global environment which have progressed at an alarming rate. The Arctic ocean has a great wealth of resources such as natural gas, petroleum and underground resources, and the outcome of monitoring climate change conducted in the Arctic ocean is very valuable in estimate global climate change.

As for the Antarctic, although it does not allow recognize, dispute, or establish territorial sovereignty claims, each country has fiercely competed themselves in the field of science research. The Arctic ocean also needs to conduct joint exploitation with surrounding countries.

This paper plans to suggest Korea's future policy direction for bipolar oceans by considering major countries' bipolar policies including those of Russia, the U.S. and Japan and by analyzing the provisions of international organizations such as UN Convention on the Law of the Sea(UNCLOS), International Maritime Organization(IMO), the Antarctic Treaty and provisions on marine environment of Arctic Council.

COMPARATIVE RESPONSE OF ARCTIC AND TEMPERATE MICROALGAE TO TEMPERATURE ELEVATION

Sreejith Kottuparambil¹, Sung-Ho Kang², Han-Gu Choi², Taejun Han^{1,3}

¹Institute of Green Environmental Research, Incheon National University, 7-46 Songdo-dong,
Yeonsu-gu, Incheon 406-840, Republic of Korea

²Korea Polar Research Institute (KOPRI), 7-50, Songdo-dong, Yeonsu-gu, Incheon 406-840,
Republic of Korea

³Department of Marine Science, Incheon National University, 12-1 Songdo-dong, Yeonsu-gu,
Incheon 406-840, Republic of Korea

hanalgae@hanmail.net

ABSTRACT

The global climate change scenario and allied temperature increase have significant detrimental effects on the survival of microalgae which form the base of all aquatic food webs. To understand how microalgae from different temperature regimes respond to global warming, we compared the growth and photosynthetic responses of two similar taxa of microalgae from the Arctic (*Chlorella* sp. KOPRI ArF 4 and *Chlamydomonas* sp. KOPRI ArF 6) and temperate (*Chlorella vulgaris* KMMCC FC 1 and *Chlamydomonas* sp. GP 34) regions to temperature variations over a range of 5 °C to 35 °C for 4 days. The Arctic strains showed growth and photosynthesis at temperatures higher than their ambient regime. The specific growth rate (μ) of Arctic and temperate species were highest at 20 °C and 30 °C, respectively. The upper limit for growth was < 35 °C for Arctic strains and at optimal temperature, μ for both species were lower in the Arctic isolates (24-26 day⁻¹) than their temperate counterparts (32-33 day⁻¹). Moreover, in comparison, temperate strains exhibited higher growth rates at elevated temperatures (< 0.16 day⁻¹ and > 0.16 day⁻¹ for Arctic and temperate species, respectively). The maximal quantum yield of PSII (F_v/F_m) in Arctic strains were consistent between 5 °C to 30 °C (0.43-0.46 and 0.42-0.48 for ArF 4 and ArF 6, respectively) while the maximal electron transport rate (ETR_{max}) was highest at 20 °C (17 and 21 $\mu\text{mol electrons m}^{-2} \text{s}^{-1}$ for ArF 4 and ArF 6, respectively). Among the temperate strains, *Chlamydomonas* showed stable F_v/F_m at all tested temperatures above 10 °C (0.58-0.61) and maximal ETR at 20 °C (46 $\mu\text{mol electrons m}^{-2} \text{s}^{-1}$) while *Chlorella vulgaris* exhibited higher F_v/F_m (0.63) and ETR_{max} (15 $\mu\text{mol electrons m}^{-2} \text{s}^{-1}$) even at 35 °C. The tested Arctic microalgae are eurythermal with wide temperature tolerance ranging from 5 °C to 30 °C which might contribute to their ability to adjust to temperature fluctuations. However, the overall data suggested that the upper temperature limits of Arctic microalgae are significantly lower than their temperate counterparts which enhance their vulnerability to increasing temperatures within the context of a globally changing environment.

BIOCHEMICAL COMPOSITONS OF PARTICULATE ORGANIC MATTER IN THE NORTHERN CHUKCHI SEA, 2011

Bo Kyung Kim, Jang Han Lee, Hui Tae Joo, Jung Woo Park, Sang Heon Lee

*Department of Earth Environmental System,
Pusan National University
bokyoung85@naver.com*

ABSTRACTS

We investigated the biochemical compositions (lipids, proteins, and carbohydrates) of particulate organic matter (POM) as a potential food source in the northern Chukchi Sea. We aimed to understand physiological status of phytoplankton, determine important controlling factors, and estimate the energetic contents of POM. The major inorganic nutrients were generally depleted at upper mixed-layer depth (> 20 m). The average chlorophyll a (chl-a) concentration was 31.9 mg m⁻² (S.D. = ± 31.3 mg m⁻²) in this study, significantly higher than that reported previously in the northern Chukchi Sea. Small phytoplankton (0.7-5 µm) accounted for 65.9% of total chl-a concentration. The overall average compositions of lipids, carbohydrates, and proteins were 50% (S.D. = ± 10.7%), 35% (S.D. = ± 11.0%), and 15% (S.D. = ± 11.2%) for POM, respectively. Along with other evidence (e.g., low N:P and protein-carbohydrate ratios), the high lipid and low protein compositions of POM in this study suggests that phytoplankton might have a nitrogen limitation and/or stationary growth phase in the northern Chukchi Sea during the cruise period, 2011. The overall average calorific content of food material (FM) was 149.2 µg L⁻¹ (S.D. = ± 36.5 µg L⁻¹) which were converted into 1.0 Kcal m⁻³ (S.D. = ± 0.2 Kcal m⁻³). The relatively higher calorific contents in the northern Chukchi Sea were due to high lipid contributions and the considerably high calorific content of FM per POC.

POSTER SESSION 3

PERMAFROST

GREENHOUSE GAS FLUX MEASUREMENT NETWORK OF KOPRI AT CIRCUM-POLAR PERMAFROST SITES

Jaeill Yoo, Taejin Choi, Sang Jong Park, Bang Yong Lee, Young Jun Yoon

*Division of Polar Climate Research,
Korea Polar Research Institute
jiyoo@kopri.re.kr*

ABSTRACTS

Arctic permafrost is known as vulnerable area to climate change and shows one of regions with rapid increase in temperature. Despite of its importance, studies on carbon cycle, one of main feedback mechanisms to the warming, based on in situ measurement are limited. Therefore, additional measurements related with carbon exchange, hydrology, surface energy budget, ecosystem, microbial activity and so on are required at geographically representative sites to cover the vast arctic region. To better understand carbon exchange over multiple permafrost sites, eddy covariance flux system has been established at Council site (Alaska, USA, 2010), Dasan station site (Ny-Alesund, Norway, 2011), and Cambridge Bay site (Nunavut, Canada, 2012) by KOPRI's CAMP program. Open-path gas analyzer (EC150, Campbell, USA) is used with sonic anemometer (CSAT3, Campbell, USA) as a reference tool. Turbulent data sampled at 10 Hz are processed using EdiRe (<http://www.geos.ed.ac.uk/abs/research/micromet/EdiRe/>). At Dasan station site, measurement system were enhanced due to availability of a 30-m walk up tower (the Amundsen Nobile Climate Change Tower established in 2009 by National Research Council(CNR), Italy) where electric power and the internet is available. Through cooperation with CNR, open path gas analyzer (LI7500, Li-cor, USA), Cavity ring-down spectroscopy (CRDS, G2301-f, Picarro, USA) and open path methane analyzer are operated at a height of 22 m to simultaneously monitor carbon dioxide and methane flux and to compare instrument performance. In the meanwhile, open path flux measurement systems were deployed at a height of 3m and 5m at Council and Cambridge Bay sites, respectively. To derive final flux data, we apply coordinate rotation to align measurement axes to mean main stream, spectral corrections to compensate for spectral loss due to line averaging, sensor separation, and limited sampling. Additional correction for tube attenuation was considered for closed path eddy covariance system. For open path eddy covariance systems, WPL correction was applied to consider density fluctuation due to temperature and water vapor flux (Webb et al., 1980). In this presentation, we will introduce our measurement systems including comparison of instruments' performance at (the Amundsen Nobile Climate Change Tower and and discuss the influence of the site-specific environment on measurement. *This research was supported by the National Research Foundation of Korea Grant funded by the Korean Government (MEST) (NRF-CIABA001-2011-0021063, PN13081).*

MEASUREMENTS OF ENVIRONMENTAL FACTORS IN POLAR REGIONS BASED ON A UBIQUITOUS SENSOR NETWORK

Namyi Chae¹, Heekwon Yang², Chankil Lee², Bang Young Lee³

¹Civil & Environmental Engineering, Yonsei University

²Department of Electronics and Communications Eng., Hanyang University

³Division of Polar Climate Research, Korea Polar Research Institute

cnamyi@yonsei.ac.kr

ABSTRACTS

To investigate the cycle of greenhouse gases in a permafrost region, major environmental factors were collected and analyzed with the proposed ubiquitous sensor network-based remote monitoring system (U-RMS), which is a basically wireless sensor network (WSN) connected to an iridium satellite network (ISN) backbone. The use of techniques for power-efficient operation and network scalability that enabled the WSN to be operated for long periods and to be deployed reliably and widely is described. The temporal and spatial variations in the soil temperature (Ts) and the soil water content (SWC) in 10 locations, and the air temperature (Ta) and the relative humidity (RH) of the near-surface in 16 locations, were measured to monitor the active layer of the permafrost in Alaska from July 2012 to January 2013. In the permafrost regions, the temporal variations in the temperature and the water content of the soil and the near-surface depended on the thawing (from July to September) and freezing (from October to January) with a snow cover. The spatial variations in the Ts and the SWC showed a high coefficient of variation (CV) which ranged from 20% to 40%. The Ta of the near-surface changed only in winter due to the snow cover, and the CV was about 30%. There was no change in the RH within 3% in the CV. Moreover, the change in the spatial variations in the Ta of the near-surface was helpful in the estimation of the effect on the snow cover in winter. Using the camera sensor, the growth of vegetation and the operating appearance of the remote WSN were also monitored. In the long term, measurements of the temporal and spatial variations in the environmental factors based on U-RMS are expected to contribute to the understanding of the carbon and water cycle in permafrost. This study was supported by the National Research Foundation of Korea Grant funded by the Korean Government (MEST) (NRF-C1ABA001-2011-0021063).

CARBON DIOXIDE EXCHANGE OVER THE ARCTIC TUNDRA IN COUNCIL, ALASKA: CONTROLLING FACTORS AND CONTRIBUTION OF VEGETATION TO CARBON CYCLE

Namyi Chae¹, Sangjong Park², Taejin Choi², Yongwon Kim³, Young Jun Yoon²,
Hojeong Kang¹, Larry Hinzman³ and Bang young Lee²

¹Department of Civil and Environmental Engineering, Yonsei University

²Division of Polar Climate Research, Korea Polar Research Institute,

³International Arctic Research Center, University of Alaska Fairbanks,

cnamyi@yonsei.ac.kr

ABSTRACTS

Carbon dioxide exchange was measured in the Council, Alaska using automated chamber measurements and eddy covariance technique to understand interaction between of atmosphere, vegetation, soil system in carbon cycle of permafrost region. The site (64°50'38"N, 163°13'38"W) is comprised of vascular plants (e.g. *Eriophorum scheuchzeri* and *Betula nana*), moss (e.g. *Sphagnum lenese pohle* and *Sphagnum russowii Warnst*) and lichen (*Cladonia stellaris*). In addition, environmental parameters were measured near the system such as soil temperature for each chamber, profile of soil temperature for each vegetation type, photosynthetically active radiation, water content and thaw depth. Net CO₂ exchange was -0.1 ~ 0.2 CO₂ mg m⁻² s⁻¹(vascular plant and moss), 0 ~ 0.2 (moss removed leaves of vascular plant), -0.2 ~ 0.2 CO₂ mg m⁻² s⁻¹ (tussock) and 0 ~ 0.1 (lichen) by chamber measurements. In the comparison both measurements, net ecosystem CO₂ exchange of eddy covariance underestimated in the night time and greatly overestimated in the day time against the net CO₂ exchange of chamber measurement system. Net CO₂ exchange was not showed general relationship on the soil temperature. We investigated controlling factors for CO₂ flux, contribution of vegetation and difference between both systems and under rainy season in permafrost. This study was supported by the National Research Foundation of Korea Grant funded by the Korean Government (MEST) (NRF-C1ABA001-2011-0021063).

GEOCHEMICAL ANALYSIS OF ALASKAN PERMAFROST SOIL: DEFINING GAS PERMEABLE LAYER AND QUANTIFYING GAS TRANSPORT

Eunji Byun¹, Jiwoong Yang¹, Yongwon Kim², and Jinho Ahn¹

¹*School of Earth and Environmental Science, Seoul National University, Seoul, Korea*

²*International Arctic Research Center (IARC), University of Alaska Fairbanks, Fairbanks,
AK, United States*

bej0728@gmail.com

ABSTRACTS

Three different types of soil cores were collected from five locations in Alaska (coastal tundra, boreal forest, and wildfire affected forest) using 90cm SIPRE auger during the Seoul National University (SNU) - University of Alaska Fairbanks (UAF) joint field trip in April/May of 2013. After drilling twelve temperature sensors and loggers were installed inside the boreholes for monitoring thermal regime of coring sites. The core samples were transported in frozen condition and stored under -20 °C at walk-in freezer of SNU and core archives are preserved in UAF. Physical and geochemical properties of the frozen soils are to be primarily analyzed, with an aim of defining gas permeable/impermeable depth intervals, and further quantifying gas transport along the frozen soil layers. Following the headspace method (Kim *et al.* 2012), 3-ml sediment subsamples are taken from every 5~10 cm depth intervals of the core sections and extruded into 20 ml glass serum vials. Then, the vials are heated under 60 °C for 30 minutes to extract gases trapped in soils. Depth profiles of CO₂ and CH₄ will allow us to distinguish gas permeable layer, which contributes surface gas flux from non-permeable layer. By this we may better understand gas mobility in permafrost from various regions in Alaska. Additional chemical analysis on soils organic carbon content and stable isotopes (C-13 and D) of CH₄ will be helpful supplement for detailed interpretation.

REFERENCE

Kim, J-H., Torres, M E., Choi, J., Bahk, J-J., Park, M-H., Hong, W-L., Inferences on gas transport based on molecular and isotopic signatures of gases at acoustic chimneys and background sites in the Ulleung Basin, 2012, *Organic Geochemistry* 43, 26-38.

POSTER SESSION 4

ARCTIC TERRESTRIAL ECOSYSTEMS

TEMPERATURE AND PRECIPITATION MANIPULATION EXPERIMENT IN CAMBRIDGE BAY, CANADIAN HIGH ARCTIC

*Kwon Hye young, Ji Young Jung, Ok-sun Kim, Namyi chae, Joo Han Lee, Tae Jjin Choi,
Young Jun Yoon, Bang yong Lee, Yoo Kyung Lee*

*Division of Life Science,
Korea Polar Research Institute, KOPRI
kkoma1023@kopri.re.kr*

ABSTRACT

Arctic is one of the sensitive ecosystems to climate change. The future climate change includes increasing temperature and changes in hydrological cycles. There have been lots of studies examining the effects of temperature or altering precipitation alone, however, a few studies focused on the interaction effects between temperature and precipitation. To understand how soil organic carbon (SOC) and soil microbe will respond to climate change in the future, a new temperature and precipitation manipulation experiment has been initiated in high Arctic Canada. In July 2012, we established a 2 × 2 factorial design that involved increasing temperature and precipitation: non-warming and non-precipitation, NWNP; non-warming and increasing precipitation, NWP; warming and non-precipitation, WNP; warming and increasing precipitation, WP. We set two types of plots for monitoring and destructive sampling to avoid any side effects from periodic soil sampling for the continuously monitored parameters for all treatments. Before starting the manipulation experiment, soil was sampled to acquire the baseline data from both plots at the end of June in 2012. In 2013, we again acquired soil samples that have been influenced by warming and increased precipitation for one year from the destructive plots. From those samples, we have been analyzing several soil parameters (soil organic carbon, total nitrogen, inorganic nitrogen, total phosphorus, available phosphorus, several cations, pH, etc.). For microbial analysis, pyrosequencing is currently undertaken to study microbial community structure.

GEOGRAPHICAL ANALYSIS OF MICROBIAL ACTIVITY IN ARCTIC SOILS

Inyoung Jang and Hojeong Kang

*School of Civil and Environmental Engineering
Yonsei Univeristy
in06029@yonsei.ac.kr*

ABSTRACTS

Arctic soils contains large amount of organic matter, therefore decomposition of these organic matter is important. Microbial activity is an important for decomposition of organic matter in soils. Microbial activity was measured using artificial substrates in arctic soils. We analyzed microbial enzyme activities related with carbon (β -glucosidase and cellulase) and nitrogen (N-acetylglucosaminidase and aminopeptidase) decomposition. In addition, we analyzed the enzyme activities which decompose recalcitrant carbon such as phenolics. We also analyzed geographical pattern of these enzymes using geostatistical analysis. Soils were collected at Cambridge Bay, in Canada and two different layers were collected (0-5 cm and 5-10 cm). Enzyme activities in upper layer were higher than lower layer. Soil organic matter content and dissolved organic carbon (DOC) in upper layer showed significant higher values than the values in lower layers. Organic matter and DOC acts as substrates for microorganisms, microbial activities exhibited higher values where the substrates were abundant. Geographical analysis exhibited the different results between upper and lower layer. Geological patterns of microbial enzyme activities were distinct in upper layer, but these patterns disappeared in lower layers.

COMPARISONS OF METABOLIC PROFILES OF *DRYAS INTEGRIFOLIA* IN RELATION WITH SOIL MICROBIAL COMMUNITY CHANGES FROM AN OPEN TOP CHAMBER EXPERIMENT IN CAMBRIDGE BAY, CANADA.

Dongwoo Yang, Jinjoo Lee, Seonah Jeong, Sangkyu Park.

*Department of Biological Sciences,
Ajou University
daphnia@ajou.ac.kr*

ABSTRACTS

To elucidate chemical interactions between dominant plant species and soil microbial communities on climate change, we monitored metabolic profile changes of leaves and roots of *Dryas integrifolia*, a dominant plant, with soil microbial in climate change simulating chambers (control: NWNP, increased precipitation: NWP, increased temperature: WNP, increased precipitation and temperature: WP) in Cambridge Bay, Canada. Averages of underground temperature in increased temperature treated site (WNP, WP) were higher than non-treated (NWNP, NWP). Mean of water contents in soil treated with precipitation (NWP, WP) were higher than non-treated (NWNP, WNP). We quenched the plant metabolism using dry ice and separated them into two parts as leaves and roots as well as soil samples for 5 blocks, 4 treatments and 3 replicates, and transferred to the laboratory near the fields in August, 2013. We weighed the leaves of the dominant plant (fresh weight and dry weight), the both are not different among the treatments. First extracted samples with a methanol were transported to our laboratory in Korea and followed the second extraction with derivative. We used 6890GC/5973i MS for the plant metabolites and soil sterols, markers of fungal communities. We identified the compounds with AMDIS and NIST library, in addition to several standard references and conducted statistical analysis as Analysis of variance (ANOVA) and Principal Component Analysis (PCA).

SPATIAL DISTRIBUTION OF BACTERIAL COMMUNITY STRUCTURE IN TUNDRA SOIL, ALASKA

Hye Min Kim^{1,2}, Ji Young Jung¹, Etienne Yergeau³, Chung Yeon Hwang¹, Sung Jin Nam¹, Ok-Sun Kim¹, Larry Hinzman⁴, Jongsik Chun², Yoo Kyung Lee¹

¹ *Division of Life Sciences, Korea Polar Research Institute, Incheon, Korea*

² *School of Biological Sciences, Seoul National University, Seoul, Korea*

³ *National Research Council of Canada, Montreal, Biotechnology Research Institute, Quebec, Canada*

⁴ *International Arctic Research Center, University of Alaska Fairbanks, Fairbanks, Alaska, U.S.A*

ABSTRACTS

Arctic soil is one of the most extreme environments for microorganisms due to low temperature. Currently, the microbial processes occurring in the Arctic soil have gained scientific attention, and these studies focused on CO₂ and CH₄ emission from the thawing permafrost. The soil microbial processes are very important to understand, and structure of soil microorganisms would be the basic and essential element to explain the microbial processes. Many studies have been conducted to reveal the community structure by using of culture-independent techniques such as DGGE, T-RFLP, etc. Recently, next generation sequencing technology has been used as a powerful tool to elucidate microbial community structures in tundra soils. Here we report the bacterial community structure in moist acidic tussock tundra soils (Council, Alaska) by using pyrosequencing technique. We collected 70 soil samples (36 of upper layer and 34 of lower layer) from a tundra region in Council, Alaska. Soil bacteria were determined through DNA extraction and pyrosequencing for 16S rRNA gene identification, and several soil physicochemical properties (moisture content, carbon and nitrogen contents, pH, etc.) were analyzed. Dominant bacterial groups in the upper layer and lower layer soils were Alphaproteobacteria and Acidobacteria, respectively. Among several soil properties, pH showed the highest correlation ($r=0.41$, $p<0.001$) with some bacterial groups in both upper and lower layer soils. However, the other soil properties that were correlated with bacterial groups between two depths were different as showing total nitrogen content ($r=0.38$, $p<0.001$) and ammonium ion concentration ($r=0.25$, $p<0.05$) for the upper layer soils and carbon/nitrogen ratio ($r=0.20$, $p<0.05$) and moisture content ($r=0.23$, $p<0.05$) for the lower layer soils. The distance decay analysis showed that there was no significant correlation between the distances among sampling sites and bacterial community composition. This study was supported by the National Research Foundation of Korea Grant funded by the Korean Government (MSIP) (NRF-2011-0021067) (PN13082, KOPRI).

CHANGES IN COMMUNITY STRUCTURE AND DEGRADATIVE CAPACITY OF SOIL HUMIC SUBSTANCES-DEGRADING BACTERIA FROM COLD ENVIRONMENTS

*Ha Ju Park and Dockyu Kim**

*Division of Life Sciences,
Korea Polar Research Institute, Korea
envimic@kopri.re.kr*

ABSTRACTS

Soil humic substances (HS), widely distributed in cold natural environments, are known as the largest constituent of soil organic matter (~60%) and are considered as a key component of the terrestrial ecosystem. The microbial degradation of HS has been studied in fungi and *Streptomyces* spp., but it is much less studied in bacteria, although they dominate even cold environments. The object of this study is to preliminarily investigate the ecological correlation between cold-adapted bacteria and HS degradation. In a microcosm experiment with subarctic tundra soil in Nome (Alaska), microbial community analysis showed that the relative abundance of phyla *Proteobacteria* (bacteria) and *Euryarchaeota* (archaea) largely increased when incubated at 5°C, indicating the involvement of proteobacteria in microbial HS degradation. During the experiment, soil organic matter including HS was subjected to significant microbial degradation, resulting in the consistent decrease of HA (humic acids, a main fraction of HS). In addition, cold-adapted HS-degrading bacteria from the Antarctic and Arctic regions showed their degradative capacities increased in parallel with temperature rise in a range of 4 - 25°C, although the bacteria could not grow over 30°C. These results show that HS degradation is in progress by bacteria even at as low temperature as 5°C, and soil temperature rise could change the bacterial community structure and HS degradative capacity. In conclusion, the information on bacterial degradative activities against HS would help us to predict the effects on polar ecosystems of climate change like global warming.

EFFECTS OF SVALBARD REINDEER (*RANGIFER TARANDUS PLATYRHYNCHUS*) GRAZING ON GAS CHROMATOGRAPHY-MASS SPECTROMETRY (GC-MS) METABOLIC PROFILES OF DWARF WILLOW (*SALIX POLARIS*) LEAVES IN AN ARCTIC REGION

Donguk Han¹, Hansoon Kwak², Sangkyu Park² and Eun Ju Lee¹

¹*School of Biological Sciences, Seoul National University, Seoul 151-742, Korea*

²*Department of Biological Sciences, Ajou University, Suwon 443-749, Korea*
ecoguideuk@gmail.com

ABSTRACTS

Korea

High-arctic tundra ecosystems on Svalbard are regarded as ‘three trophic level ecosystems’ with the only mammalian herbivore, Svalbard reindeer (*Rangifer tarandus platyrhynchus*). Recent development of plant metabolomic approach made it possible to monitor untargeted metabolic changes in plants. To understand the anti-herbivore response of dwarf willow (*Salix Polar*) to Svalbard reindeer grazing, we analyzed Gas chromatography-mass spectrometry (GC-MS) profiles of *S. polaris* leaves in grazing and non-grazing sites in a high-arctic tundra ecosystem on the Svalbard archipelago. We developed a metabolomic work frame for GC-MS data. An MSeasy R package found mass spectral tags (MSTs) from raw data and produced aligned data matrices for further multivariate analysis such as principal component analysis (PCA), partial least square discriminant analysis (PLS-DA) and orthogonal PLS-DA (OPLS-DA). Selected mass spectral tags (MSTs) from the multivariate analyses were annotated by offline libraries and online queries such as MassBank. PCA, PLS-DA, and OPLS-DA clearly separated GC-MS profiles of *S. polaris* leaves with and without grazing along the first component. Maleic acid, Malonic acid, trans-Caffeic acid, and 4-hydroxycinnamic acid appear to have increase with reindeer grazing while L-Phenilalanine, Glucopyranose, Gulose, Digalctosylglycerol, Raffinose, and L-Tryptophan decreased with reindeer grazing. Reindeer grazing appear to induce lignin biosynthesis through phenylpropanoid pathway. Our study shows the usefulness of metabolic approach in studying chemical ecology between plants and other interacting organisms.

Keywords: dwarf willow · *Salix polaris* · Leaves · Svalbard Reindeer · *Rangifer tarandus platyrhynchus* · Grazing · anti-herbivore response · GC-MS · Metabolomics

TURNOVER TIME OF SOIL ORGANIC CARBON IN PERMAFROST USING RADIOCARBON AND THEIR APPLICATION FOR DETERMINING LONG AND SHORT TERMS CARBON BALANCES: CASE STUDY IN ALASKAN TUNDRA AND BOREAL FOREST

Miyuki Kondo¹, Masao Uchida¹, Motoo Utsumi², Go Iwahana³, Kenji Yoshikas³, Hiroki Iwata⁴, Yoshinobu Harazono³, Taro Nakai^{3,5}, Kiyoshi Tanabe¹, and Yasuyuki Shibata¹

¹ National Institute for Environmental Studies

² University of Tsukuba, ³ University of Alaska, Fairbanks

⁴ Kyoto University, ⁵ Nagoya University

ABSTRACTS

The high-latitude regions, where a serious warming is expected, currently store large amounts of soil organic carbon (SOC) in active-layer soils and permafrost, accounting for nearly half of the global belowground organic carbon pool. Despite the importance of these regions in the present carbon cycle, the soil C fluxes and budget are still only poorly known. Here, we use radiocarbon as the tool for quantifying the C balance of the inputs and decomposition in tundra and boreal soil. We evaluated the C inputs (I) and decomposition rates (k, inverse of turnover time) and net C accumulation (CA), using ¹⁴C approaches. Tundra and boreal soils show different patterns of depth distribution and C storage. Cumulative organic carbon stocks in boreal forest are 5.3 and 19.2 kgCm⁻², in surface organic layer (0-25 cm), and deep organic and mineral layers (25-70 cm), respectively. Large annual C input (0.249 kgCm⁻² yr⁻¹) and relatively slow decomposition (27 years) lead to rapid CA (0.052 kgCm⁻² yr⁻¹) in surface organic layer in boreal forest. Deep organic and mineral layers including near-surface permafrost show slower rate of input (0.031 kgCm⁻² yr⁻¹) and turnover (617 years) and CA about 20 times slower (0.003 kgCm⁻² yr⁻¹) than surface organic layer. By using above values of the input and decomposition rate, heterotrophic respiration rate, decomposition of organic matter (Rh), which in accord with C losses from both surface and subsurface layers, was 0.225 kgCm⁻² yr⁻¹. This value also agreed well with Rh (0.227 kgCm⁻² yr⁻¹) simulated by process-based models that simulate the biogeochemical and hydrologic cycle, where Rh was averaged 45% of ecosystem respiration and 59% of soil respiration². In contrast, In tundra, large amount of SOC (36.4 kg m⁻²) have accumulated over millennia (turnover time: 4540 yrs) below the thin organic layer. The CA of mineral layer and permafrost is close to zero (0.003 kgCm⁻² yr⁻¹), and Rh is 0.008 kgCm⁻² yr⁻¹. Our radiocarbon data show that the most SOC in tundra soil was made of stabilizing OC by permafrost and steady-state SOC stocks under current C balance.

References

1. Ueyama M., Y. Harazono, Y. Kim and N. Tanaka, Response of the carbon cycle in sub-arctic black spruce forests to climate change: Reduction of a carbon sink related to the sensitivity of heterotrophic respiration, *Agric. For. Meteorol.*, 149, 582–602, 2009.

EFFECTS OF CLIMATE MANIPULATIONS ON SOIL ORGANIC MATTER UNDER CASSIOPE TETRAGONA IN ZACKENBERG, GREENLAND

*Ji Young Jung¹, Anders Michelsen², Niels Martin Schmidt³, Yoo Kyung Lee^{*1}*

¹ Division of Life Sciences, Korea Polar Research Institute

² Department of Biology, University of Copenhagen

² Centre for Permafrost (CENPERM), University of Copenhagen

³ Arctic Resesarch Centre, Aarhus University

ABSTRACT

It is projected that climate change will be more pronounced in the Arctic than further south. Climate change will affect soil organic carbon (SOC) pools which are directly related to carbon dioxide fluxes. Thus, it is crucial to understand how soil will respond to climate change in the Arctic where large amount of SOC is accumulated in many ecosystem types due to low temperature reducing decomposition. In this study, we aimed to understand the characteristics of SOC and the effects of climate manipulation on SOC under two high arctic heaths. We hypothesized that change in temperature and in growing season length would affect microbial activities and thus the amount and chemical composition of SOC.

This study was conducted in the long-term climate manipulation plots established in Zackenberg, Greenland in 2004 by Prof. Michelsen and coworkers. There are one control (C) and four treatments plots: warming (T), shading (S), short growing (SG), and long growing (LG). Detailed explanation for the manipulation was described in Klitgaard et al. (2006). Soil sampling was conducted in the Cassiope tetragona site in 2011. Soil temperature, litter layer thickness, and thawing depth were measured in the field. Three 15 cm depth soil cores (5 cm diameter) were taken in one plot, and each soil core was divided as the litter layer, 0-5, 5-10, and 10-15 cm depths, and then three cores in the same depth interval were pooled together. Air-dried soil samples were passed through a 2-mm sieve for further physical and chemical analyses. Total carbon and inorganic carbon were measured, and the difference was regarded as soil organic carbon (SOC). Density fractionation (sodium polytungstate, 1.55 g cm⁻³) separated SOC as free light fraction (FLF), occluded light fraction (OLF), and heavy fraction (HF). For statistical analyses, one-way ANOVA was used and the significance level was set as 0.1.

Preliminary analyses show that thawing depth and litter layer thickness were not significantly different among treatments. Soil temperature in the T treatment was 1.2-1.5 °C higher than in the other treatments. Bulk density, moisture content, and soil pH did not vary among treatments. There were no statistical differences in SOC, and SOC in the 0-5 cm depth was in a range of 3.5 to 5.2 %. Total inorganic carbon was rarely or never detected across all treatments. Density fractionation showed that there were differences in FLF, with a lower amount of FLF in the T and SG treatments than that in control. Further analysis for SOC fractions is currently taking place.

Reference

Klitgaard, A.B., Rasch, M., and Caning, K. (eds.) 2006. Zackenberg Ecological Research Operations, 11th Annual Report, 2005. Danish Polar Center, Ministry of Science, Technology and Innovation, Copenhagen, Denmark. 111 pp.

POSTER SESSION 5

ARCTIC PALEOCEANOGRAPHY

SEDIMENTARY FACIES ANALYSIS OF LATE PLEISTOCENE CORE SEDIMENTS RECOVERED FROM THE CHUKCHI SEA, THE WESTERN ARCTIC OCEAN

Young-Jin Joe¹, Seok-Hoon Yoon¹, & Seung-Il Nam²

¹*Department of Earth and Marine Sciences, Jeju National University*

²*Korea Polar Research Institute, Incheon, Korea*

yjoe011@jejunu.ac.kr

ABSTRACT

In this study, we present the results of sedimentary facies analysis of 5 gravity cores obtained during the 2011 Arctic expedition of R/V Araon (operated by Korea Polar Research Institute) in the Chukchi Sea, the western part of the Arctic Ocean. Based on grain-size analysis and detailed description of sedimentary structures on X-radiographs, 5 sedimentary facies are classified: (1) bioturbated mud, (2) couplet or alternation of thinly-laminated (sandy) mud and homogeneous mud, (3) indistinctly-layered mud, (4) wispy-layered mud, and (5) disorganized sandy mud. The bioturbated mud, the most predominant facies recognized in all cores, is characterized by intense occurrence of burrows without primary sedimentary structures except for diffuse banding or layering. The facies boundaries are irregular and poorly defined, and the facies thickness is highly variable. This is suggestive of hemipelagic sedimentation and/or contour-current deposition during the interglacial period. Thinly-laminated (sandy) mud and homogeneous mud commonly occur as couplets of a thin silt layer and the overlying clay layer. The lower silt layers ranging in thickness from a few mm to more than a decimeter generally show thin parallel to cross lamination that is recognized by alternation of thin silt-rich and clay-rich mud laminae and occasionally normally graded by upward decrease in silt content. The overlying homogeneous mud layers usually consist of relatively well-sorted, clay-size particles, ranging in thickness less than 5 cm and commonly show bioturbation. These intimately-occurring facies are generally accepted as deposits of low-density fine-grained turbidity currents in deep-sea environments. The indistinctly-layered mud exhibits crude and discontinuous layering with minimal bioturbation. The grain-size distribution within this facies most likely suggests a major contribution of hemipelagic settling from sea ice during the glacial period. On the other hand, wispy-layered (or laminated) mud generally occurs as poorly-sorted, commonly-bioturbated mud showing irregular and discontinuous wavy lamination or layering, and occasionally discontinuous trains of horizontally oriented coarse grains. The lower and upper boundaries of the facies are sharp or gradational, and the thickness is variable. This facies is most likely suggestive of deposition by contour currents, tail of turbidity currents or melt water plumes during the late deglaciation and interglaciation periods. In the disorganized sandy mud, coarse-grained angular clasts are randomly scattered in fine matrix without internal organization, and bioturbation is usually suppressed. This facies is interpreted to represent the settling of coarse debris from the drifting icebergs or ice-sheet margins. The sedimentological characteristics of the sedimentary facies presented in this study can be used as proxies for reconstruction of modern and ancient glacio-

marine depositional environments in the Arctic Ocean.

PALEOCEANOGRAPHIC RECORDS IN THE CHUKCHI PLATEAU, WESTERN ARCTIC OCEAN

Kwang-Kyu Park¹, Boo-Keun Khim¹, Kenichi Ohkushi²

*¹Department of Oceanography,
Pusan National University, Korea
bkkhim@pusan.ac.kr*

*²Faculty of Human Development,
Kobe University, Japan*

ABSTRACT

Two piston cores PC01 (75°28.1' N, 165°40.4' W, 558 m water depth, 587 cm) and PC04 (74°26.3' N, 165°44.3' W, 370 m water depth, 928 cm) along with multiple cores PL01 and PL04 were collected from the southern part of the Chukchi Plateau in the western Arctic Ocean during the R/V Mirai Cruise MR09-03 for the purpose of establishing the stratigraphy and unraveling the paleoceanographic history. Multiple cores were used to compensate for the top-loss of piston cores, based on the comparison of sediment color profiles. As a result, two composite cores were obtained successfully. Age of core PC01 was estimated by nine AMS ¹⁴C dates as well as by correlation of geochemical properties and ice-rafted debris (IRD) abundance with the well-dated cores nearby our core site. Age of PC04 was decided by correlation of lithologic units with core PC01. Both composite cores are divided distinctly into three lithologic units: Unit I - Last glacial gray mud layer including intervened IRD layer, Unit II - deglacial thick IRD layer, Unit III - Holocene brownish sandy mud layer. Glacial massive or laminated mud sediments in Unit I might be deposited by suspension settling from meltwater plume of local glacier. Absence of coarse-grained sediments in Unit I is attributed to the limited drifting icebergs due to relatively thick sea-ice cover during the last glacial period. Unit I is characterized by low CaCO₃ content (< 2%), low total organic carbon (TOC) content (0.1~0.6%), low C/N ratio (2.3~7.6), fairly high δ¹³C value (-25.3~-24.0‰), and low kaolinite/chlorite (K/C) ratio (0.5~0.8). Based on the microscope and SEM observation on the deglacial IRD, the IRD constituents are mineralogically diverse, but mainly composed of carbonate minerals. It implies that IRD were transported from the Canadian Arctic Archipelago. Unit II also shows high CaCO₃ (2~6%) and TOC content (0.9~1.8%), high C/N ratio (7.5~16.6), and low δ¹³C value (-26.5~-25.4‰). These properties clearly indicate an increased terrestrial contribution. Further, high K/C ratios (up to 1.2) of Unit II support the increase of kaolinite, confirming the source of IRD particles. Holocene Unit III consists of brownish silty mud sediments, characterized by high opal content (up to 18%) in PC04, and high TOC content (0.4~1.4%), very low C/N ratio (0.3~1.3), and high δ¹³C value (up to -22.0‰) in both cores. These properties clearly indicate an increase in diatom production and marine influence.

A HIGH PRECISION GAS EXTRACTION SYSTEM FOR MEASUREMENT OF ATMOSPHERIC METHANE AND TOTAL AIR CONTENT IN POLAR ICE CORE

Jiwoong Yang¹, Jinho Ahn¹, Yoo-hyeon Jin¹, Ed Brook²

¹School of Earth and Environmental Sciences, Seoul National University, Seoul 151-747,
South Korea.

²Department of Geosciences, Oregon State University, Corvallis, Oregon 97331-5506, USA
luckyno44@gmail.com

ABSTRACTS

We designed an improved high-precision method for measurement of the CH₄ mixing ratio and total air content in polar ice core samples. The occluded air in ice samples of ~50 g is extracted by melting-refreezing process, known as wet-extraction technique, and entrapped in headspace of sample flasks (Grachev et al., 2009). To minimize disturbance by water vapor the sample flasks are submerged ethanol which is chilled to -80 °C. The air is injected to gas chromatograph (Agilent® 7890A GC) for CH₄ analysis and the modified barometric method is employed for air content measurement calculated from pressure and volume of sample gas (Lipenkov et al., 1995; Jiule et al., 2011). The GC system is calibrated by two standard airs of known CH₄ concentration (721.31 or 895.03 ppbv) from US National Oceanic and Atmospheric Administration (NOAA). Data corrections of gas solubility effect and ice cutting effect are considered. Results of blank tests using bubble-free artificial ice show <1.0% standard deviations for CH₄ measurement. Comparisons of Siple Dome CH₄ data measured at Seoul National University with previously published data from Oregon State University show a good agreement within error bars. This technique is applicable to reconstruct the paleoatmospheric CH₄ and air content variations with high temporal resolutions. The high resolution CH₄ records will contribute to better understanding of terrestrial carbon cycle and global climate change, while air content gives good constrains of past summer temperature (Herron et al., 1981; Hou et al., 2007) and site elevation (Herron and Langway, 1987).

REFERENCES

- Herron, M.M., Herron, S.L., and Langway C.C., 1981, Climatic signal of ice melt features in southern Greenland, *Nature*, 293, 389-391.
- Herron, S.L., and Langway, C.C., 1987, Derivation of paleoelevations from total air content of two deep Greenland ice cores, *IAHS Publ.*, no. 170, 283-295.
- Hou, S., Chappellaz, J., Jouzel, J., Chu, P.C., Masson-Delmotte, V., Qin, D., Raynaud, D., Mayewski, P.A., Lipenkov, V.Y., and Kang, S., 2007, Summer temperature trend over the past two millennia using air content in Himalayan ice, *Climate of the Past*, 3, 89-95.
- Jiule, L., Baiqing, X., and Chappellaz, J., 2011, Variations of air content in Dasuopu ice core from AD 1570-1927 and implications fore climate change, *Quaternary International*, 236, 91-95.

- Lipenkov, V., Candaudap, F., Ravoire, J., Dulac, E., and Raynaud, D., 1995, A new device for the measurement of air content in polar ice, *Journal of Glaciology*, 41, 138, 423-429.
- Grachev, A.M., Brook, E.J., Severinghaus, J.P., and Pias, N.G., 2009, Relative timing and variability of atmospheric methane and GISP2 oxygen isotopes between 68 and 86 ka, *Global Biogeochemical Cycles*, 23, GB2009, doi: 10.1029/2008GB003330.

**VEGETATION CHANGES IN THE WESTERN ARCTIC DURING THE
HOLOCENE:
PRELIMINARY RESULTS FROM POLLEN AND SPORE RECORDS
FROM THE SHELF SEDIMENTS IN THE CHUKCHI SEA**

So-Young Kim¹, Seung-Il Nam¹, Irina Delusina²

¹Division of Polar Climate Research, Korea Polar Research Institute, Incheon, Korea

²Geology Department, University of California, Davis, California, USA

ABSTRACTS

Remnants of microscopic organisms in marine sediments such as pollen and spore have been suggested as a useful tool for reconstructing past terrestrial environments through geological time. In this study, sediments recovered from the Arctic Ocean shelf have been identified as important and under-exploited paleoclimate archives for obtaining integrated oceanic and terrestrial records of natural instabilities over the Arctic regions on millennial to decadal scales. Within this context, we investigated one marine sediment core (ARA02B/01A-GC) with surface sediments recovered from the Chukchi Sea shelf, western Arctic Ocean, to reconstruct paleo-vegetation changes during the entire Holocene based on pollen and spore records. Eight radiocarbon dates indicate that the Chukchi Sea shelf sediment record spans over 10,000 years BP. The Holocene terrestrial palynomorph records show substantial differences in the paleo-vegetation changes in the western Arctic regions, probably reflecting the response of land vegetation to ocean-atmosphere systems over the western Arctic region.

SEDIMENTARY ORGANIC MATTER VARIATIONS IN THE CHUKCHI BORDERLAND OVER THE LAST 155 KYR

Masao Uchida, Stephan Rella, Miyuki Kondo

National Institute for Environmental Studies
uchidama@nies.go.jp

ABSTRACTS

Knowledge on past variability of sedimentary organic carbon in the Arctic Ocean is important to assess natural carbon cycling and transport processes related to global climate changes. However, the late Pleistocene oceanographic history of the Arctic is still poorly understood. In the present study we show sedimentary records of sedimentary organic carbon (TOC, $\delta^{13}\text{C}$), CaCO_3 , benthic and planktonic foraminiferal $\delta^{18}\text{O}$, molecular markers (BIT index) and the coarse grain size fraction from a piston core recovered from the northern Northwind Ridge in the far western Arctic Ocean, a region potentially sensitively responding to past variability in surface current regimes and sedimentary processes such as coastal erosion. An age model based on oxygen stratigraphy, radiocarbon dating and lithological constraints suggests that the piston core records paleoenvironmental changes of the last 155 kyr. Sedimentary organic carbon content shows orbital-scale increases and decreases that can be respectively correlated to the waxing and waning of large ice sheets dominating the Eurasian Arctic, suggesting advection of fine suspended matter derived from glacial erosion to the Northwind Ridge by eastward flowing intermediate water and/or surface water and sea ice during cold episodes of the last two glacial interglacial cycles. At millennial scales, increases in TOC might correlate to a suite of Dansgaard-Oeschger Stadials between 120 and 45 ka before present (BP) indicating a possible response to abrupt northern hemispheric temperature changes. Between 70 and 45 ka BP, closures and openings of the Bering Strait could have additionally influenced TOC variability. CaCO_3 content tends to anti-correlate with TOC on both orbital and millennial time scales, which we interpret in terms of enhanced sediment advection from the carbonate rich Canadian Arctic via an extended Beaufort Gyre during warm periods of the last two glacial-interglacial cycles and increased organic carbon advection from the Siberian Arctic during cold periods when the Beaufort Gyre contracted.

**MULTIBEAM BATHYMETRIC AND SEDIMENT PROFILER
EVIDENCES FOR POCKMARKS AND ICE GROUNDING SCOURS ON
THE CHUKCHI BORDERLAND AND BEAUFORT SEA**

Masao Uchida, Akihiko Shibahara

National Institute for Environmental Studies
uchidama@nies.go.jp

ABSTRACTS

Multibeam bathymetry and subbottom profiler data collected from the Japanese R/V Mirai in 2004 and 2008 provide convincing evidence for ice grounding scour and mega pockmarks on the Chukchi borderland and Beaufort Sea, Arctic Ocean. The data presented here were collected hull-mounted multibeam echo sounder and 12 kHz subbottom profiler. The multibeam bathymetry soundings were compiled into digital terrain models with a Polar Stereographic projection and its grid resolution of the digital terrain models are 25 to 100m. The size of pockmarks and scours are measured on the digital terrain models to determine pockmarks diameter and scour width. We also measured scour direction and displayed them as a rose diagram. In this study, we obtained a bathymetric dataset of approximately 610000 km² in the area. The running time of the seabeam system was more than about 700 hours. Seabeam data were converted and visualized by CARIS (Geospatial Software Solutions) and ArcGIS (ESRI).

TERRESTRIAL *N*-ALKANES SIGNATURES IN SEDIMENT OF THE NORTH ATLANTIC ODP SITE 980: PALEOCLIMATOLOGICAL IMPLICATIONS

Sangmin Hyun¹, Yean Jee Suh² and Minoru Ikehara³

¹Korea Institute of Ocean Science and Technology (KIOST), Korea

²Department of Geology, University of Cincinnati, Cincinnati, OH 45221-0013, USA

³Kochi Core Center, Kochi University, Japan

ABSTRACTS

Terrestrial biomarker *n*-alkanes, was analyzed from the core sediment of North Atlantic ODP Site 980 for the reconstruction of its distribution in conjunction with the past paleoclimatological evolution. Since the changes in the sedimentary *n*-alkanes distribution over the time were primarily driven by variable inputs from plant leaf-waxes in response to changing plant community composition, the distribution of *n*-alkanes chain length directly indicate environmental variations in land plant source areas.

There were drastic changes in the abundance of individual *n*-alkanes; predominant existence of *n*C29 occurred at 106.51 kyr, 399.12 kyr and 477.14 kyr. Similarly, strong abundance of *n*C25 was founded in sediment of 112.50 kyr. This shift and/or occurrence of specific chain lengths (*n*C25, *n*C29) in specific time can be explained by changes in plants habitat of source areas. Usually, it is thought that land plant community is strongly related with the landscape condition that has been repeated between dry conditions during glacial period and humid condition during interglacial period. In most grasses and herbs the *n*-alkanes *n*C31 or *n*C33 dominate, whereas in most trees and shrubs the *n*-alkanes *n*C27 or *n*C29 dominate.

Our *n*-alkanes distribution is characterized by the dominance of *n*C31 during present to approximately 100 kyr ago, and this pattern switched into *n*C29 dominant pattern at 106.5 kyr, and further it switched into *n*C25 dominant pattern at 112.50 kyr. This *n*-alkanes distribution, therefore suggest vegetation changes, thus climatic changes of source areas has been maintained and repeated during the last 500 kyr. In previous studies, distinctive 100 kyr periodicity in biogenic carbonate production was observed in this site. It is needed to further study whether this vegetation, climatic changes are associated with oceanic variations in carbonate production or not.

NEOGENE BIOSTRATIGRAPHY AND PALAEOENVIRONMENT ACROSS THE FRAM STRAIT GATEWAY

– Reappraisal for the application of dinocysts in Arctic deep time reconstructions –

M. Schreck¹, M. Meheust², J. Matthiessen², R. Stein², M.J. Head³

¹Arctic Research Centre, Korea Polar Research Institute

Michael.Schreck@kopri.re.kr

²Alfred Wegener Institute Helmholtz Centre for Polar and Marine Research, Germany

³Department of Earth Science, Brock University, Canada

ABSTRACT

Continuous Neogene high northern latitude paleoclimate records with an unequivocal age model that allow tackling Miocene climate variability are rare. Moreover, owing to a generally low carbonate deposition/preservation and the scarcity of calcareous microfossils in these sediments, which seriously hampered the establishment of a consistent chronostratigraphic framework, most previous studies focussed on reconstructing the paleoclimatic history of the high latitudes only since the onset of large-scale Northern Hemisphere glaciations whereas the Miocene paleoenvironmental evolution still remains enigmatic.

ODP Hole 907A in the Iceland Sea is located close to the growing Greenland ice sheet and experienced the effects of sea-ice cover, migrating wind fronts and ocean currents. Its continuous Middle through Late Miocene sediment sequence and a pristine paleomagnetic record predisposes it for detailed investigations on the response of the high northern latitudes to major Neogene climate deteriorations. To bypass the virtual absence of biogenic carbonates, organic-walled marine palynomorphs (dinoflagellate cysts, prasinophyte algae and acritarchs) have been utilized in this study as they are continuously present within this time-interval and show relatively high abundance and diversity in the high northern latitudes hemipelagic sediments.

Here we summarize latest progress in the application of marine palynomorphs for both biostratigraphy and paleoceanographic reconstructions in the Neogene of the high northern latitudes, a region critical for Earth's Cenozoic climate development. Build upon a refined palynostratigraphic framework for ODP Hole 907A, which suggests that some age models of previously drilled ODP/IODP Sites have to be revised, we present new insights into short-term Miocene climate variability superimposed on the gradual Neogene cooling, and discuss the initiation and subsequent development of the East Greenland Current across the Middle Miocene Climate Transition.